

**SYNTHESIS OF A CONGESTED HEPTAMINE AS A POTENTIAL PRECURSOR TO
HYPERVALENT (10-N-5) NITROGEN, AND EFFECTS OF REMOTE SUBSTITUENTS
ON PLANARIZATION OF NITROGEN IN TRIALKYLAMINES**

by

David Sujee Makhanu

A dissertation submitted to the Graduate Faculty of
Auburn University
in partial fulfillment of the
requirements for the Degree of
Doctor of Philosophy

Auburn, Alabama
August 4, 2012

Keywords: hypervalency, heptamine, congestion, planarity, hyperconjugation.

Copyright 2012 by David Sujee Makhanu

Approved by

Peter D. Livant, Chair, Associate Professor of Chemistry
Edward J. Parish, Professor of Chemistry
Orlando Acevedo, Associate Professor of Chemistry
Michael E. Squillacote, Associate Professor of Chemistry

Abstract

The challenging synthesis of a congested heptamine **10**, as a potential precursor to hypervalent (10-N-5) nitrogen, was pursued by employing four different strategies. Even though these strategies didn't lead to a successful synthesis of **10**, strategy 4 seems more likely the way forward if deprotection of a single acetonide group of **105** is possible in the future.

Investigation into the unprecedented formation of ester-amides **85** and **87** in $\text{Rh}_2(\text{OAc})_4$ catalyzed N-H insertion with dimethyl diazomalonate **19** led to the identification of other minor side products **88**, **89**, **90** and **91**. The 1:1 ratio of ester-amides **85/87** with **88** led us to propose a mechanism that involves a novel thermal *intermolecular* Wolff rearrangement.

Analysis of planar and nearly planar trialkylamines **20**, **85**, **86**, **87** and **105**, gave anomalies that could not only be explained by steric congestion around nitrogen as it is in the case of triisopropylamine. Planarization of these trialkylamines can be explained by a simple p- σ^* hyperconjugation argument. Hyperconjugation was also supported through computational methods *i.e.* Natural Bond Orbital analysis.

Acknowledgments

First and foremost I would like to express my deep appreciation to my advisor Dr. Peter Livant, for his guidance and encouragement throughout my studies here at Auburn University. I am also grateful to my dissertation committee members, Dr. Edward J. Parish, Dr. Orlando Acevedo, Dr. Michael E. Squillacote and university outside reader Dr. Jack DeRuiter, for taking their time to read and offer meaningful suggestions for my dissertation.

I am grateful to Dr. Anna-Gay Nelson, Dr. Andrea Alsobrook, Mr. Branson Maynard, Dr. John Gorden and Dr. Thomas Albrecht-Schmitt for completing X-ray structure determinations. I would also like to thank Dr. Yonnie Wu for the extended help with Mass spectroscopy and Dr. Mike Meadows for helping with the NMR instrument.

I thank all my group members and friends here in Auburn for their friendship and encouragement. I also thank the faculty and staff in the Chemistry & Biochemistry Department for my smooth transition and stay here in Auburn.

Lastly, I would like to thank my mum who has been a source of inspiration and encouragement throughout my life especially as I have been undertaking my studies.

TABLE OF CONTENTS

ABSTRACT	ii
ACKNOWLEDGMENTS	iii
LIST OF TABLES.....	vii
LIST OF SCHEMES.....	viii
LIST OF FIGURES	ix
1. INTRODUCTION	1
2. RESULTS AND DISCUSSION	6
2.1. Synthesis of amine hexaalcohol 22	6
2.1.1. Some properties of DDM 19	9
2.1.1.2. Solid state structural features of DDM	9
2.2. STRATEGY 1. Introduction of N-Alkyl group at the end of the synthesis of 22	14
2.2.1. Traditional method of converting a primary alcohol to amine.....	14
2.2.2. Direct conversion of alcohol to amine via Mitsunobu reaction	16
2.2.3. Use of borrowing-hydrogen methodology to convert alcohols to amines	19
2.3. Introduction of a synthetic route incorporating N-alkyl groups	20
2.3.1. STRATEGY 2. Introduction of N-alkyl groups to an intermediate appearing along the synthetic path to 22	21
2.3.1.1. Aminolysis of amino diesters.....	21
2.3.1.2. Aminolysis of dimethyl malonate.....	23
2.3.1.3. Synthesis of diazo malonamides.....	24

2.3.1.4. Aminolysis of DDM	24
2.3.1.5. Aminolysis of dimethyl malonate with Boc-protected <i>tert</i> -butylamine	25
2.3.1.6. Protection of malonamide N-H with Boc group	25
2.3.2. STRATEGY 3. Introduction of N-alkyl groups at the beginning of the synthetic path.....	26
2.3.2.1. Synthesis of a protected N-alkylated ketone.....	27
2.3.2.2. Double reductive amination of ketone 54	31
2.3.2.3. Synthesis of heterocyclic protected ketones with N-alkyl groups	33
2.3.2.4. Double reductive amination of heterocyclically-protected ketones 64 and 67	35
2.3.2.5. Oxime synthesis from ketones 64 and 67	36
2.3.2.6. Double reductive amination of 67 with PEMB.....	36
2.3.2.7. Synthesis of diazo barbiturate 73	37
2.3.2.8. Rhodium catalyzed N-H insertions	38
2.3.2.8.1. Synthesis of diazo DDDU	41
2.3.2.9. Screening of new catalyst for N-H insertions	42
2.4. STRATEGY 4. Double Fukuyama-Mitsunobu reaction	44
2.4.1. Fukuyama-Mitsunobu reaction of 21	45
2.4.2. Attempted deprotection of only one acetonide group of 79	46
2.4.3. Acetonide deprotection of 79	48
2.4.4. Quadruple Fukuyama-Mitsunobu reaction of 80	48
2.4.5. Nosyl group deprotection of 79	51
2.4.6. Urea cyclized protection of 83	51
3. RESULTS AND DISCUSSION	54
3.1 Investigations of the unprecedented ester-amides in N-H carbene insertions	55

3.1.1. Aminolysis	55
3.1.2. Reaction progress monitored by NMR	57
3.1.3. Proposed reaction mechanism in formation of ester-amides 87/85 and 88	61
3.1.4. Partial evidence supporting the proposed mechanism	63
3.2. Nitrogen Planarity of trialkylamines 20 , 21 , 85-87 and 104	66
3.2.1. Planarity at Nitrogen in compounds 20 , 21 , 85 , 86 , 87 and 105	67
3.2.2. A rationale for Trends in Nitrogen Planarity	72
3.2.3. Hyperconjugation.....	74
3.2.4. Computational analysis.....	76
4. EXPERIMENTAL.....	84
5. REFERENCES	147
6. APPENDICES	157

List of Tables

Table 2.1 Structural parameters of DDM and related compounds	10
Table 2.2 Room temperature double reductive aminations	31
Table 2.3 Conditions of acetonide deprotection of 79	47
Table 2.4 Attempted reaction conditions for quadruple F-M reaction of 80	49
Table 3.1. Effect of ratio of reactants on product distribution	56
Table 3.2. Aminolysis of 86 by DCHA	56
Table 3.3. Selected geometrical parameters of amines 20 , 21 , 80 , 85 – 87 and 105	68
Table 3.4. Comparison of calculated and exptl geometrical parameters of trialkylamines; 11 , 20 , 84-133 , 105-107	79
Table 3.5. NBO $E(2)$ energies associated with N2p - (C-A) σ^* interactions	81
Table 3.6. Comparison of NBO E_{del} and $\sum E(2)$ energies.....	82

List of Schemes

Scheme 1.1. Plan to synthesize hypervalent (10-N-5) nitrogen.....	1
Scheme 1.2. Attempted synthesis of 2	1
Scheme 2.2. Synthesis of hexaalcohol 22	7
Scheme 2.2. Conformations of DDM	12
Scheme 2.3. Work-up of Mitsunobu reaction with DIAD	17
Scheme 2.4. Work-up of Mitsunobu reaction with DTBADM	18
Scheme 2.5. Borrowing-hydrogen methodology	19
Scheme 2.6. Retrosynthesis of 38	21
Scheme 2.7. Enolate formation.....	23
Scheme 2.8. Retrosynthetic analysis of diamide 39	23
Scheme 2.9. General retrosynthesis of new synthetic route beginning with N-alkyl groups, STRATEGY 3	26
Scheme 2.10. Retrosynthesis of a ketone with protected N-alkyl groups	27
Scheme 2.11. Jie's efforts towards synthesis of 22	32
Scheme 2.12. Modified retrosynthesis to introduce N-alkyl groups, according to STRATEGY 3	33
Scheme 2.13. Retrosynthesis involving double Fukuyama-Mitsunobu (F-M) reactions, STRATEGY 4	44

List of Figures

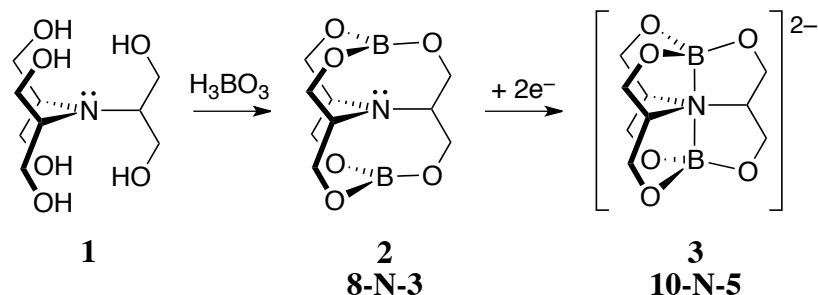
Figure 1.1. Intermolecular association of alumatrane	2
Figure 1.2. Bidirectional association of 2 leading to a polymer	3
Figure 1.3. New target molecules	4
Figure 1.4. Definition of parameter <i>h</i>	4
Figure 2.1. The X-ray crystal structure of compound 17	8
Figure 2.2. The X-ray crystal structure of DDM 19	9
Figure 2.3. <i>c</i> and <i>a</i> axis views of two adjacent DDM molecules in the unit cell	11
Figure 2.4. ¹ H-NMR spectra of ketone 54 at T = 296 K (red) and at T = 323 K (blue)	29
Figure 2.5. ¹³ C-NMR spectra of ketone 54 at T = 293 K (red) and at T = 323 K (blue)	30
Figure 2.6. Stabilities and reactivities of diazo compounds	40
Figure 2.7. Stability and reactivity comparison of diazoamides 73 and DDDU	41
Figure 2.8. Formation of MBH betaine in the first step of a Mitsunobu reaction	51
Figure 2.9. Possible interference by –OH groups in F-M reaction of 21 and 80	51
Figure 2.10. Plausible side reaction in the quadrupole F-M reaction	52
Figure. 3.1. The Rh ₂ (OAc) ₄ -catalyzed N-H insertion reaction of DCHA with DDM (in the ratio of 1.17:1.00 respectively) in refluxing C ₆ D ₆	58
Figure. 3.2. The Rh ₂ (OAc) ₄ -catalyzed N-H insertion reaction of DIPA with DDM (1.20:1.00 ratio respectively) in refluxing C ₆ D ₆	59
Figure 3.3. Proposed mechanism of formation of 88 and 85/87	62
Figure 3.4. Comparison 1	69
Figure 3.5. Comparison 2	70

Figure 3.5. Comparison 3	71
Figure 3.6. Comparison 4	71
Figure. 3.7. Orbital interaction diagram for a planar trialkylamine, N(CH ₂ A) ₃ where A represents any atom. Only one -CH ₂ substituent of three is shown. For clarity, the analogous σ _{C-A*} that involves the bottom atom A is not shown	73
Figure 3.8. A-C-A group σ* orbitals of 86 and 105	74
Figure 3.9. Hyperconjugation as described by VB theory (a) and MO theory (b)	75
Figure 3.10. N2p - (C-A) σ* orbitals interaction.....	80
Figure 4.1. Partial 400 MHz ¹ H-NMR spectrum (<i>ca.</i> 2.90 - 5.10 ppm) of the crude reaction mixture (experiment J4(a)) at <i>t</i> = 120 min	129
Figure 4.2. Partial 400 MHz ¹ H-NMR spectrum (<i>ca.</i> 2.96 – 3.58 ppm) of the crude reaction mixture (experiment J4(b)) at <i>t</i> = 0, 3, 6, 9, & 12 min	131
Figure 4.3. Partial 400 MHz ¹ H-NMR spectrum (<i>ca.</i> 4.20 – 5.00 ppm) of the crude reaction mixture (experiment J4(b)) at <i>t</i> = 0, 3, 6, 9, & 12 min	132
Figure 4.4. Partial 400 MHz ¹ H-NMR spectrum (<i>ca.</i> 2.96 – 5.05 ppm) of the crude reaction mixture (experiment K2) at <i>t</i> = 105 min (Compounds were identified as indicated above)	134
Figure 4.5. Partial 400 MHz ¹ H-NMR spectrum (<i>ca.</i> 4.20 – 5.10 ppm) of the crude reaction mixture (experiment L1)	138
Figure 4.6. Partial 100 MHz ¹³ C-NMR spectrum (<i>ca.</i> 61.0 – 80.0 ppm) of the crude reaction mixture (experiment L1)	139
Figure 4.7. Partial 400 MHz ¹ H-NMR spectrum (<i>ca.</i> 4.24 – 5.07 ppm) of the crude reaction mixture (experiment L2)	141
Figure 4.8. Partial 100 MHz ¹³ C-NMR spectrum (<i>ca.</i> 61.3 – 79.5 ppm) of the crude reaction mixture (experiment L2)	142

1. INTRODUCTION

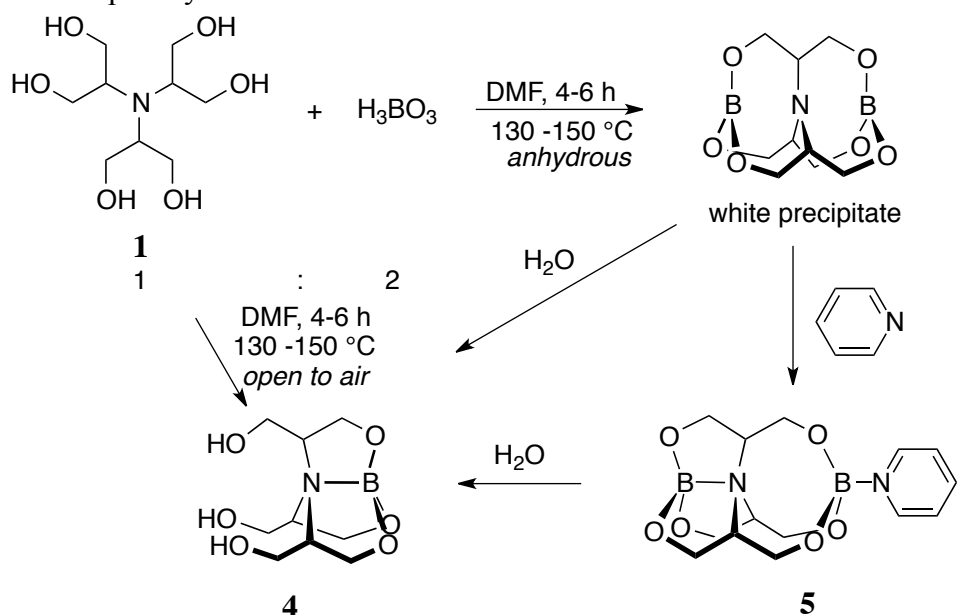
Our laboratory has been interested in synthesizing an isolable hypervalent (10-N-5) nitrogen compound. The idea was to synthesize hypervalent nitrogen species **3** from **1** as shown in Scheme 1.1.

Scheme 1.1. Plan to synthesize an example of a hypervalent (10-N-5) nitrogen species.



A previous student in our lab, Yuanping Jie, tried to synthesize **2** as shown in Scheme 2.¹ Reaction of **1** with boric acid in the open air gave **4**. When performed under anhydrous conditions, the reaction produced a white precipitate (maybe **2**) that was insoluble in all common solvents. Also, it neither melted nor sublimed below 400 °C and 2 torr. The lack of solubility precluded characterization of the white precipitate by NMR spectroscopy. Further, the solid was extremely moisture-sensitive, hydrolyzing rapidly to **4**. The intractable precipitate was found to dissolve in dry pyridine, forming an adduct, **5**, that was characterized using x-ray crystallography. Therefore, the precipitate was most probably **2**, because the pyridine adduct **5** incorporated two boron atoms.

Scheme 1.2. Attempted synthesis of **2**.



It was hypothesized that the lack of solubility exhibited by **2** might be due to intermolecular association. This type of association is illustrated by alumatrane **6** and **7**, which form dimers, Figure 1.1.² Compound **7** dimerizes when $R = CH_3$, but not when $R = SiMe_3$ or $SiMe_2-t-Bu$.³

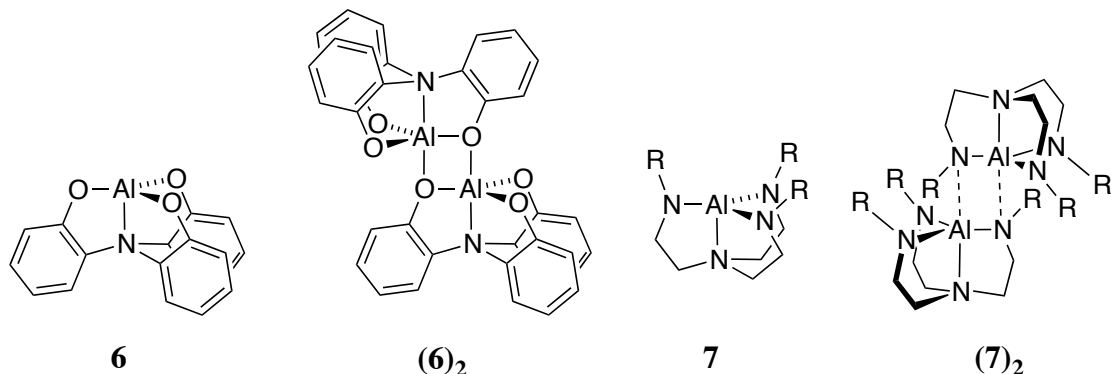


Figure 1.1. Intermolecular association of alumatrane

In the case of **2**, there is a functional group required for intermolecular association, $B(OR)_3$, at both ends of the structure, instead of at only one end as in **6** and **7** ($Al(OR)_3$ or $Al(NRR')_3$, respectively). Therefore, with **2**, association results in a polymer rather than a dimer. This is shown in Figure 1.2. The polymeric nature of the product accounts for its insolubility.

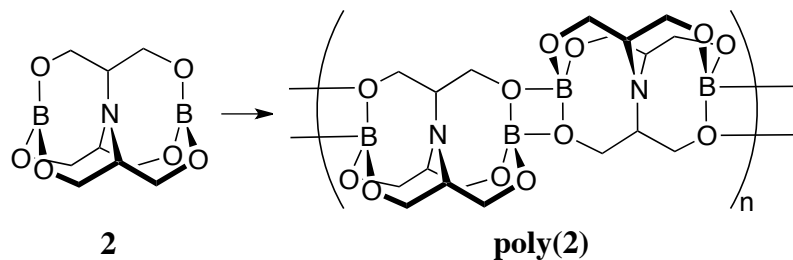
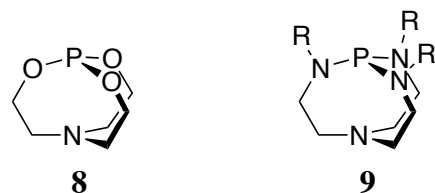


Figure 1.2. Bidirectional association of **2** leading to a polymer

Clearly, it is critical to limit or prevent this aggregation. We were inspired by the success experienced by Verkade and his coworkers in replacing the oxygen atoms of **8** with alkylamino groups, as in **9**.



Phosphorane **8** was a difficult compound that was very hard to work with. Synthesis of **8** gave mainly an “uncharacterized polymer.”⁴ Vacuum sublimation of **8** produced “violent pyrolysis.”⁴ However, **9** behaved beautifully, and it launched decades of fruitful research for the Verkade group.⁵ Therefore we sought to replace **1** with **10** as a target molecule (Figure 1.3).

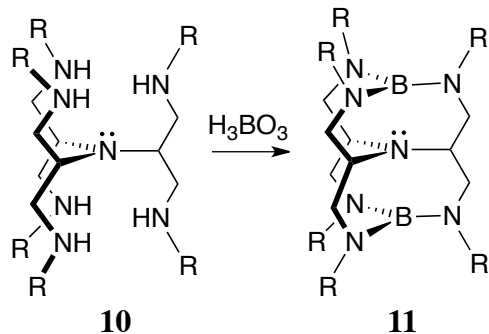


Figure 1.3. New target molecules ($R = iso\text{-}Pr, Bn$).

Converting **10** to **11** would provide a compound prevented by the steric bulk of the R groups from associating, and hence polymerizing. This would allow us to characterize the bonding, or lack of it, along the B-N-B triad. Chapter 2 will present work directed at a synthesis of **10**.

In previous work by Jie, *et al.*⁶ trialkylamines were obtained that exhibited central nitrogen atoms that were significantly flattened.⁷ In the work on the synthesis of **10**, to be discussed in Chapter 2, further examples of this unusual amine planarization were found.

A survey of the Cambridge Crystallographic Database revealed a number of examples of flattened trialkylamines, where the term trialkylamines was taken to refer to compounds with nitrogen atoms attached to three sp^3 (tetrahedral) carbon atoms. A convenient measure of nitrogen planarity is the distance from N to the plane defined by the three carbon atoms attached to N. We will call this parameter “ h ” (Figure 1.4)

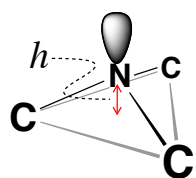
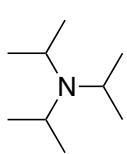
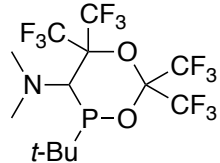


Figure 1.4. Definition of parameter h

For ordinary trialkylamines, h is roughly 0.45 Å. Trialkylamines with h less than 0.30 Å were considered flattened in the survey of the crystallographic database. These trialkylamines fell into several categories: (i) bicyclic or tricyclic amines with bridgehead N, (ii) medium-ring or macrocyclic trialkylamines, (iii) trialkylamines with multidentate contacts to a metal, (iv) highly fluorinated trialkylamines, and (v) others.⁷ Since the trialkylamines we were dealing with in our work were all acyclic, we focused on the fifth category. Many trialkylamines in this group had three branched carbon atoms attached to N, e.g. triisopropylamine **12** ($h = 0.282$ Å)⁸. This would suggest that steric congestion necessarily results in flattening of the nitrogen. Yet tricyclopropylamine, a trialkylamine in which every α -carbon is branched, has $h = 0.47$ Å, typical of an ordinary trialkylamine. Also, there were many examples of quite flattened nitrogens in trialkylamines in which only one alkyl group attached to N could be considered bulky, e.g. **13** in which two alkyl groups attached to nitrogen are methyl groups. The factors controlling planarity at N are not simple.



$$h = 0.282 \text{ \AA}$$



$$\mathbf{12}, h = 0.191 \text{ \AA}$$

Chapter 3 discusses flattened trialkylamines we have synthesized, and offers an explanation of the geometries we have encountered.

2. SYNTHESIS OF A CONGESTED HEPTAMINE AS A POTENTIAL PRECURSOR TO HYPERVALENT (10-N-5) NITROGEN

Results and Discussion

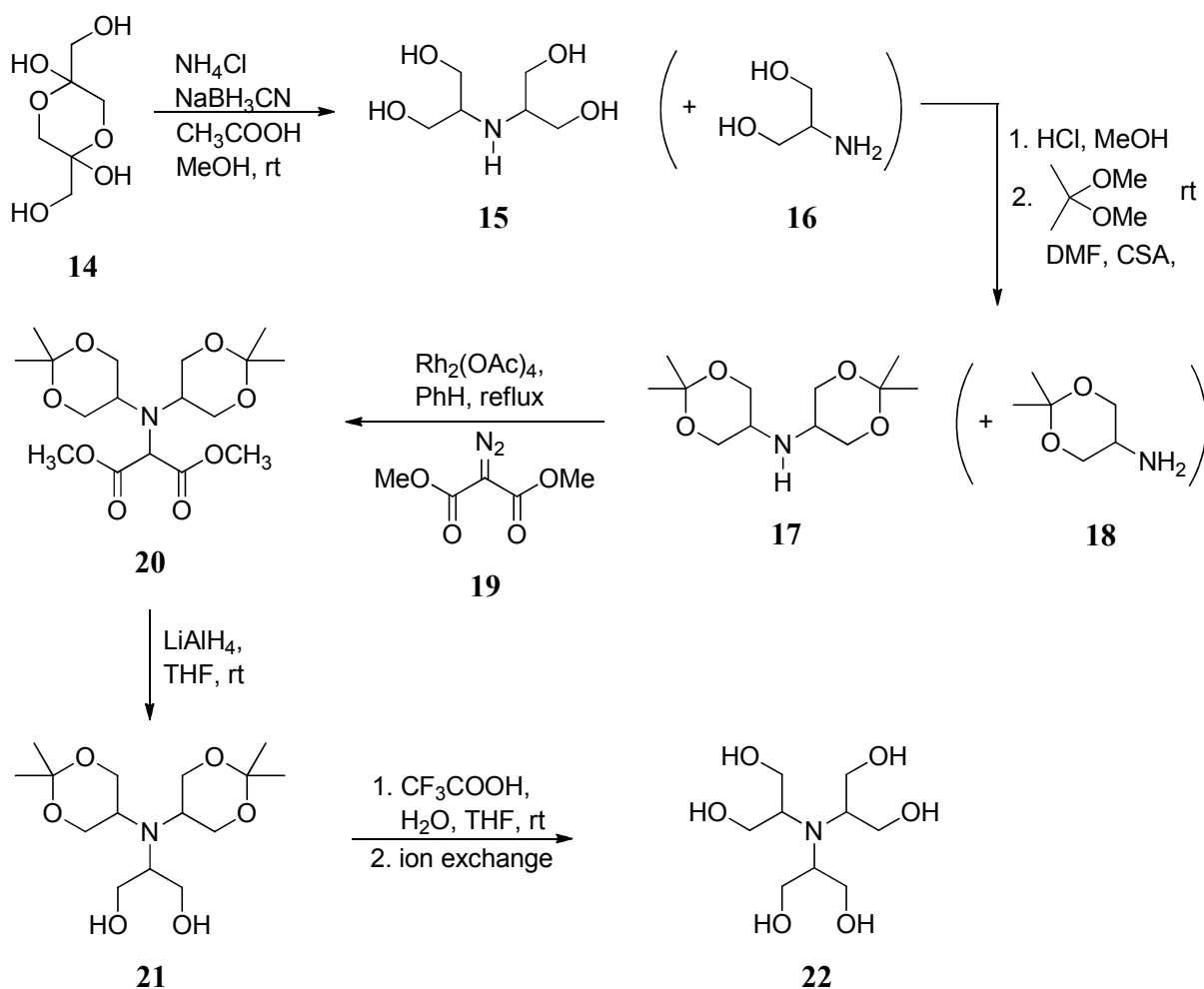
To embark on the synthesis of heptamine **10**, we chose to introduce the N-alkyl groups after the synthesis of amine hexaalcohol **22**. To achieve this, we required gram scale quantities of **22** for use in investigations of various functional group manipulations that were to be carried out.

2.1. Synthesis of amine hexaalcohol **22.**

Following Jie's protocol (Scheme 1),³⁵ a large scale synthesis of **22** starting with the commercially available dihydroxyacetone dimer **14**, was achieved in five steps. Under reductive amination conditions, tetraalcohol **15** was synthesized from dihydroxyacetone dimer **14** and NH₄Cl, although the monoamination product **16** was observed as a contaminant that could not be easily separated.

Protection of tetraalcohol **15** was achieved by first preparing and isolating a mixture of hydrochloride salts of **15** and **16**, then using this dry solid product in the reaction with 2,2-dimethoxypropane. In this reaction we found that minimizing any traces of water led to better yields of **17**, therefore hygroscopic *p*-toluenesulfonic acid (*p*-TSA) was replaced by camphorsulfonic acid (CSA) as the catalyst, and 4A molecular sieves were added. Recrystallization of the product from hot hexanes provided **17** free of **18**, and suitable for the next step: carbenoid N-H insertion.³⁵

Scheme 2.1. Synthesis of hexaalcohol **22**.



In the quest to improve the purity of **17**, vacuum ($< 1 \text{ mm Hg}$) sublimation at 35°C of the product gave colorless needle crystals with a sharp mp 61°C . The yield dropped immensely from 73% (reported)^{35a} to 29% in our case but we had over 10 g at hand to proceed with a large scale synthesis of **22**. Compound **17** was unusual in that it dissolved in both CDCl_3 and D_2O solvents, and NMR spectra of **17** were obtained in both solvents. It was quite intriguing that amine **17** could dissolve in both a relatively non-polar solvent (hot hexanes) and a highly polar solvent (water at rt). The crystal structure of **17** is shown in Fig. 2.1.

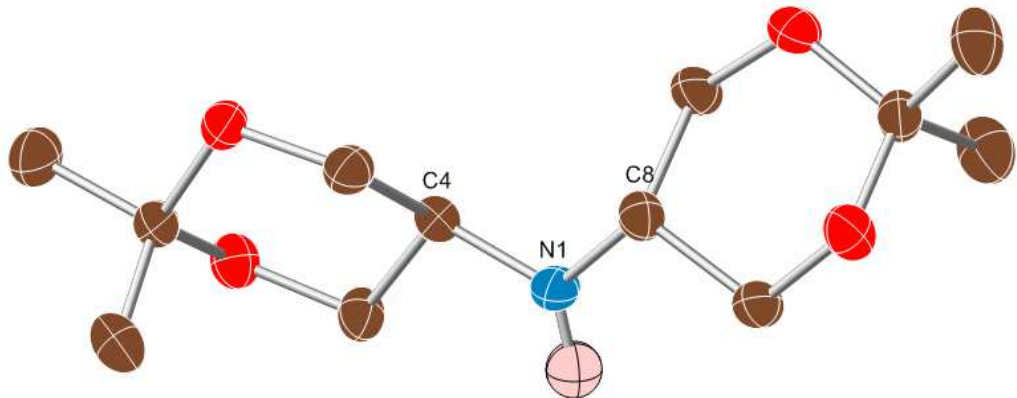
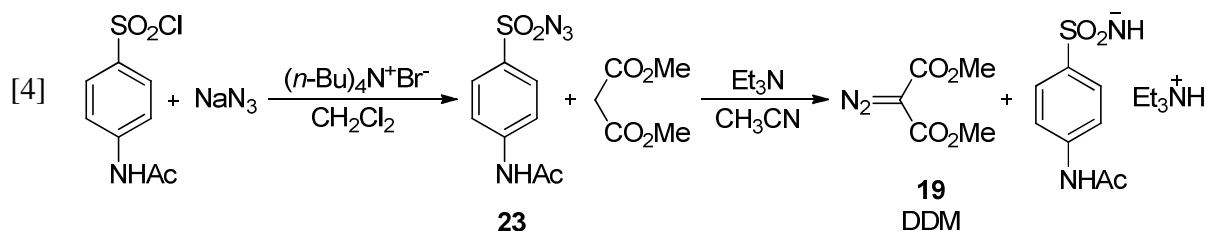


Figure 2.1. The X-ray crystal structure of compound **17**. Thermal ellipsoids are illustrated at 50% probability level. Carbon is brown, oxygen is red, nitrogen is blue. For clarity, all hydrogens have been omitted, except N-H. Hydrogen is depicted in pink.

The average length of the two C–N bonds of **17**, 1.456(4) Å, is relatively short compared to the average C(sp³)–N(sp³) bond length 1.469 ± 0.014 Å, a value determined by systematic searching of the Cambridge crystallographic database.⁶¹

Synthesis of **20** called for a $\text{Rh}_2(\text{OAc})_4$ -catalyzed N-H insertion of the carbenoid obtained from dimethyl diazomalonate **19** (“DDM”) into **17**, a method that has been developed in our lab and will be further discussed in a subsequent chapter. Diazo compound **19**, whose properties will be discussed shortly, was synthesized using the diazo transfer reaction shown in eq [4].⁸⁹



2.1.1. Some properties of DDM 19.

Diazo compounds in general are commonly thought to be unstable. However we were surprised by the stability of **19** under various conditions: in air at rt; under both basic and acidic conditions in air at rt; and under N₂ at 90 °C for a period of 24 h. DDM decomposed under N₂ at temperatures above 110 °C. On storage at -15 °C, DDM solidified but gradually melted on return to rt. A single crystal was carefully obtained from solidified DDM at -15 °C and used to get the crystal structure, shown in Fig. 2.2.

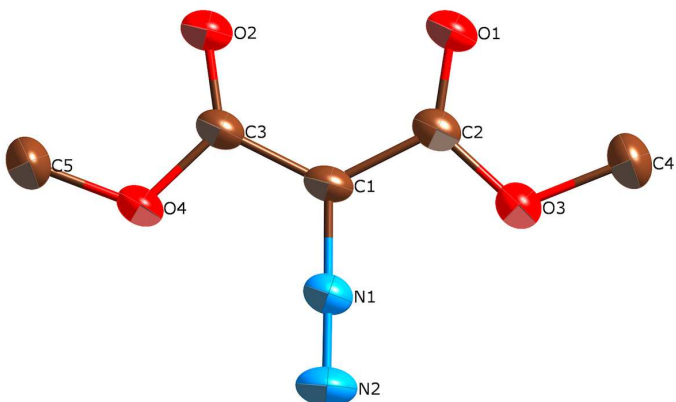


Figure 2.2. The X-ray crystal structure of DDM **19**. Thermal ellipsoids are illustrated at 50% probability level; carbon is brown, oxygen is red and nitrogen is blue. All hydrogens are omitted.

2.1.1.2. Solid state structural features of DDM.

Table 2.1 shows geometry comparisons between DDM and other compounds or groups of compounds defined in Chart 1.

Chart 2.1. Structures of diazo compounds, and model compounds in Table 2.1.

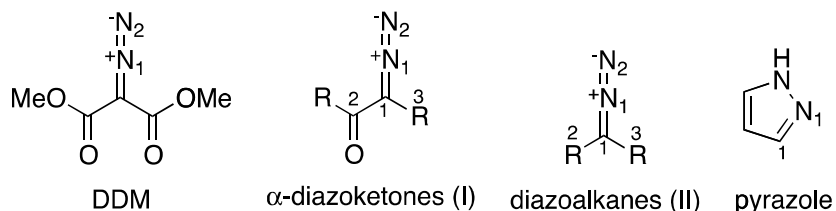


Table 2.1. Structural parameters of DDM and related compounds.

(a) Bond Length (Å)					
	N ₁ =N ₂	C ₁ =N ₁	C ₁ -C _{2/3} ^a	C=O	C _{2/3} -OMe
DDM	1.112(2)	1.325(2)	1.458(2)	1.202(2)	1.337(2)
I ^b	1.115(3)	1.328(5)	1.436(3)	1.222(2)	
II ^c	1.133(2)	1.301(2)			
pyrazoles ^d		1.329(3)			
N ₁ =N ₂ =N ₃ -R ^e	1.124(15)				
C-N=N-C ^f	1.240(12)				
C=N-OH ^g		1.281(13)			
C _{ar} -C=N-C ^h		1.279(8)			

(b) Bond Angle (°)						
	N ₁ =N ₂ -C ₁	C ₃ -C ₁ -C ₂	N ₁ =C ₁ -C ₂	N ₁ =C ₁ -C ₃	C ₁ -C ₂ -OMe	C ₁ -C ₃ -OMe
DDM	179.23(18)	126.81(14)	116.86(15)	116.33(14)	110.64(13)	109.92(14)
I ^b	177.2(3)	124.9(14)	116.4(7)	117.9(19)		
II ^c	178.5(6)	114.6(30)	122.8(14)	122.5(19)		

^amean of C1-C2 and C1-C3 bond lengths ^bmean of 23 α -diazoketones compounds, ref 71a ^cmean of 6 diazoalkanes, ref 71a ^dmean of C=N double bond length in various delocalized systems, ref. 71a ^emean of 19 azides, ref. 71c ^fmean of 27 azo compounds, ref. 71c ^gmean of 67 oximes, ref. 71c ^hmean of 75 aryl alkyl imines, ref. 71c

The N=N bond length of DDM, 1.112 Å, is comparable to those of α -diazoketones, but 0.021 Å shorter than diazoalkane N=N bonds. The C=N double bond in **19**, 1.325 Å, is about 0.045 Å longer than C=N bonds in oximes (1.281(13) Å) or aromatic imines (1.279(8) Å),^{71c} both of which are not strongly delocalized, but comparable to a strongly delocalized C=N bond, *e.g.* pyrazole (1.329 Å). The N=C-C=O (C1-C2/C3) bond of DDM, 1.458(2) Å, is shorter than the

average central C-C bond length of 211 conjugated C=C-C=O systems, 1.464(18) Å.^{71c} The ester C=O bond, 1.202(2) Å, is slightly shorter than both the α -diazoketone group (I) and the mean C=O bonds of a sample of 113 conjugated esters (1.199(9) Å).^{71c} The molecule is planar. The average deviation from the best plane through the non-hydrogen atoms of DDM is 0.000 Å.

The molecule has a high symmetry *i.e.* space group *Cmca*, consisting of a repeating double layer of oppositely arranged adjacent molecules (relative to C=N=N direction) as shown in Fig. 2.3, with an interlayer distance of 3.160 Å.

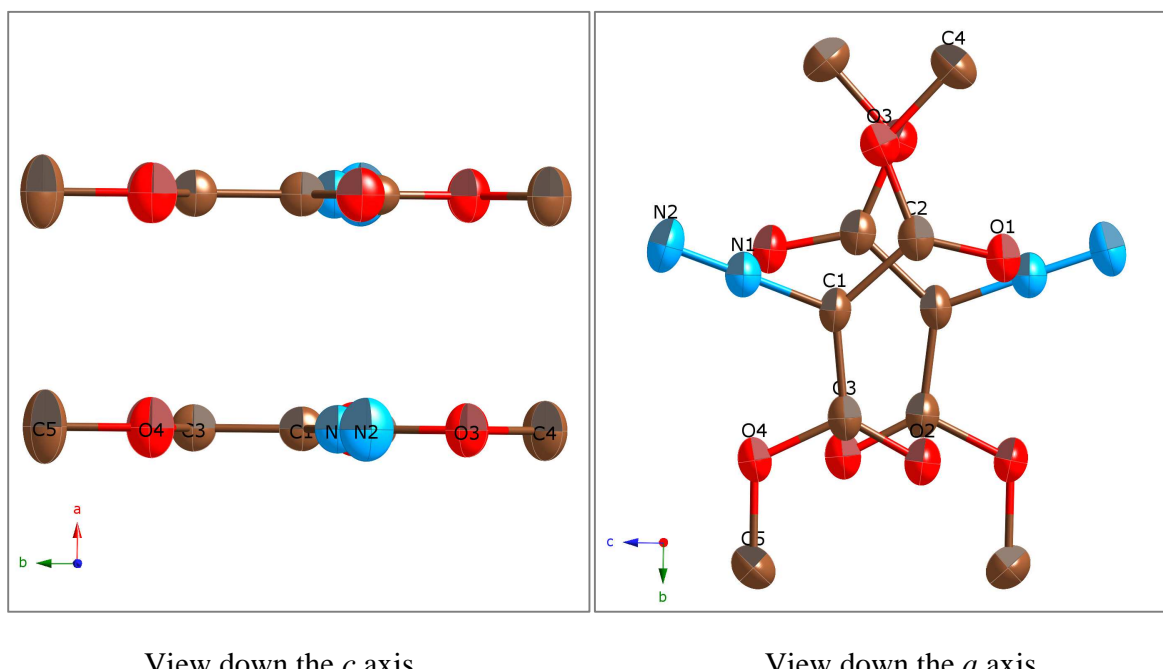
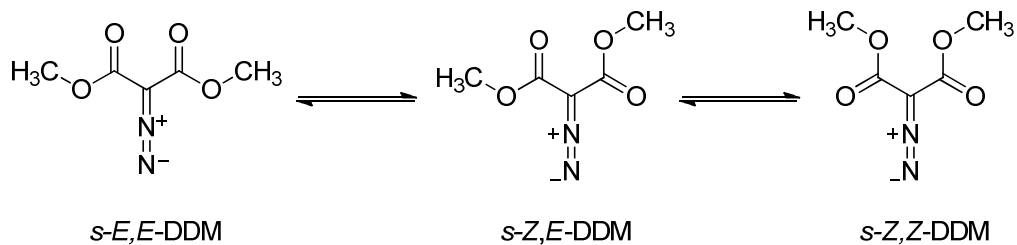


Figure 2.3. *c* and *a* axis views of two adjacent DDM molecules in the unit cell.

From *c* and *a* axis views, a slight shear between molecules in adjacent bilayers can be seen, coupled with the longer intermolecular distance 3.440 Å (between C1 of the two molecules). This arrangement could be due to Coulombic attraction between partially positively charged N1 and electron rich carbonyl oxygen (O1) as shown in the view down the *a* axis of Fig. 2.3.

DDM can exist in an equilibrium of three conformations as shown in Scheme 2.2.

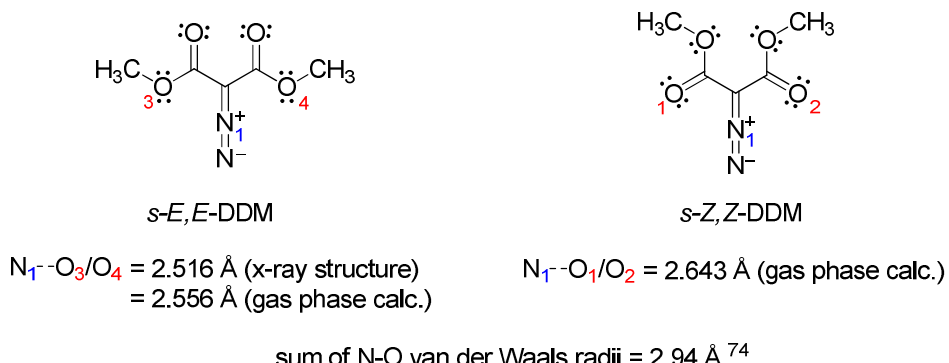
Scheme 2.2. Conformations of DDM.



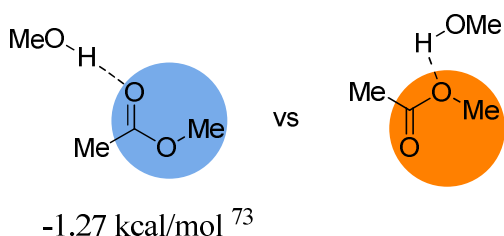
In the solid state, DDM adopts the *s-E,E* conformation. Based on low-temperature NMR experiments with diethyl diazomalonate (DEDM), and on gas-phase DFT/MP2 calculations on DDM,⁷² the *s-E,E* conformation of α -diazodicarbonyl compounds has been suggested to be the least favored conformation in solution. However, in α -diazoketones and esters, it has been suggested that bulky alkyl groups attached to either the ketone carbonyl carbon or attached to the ester oxygen (-OR) can stabilize the *s-E,E* conformation relative to the other two.⁷² One wonders if the *s-E,E* conformation observed for DDM arises because the methyl groups are bulky substituents, or because of crystal packing forces.

In DDM, intramolecular Coulombic attraction between electron rich centers and N1, which has a formal positive charge, might arise from either the carbonyl oxygens (O1/O2 in the *s-Z,Z* conformation) or the ester's "ether" oxygen (O3/O4 in the *s-E,E* conformation). From the x-ray crystal structure of DDM, (*s-E,E*-conformer), has an average distance of 2.516 Å between N1 and O3/O4 which is 0.040 Å shorter than the gas phase optimized *s-E,E*-conformer obtained from DFT [B3LYP/6-311+G(3df,2p)] calculation (2.556 Å)⁷² (see Chart 2.2). The average distance between N1 and (O1/O2) for a gas phase optimized DFT [B3LYP/6-311+G(3df,2p)] calculation of DDM *s-Z,Z*-conformer is 2.643 Å⁷² (see Chart 2.2).

Chart 2.2. Intramolecular Coulombic attraction in DDM conformers.



In both *s*-*E,E* and *s*-*Z,Z* conformers of DDM the N-O distances are shorter than the sum of N-O van der waals distance (2.94 Å).⁷⁴ Also preference of the ester's ether oxygen for Coulombic attraction over the carbonyl oxygen is noted which is contrary to reported nucleophilicity of ester's oxygens as donor groups. From calculations, it has been reported that intermolecular H-bond in its optimum geometry is only slightly stronger when formed to carbonyl oxygen than to an ester's ether oxygen as shown below.⁷³



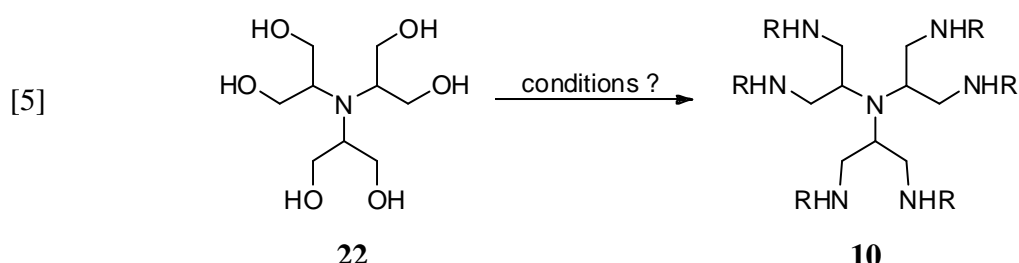
The N-H insertion reaction of DDM into **17** with a catalyst loading of 1 mol% gave compound **20** with a yield of 69%. Crystals of **20** were obtained from the slow evaporation of a solution of **20** in ethyl acetate at rt. X-ray crystallography gave the structure (see Appendix 1).

Reduction of amine diester **20** with three-fold excess lithium aluminium hydride (LiAlH_4), gave amine diol **21** with a yield of 94%. Recrystallization of **21** gave crystals whose structure was obtained through X-ray crystallography (Appendix 7). The next step, deprotection of the acetonide groups of **21**, could be accomplished with either crude or purified **21**. Treatment of diol

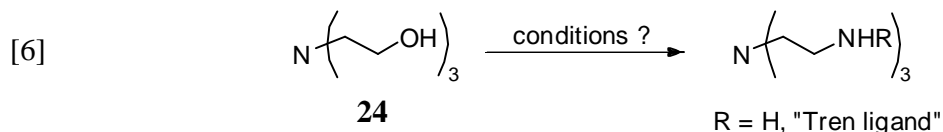
21 with trifluoroacetic acid (TFA) followed by ion exchange purification gave amine hexaalcohol **22**.

2.2. STRATEGY 1. Introduction of N-alkyl groups at the end of the synthesis of **22**.

The initial plan was to search for the optimal conditions that would convert all six alcohol functions in **22** to secondary amines, as shown below in eq [2].



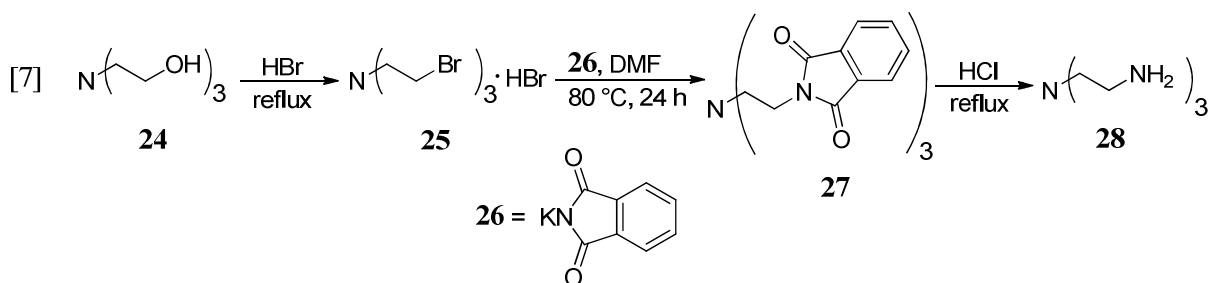
But based on the insolubility of **22** in common organic solvents and the expense involved in its synthesis, triethanolamine **24** was chosen as a model for **22** since it is a commercially available reagent and soluble in medium-polarity organic solvents. Equation [6] shows the model reaction, the conversion of triethanolamine to a tri-N-alkylated “tren” ligand.



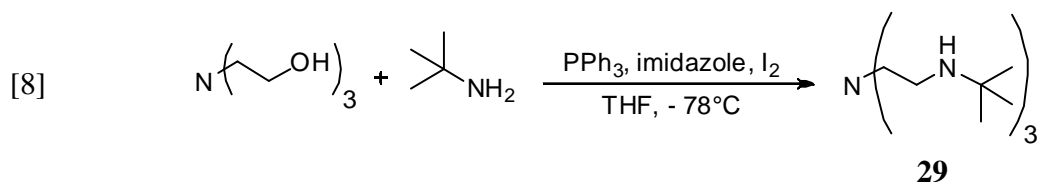
2.2.1. Traditional method of converting a primary alcohol to amine.

Synthesis of **28** can be attempted by first converting the three primary alcohols of **24** into an alkyl trihalide, followed by reaction with a phthalimide and finally hydrolysis of the product. Compound **24** was refluxed in 48% aq HBr¹¹ to give salt **25**³⁷ with 60% yield, which was used without further purification, to react with three equivalents of potassium phthalimide **26** in DMF to give an intractable white solid **27** (eq. [7]). Efforts at dissolving **27** in any deuterated solvent

for NMR analysis were futile. The solid had a high mp, 225-227 °C (lit. 183 °C).³⁸ This made it more suspect, since impurities usually lower the mp. In the spirit of joyful forward progress to obtain **28**, whose characterization is well supported in the literature, hydrolysis of **27** was carried out by refluxing it in conc HCl. That treatment yielded a colorless solid whose mp was greater than 320 °C.

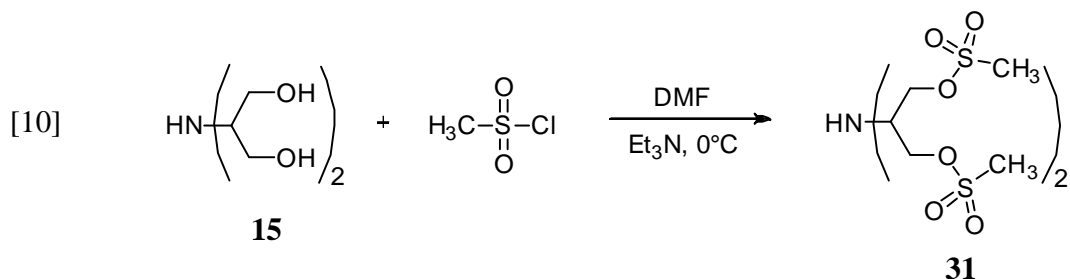
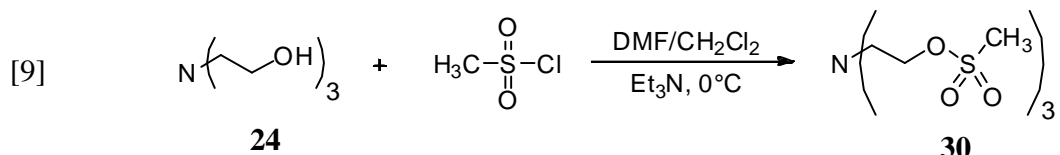


Based on our objective of replacing alcohol groups with secondary amine groups, **54** would have to undergo a successful triple alkylation *e.g.* reductive amination afterwards. With this in mind, a one pot synthesis of **55** without isolating the intermediate trihalide compound was performed on **50** with triphenylphosphine, iodine, imidazole and *tert*-butylamine (eq. [8]).⁶² Unfortunately, the use of stoichiometric amounts of the reagents as well as iodine made monitoring the reaction progress by TLC a daunting task. The reaction was quenched after 12 h with satd. aq. NaS₂O₃, followed by extraction to give an inseparable mixture of products (on TLC).



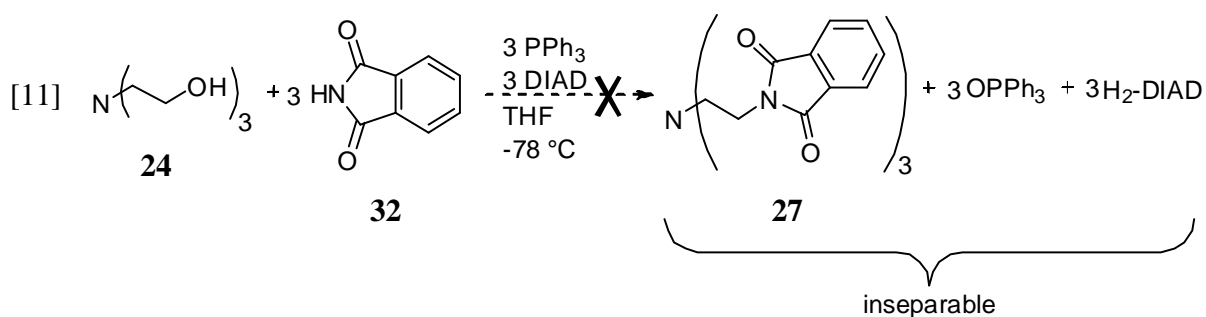
Next, attention was focused on trying to convert each -OH group of **24** to a good leaving group that would undergo an S_N2 reaction with an amine nucleophile. Synthesis of **30** and **31** by reacting triethanolamine **24** or tetraol **15** with mesyl chloride in DMF were met with inseparable

mixtures in both cases (eqs. [9] and [10]). Using methylene chloride as the solvent, as in eq. [9], didn't give a successful result either.



2.2.2. Direct conversion of alcohol to amine via Mitsunobu reaction.

The Mitsunobu reaction is a versatile reaction that has been widely used successfully to replace alcohols by amine functional groups.²² Synthesis of **27** was once again targeted under Mitsunobu conditions *i.e.* triphenylphosphine (TPP) and diisopropyl azodicarboxylate (DIAD) with phthalimide **32** as shown in eq. [11]. This gave an inseparable mixture.

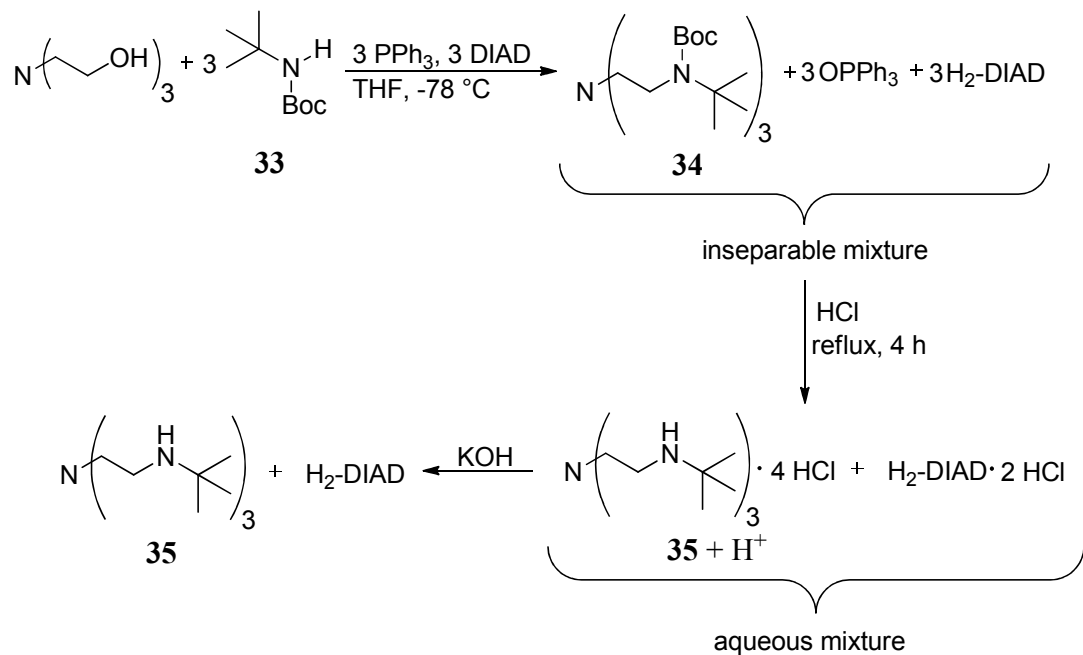


The main disadvantage of the Mitsunobu reaction that has discouraged its utilization is the use of stoichiometric amounts of TPP and DEAD (or a derivative *e.g.* DIAD) in the reaction, which yields equal by-product amounts of triphenylphosphine oxide (TPPO) and reduced DEAD (H₂-DEAD) that makes the work-up process messy and challenging. Significant progress has

been made in use of other derivatives of TPP and DEAD whose by-products can be easily separated (*e.g.* filtered off) to ease tedious chromatographic work-up.²⁶⁻²⁸

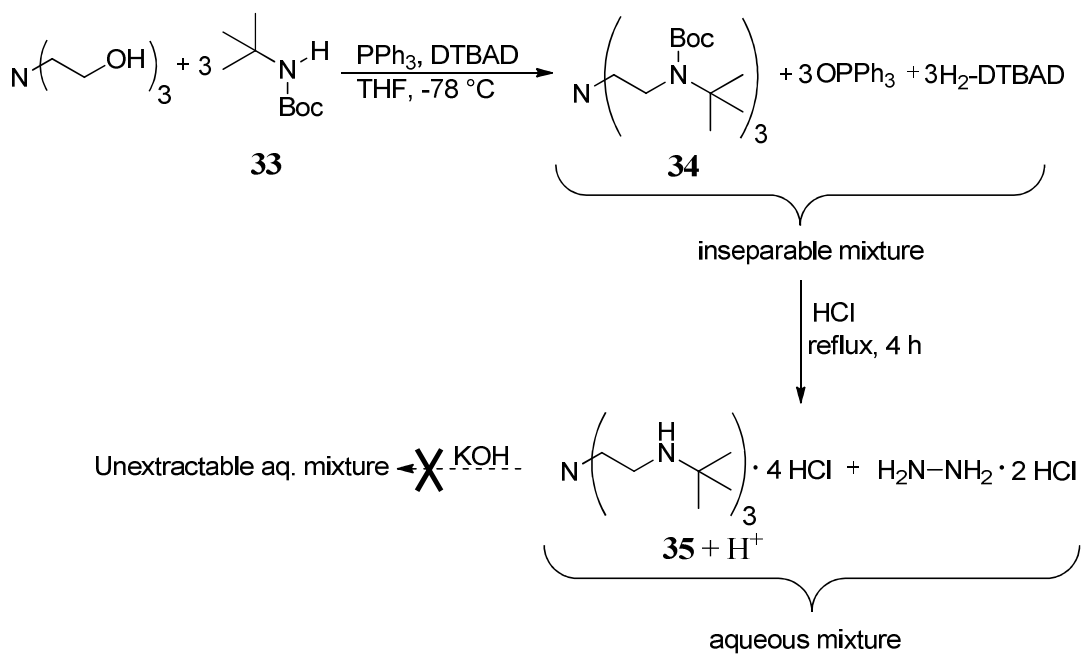
In eq. [11] the use of a three equivalents of **32**, TPP and DIAD made isolation of one equivalent (at most) of **27** from a mixture containing three equivalents each of TPPO and H₂-DIAD clearly impractical. To overcome this challenge, phthalimide **32** was replaced with Boc-protected *tert*-butylamine **33** to obtain compound **34** and the associated byproducts under Mitsunobu conditions as indicated by Scheme 2.3. Treatment of this mixture with HCl served two purposes; (*i*) to cleave the protecting groups and (*ii*) to obtain the HCl salt of **35** in the aqueous layer. Upon extraction of the acidified mixture with CH₂Cl₂, which removed only TPPO, we obtained aqueous mixtures of protonated **35** and protonated reduced DIAD (H₂-DIAD·HCl). KOH treatment of the concentrated aq. mixture followed by CH₂Cl₂ extraction, gave a chromatographically inseparable mixture of **35** and H₂-DIAD.

Scheme 2.3. Work-up of Mitsunobu reaction with DIAD.



To solve the protonation of H₂-DIAD in the acidified work-up of compound **35**, use of a different DEAD derivative is required. Di-*tert*-butyl azodicarboxylate (DTBAD), a DEAD derivative, has been used successfully to ease the work-up procedures of Mitsunobu reactions. Its reduced by-product (H₂-DTBAD) readily decomposes to gaseous by-products (CO₂, C₄H₈) and hydrazine on treatment with mineral acids *e.g.* HCl.⁹ Synthesis of compound **35** was repeated using DTBAD, the reaction mixture was treated with HCl, and TPPO removed by extracting with CH₂Cl₂. The concentrated aq. mixture was treated with 50% KOH but the product could not be extracted with any organic solvent. Hence synthesis of an isolable **35** with this method was not achieved (Scheme 2.4).

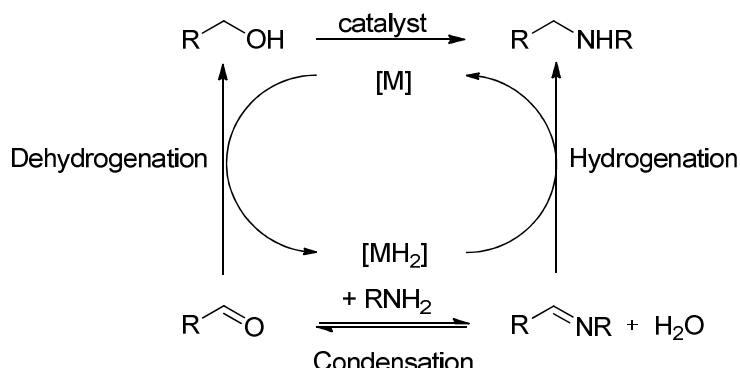
Scheme 2.4. Work-up of Mitsunobu reaction with DTBAd.



2.2.3. Use of “borrowing-hydrogen” methodology to convert alcohols to secondary amines.

Borrowing-hydrogen methodology is a relatively new synthetic technique. It is illustrated in Scheme 2.5 for the conversion of an alcohol RCH_2OH to an amine RCH_2NHR .

Scheme 2.5. Borrowing-hydrogen methodology.

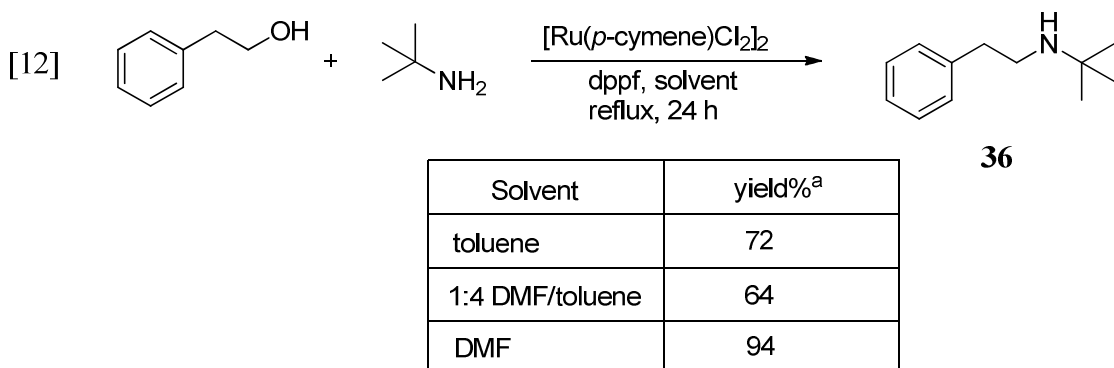


The metal catalyst M “borrows” H_2 from the alcohol, giving an aldehyde intermediate and MH_2 . The aldehyde may undergo various transformations, such as imine formation as in Scheme 2.5, or Wittig reaction, for example. The catalyst then returns the “borrowed” H_2 to the product of the aldehyde transformation. In the example in Scheme 2.5, the imine is reduced to an amine, which corresponds overall to replacement of $-\text{OH}$ by $-\text{NHR}$.

The main advantage of this strategy is loss of water as a by-product that makes this reaction both “green” and atom economical.⁶³

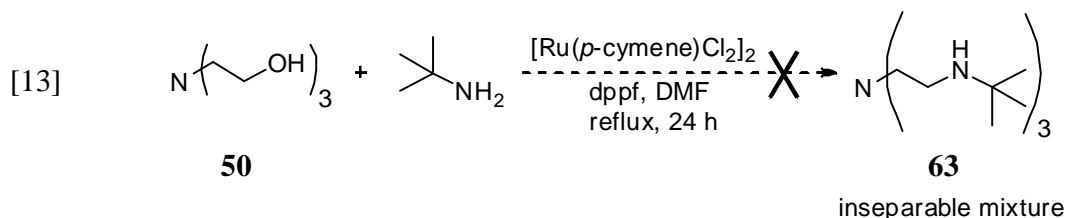
Synthesis of compound **36** from 2-phenylethanol and *tert*-butylamine in a sealed reaction tube was replicated in our lab as described in Williams *et al.*^{64a} using $[\text{Ru}(\text{p-cymene})\text{Cl}_2]_2$ and dppf in catalytic amounts and various solvents (eq. [12]). Using toluene as the solvent, Williams and coworkers achieved an 88% yield. We got a 72% conversion. DMF gave the best conversion: 94%. This was surprising in two ways: DMF, a polar aprotic solvent has never been

used for this reaction, and, secondly, under our reaction conditions, DMF gave the best conversion.



^a yield determined by $^1\text{H-NMR}$ integration of **36** relative to 2-phenylethanol

Armed with this exciting result, effort was put to extend this reaction to synthesize **63** from triethanolamine **24** and *tert*-butylamine under similar conditions, as shown in eq. [13]. This gave a mixture of compounds as evidenced by a complicated NMR spectrum and a chromatographically inseparable mixture (several spots on TLC). Cyclized^{64b} and incompletely aminated products may possibly exist in this mixture.



2.3. Introduction of a synthetic route incorporating N-alkyl groups.

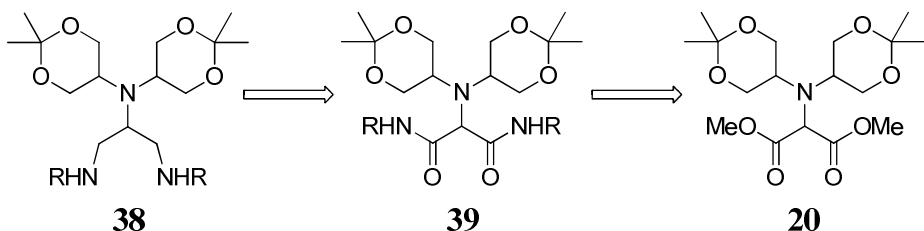
The lack of clear success in replacing *three* OH groups of **50** with N-alkyl groups as we have described gave us reason to conclude that replacing *six* OH groups in **49** (*i.e.* Strategy 1) would be even harder. Therefore, two new strategies were pursued: (*i*) Strategy 2: Introduction of N-

alkyl groups to an intermediate appearing along the synthetic path to **22**, and (ii) Strategy 3: Designing a new synthetic route that would incorporate N-alkyl groups from the beginning.

2.3.1. STRATEGY 2. Introduction of N-alkyl groups to an intermediate appearing along the synthetic path to **22**.

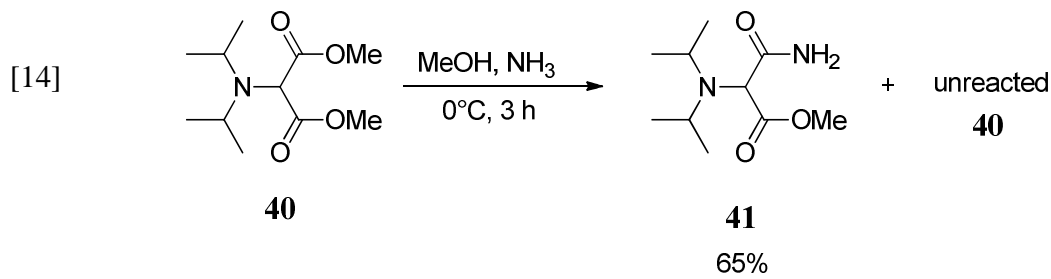
Along the synthesis of **22** (see Scheme 7), an intermediate diester **20** was synthesized. Aminolysis of the ester groups of **20** could give diamide **39**, whose reduction would furnish **38** and hence achieve the feat of introducing two secondary amines, as shown by the retrosynthetic analysis of Scheme 2.6.

Scheme 2.6. Retrosynthesis of **38**.

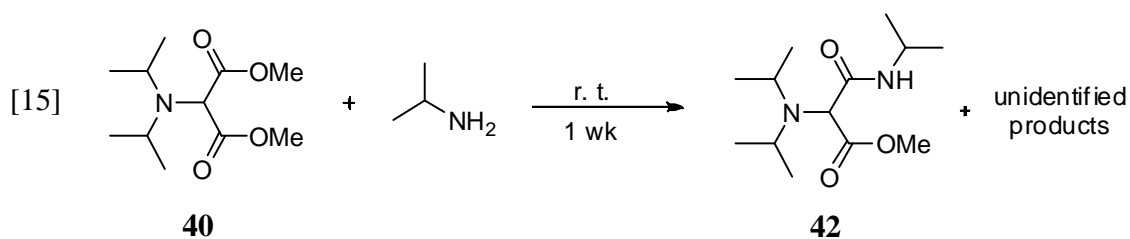


2.3.1.1. Aminolysis of amino diesters.

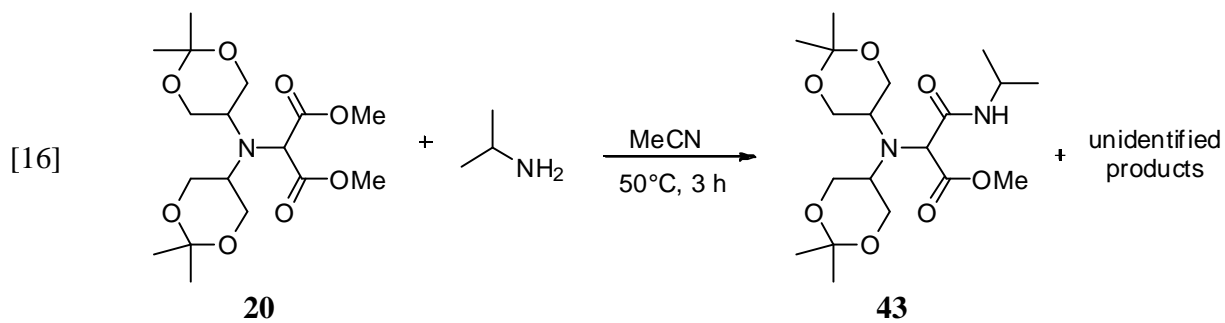
To attempt this hypothesis, dry ammonia gas was bubbled through a cooled solution of diester **40** in methanol for three hours (eq. [14]) to yield the monoaminated product **41** with a yield of 65% relative to starting material **40** (determined by ¹H-NMR integration). This monoaminated product could arise from two possibilities; incomplete aminolysis or formation of an enolate under basic conditions on one of the ester groups.



To circumvent the incomplete aminolysis problem, ammonia was replaced by isopropylamine, a liquid at rt that can be precisely measured to guarantee at least two equivalents relative to diester **66**. Longer reaction time was used to ensure reaction went to completion. A mixture of **66** and six equivalents of isopropylamine as solvent was stirred at rt under N₂ for 1 week to yield a complicated mixture (multiple spots on TLC) of **68** with other unidentified products (as per careful ¹H and ¹³C NMR analysis of the concentrated crude reaction mixture) as in eq. [15].

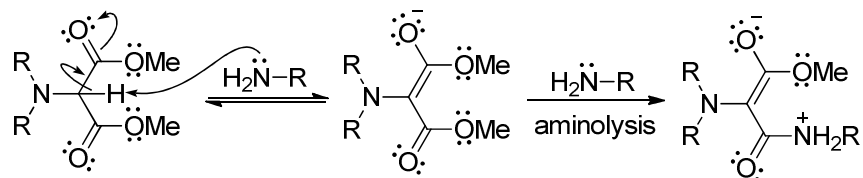


Likewise the reaction of **20** with excess isopropylamine in acetonitrile at 50 °C for 3 h gave a mixture of **69** and unidentified products (eq. [16]).



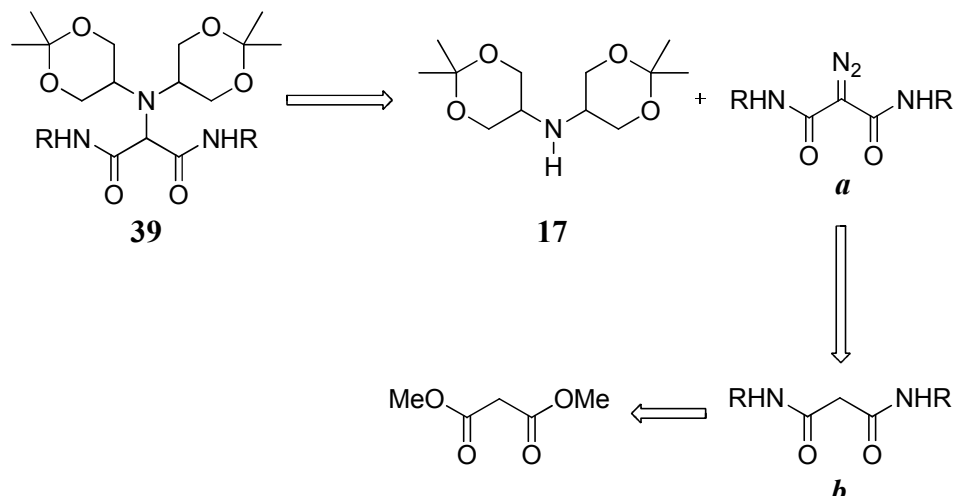
With these results, enolate formation, formed by abstraction of the acidic proton between the ester groups of amino malonates **20** and **40** under basic conditions as shown in Scheme 2.7, seems the most probable cause that prevents the desired double aminolysis.

Scheme 2.7. Enolate formation.



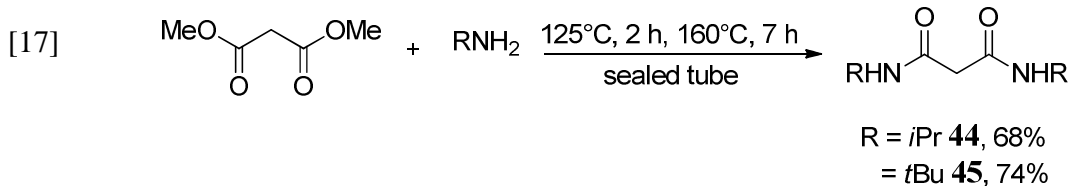
To overcome this setback we rationalized as shown in Scheme 2.8, that diamide **39** could be obtained from the commercially available dimethyl malonate through synthesis of two intermediates; malonamide (**b**) and diazomalonamide (**a**).

Scheme 2.8. Retrosynthetic analysis of diamide **39**.



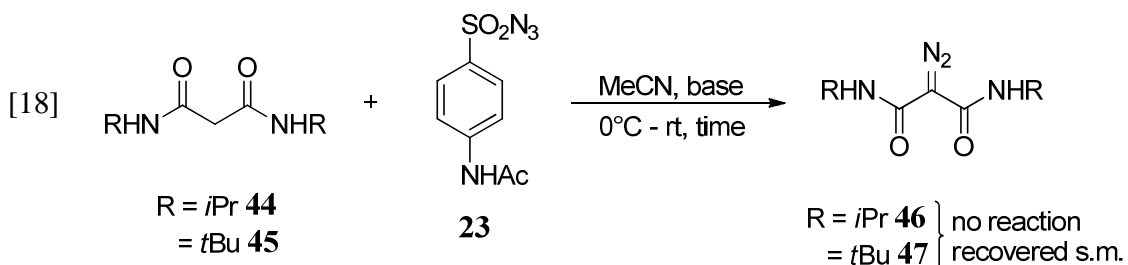
2.3.1.2. Aminolysis of dimethyl malonate.

Malonamides **44** and **45** were synthesized through aminolysis of dimethyl malonate with isopropylamine and *tert*-butylamine respectively in a modified solvent-free technique involving heating in a sealed tube at high temperatures to give moderate yields of 68% and 74% respectively as shown in eq. [17].



2.3.1.3. Synthesis of diazo malonamides.

With malonamides **44** and **45** in hand, synthesis of diazomalonamide would involve a diazo transfer reaction (eq. [18]) similar to that used to prepare DDM **19**. Replicating the exact conditions used in the DDM case, synthesis of diazo malonamide **46** (entry 1) was unsuccessful and starting materials were recovered. By varying base and reaction time none of the diazomalonamide **46** and **47** were obtained (entries 2-4).

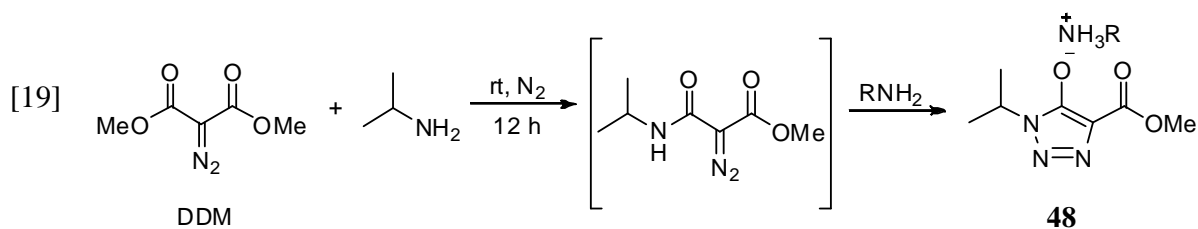


	R	Base	Time
1	<i>i</i> Pr	NEt ₃	16 h
2	<i>i</i> Pr	DABCO	16 h
3	<i>i</i> Pr	DABCO	3 wk
4	<i>t</i> Bu	DABCO	3 wk

2.3.1.4. Aminolysis of DDM.

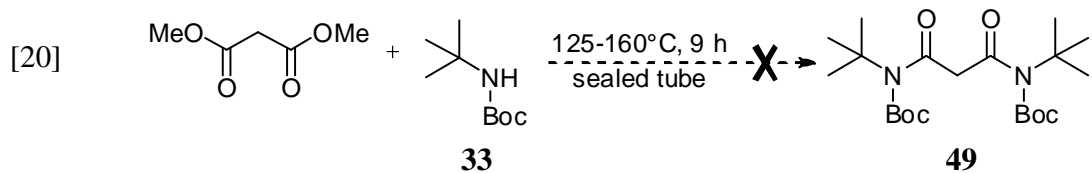
Unsuccessful synthesis of diazomalonamide via diazo transfer led us to attempt an alternate route via aminolysis of DDM with isopropylamine at rt (eq. [19]). The reaction precipitated a white solid with a mp >220 °C (dec) and soluble only in polar solvents (DMSO, DMF, *n*-BuOH

at rt and MeCN at 60 °C). Structure of solid **48** was deduced from NMR data ($\text{DMSO}-d_6$ solvent) and also from the reported reaction of DDM with primary amines that yield alkylammonium salts of 5-hydroxy-1,2,3-triazoles (eq. [19]).⁶⁵ Extension of this triazole formation lends insight to the failed synthesis of diazomalonamide via diazo transfer.



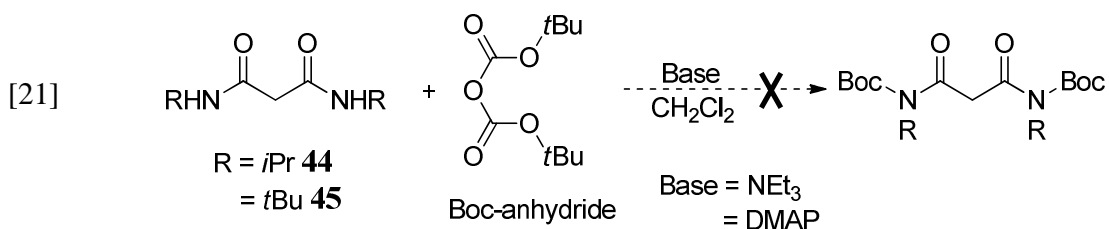
2.3.1.5. Aminolysis of dimethyl malonate with Boc-protected *tert*-butylamine.

Led by literature reports of examples of amide N-H carbenoid insertions,⁶⁸ synthesis of **39** would require protected diazomalonamide before insertion into **17** and equally the protection aids in the diazo transfer reaction by preventing formation of a triazole. To achieve this, aminolysis of dimethyl malonate with **33** to give protected malonamide **49** (eq. [20]) was carried out but with no success, though starting material was recovered.



2.3.1.6. Protection of malonamide N-H with Boc group.

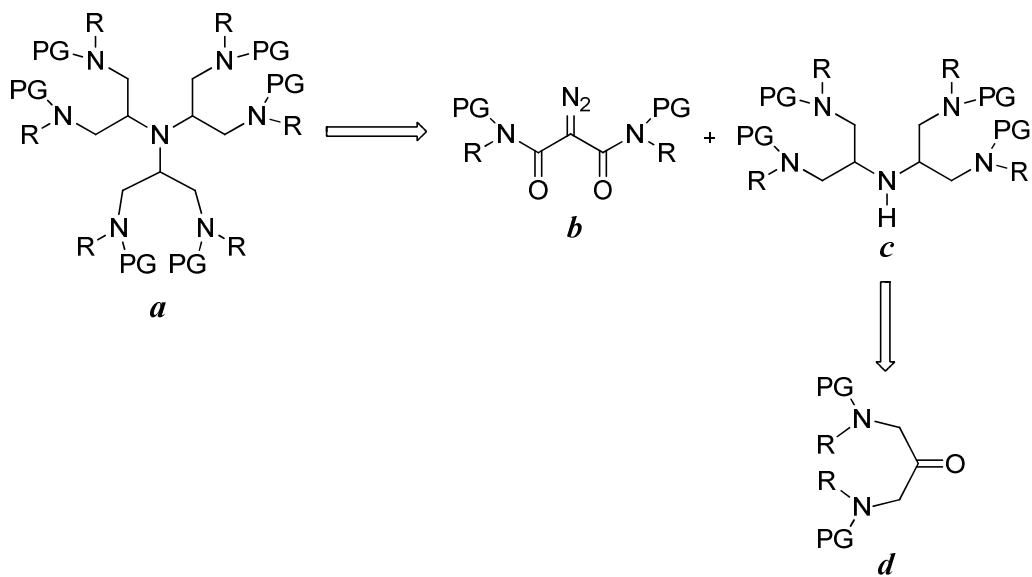
In a display of desperate curiosity, and while being aware of the potential problems caused by the presence of acidic CH₂ protons, an attempt was made, nonetheless, to protect the N-H groups of malonamides **44** and **45** (eq. [21]) with Boc groups. The reaction did not work.



2.3.2. STRATEGY 3. Introduction of N-alkyl groups at the beginning of the synthetic path.

In keeping with the wisdom of not trying to “reinvent the wheel”, inspiration from some main steps in the synthesis of amine hexaalcohol **22** were incorporated in the design of a new synthetic scheme, as shown in Scheme 2.9.

Scheme 2.9. General retrosynthesis of new synthetic route beginning with N-alkyl groups, STRATEGY 3.



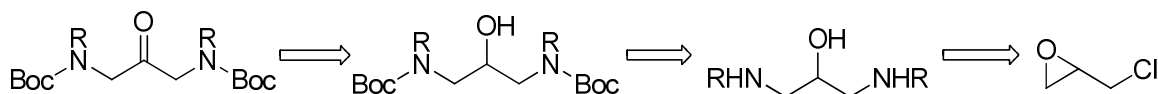
The main general reactions extended from synthesis of **22** to this design are as follows; (*i*) double reductive amination of a ketone with N-alkyl groups, **d**, to form secondary amine **c**, (*ii*) a

diazomalonamide, **b**, carbenoid insertion to give a protected tertiary amine **a**, and finally (*iii*) removal of the protecting groups.

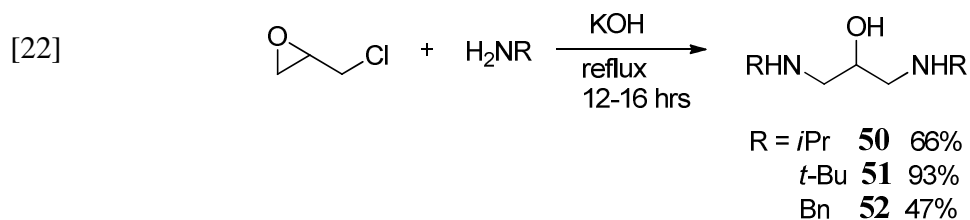
2.3.2.1. Synthesis of a protected N-alkylated ketone.

Synthesis of a ketone analogous to dihydroxyacetone dimer for reductive amination can be achieved using the retrosynthesis in Scheme 2.10, starting with commercially available epichlorohydrin.

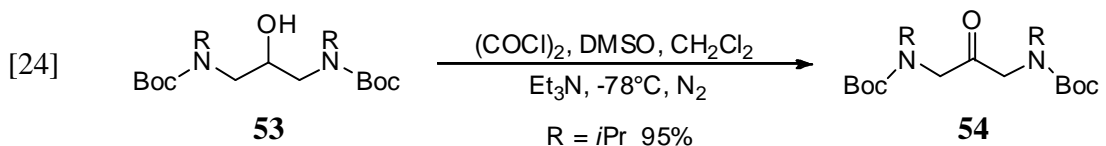
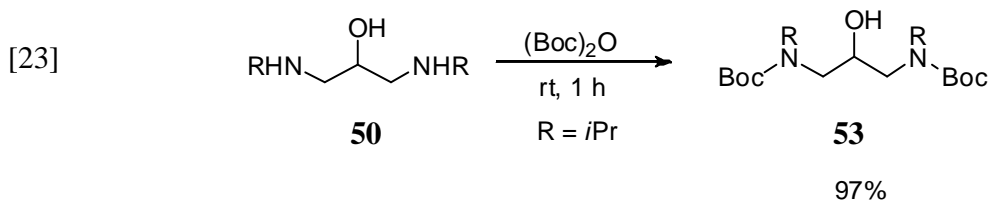
Scheme 2.10. Retrosynthesis of a ketone with protected N-alkyl groups.



Using a reported method,⁷⁰ alkylated 1,3-diamino-2-propanols **76**, **77** and **78** were easily prepared through reactions of epichlorohydrin with primary amines. Isopropylamine, *tert*-butylamine and benzylamine respectively in sealed tubes were reacted with KOH and epichlorohydrin under reflux as in eq. [22].



To protect the amino groups of alkylated 1,3-diamino-2-propanols a newly reported “solvent free” Boc protecting methodology⁴⁰ was employed in the synthesis of **53** (eq. [23]). Reaction time was short and work-up was easy, affording a 97% yield of **53**. ¹H-NMR peaks were broad, and **53** was used without further characterization to synthesize ketone **54**. Swern oxidation of **53** gave ketone **54** with a yield of 95% (eq. [24]).



In characterizing this new ketone **54**, we were once again amazed with the broad peaks in its ¹H-NMR spectrum. We suspected that some sort of dynamic effect might be in operation in CDCl₃ solvent. Therefore, the probe temperature was raised from 293 K (rt) to 323 K (50 °C) and experiments performed. ¹H and ¹³C-NMR spectra are shown in Figs. 2.4 and 2.5.

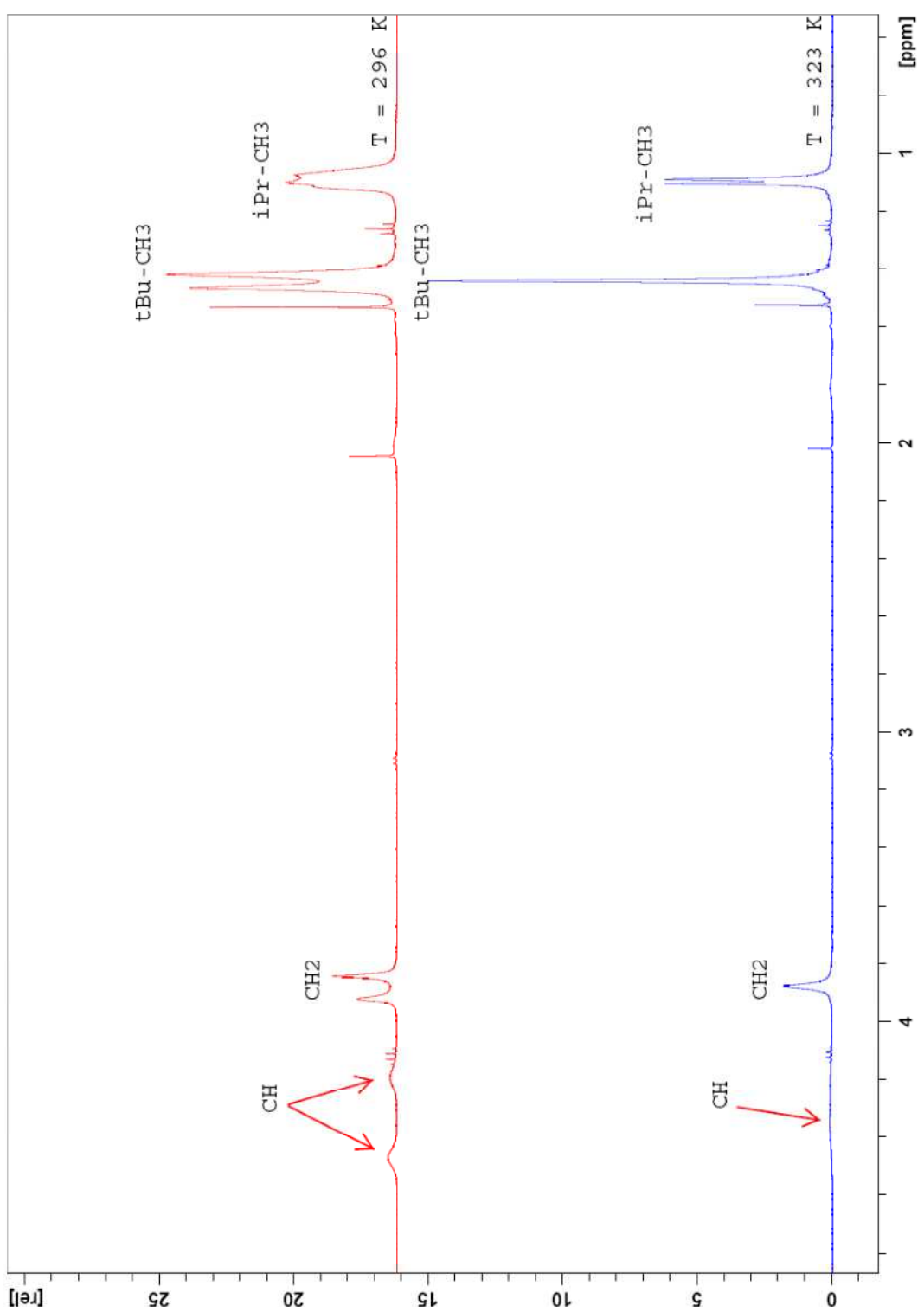


Figure 2.4. ¹H-NMR spectra of ketone **54** at $T = 296\text{ K}$ (red) and at $T = 323\text{ K}$ (blue).

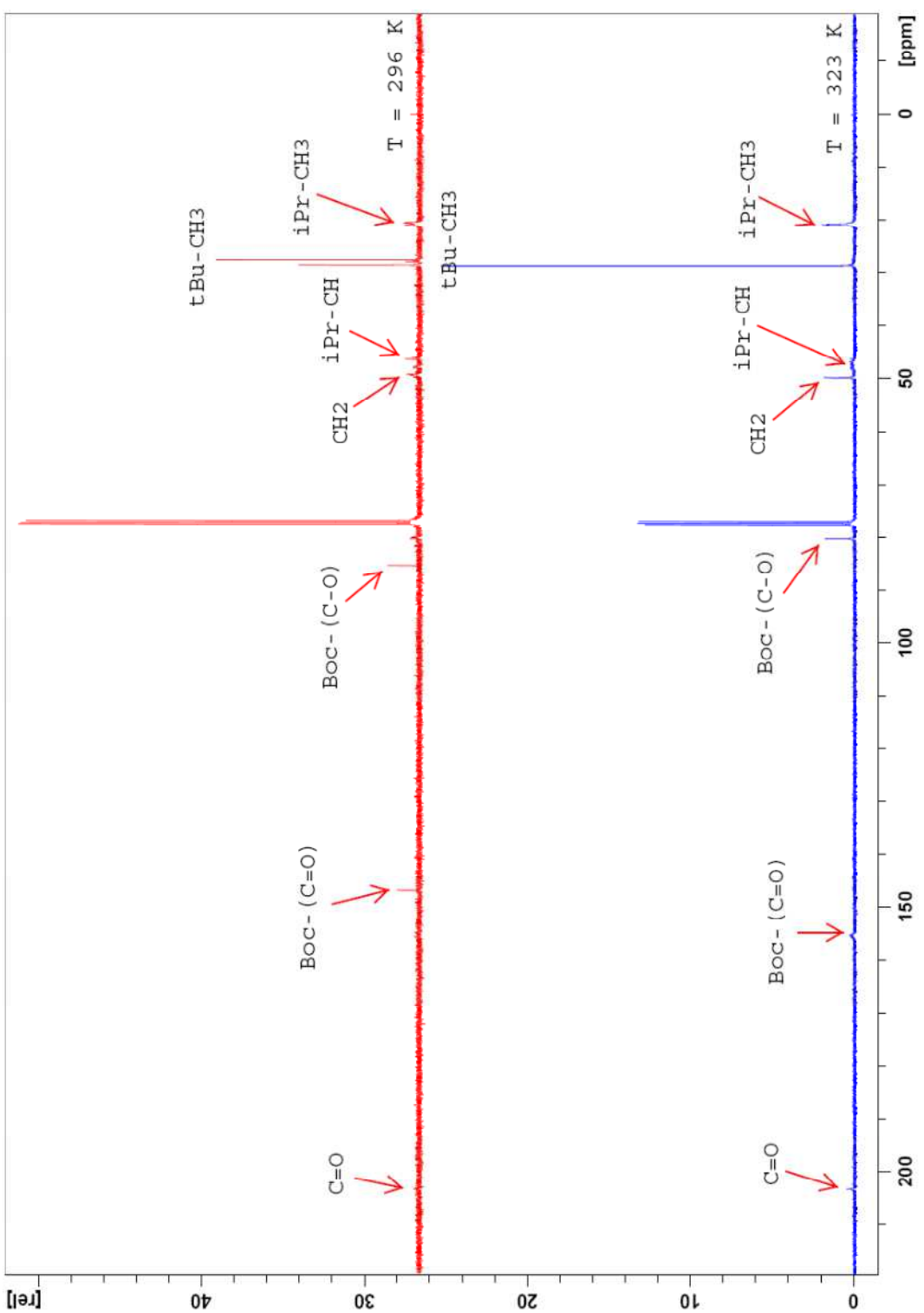


Figure 2.5. ^{13}C -NMR spectra of ketone **54** at $T = 293\text{ K}$ (red) and at $T = 323\text{ K}$ (blue).

At 323 K, the ^1H -NMR spectrum was well resolved with the exception of the isopropyl methine proton peak that is too weak. On the other hand, in the ^{13}C -NMR spectrum all carbon peaks were well resolved with the exception of the Boc group carbonyl and methine carbon of isopropyl group both attached to nitrogen.

2.3.2.2. Double reductive amination of ketone **54** ($d \rightarrow c$ in Scheme 10).

Double reductive amination of ketone **54** under various reactions conditions (entries 1–4 in Table 2)⁶⁰ to obtain **55** was unsuccessful (eq. [25]).

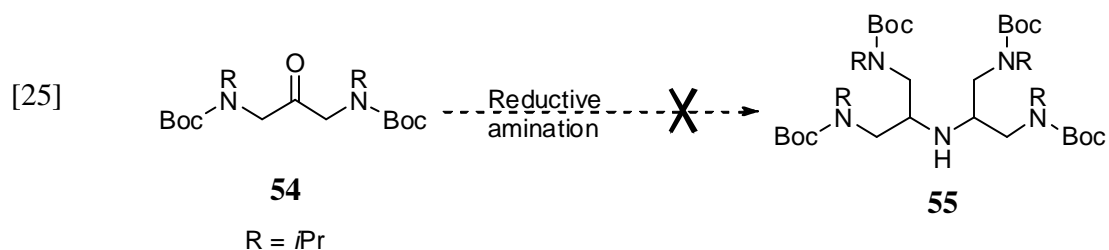


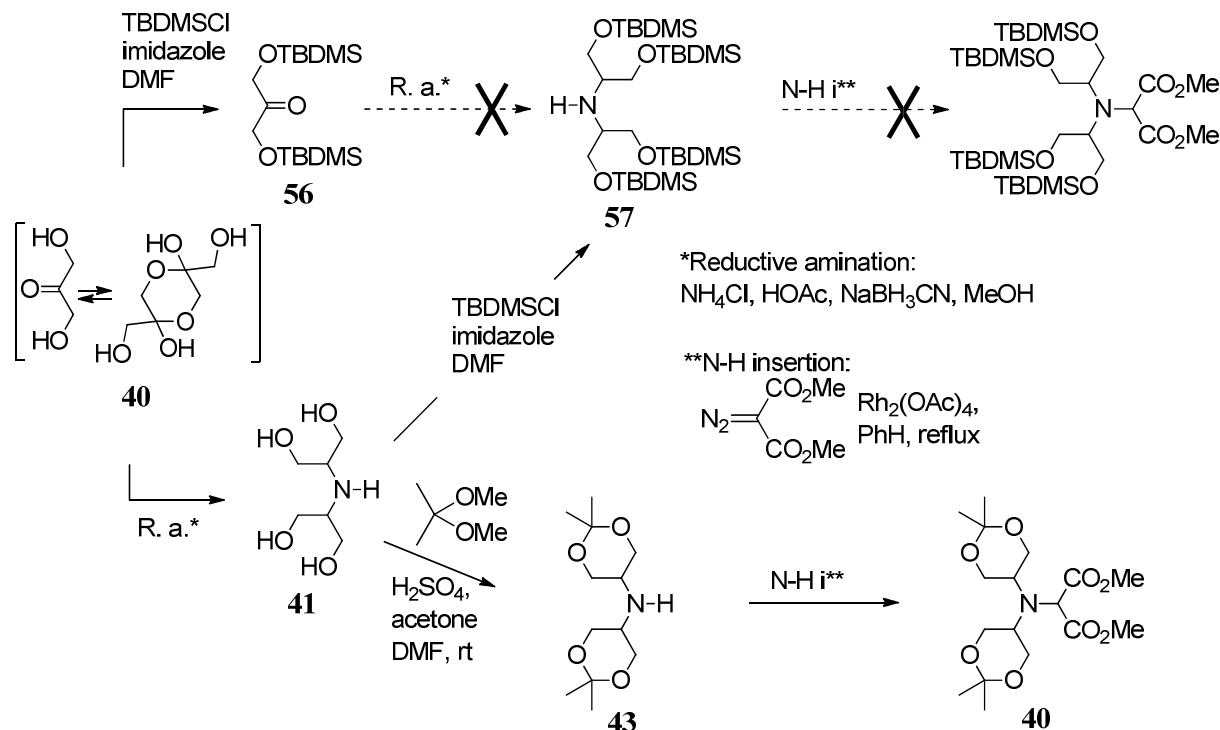
Table 2.2. Room temperature double reductive aminations.

Entry	Solvent	Acetic Acid	Reducing agent	Amine Source	Time
1	MeOH	–	NaBH ₃ CN	NH ₄ Cl	72 h
2	MeOH	+	NaBH ₃ CN	NH ₄ Cl	20 h
3	MeCN	–	NaBH(OAc) ₃	NH ₄ Cl	72 h
4	MeCN	–	NaBH(OAc) ₃	NH ₄ OAc	48 h

In order to understand and offer an explanation of our inability to synthesize secondary amine **55** by reductive amination, it was noticed from Jie's earlier efforts on synthesizing amine hexaacohol **22** (Scheme 2.11)^{35a} that secondary amine synthesis was achieved from a ketone with

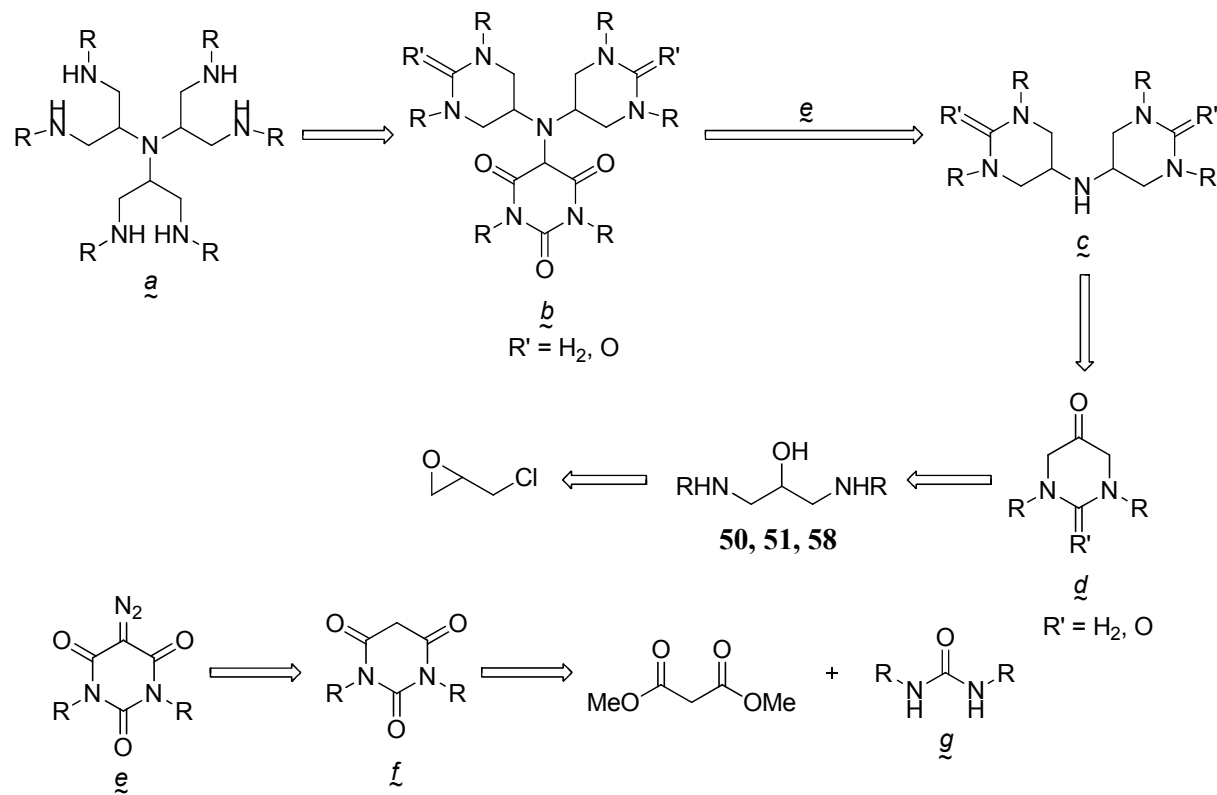
less bulky substituents (**40** compared to **56**) and also the insertion reaction favored less bulky cyclic protected groups compared to the bulky acyclic ones (**17** compared to **57**).

Scheme 2.11. Jie's efforts towards synthesis of **22**.^{35a}



In the synthesis of spermidine, a polyamine similar to our targeted heptamine, formaldehyde and carbonates have been used as protecting groups for N-alkyl-1,3-diamino moieties as aminals and urea respectively in a cyclic fashion.⁶⁶ Therefore the synthetic route to heptamine was modified as shown by the retrosynthesis in Scheme 2.12.

Scheme 2.12. Modified retrosynthesis to introduce N-alkyl groups, according to STRATEGY 3.

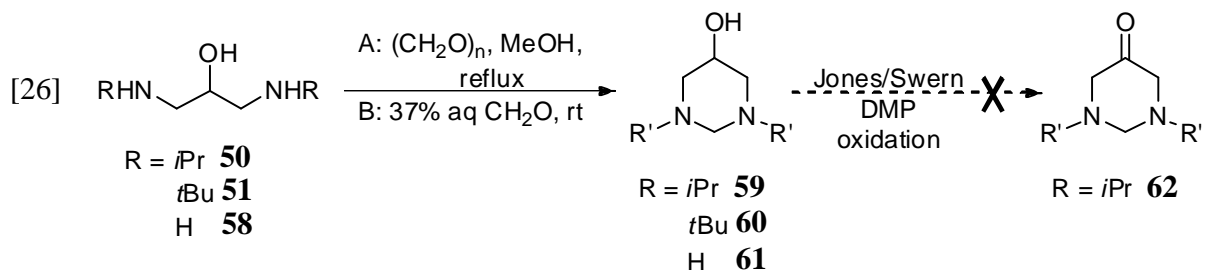


The main modification is the cyclic protection in both the starting ketone **d** and diazo compound **e** as urea or aminals. We will refer to these as “heterocyclically protected.” This route also gives a heterocyclically protected diazo compound, **e**, obtained through a two step synthesis involving **f** and **g**. Deprotection of **b** to give the final target compound **a** would entail either the reduction or basic hydrolysis of ureas, and hydrolysis of aminals.

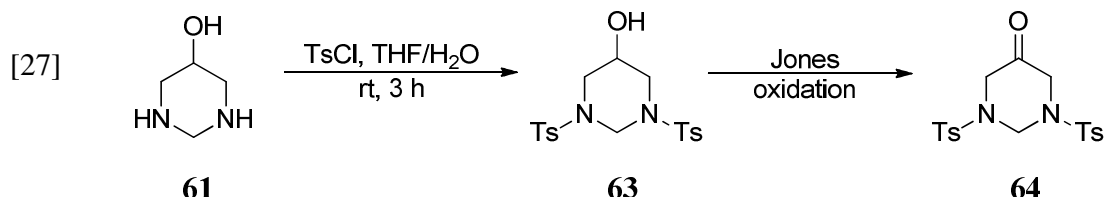
2.3.2.3. Synthesis of heterocyclically protected ketones with N-alkyl groups.

N-Alkyl-1,3-diamino-2-propanol **50**, **51** and **58** (eq. [26]) were either reacted with paraformaldehyde in refluxing MeOH (procedure A), or stirred at rt with 37% aq. formaldehyde (procedure B).⁴⁴ Diaminoalcohols **50** and **58** gave hexahydropyrimidines **59** and **61** in 99% and 65% yields, respectively. Diaminoalcohol **51** led to a product mixture from which **60** could not be isolated for both procedures A and B. Several oxidation procedures (*e. g.* Jones, Swern and

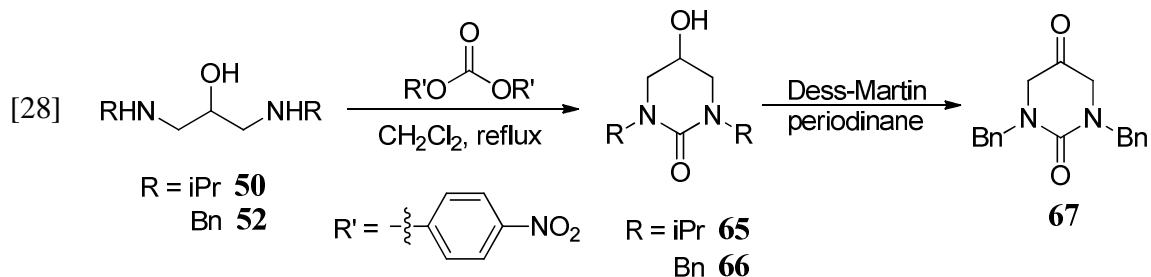
Dess-Martin periodinane) were employed in the attempt to synthesize ketone **62**, but all were unsuccessful, and only under Dess-Martin conditions was the recovery of starting material made.



To oxidize **61**, protection of the N-H group was required, and was done using tosyl chloride to give **63** in 54% yield. Oxidation of **63** to **64** under Jones conditions gave a relatively low yield of 54% compared to the reported yield 76% (eq. [27]).⁴⁴



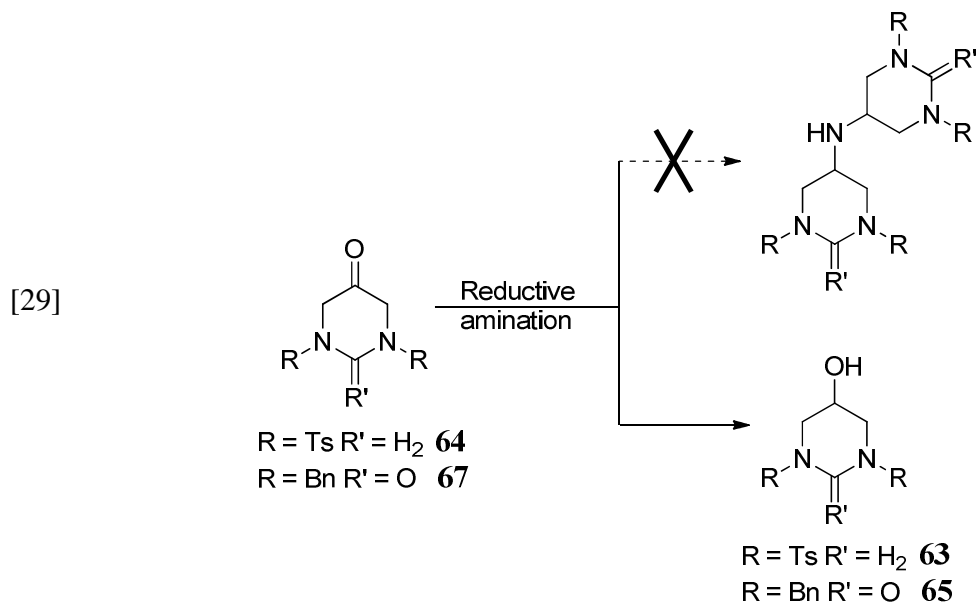
Referring to Scheme 2.12, we could obtain only one example of *d* with $R' = H_2$, *viz.* ketone **64**. Inclined to be on the cautious side, effort was directed towards the synthesis of a urea protected ketone (Scheme 2.12, *d*, $R' = O$) using a published method.⁴⁵ Refluxing of **50** and **52** with bis(4-nitrophenyl) carbonate (eq. [28]) gave the heterocyclically protected ketones **65** and **66** in 14% and 92% yields respectively.⁴⁵ With the low yield of **65**, only oxidation of **66** was performed under Dess-Martin conditions to give ketone **67** in 84% yield.



2.3.2.4. Double reductive amination of heterocyclically-protected ketones **64**

and **67**.

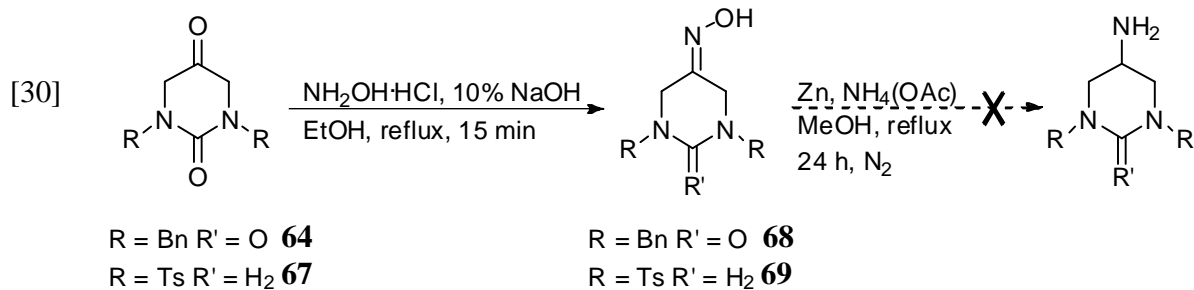
Reductive amination reactions,⁶⁰ were carried out for **64** and **67** using sodium triacetoxyborohydride in neutral conditions with both ammonium acetate and benzylamine as amine sources. These reactions gave neither primary nor secondary amines. Rather, the ketones were reduced to alcohols **63** and **65** as in eq. [29].



In order to understand the failures depicted in eq [29], validation of ketones' **64** and **67** ability to form imines was attempted with the synthesis of their corresponding oximes. These could be reduced to primary amines and used as an amine source for a more efficient mono reductive amination.

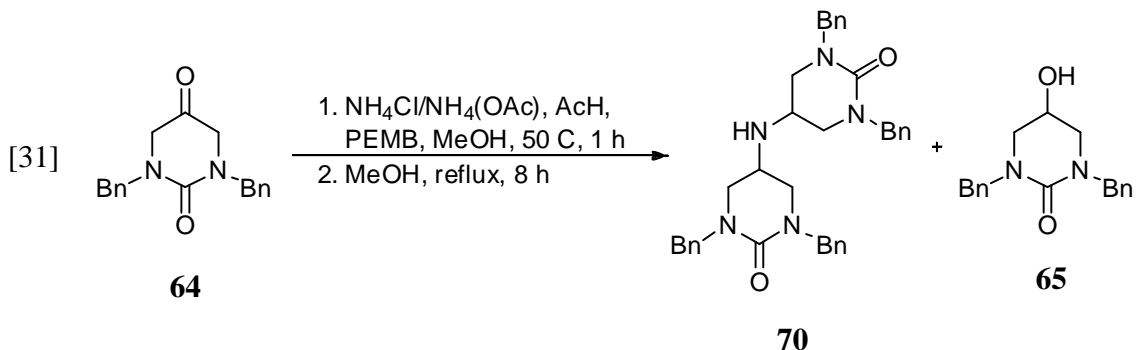
2.3.2.5. Oxime synthesis from ketones **64** and **67**.

The reactions of hydroxylamine hydrochloride with ketones **64** and **67** gave oximes **68** and **69** in 72% and 87% yields (eq. [30]).⁴⁸ Reduction of these oximes **68** and **69** using zinc metal and ammonium acetate was not successful.



2.3.2.6. Double reductive amination of **90** with PEMB.

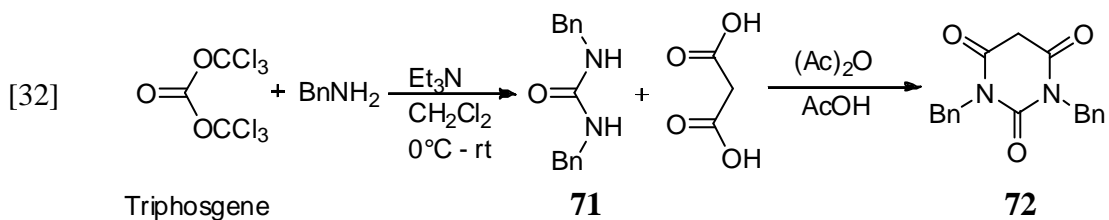
The most commonly employed reductive amination reducing agents are sodium cyanoborohydride (NaBH_3CN) and sodium triacetoxyborohydride [$\text{NaBH}(\text{OAc})_3$]. Recently Coleridge and co-workers,⁵² have reported 5-ethyl-2-methylpyridine borane (PEMB), a new reducing agent for reductive aminations. Reductive amination of **64** under acidic conditions with ammonium acetate and PEMB at 55 °C gave secondary amine **70** with a yield 5.31% and **65** (67%) was recovered (eq. [31]).



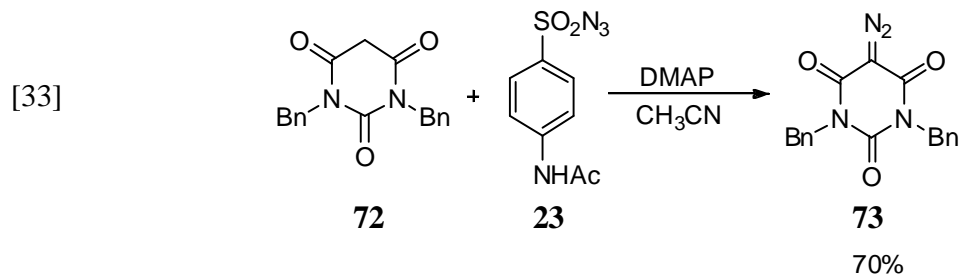
With PEMB double reductive amination was achieved in getting secondary amine **70** even though in very low yield. The main product of this reaction was the reduced ketone **65** that could be oxidized and therefore recycled to obtain more of amine **70**. This “double reductive amination” reaction seems to be an inefficient route to synthesize secondary amines, especially when the starting ketone is not readily available. By contrast, dihydroxyacetone dimer, used in the synthesis of **15**, is commercially available. In the synthesis of **15**, the monomer of dihydroxyacetone dimer **14** was also reduced to glycerol.^{35a}

2.3.2.7. Synthesis of diazobarbiturate 73.

Using reported literature methods in the synthesis of disubstituted barbiturates, dibenzyl barbiturate **72** was synthesized in two steps (eq. [32]): the reaction between triphosgene and benzyl-amine gave dibenzylurea **71**⁴⁹ and the condensation of **71** with malonic acid⁵⁰ gave **72** with an overall yield of 84% for the two steps.



Employing the diazo transfer reaction previously used to synthesize DDM, dibenzyl barbiturate **98** was used to synthesize its diazo derivative **73** (eq. [33]). Triethylamine used as a base in the DDM reaction was replaced with DMAP⁵² in this reaction.

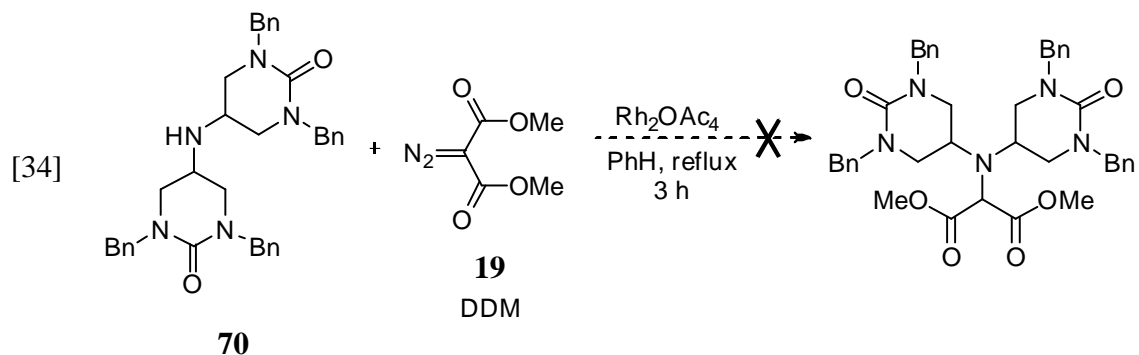


2.3.2.7. Rhodium catalyzed N-H insertions.

Synthesis of sterically hindered trialkylamines using rhodium-catalyzed insertions of carbenoids into the N-H bonds of secondary amines has been developed and studied in our lab.³⁴ Prior to attempting the insertion of diazo compound **73** into amine **70**, insertion reactions were performed separately with other reagents as follows:

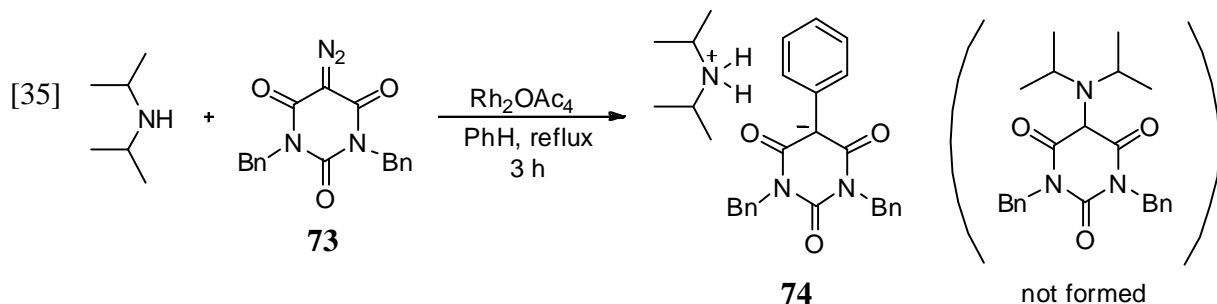
(a) Reaction of secondary amine **70** with DDM.

The N-H insertion reaction of amine **70** with DDM **19**, in benzene didn't give the insertion product as in eq. [34]. The solution turned red and **70** was recovered. The significance of the red color will be discussed shortly.



(b) Reaction of diazo barbiturate 73 with diisopropylamine.

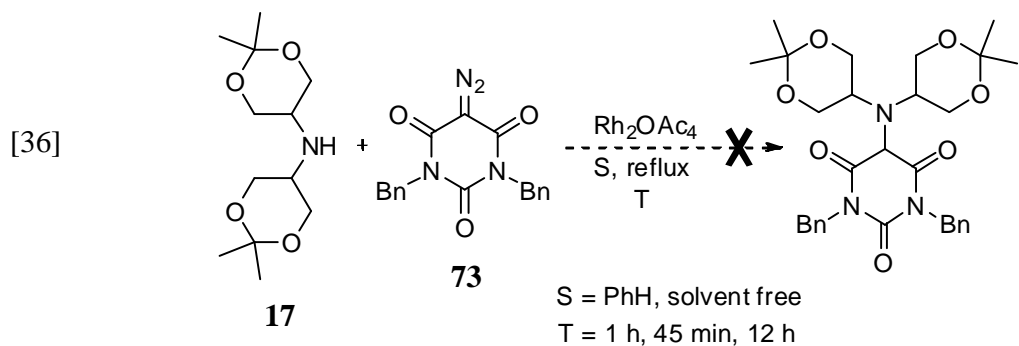
The N-H insertion reaction of **73** with diisopropylamine (eq [35]) didn't give the insertion product, but instead formed **74** even though the solution turned red. Carbenoid insertion into solvent (benzene) has been reported.



previously by Yang,³⁴ hence obtaining **74**, a salt of the insertion product of **73** with benzene with diisopropylamine wasn't surprising, even though it was unanticipated. The fact that the product of insertion into solvent was the sole product means that the desired N-H insertion process is extremely sluggish.

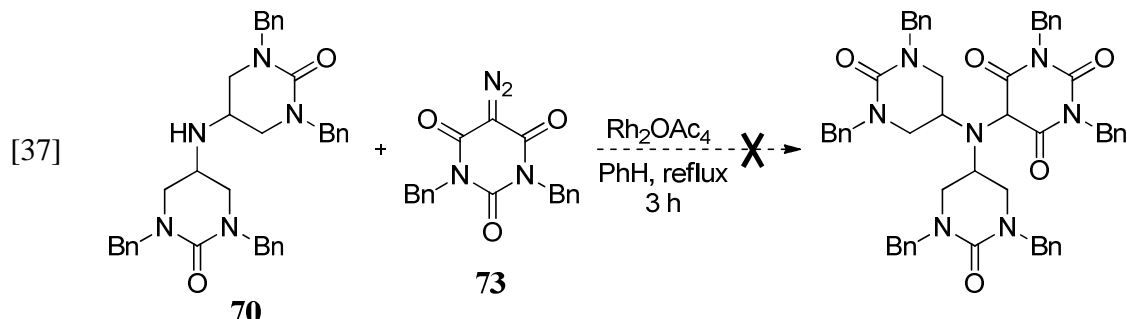
(c) Reaction of diazobarbiturate 73 with 17.

The N-H insertion reaction of **73** with **17** never gave the insertion product irrespective of using solvent or not as well as varying the reaction time as in eq. [36]. The reaction mixture turned red in all cases.



(d) Reaction of amine 70 with diazobarbiturate 73.

The reaction of amine **70** with **73** was carried out in refluxing benzene for 3 h and didn't yield the N-H insertion product as in eq. [37]. The solution turned red and both **70** and **73** were recovered.



In each of the cases just discussed, (a)-(d), the reactions turned red, which indicates that the rhodium catalyst has been poisoned.⁶⁵ Poisoning of $\text{Rh}_2(\text{OAc})_4$ has been reported to occur when sterically uncongested amines - *e.g.* primary amines^{65a} and diallylamine³⁴ - form complexes (red color) with the catalyst, effectively turning off all catalytic activity.

The rate of catalytic decomposition of diazo compounds depends on the presence or absence of adjacent carbonyl groups, and the type of adjacent carbonyl groups. Stabilities range from the least stable diazomethane to the most stable diazo amides, while reactivity is the opposite, as shown in Figure 2.6.

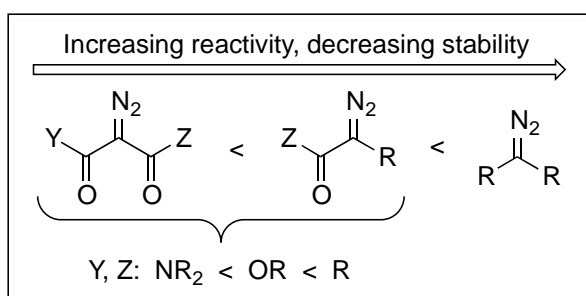


Figure 2.6. Stabilities and reactivities of diazo compounds.^{67a}

With this understanding about stabilities of diazo compounds, it is reasonable to assert that one way to make **73** more reactive would be to eliminate one adjacent carbonyl group. This leads to dibenzyl diazodihydrouracil (DDDU) with a single carbonyl (Figure 2.7). The synthesis and assessment of insertion chemistry of dibenzyl diazodihydrouracil was undertaken.

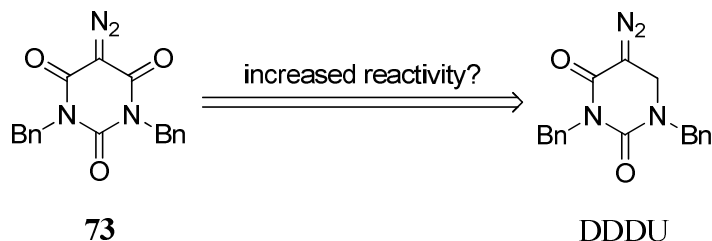
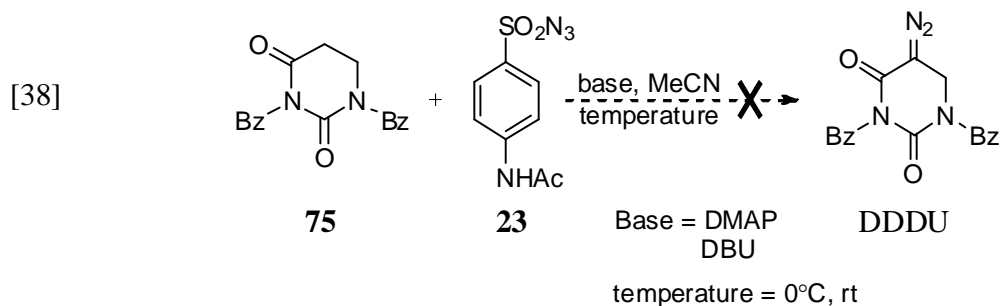


Figure 2.7. Stability and reactivity comparison of diazoamides **73** and DDDU.

2.3.2.7.1. Synthesis of diazo DDDU.

Utilizing a diazo transfer reaction similar to that used in DDM synthesis, **75** was reacted with **23** in the presence of various bases, as shown in eq. [38]. We had no success getting DDDU. At this time, several other routes to the target were being pursued, and we decided to focus our efforts elsewhere, rather than trying to get the reaction of eq [38] to work.



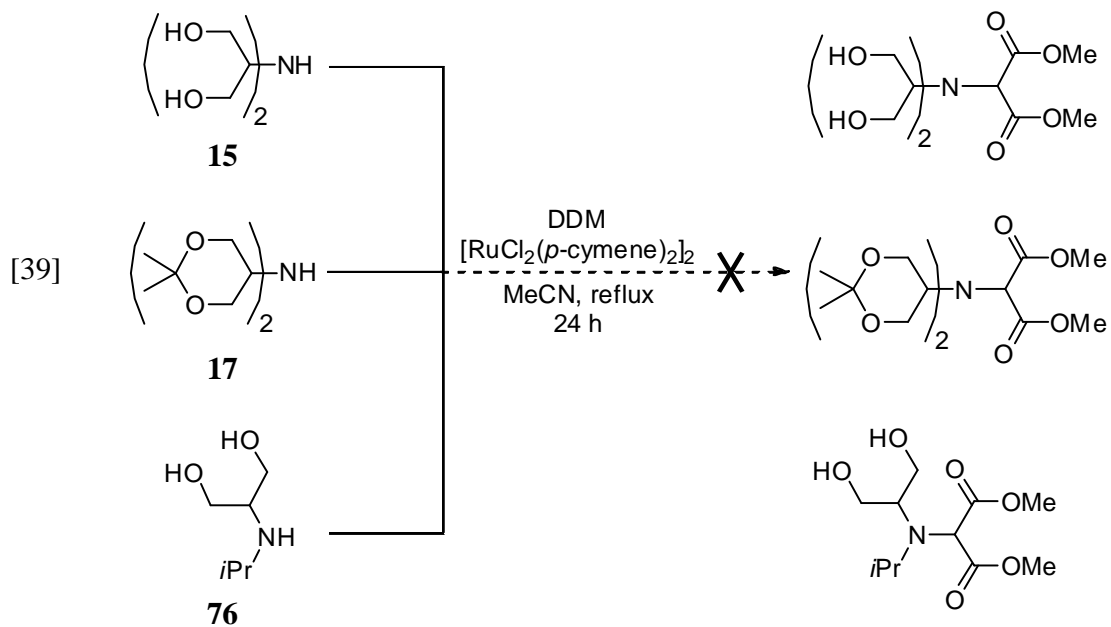
It became obvious that the most reliable catalyst known in our lab for carbenoid insertion into sterically congested amines, $\text{Rh}_2(\text{OAc})_4$, was not the suitable catalyst for the insertion reaction of diazobarbiturate **99** with amine **96**. Also, one wonders whether amine **96** is so sterically congested around nitrogen that N-H insertion is impossible.

2.3.2.8. Screening of a new catalyst for N-H insertions.

Recently Deng and coworkers⁵⁸ reported a ruthenium catalyst, $[\text{RuCl}_2(p\text{-cymene})]_2$, that can be used in the catalytic decomposition of a diazo compound for carbenoid N-H insertion in presence of MeOH with undetected O-H insertion. There exist very few examples with ruthenium as a catalyst in carbenoid reactions, and when used, the reactions are known to require longer times.^{67a} The following reactions were performed to investigate N-H insertion catalysis by $[\text{RuCl}_2(p\text{-cymene})]_2$:

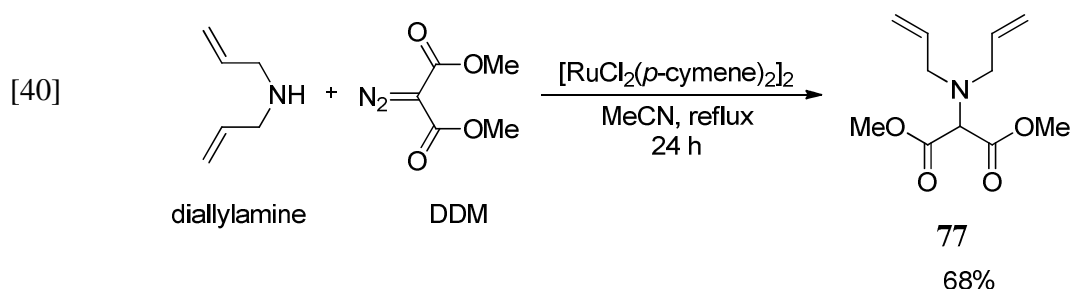
(a) $[\text{RuCl}_2(p\text{-cymene})]_2$ catalyzed N-H insertion of sterically hindered amines.

Amines **15**, **17** and **76** were refluxed with DDM and 1 mol% $[\text{RuCl}_2(p\text{-cymene})]_2$ for 24 h and no insertion product was obtained for these reactions (eq. [39]).



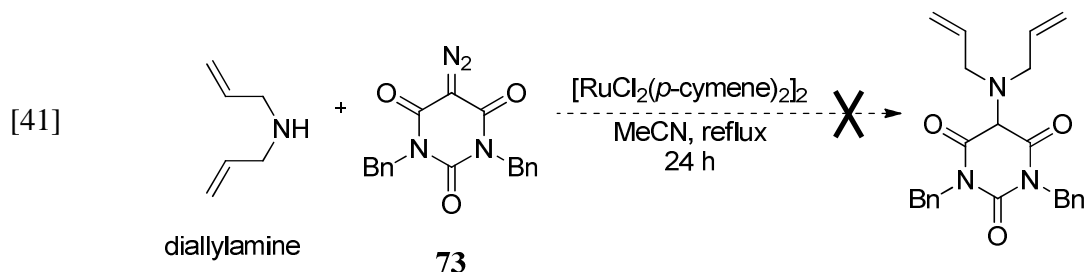
(b) $[\text{RuCl}_2(p\text{-cymene})]_2$ catalyzed N-H insertion of sterically unhindered amines.

DDM was successfully inserted into diallylamine, a sterically unhindered amine which is known to poison $\text{Rh}_2(\text{OAc})_4$,³⁴ when catalyzed with 1 mol% $[\text{RuCl}_2(p\text{-cymene})]_2$ (eq. [40]).



(c) $[\text{RuCl}_2(p\text{-cymene})]_2$ -catalyzed N-H insertion of diallylamine with 73.

Diallylamine was refluxed with **73** with a catalytic loading of 1 mol% $[\text{RuCl}_2(p\text{-cymene})]_2$ that gave mixture (several spots on TLC) with no insertion product (from NMR of mixture) (eq. [41]).



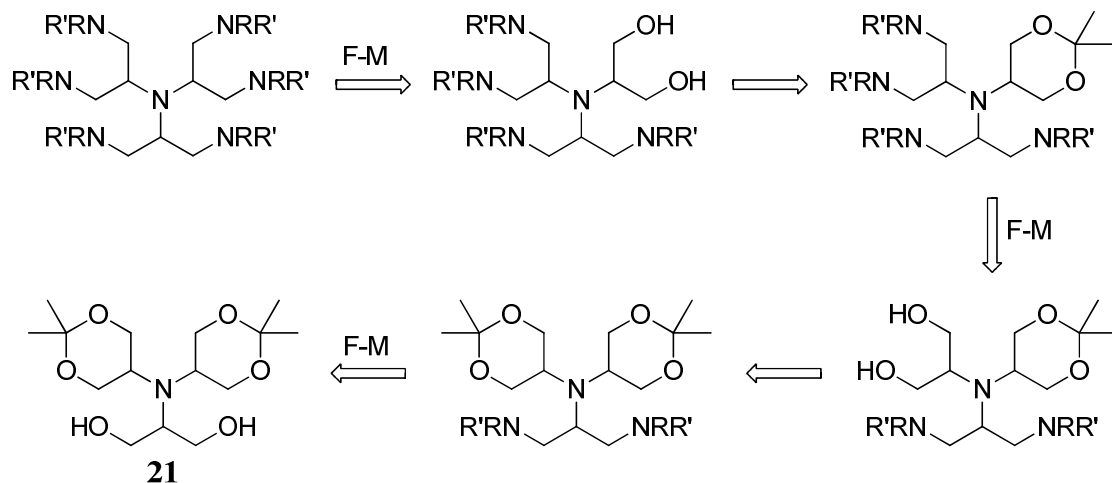
With ruthenium catalysis not working to our favor, the new synthetic route to the target heptamine, STRATEGY 3, couldn't be pursued further. In the event a better catalyst is identified and can be used efficiently for the decomposition of relatively stable diazo amides for carbenoid N-H insertions, this synthetic route may be viable.

2.4. STRATEGY 4. Double Fukuyama-Mitsunobu reaction.

After an exhausting whirlwind tour through the challenging exploratory synthesis of heptamine **30**, attention was reverted back to the synthesis of amine hexaalcohol **22**. Our earlier strategy was to convert all six OH groups of **22** to six N-alkyl groups in one step. It occurred to us that a more manageable plan would be to attempt the OH to N-alkyl conversions in smaller bites, for example one at a time or two at a time. Our inspiration for this idea came from noting that **22** is prepared *via* the precursor **21** (see Scheme 1), and that the two OH groups of **21** might be amenable to a double Fukuyama-Mitsunobu (F-M) reaction.⁹⁰ Revealing two more OH groups, converting them to N-alkyl groups via double F-M, and finally revealing the last two OH groups and converting them via double F-M, plus some manipulations of the groups on N, would afford the target. This is shown retrosynthetically in Scheme 2.13.

Scheme 2.13. Retrosynthesis involving double Fukuyama-Mitsunobu (F-M) reactions,

STRATEGY 4.



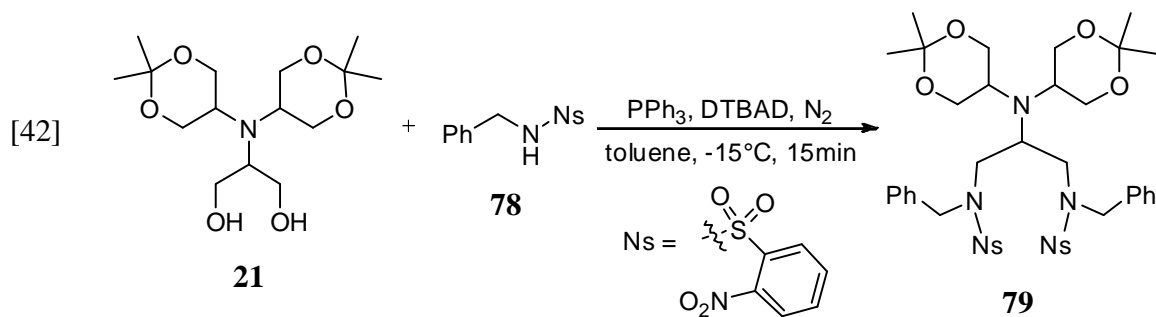
Hexaalcohol **22** is soluble only in very polar solvents, *e.g.* H₂O, or DMF at elevated temperatures (*ca.* 130 °C), making it a challenging compound to do organic reactions with. However **21** easily dissolves in most ordinary organic solvents, *e.g.* THF, CH₂Cl₂, or toluene. This increases

the chances that a standard Fukuyama-Mitsunobu reaction might be successful, and therefore a double F-M reaction might be successful. Other points supportive of the plan shown in Scheme 16, with emphasis on the possibility of the double F-M, are listed here:

- (a) Compound **21** is a compound whose synthesis is well established.
- (b) Compound **21** has one fewer OH group than triethanolamine (see section 2.2.2), therefore the work-up maybe less daunting chromatographically due to the stoichiometric amounts of TPP and DEAD reagents used.
- (c) The F-M protocol calls for the use of a nosyl (*o*-nitrophenylsulfonyl) group on the amine nitrogen (see below). The nosyl groups can be retained until the latter steps, and so provide protection of the amines already present while subsequent amines are added.
- (d) Sequential replacement of acetonide groups with nosylalkylamine groups or nosylarylamine groups would maintain or perhaps increase the solubility of the synthetic intermediates in ordinary solvents.

2.4.1. Fukuyama-Mitsunobu reaction of **21**.

Amine diol **21** was reacted with **78** under F-M conditions; TPP and DTBADM, in 15 min to give **79** in 69% isolated yield (eq. [42]).



This reaction was amazing in three ways: the short reaction time, the high yield, and the ease of work-up. The chromatographic separation was uncharacteristically clear. On TLC (silica gel), the reaction mixture displayed only three spots, with **79** having a yellow coloration. Therefore, when the reaction mixture was subjected to column chromatography, it was quite easy to trace the elution in a glass column, especially when the reaction was done in gram quantities. **79** is a foamy yellow solid that foamed rapidly to fill the flask as solvent was being removed under vacuum.

2.4.2. Attempted deprotection of only one acetonide group of **79.**

Deprotection of acetonides have commonly been done using either acids (e.g. HCl, TFA) though other catalytic methods have been successfully been used *e.g.* 1% I₂/MeOH³⁰ and DDQ/H₂O/MeCN⁹¹ *etc.* From literature, 1% I₂/MeOH and DDQ/H₂O/MeCN have been reported to deprotect a single acetonide in the presence of another acetonide by varying the conditions.⁹¹ Monodeprotection of diacetonide **79** was attempted by varying conditions and reagents (entries 1-6 in Table 2.3) with no success of isolating the monoacetonide diol as shown in eq. [43]. The reaction progress was monitored by both TLC and NMR.

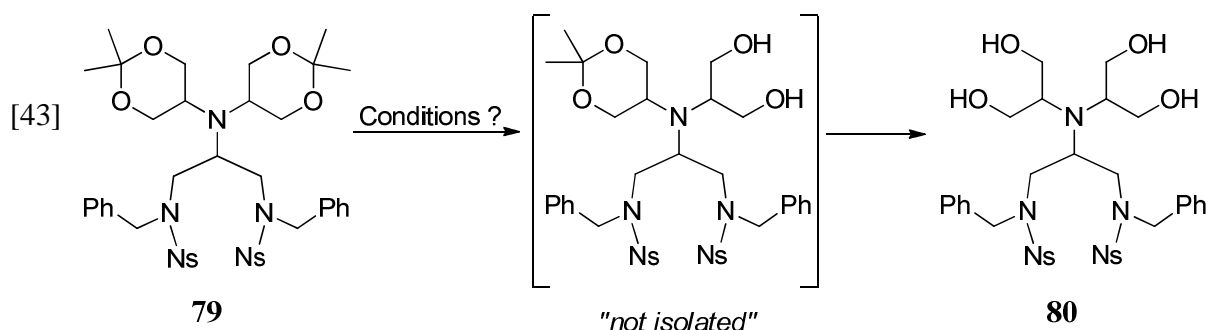
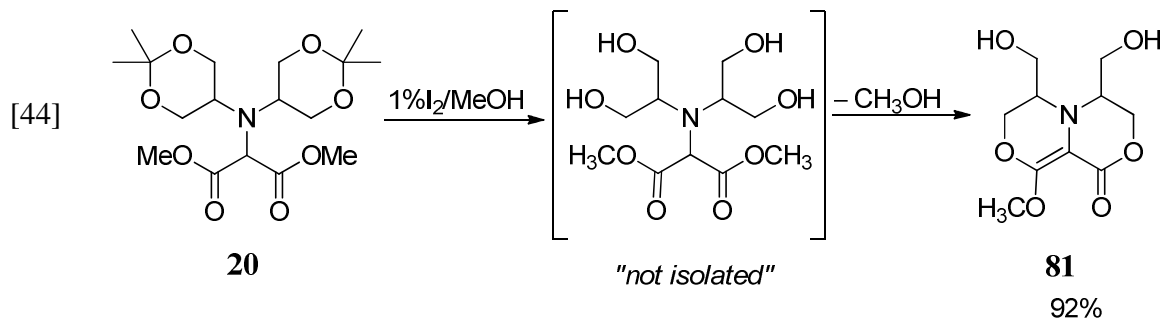


Table 2.3. Conditions of acetonide deprotection of **79**.

Entry	Conditions	Time
1	1% I ₂ /MeOH, rt ^a	12 h
2	1% I ₂ /MeOH, rt	4 h
3	0.5% I ₂ .MeOH-CH ₂ Cl ₂	4 h
4	DDQ, MeCN-H ₂ O (9:1), rt ^b	4 h
5	DDQ, MeCN-H ₂ O (9:1), 0 °C	9 h
6	DDQ, MeCN, 0 °C	6 h

^aref 30, ^bref 91

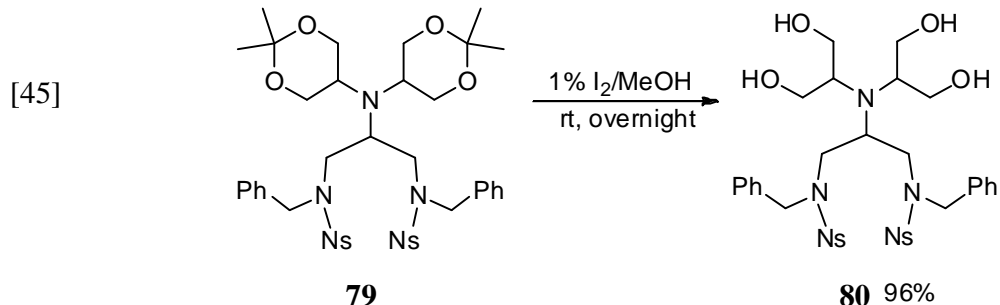
When **20** was used as model reaction for deprotection of one acetonide group using 1% I₂/MeOH (rt, 1 h), compound **81** was surprisingly obtained rather than the anticipated diol nor tetraol as shown in eq [44].



Unable to find optimal conditions for deprotection of a single acetonide group of **79**, the manageable systematic double F-M reaction strategy envisioned earlier (see section 2.4) was abandoned. Throwing caution to the wind, we decided to attempt a quadruple F-M reaction of tetraol **80** even though the 4:1 stoichiometry of TPP and DTBADD versus **80** was worrisome.

2.4.3. Acetonide deprotection of **79**.

Deprotection of acetonide groups of **79** was successfully achieved using a solution of 1% I₂/MeOH³⁰ to give amine tetraalcohol **80** in 96% yield (eq. [45]).



As initially hypothesized, **80** is soluble in non-polar organic solvents e.g. CH₂Cl₂ and toluene compared to amine tetraalcohol **15** which is only soluble in polar solvents e.g. MeOH, H₂O, DMF, etc.

2.4.4. Quadruple Fukuyama-Mitsunobu reaction of **80**.

Tetraalcohol **106** was reacted with nosylbenzylamine **78**, TPP, and DTBADM without any success as shown in eq. [46]. Varying stoichiometric amounts of F-M reagents (TPP, DTBADM and **78**), reaction time, and temperature, or substituting TPP with polymer-bound TPP (resin-TPP) to ease work-up by filtration of polymer-bound TPPO^{25, 27-29} never gave the desired product, as shown in Table 4.

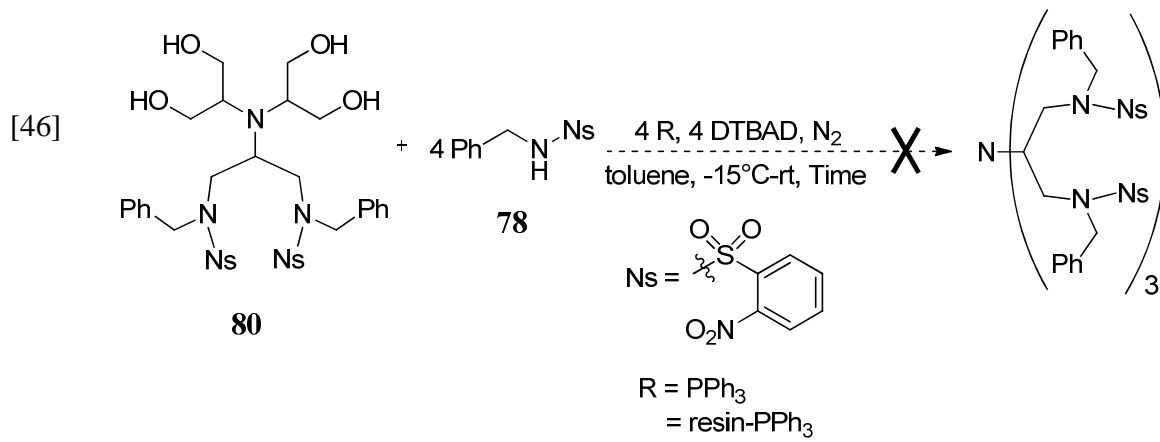


Table 2.4. Attempted reaction conditions for quadruple F-M reaction of **80**.

Entry	Conditions	Time (h)
1	4 eq. TPP, 4 eq. DTBADM, 4 eq. 78	2
2	4 eq. resin-TPP, 4 eq. DTBADM, 4 eq. 78	12
3	10 eq. resin-TPP, 4.8 eq. DTBADM, 4 eq. 78	12 (rt), 12 (reflux)

Even though, the planned quadrupole Fukuyama-Mitsunobu (F-M) reaction did not proceed as desired, a few observations were noted in the course of monitoring the reaction progress (by TLC and NMR).

From TLC the following were noted:

- (i) The spot associated with **80** was absent and no new spot to account for a new product was observed.
- (ii) Almost an unchanged quantity of **78** was present (which is inconsistent with a successful F-M reaction).
- (iii) The usual by-products of a Mitsunobu reaction; reduced DTBADM (H_2 -DTBADM) was present while TPPO was absent.

From NMR the following were noted:

- (i) Careful analysis of 1H -NMR spectrum revealed the presence of **78** and H_2 -DTBADM.
- (ii) ^{31}P -NMR spectrum revealed the Morrison-Brunn-Huisgen (MBH) betaine (see figure 2.7) at δ_P 42.6 ppm (lit. δ_P 42.6 ppm).²⁶ A peak at 25.1 pp was assigned as TPPO.

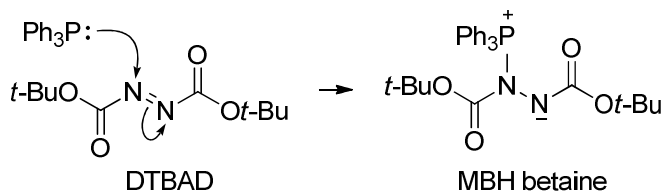


Figure 2.8. Formation of MBH betaine in the first step of a Mitsunobu reaction.

These observations seem to imply **80** could not have been consumed by reaction with **78**, or by known process. Amine **78** was mostly unconsumed, however. The first step in Mitsunobu reaction did indeed occur, because the betaine was present (see Figure 2.8), but since it was not fully consumed, it was still present at the end of the reaction. The hydrazine corresponding to reduction of DTB BAD (H_2 -DTB BAD) was produced.

The negative results of the quadruple F-M reaction of tetraol **80** are in stark contrast to the success of the double F-M reaction of diol **21**. In the case of **21**, the unreacted alcohol group cannot compete with nosylbenzylamine **78**, in nucleophilic attack on the phosphonium species (see Figure 2.9). However, in the case of **80**, interference by a remote $-OH$ group seems more plausible.

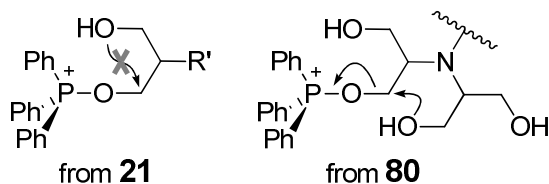


Figure 2.9. Possible interference by $-OH$ groups in F-M reaction of **21** and **80**.

Perhaps, the remote $-OH$ groups of **80** might enable formation of a cyclic phosphorane, as shown in Figure 2.10. Were this to happen, one equivalent of **80**, the entire amount present, would be consumed by reaction with one of the four equivalents of the betaine present, forming

one equivalent of H₂-DTBAD, while leaving 3 equivalents of the betaine and 4 equivalents of **78** unreacted (see Figure 2.10).

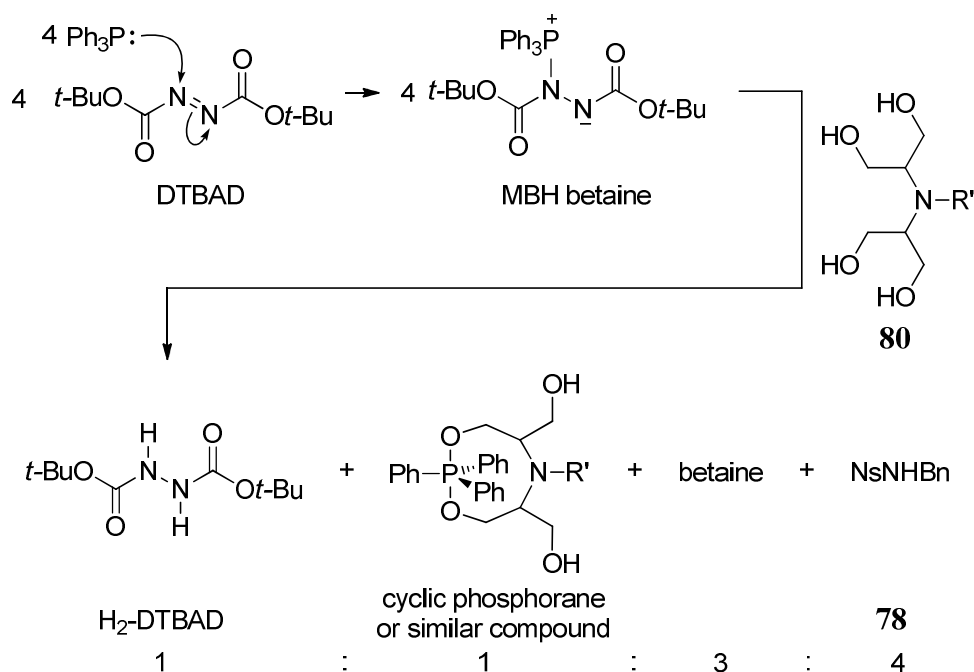


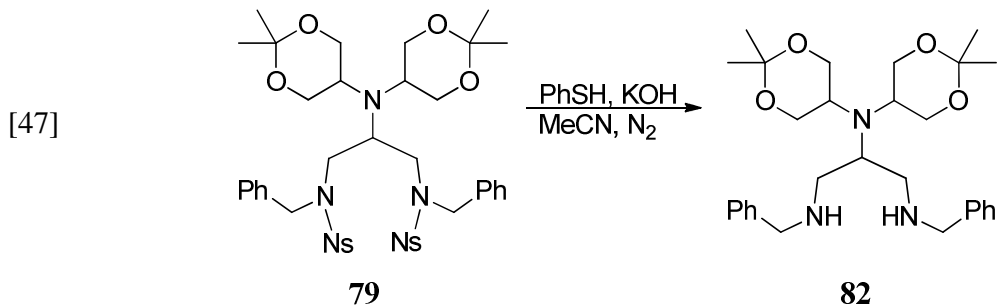
Figure 2.10. Plausible side reaction in the quadrupole F-M reaction.

Because of time constraints, further work on this challenging reaction could not be pursued. The key lies in stepwise deprotection of hydroxyl protecting groups, *e.g.* a single acetonide of **79**. Another approach is complete deprotection followed by re-protection of only one diol.

Some additional reactions relating to Strategy 4 were also carried out.

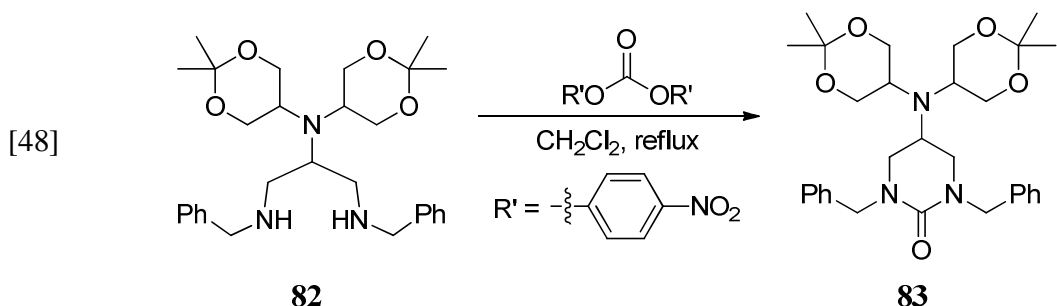
2.4.5. Nosyl group deprotection of **79**.

Deprotection of the nosyl groups was achieved by treating **79** with thiophenol and KOH to give diamino **82** in a moderate yield of 38% (eq. [47]).



2.4.6. Urea cyclized protection of **83**.

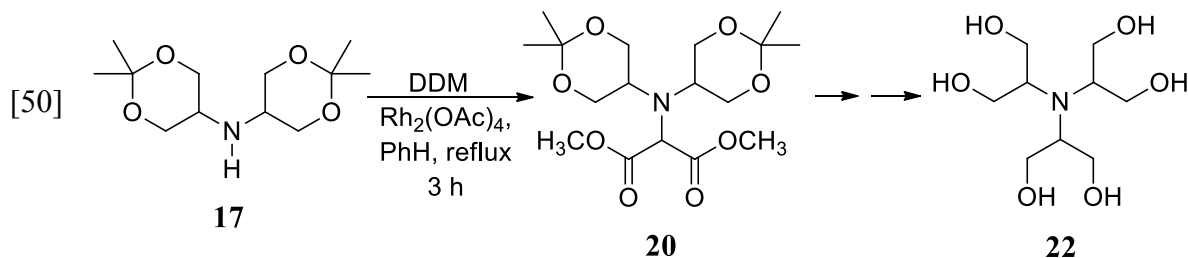
Refluxing **82** with bis(4-nitrophenyl) carbonate in CH₂Cl₂ gave the protected cyclized urea **83** with a yield of 63% (eq. [48]).



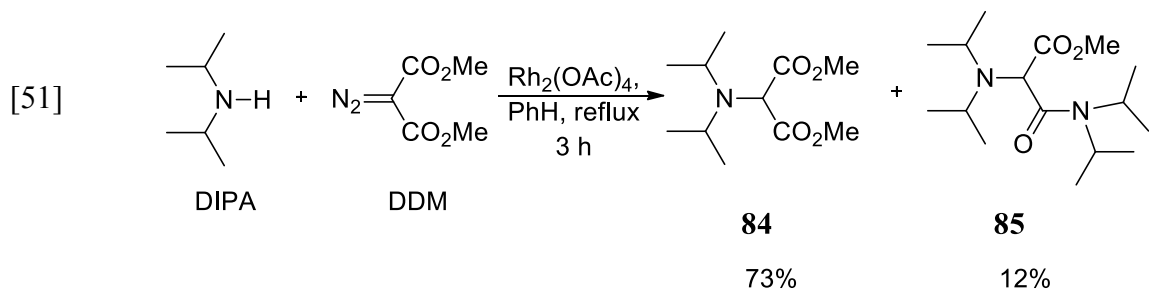
3. EFFECTS OF REMOTE SUBSTITUENTS ON PLANARIZATION OF NITROGEN IN TRIALKYLAMINES

Results and Discussion

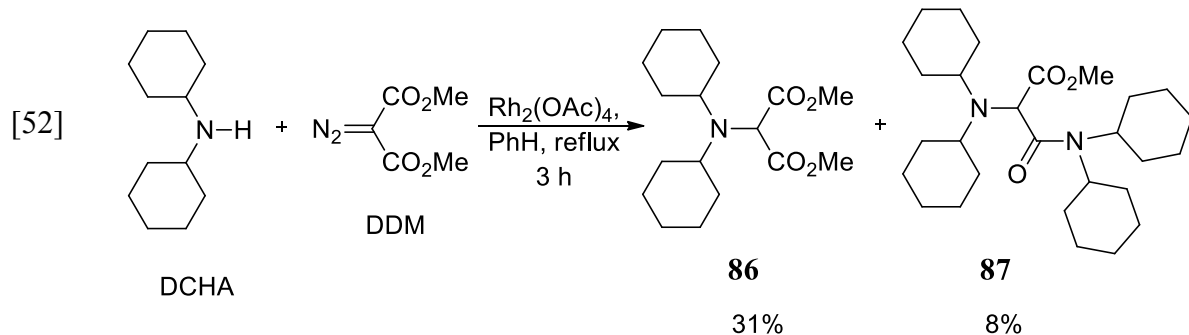
In developing a synthetic route to **22**, amine diester **20** was prepared by a Rh-stabilized carbene N-H insertion reaction into a sterically hindered secondary amine, *viz.* **17** (eq. [50]).^{34,35}



In studies of the scope of that reaction, a previous student in our lab, Minmin Yang, found (eq. [51]) that an amide side product **85** accompanied the expected amine diester product **84**, in the case of diisopropylamine (DIPA).³⁴ At that time, with no other similar cases known, it was easily accepted that aminolysis of amine diester **84** with excess diisopropylamine gave **85**.



Later on, when this type of insertion reaction was done by us using dicyclohexylamine (DCHA) as the substrate, we also encountered an amide side product (eq. [52]). Intense efforts at chromatographic separation of a mixture containing **86** and **88** (with similar R_f on TLC) were unsuccessful, but eventually the separation was achieved by vacuum sublimation of the solid mixture.



With this result, coupled with obtaining intriguing x-ray crystal structures of **85-87** (that will be discussed later), inquiry into the unprecedented formation of these amides was begun.

3.1. Investigations of ester-amides formed in carbene N-H insertion reactions.

3.1.1. Aminolysis.

The amide products **85** and **87** were thought at first to arise from aminolysis of the diester products **84** and **86** by excess amine DIPA or DCHA respectively. The following experiments were performed to test this rationale:

- I. Effect of residual excess DCHA. The results in Table 3.1 show that the yields of **86** and **87** were essentially independent of whether DCHA was deficient or in excess.

TABLE 3.1. Effect of ratio of reactants on product distribution.

DCHA	DDM	$\xrightarrow[\text{PhH reflux, 3 h}]{\text{Rh}_2(\text{OAc})_4^a}$	86^b	87^b
1.19	1.00		72%	28%
1.00	1.32		73%	27%

^a 1 – 4 mol% ^b from NMR integration of peaks of these products only

II. Aminolysis of insertion product 132. Amine diester **86** was reacted with an excess of DCHA in the presence and the absence of Rh₂OAc₄ catalyst under the same N-H insertion conditions and time duration (3 h, as shown in Table 3.2). The yields obtained were inconsistent with yields observed in the same time period for the N-H insertion reaction.

TABLE 3.2. Aminolysis of **132** by DCHA.

86	DCHA	Rh ₂ (OAc) ₄	$\xrightarrow[\text{reflux, 3 h}]{\text{C}_6\text{D}_6}$		
				86^a	87^a
1.00	2.50	2.5 mol%		100%	0%
1.00	2.50	none		97%	3%

^a from NMR integration of peaks of these products only

III. Uncatalyzed reaction of amine and DDM. From previous work,⁴³ DDM was found to undergo aminolysis with primary amines (though the resulting malonamide was not isolated) and therefore we wondered if aminolysis of DDM occurred first followed by insertion. The reaction was repeated for both DCHA and DIPA without Rh₂OAc₄ catalyst for the same duration. Neither gave insertion product or DDM-amide product.

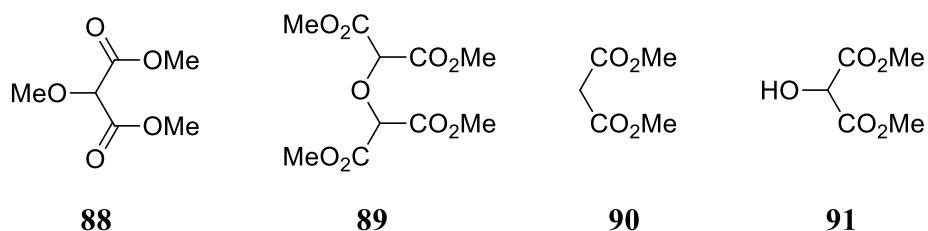
These results show that the occurrence of **87** as a product was *not* the result of an aminolysis of **86**, and, by extension, **85** did not arise by aminolysis of **84**. Also, it did not arise via

aminolysis of DDM followed by insertion. This left us with no readily apparent explanation for the formation of **87**. These doubts about the provenance of **87** spurred us to follow these N-H insertion reactions carefully over time by NMR.

3.1.2. Reaction progress monitored by NMR.

When the reaction progress was carefully monitored by NMR, the following three surprising observations were noted:

- i.* On close examination of the NMR spectra, some minor products that had been overlooked earlier were detected and identified. The products newly identified were dimethyl 2-methoxymalonate, **88**, tetramethyl 2,2'-oxybis(malonate), **89**, dimethyl malonate, **90**, and 2-hydroxymalonate, **91**⁹² (observed on short time scale only).



The evolution of **86**, **87**, and **88 – 90** over 3 h is shown in Figure 3.1. Also shown in the Figure is a product distribution assessed at $t = 48$ h.

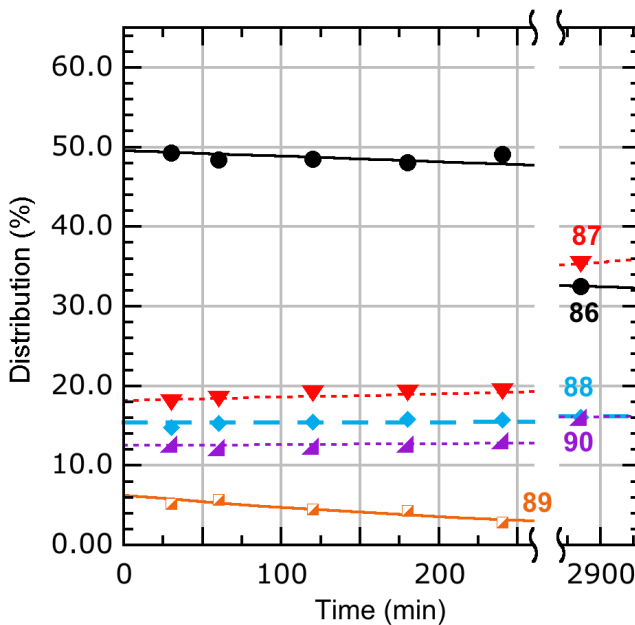


Figure. 3.1. The $\text{Rh}_2(\text{OAc})_4$ -catalyzed N-H insertion reaction of DCHA with DDM (in the ratio of 1.17:1.00 respectively) in refluxing C_6D_6 . Products are **86** (black circles), **87** (red triangles), **88** (blue diamonds), **89** (orange squares), and **90** (purple triangles). The curves are not best fits; they are meant only to enhance readability. Product distributions were measured by NMR integration.

- ii.* The insertion reaction was over in less than 30 minutes at reflux, a much shorter duration than our standard 3 h protocol. The product distribution observed in the first NMR spectrum was preserved with little change in subsequent spectra up to $t = 3$ h.
- iii.* After 2 days in refluxing benzene, about one third of diester **86** present at $t = 3$ h had undergone aminolysis at the hands of DCHA and formed ester-amide **87**.

Reexamination of the reaction of DIPA with DDM was also conducted. The results, shown in Figure 3.2, were similar to the results of the dicyclohexylamine case. The difference was the first two time points of the DIPA reaction showed DDM being consumed, while in the DCHA case

DDM had been completely consumed before the first time point.

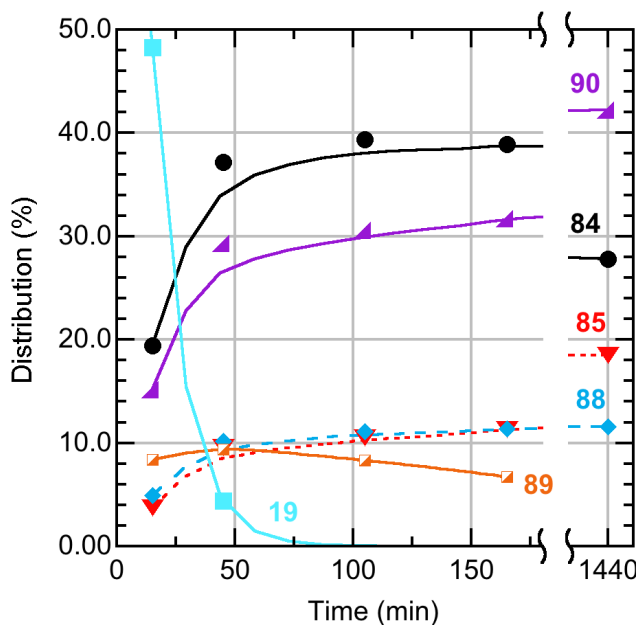
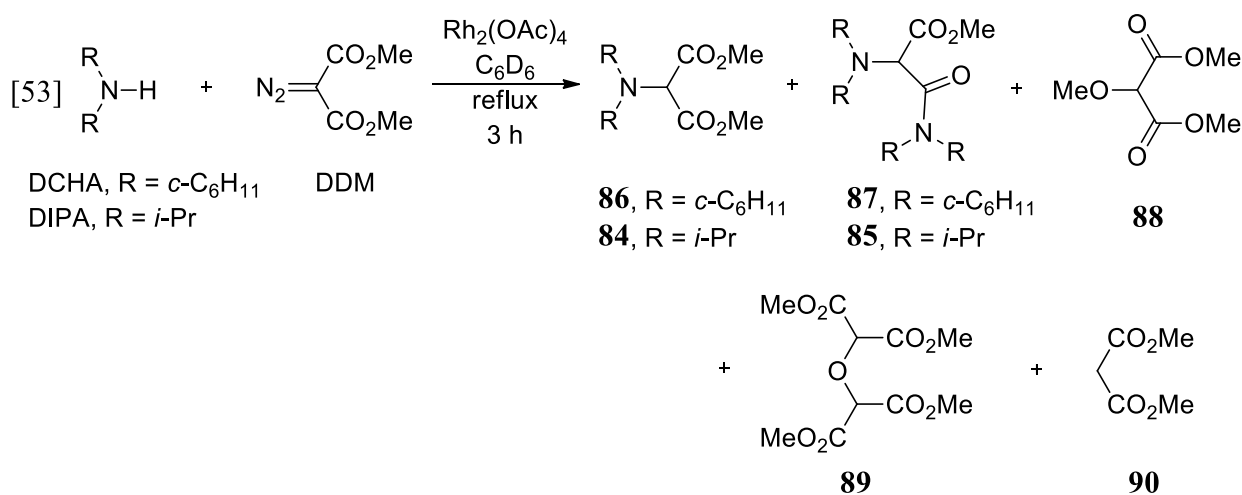


Figure. 3.2. The $\text{Rh}_2(\text{OAc})_4$ -catalyzed N-H insertion reaction of DIPA with DDM (1.20:1.00 ratio respectively) in refluxing C_6D_6 . Products are **84** (black circles), **85** (red triangles), **88** (blue diamonds), **89** (orange squares), and **90** (purple triangles); DDM is represented by light blue squares. The curves are not best fits; they are meant only to enhance readability. Product distributions were measured by NMR integration.

Equation [53] below summarizes both (DCHA and DIPA) N-H insertion reactions.

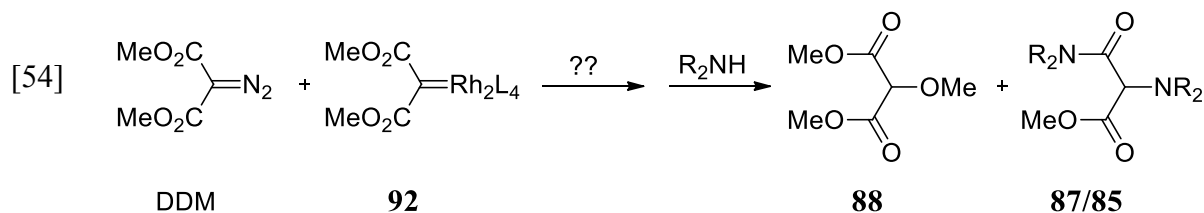


As can be seen in Figures 1 and 2, the ester-amide side product (**87** or **85**) is formed in significant amount by either the first or second time point (30 or 45 minutes). That amount remained essentially unchanged until $t = 2.75\text{ h} - 3.00\text{ h}$, when hourly measurements were suspended. Over the ensuing 1 – 2 days, the “normal” NH insertion product (diester **86** or **84**) diminished, and the ester-amide side product (**87** or **85**) increased, which is clear evidence of slow aminolysis. Therefore, the ester-amides **87** and **85** are formed by two processes: a rapid initial process (as yet unspecified) that is complete in well under an hour, and by a much slower aminolysis that proceeds on a timescale of days.

Another salient feature of these reactions shown by Figures 1 and 2 is the formation of methoxymalonate **88** and the ester-amide side product (**87** or **85**) in an approximate 1:1 ratio at $t \leq 3\text{ h}$. This suggests that **88** and **87** (or **85**) are formed either in the same mechanistic step, or along the same mechanistic branch.

The finding that DDM (with two methoxy groups) generates **88** (with three methoxy groups) requires either methanol, or some source of a methoxy group. If methanol were present in the reaction medium, insertion of the Rh-carbenoid derived from DDM into the O-H bond of methanol – a well known process^{67b} – would nicely explain the formation of **88**. However, methanol is undetectable by NMR at $t = 0$. There is clearly not enough methanol initially present to account for **88** being formed by insertion of the carbenoid into the O-H bond of adventitious methanol, because while methanol is initially undetectable, ultimately **88** certainly *is* detectable. Therefore, the appearance of **88** as a product poses an interesting mechanistic conundrum: where does the “extra” methoxy group come from? Because the “extra” methoxy group of **88** is not obtained from methanol, one is led to propose it comes either directly or indirectly from a methyl ester group of DDM. Indeed, **88** has one methoxy group more than DDM, and **87** (or **85**) has one

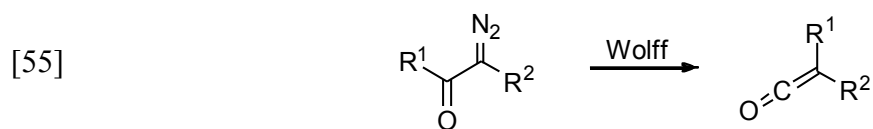
methoxy group less. Since DDM is unreactive at these temperatures without $\text{Rh}_2(\text{OAc})_4$ catalyst, it is reasonable to guess it is not DDM, but rather **92**, the Rh-carbenoid derived from DDM, that reacts with DDM in some way that results in transfer of a methoxy group, and also leads (either directly or in subsequent steps) to ester-amide products (**87** or **85**). This idea is sketched out in eq [54].



When neat DDM is heated for 15 minutes in the presence of catalytic $\text{Rh}_2(\text{OAc})_4$, an NMR spectrum of the cooled reaction mixture (C_6D_6 solvent) revealed that a small amount of **134** had been formed (among a number of other products), which lends support to the idea expressed in eq. [54]. (In this experiment, some **135** was also observed. This product is discussed later).

3.1.3. Proposed reaction mechanism in formation of ester-amides **87/85** and methoxymalonate **88**.

A fuller mechanism is shown in Figure 3.3, one that provides a pathway to formation of **88** and **87** or **85** in a 1:1 ratio. The key step is the first one, which transfers a methoxy group from DDM to Rh-carbenoid **92**, forming methoxymalonate derivative **a** and ketene **b**. This step is reminiscent of the Wolff rearrangement, which is shown in general form in eq. [55].



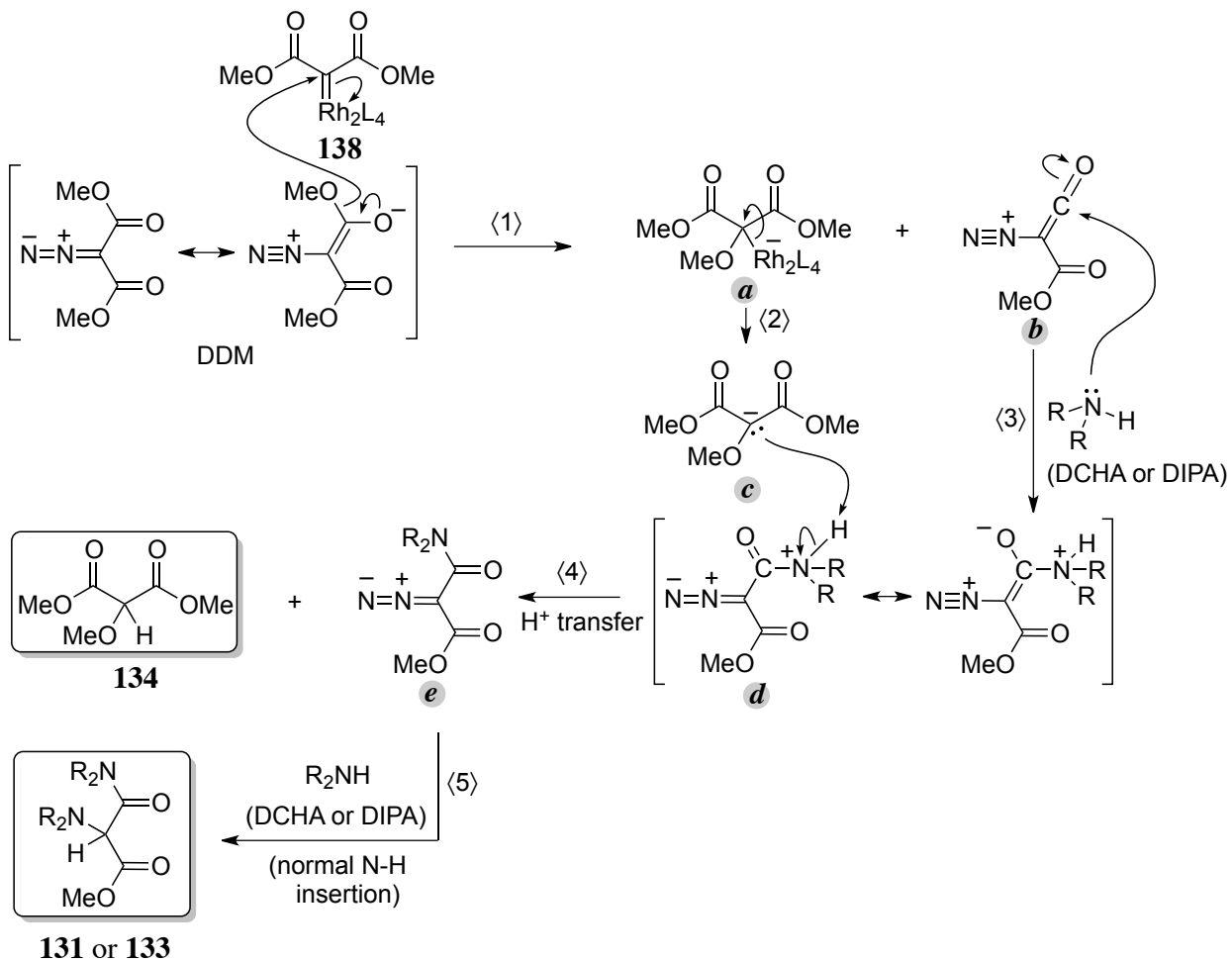


Figure 3.3. Proposed mechanism of formation of **88** and **85/87**.

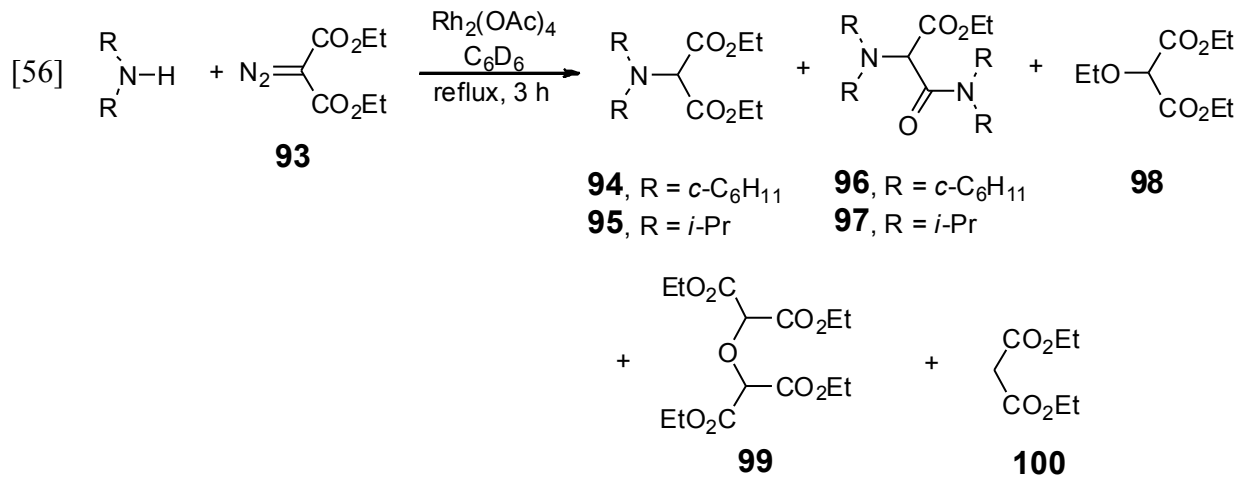
The classical Wolff rearrangement (*i*) is intramolecular, (*ii*) may be either photochemical or thermal, and (*iii*) usually involves migration of alkyl or aryl groups (R^1 in eq [55]).⁸³ Step $\langle 1 \rangle$ in the proposed mechanism is *intermolecular*, and involves transfer of a methoxy group, which has poor migratory ability in the standard Wolff rearrangement.⁸³ Nevertheless, we propose that the reaction written as step $\langle 1 \rangle$ is a novel thermal *intermolecular* Wolff rearrangement. The step leads to equimolar amounts of intermediates **a** and **b**. Intermediate **a** loses $\text{Rh}_2(\text{OAc})_4$ (step $\langle 2 \rangle$) to generate methoxymalonate anion **c**. Ketene **b** is attacked by the secondary amine (DCHA or DIPA) (step $\langle 3 \rangle$), leading to protonated diazo ester amide **d**.⁹⁴ Deprotonation of **d** by anion **c**

(step <4>) forms product **88** and diazo ester amide *e* in equal amounts. Compound *e* undergoes standard N-H insertion with either DCHA or DIPA to give amine-ester-amide **85** or **87**.

3.1.4. Partial evidence supporting the proposed mechanism.

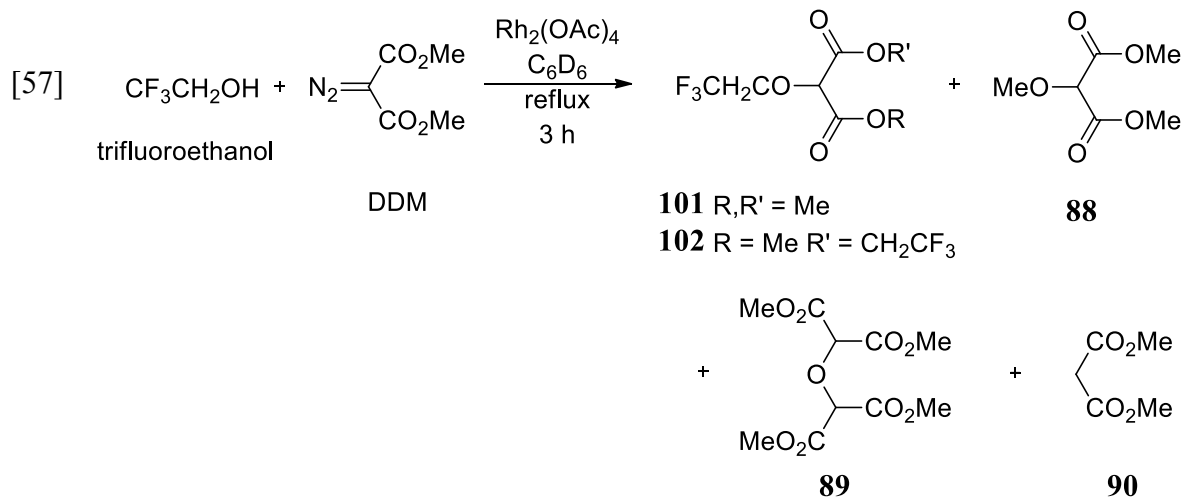
The following reactions were conducted to find collaborative evidence supporting the suggested mechanism.

(i) To completely rule out any adventitious MeOH present in the reaction, DDM was replaced with its homologous diazo compound, diethyl diazomalonate **93** and the reaction was repeated under the same reaction conditions for 45 mins. Careful analysis of the NMR spectra of the crude reaction mixture enabled us to identify the products shown in eq. [56], which were confirmed by mass spectrometry. These products differ from those identified in DDM case eq. [53] only by the presence of an ethyl group where a methyl group had previously been. The methanol insertion product **88** was absent.



This clearly suggests **88** doesn't arise from adventitious methanol. The formation of the alkoxy transfer product **98** provides additional support for the intermolecular methoxy migration (that is, Wolff rearrangement) proposed in Figure 3.3.

(ii) The proposed mechanism indicates that the amine first participates in step $\langle 3 \rangle$, after the intermolecular methoxy transfer is complete. Therefore, trapping the ketene **b** with a species other than a secondary amine should not interfere with the formation of **88**. We decided to trap the ketene with an alcohol rather than an amine. After some initial work with *tert*-butanol and CD₃OD, 2,2,2-trifluoroethanol was chosen, on the basis of (i) uncomplicated NMR spectra, (ii) low molecular weight, and resulting higher volatility of expected products which would be conducive to analysis by GC or GC-MS and (iii) different molecular weights of expected analogous products similar to eqs. [53] and [56]. The insertion reaction of 2,2,2-trifluoroethanol with DDM was followed by NMR and through careful examination of the spectra, the products shown in eq [57] were observed. There was no detectable MeOH at $t = 0$ min; the reaction was over in 15 min, and included the normal O-H insertion product **101**. Other products analogous to those of eqs. [53] and [56] were formed, *i.e.* 1:1 product ratio of methoxy diester **88** and trifluoroethoxy unsymmetrical esters **102**, and **90**. The identities of these products and the 1:1 ratio of **88** and **102** were confirmed by GC and GC-MS.



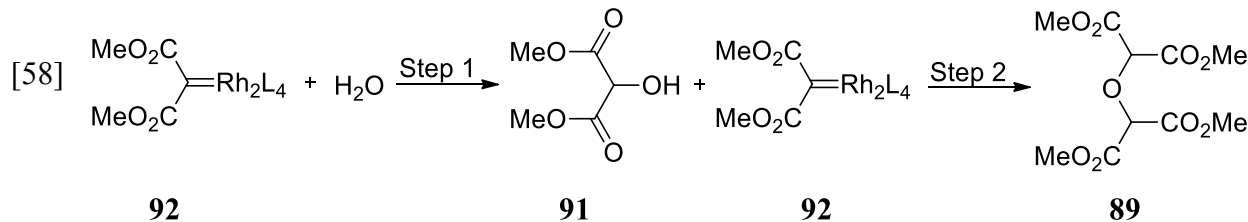
(iii) In trying to curb step $\langle 1 \rangle$ (*intermolecular* Wolff rearrangement) from occurring, efforts were made to minimize the quantity of DDM present in the reaction mixture. DDM was slowly

added (approx. 15 min) to a refluxing mixture of DCHA and $\text{Rh}_2(\text{OAc})_4$ in C_6D_6 , which gave similar products as eq. [53]. This was inconclusive since the slow addition was merely based on previous observation *i. e.* the reaction is essentially over within 15 min.

(iv) To investigate the effect of temperature we recalled that in all Rh-carbenoid insertion reactions done, crude reaction mixture was brought to reflux by subjecting the flask contents to a preheated oil bath at 80 °C. A control experiment was done by gradually increasing the oil bath temperature (rt-80 °C; $t = 100$ min) together with the reaction flask contents (DCHA, DDM and $\text{Rh}_2(\text{OAc})_4$ in C_6D_6) with no variation of products obtained in eq. [53].

With these results, it is highly plausible that formation of **88** could only arise from an intermolecular migration of a methoxy group of DDM to Rh-carbenoid **92** to give intermediates **a** and **b** (Figure 3.3) and consequently a 1:1 product ratio of methoxy diester **88** and ester-amide similar compounds. To the best of our knowledge this is the first example of a thermal *intermolecular* Wolff rearrangement.

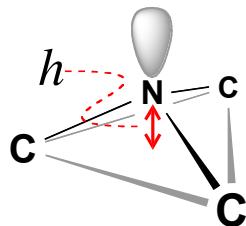
Compounds **89** and **91** could have possibly arisen from Rh-carbenoid **92** insertion into adventitious water (twice and once respectively) which has been previously suggested.⁹² First is insertion of **92** into water to give **91** (step 1), that was only identified when the reaction was followed by NMR on short time scale (3-6 min), which fades away after $t = 9$ min possibly due to a second insertion of **92** into **91** (step 2) to finally give **89** as shown in eq. [58].



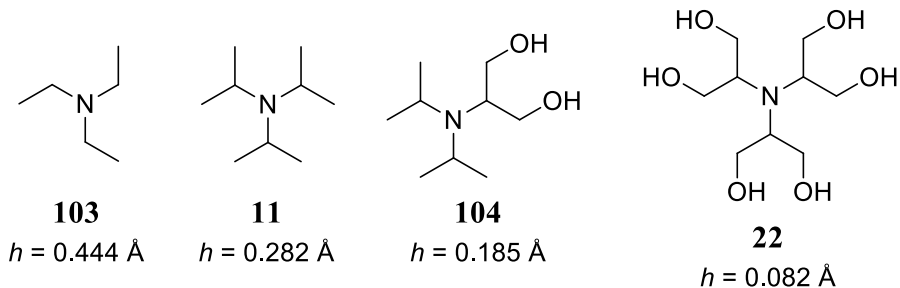
3.2. Nitrogen planarity of trialkylamines **20**, **21**, **85-87** and **104**.

Trialkylamines ($\text{N}(\text{Csp}^3)_3$) that are planar or nearly planar are rare, and therefore intriguing.

A measure of planarity, out-of-plane distance h , is defined graphically below. This parameter is $\sim 0.45 \text{ \AA}$ for ordinary trialkylamines (*e.g.* for Et_3N , $h = 0.444 \text{ \AA}$ ⁸⁴).

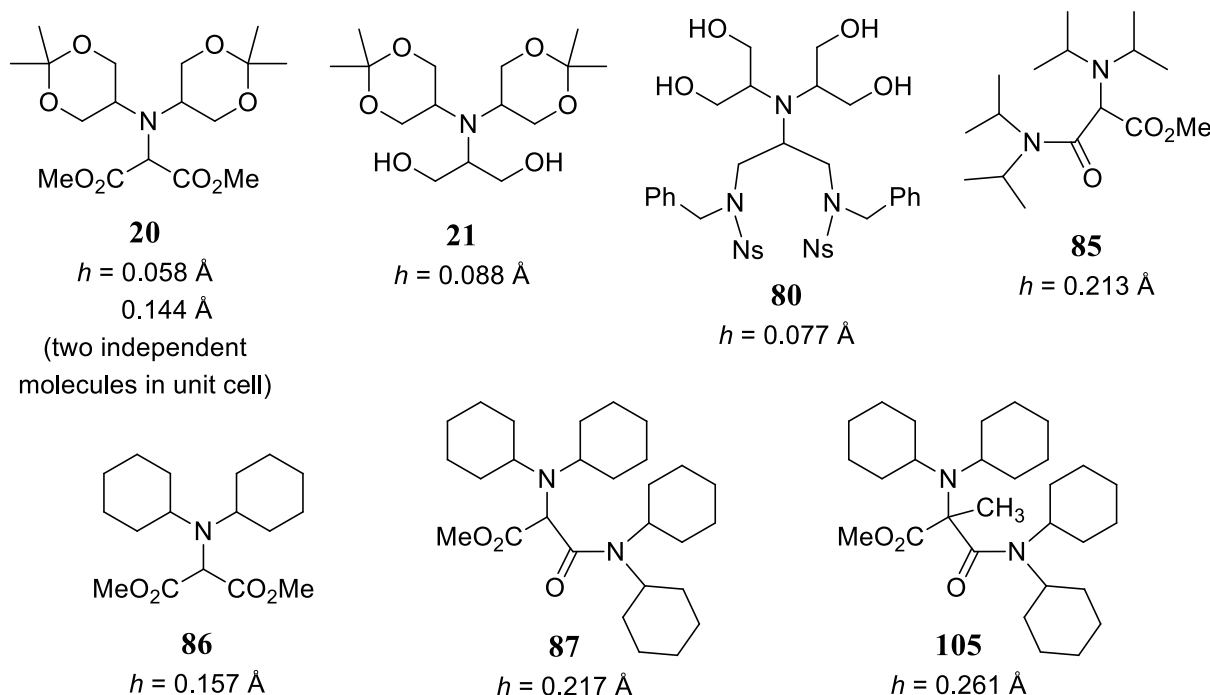


Triisopropylamine, **11**, once thought to be planar, is in fact pyramidal but significantly flattened; $h = 0.28 \text{ \AA}$.⁸⁵ Recently, our laboratory reported the structures of several trialkylamines more planar than **11**; two examples (**104** and **22**) are shown.^{35b,86}



In the course of this study new planar or nearly planar trialkylamines **20**, **21**, **85**, **86**, **87** and **105** were obtained (Chart 1) and their x-ray crystals structures (Appendices 1, 3-7) analyzed to understand the planarization of nitrogen.

Chart 3.1. New planar or nearly planar trialkylamines.



3.2.1. Planarity at nitrogen in compounds 20, 21, 85, 86, 87 and 105.

Solid state structures of **20**, **21**, **85**, **86**, **87** and **105**, were analyzed with attention directed largely to the geometry at nitrogen. Relevant geometrical parameters for these amines are collected in Table 3. Focus shall be emphasized on the out-of-plane parameter *h*. It is important to ask, when comparing structures, how small a difference between *h* values should one take account of? It has been suggested that a difference in *h* less than 0.030 Å should be considered insignificant.⁸⁶ This suggestion is based on three comparisons of *h* values of non-identical versions of the same molecule in a unit cell. All differed by less than 0.030 Å.⁸⁶ Consider, for example, the small difference between the *h* of tetracyclohexyl ester-amide **87** (0.217 Å) and that of tetraisopropyl ester-amide **85** (0.213 Å), $\Delta h = 0.004 \text{ \AA}$. Employing the 0.030 Å test, we would consider **87** and **85** to be equally planar. This conclusion makes sense, since a cyclohexyl group and an isopropyl group are about the same “size” in the vicinity of nitrogen. (Equatorial

preferences, *i.e.*, A-values, for cyclohexyl⁸⁷ and isopropyl⁷⁵ are 2.15 (305 K) and 2.21 kcal/mol (300 K) respectively).

Table 3. Selected geometrical parameters of amines **20, **21**, **80**, **85 – 87** and **105**.**

Cmpd	<i>h</i> (Å) ^a	C-N bond length (Å) ^b	$\Sigma_{\text{C-N-C}}$ (°) ^c
20(A)^d	0.058	1.449 (1.453, 1.457, <i>1.437</i>)	359.53
20(B)^d	0.144	1.454 (1.461, 1.452, <i>1.450</i>)	357.11
21	0.088	1.446 (1.444, 1.443, <i>1.451</i>)	358.91
80	0.077	1.460 (1.456, 1.465, 1.458)	359.18
85	0.213	1.460 (1.469, 1.470, <i>1.442</i>)	353.74
86	0.157	1.446 (1.455, 1.462, <i>1.421</i>)	356.52
87	0.217	1.461 (1.472, 1.472, <i>1.438</i>)	353.50
105	0.261	1.474 (1.467, 1.486, 1.469)	350.78

^a Perpendicular distance from the non-amide nitrogen to the plane define by its three ipso carbons. ^b For the non-amide nitrogen, the average of the three C-N bond lengths. The values in parentheses are the individual C-N bond lengths, with the bond to the carbon bearing an ester or amide group in italics. ^c sum of C-N-C angles ^d (A) and (B) refer to non-identical molecules in the unit cell.

In examining the nitrogen geometries of **20**, **21**, **85**, **86**, **87** and **105**, several cases of counterintuitive geometries were found, which are presented as a series of comparisons.

Comparison 1. For the reasons laid out in the preceding paragraph, one may consider triisopropylamine **11** to be sterically equivalent to the (not-yet-synthesized) dicyclohexyl-

isopropylamine, **106**. Therefore we estimate h for **106** to be 0.28 Å, *i.e.*, the same as for **11**. When we compare **106** to **86**, we see the effect of replacing two -CH₃ groups with two -CO₂CH₃ groups: the nitrogen becomes more planar. But the A-values of -CH₃ and -CO₂CH₃ are, for -CH₃, 1.74 (300 K)⁷⁵ or 1.6 (163 K)⁷⁶, and, for -CO₂CH₃, 1.12 (195 K),⁷⁷ 1.27 (298 K),⁷⁸ or 1.31 (195 K)⁷⁹ kcal/mol. Therefore, *replacing bulkier -CH₃ groups with less bulky -CO₂CH₃ groups causes the nitrogen to become more planar.*

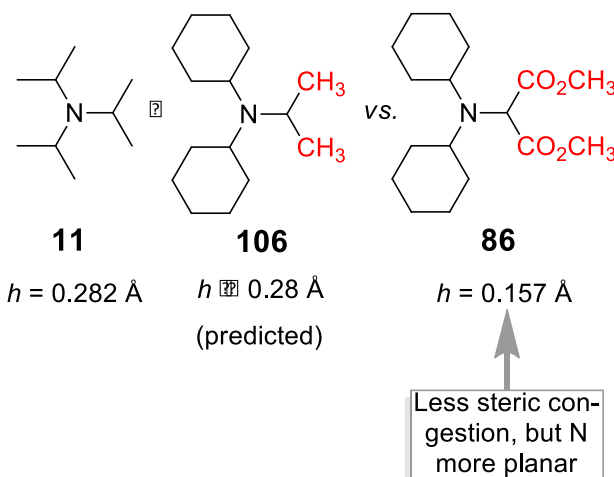


Figure 3.4. Comparison 1.

Comparison 2. Comparing **87** to **86** reveals that a change at a site remote from the nitrogen (namely, γ to nitrogen) has a large effect on planarity. That the effect operates over a large distance militates against a purely steric rationale. The A-value for the -N(cyclo-C₆H₁₁)₂ group is not known, but could be roughly estimated by the A-value for the -N(CH₃)₂ group, for which values of 1.31 (183 K),⁸⁰ 1.53 (183 K),⁸⁰ and 2.1 (293 K)⁸¹ kcal/mol have been reported. The A-value for the -OCH₃ group is 0.75 kcal/mol (180 K).⁸² (That of -OCD₃ is 0.55 kcal/mol (191 K).⁷⁹ So, in addition to its being a remote effect, the effect of the dicyclohexylamino-to-methoxy change is “counter-steric,” that is, *replacing a bulkier -N(cyclo-C₆H₁₁)₂ group with a less bulky -OCH₃ group causes nitrogen to become more planar.*

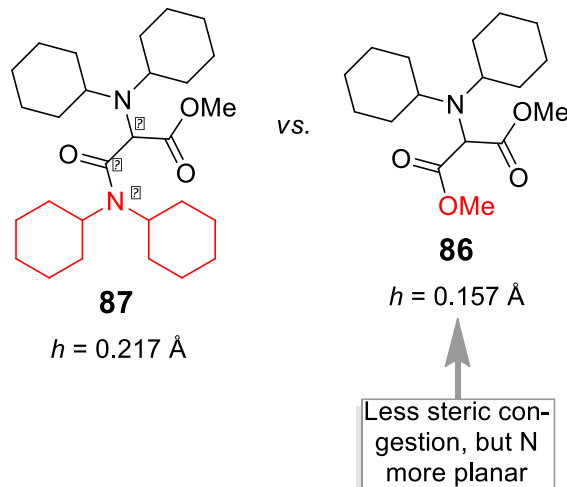


Figure 3.5. Comparison 2.

Comparison 3. At sites remote from nitrogen (again γ to nitrogen) methylene groups are replaced by oxygen atoms on going from **86** to **20**. As with Comparison 2, the large distance between the point of replacement and the nitrogen atom leads one to conclude that steric effects are an unlikely cause for any change in the planarity of nitrogen. Also, like Comparison 2, the change in steric bulk is significant here. One way to quantitate the difference in size between $-\text{CH}_2-$ and $-\text{O}-$ is to compare the A-values of $-\text{CH}_2\text{CH}_3$ (1.79 kcal/mol (300 K))^{75a} and $-\text{OCH}_3$ (0.75 kcal/mol (180 K)).⁸² Therefore, again, *remote replacements of larger groups ($-\text{CH}_2-$) with smaller groups ($-\text{O}-$) leads to substantial flattening of central nitrogen.*

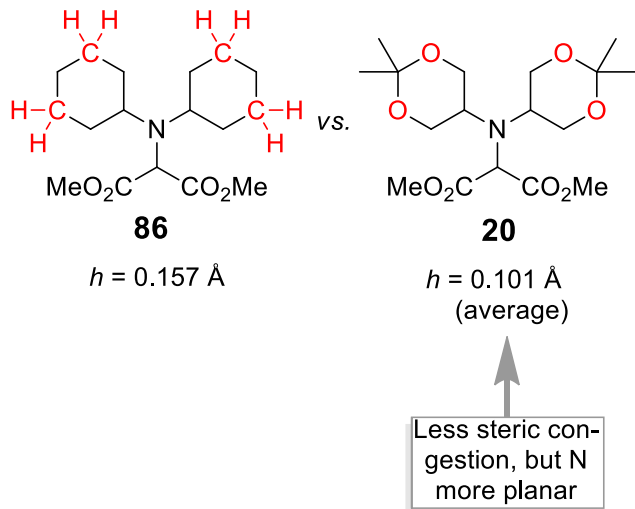


Figure 3.5. Comparison 3.

Comparison 4. The difference between **87** and **105** is the addition of a methyl group α to nitrogen. Here the effect is not remote. Replacing an α -H with an α - CH_3 results in a less planar structure. Why?

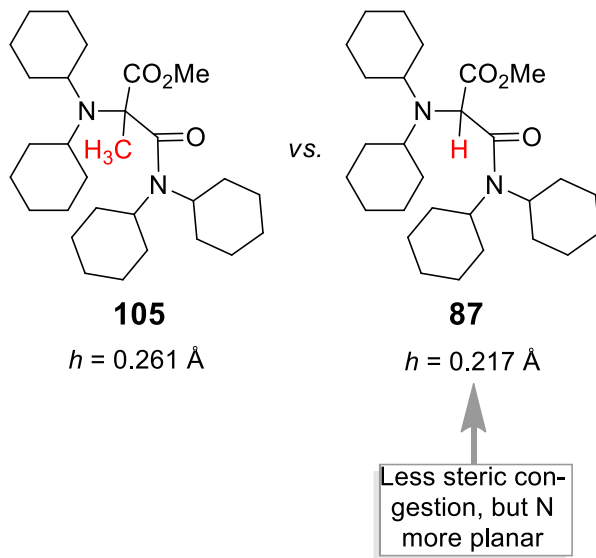


Figure 3.6. Comparison 4.

3.2.3. A rationale for trends in nitrogen planarity.

How can the foregoing comparisons be explained? These are cases in which solely steric arguments are inadequate. Therefore, we posit the following qualitative electronic argument as a complement to the standard steric ones.

Consider a planar trialkylamine. For simplicity, we discuss the case in which the three alkyl groups are identical. A planar geometry is stabilized by the filled orbital-empty orbital interactions between the occupied N 2p orbital (*i. e.*, the nitrogen lone pair orbital) and an adjacent unoccupied σ^* orbital on each of the alkyl groups to which nitrogen is bonded. This is shown in Figure 3. In the context of the comparisons under discussion, A might be the CH carbon of a cyclohexyl group, or the carbonyl carbon of a $-\text{CO}_2\text{CH}_3$ group, for example. In Figure 4, the roughly parallel disposition of the A-C-A group relative to the symmetry axis of the nitrogen lone pair orbital reflects the observed geometry in the congested trialkylamines we have studied, both those reported here, and others.^{35b, 86, 88}

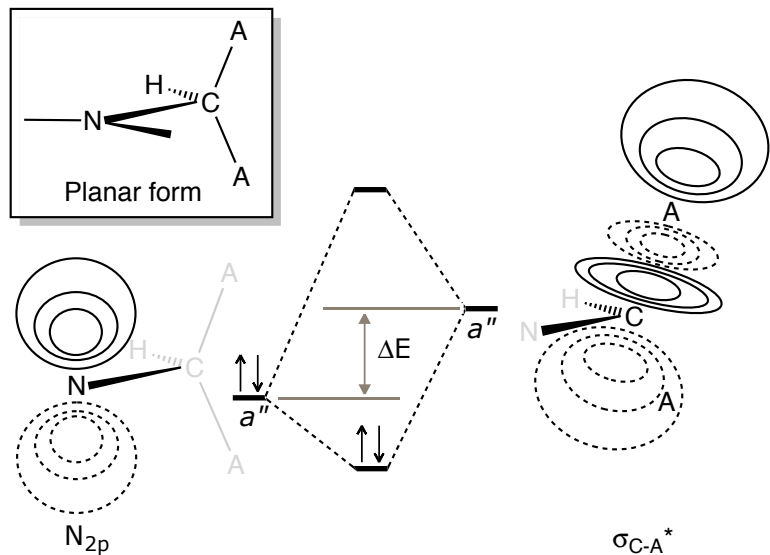


Figure. 3.7. Orbital interaction diagram for a planar trialkylamine, $\text{N}(\text{CHA}_2)_3$, where A represents any atom. Only one $-\text{CHA}_2$ substituent of three is shown. For clarity, the analogous $\sigma_{\text{C}-\text{A}}^*$ that involves the bottom atom A is not shown.

The strength of the $2\text{p}-\sigma^*$ interaction is governed in part by ΔE ; as ΔE becomes smaller, the $2\text{p}-\sigma^*$ interaction becomes stronger. Therefore, any factor that lowers the energy of the σ^* orbital (or raises the energy of the nitrogen 2p orbital) will tend to favor the planar geometry.

This idea can explain comparisons 1 – 4. Comparison 2 and 3 especially support an electronic argument, because steric changes occur at sites that are quite remote from nitrogen. To make sense of comparison 4, we must note that in **86** $-\text{CO}_2\text{CH}_3$ and $-\text{CONR}_2$ groups are part of the crucial σ^* orbital, but in **105**, $-\text{CO}_2\text{CH}_3$ and $-\text{CH}_3$ are part of the σ^* orbital (see Fig. 3.8). Therefore in **105** the $2\text{p}-\sigma^*$ interaction is weaker and the nitrogen is not as planar.

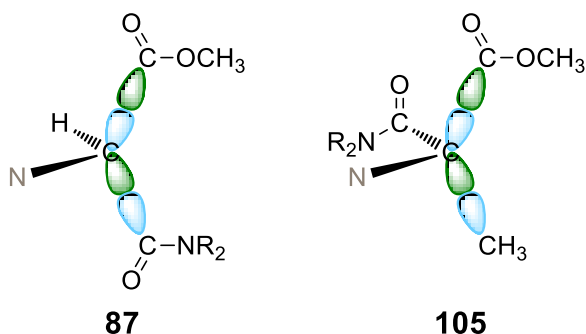


Figure 3.8. A-C-A group σ^* orbitals of **87** and **105**.

Structural data from X-ray crystallography revealed amine nitrogen geometries that are significantly flattened. In comparing nitrogen planarities quantitatively among **20**, **85**, **86**, **87** and **105**, some surprising anomalies were found. All these could be explained by a very simple p- σ^* hyperconjugation argument.

3.2.3. Hyperconjugation.

Hyperconjugation is a stabilizing interaction between electronic orbitals in molecules describing the electronic consequence of delocalization. Hyperconjugative interactions have been known to lead to significant changes in geometry, electron density, molecular orbital energies, bond strengths and NMR properties.⁹⁵ In valence bond theory, hyperconjugation arises from the presence of additional resonance structures *i.e.* “the double bond/no double bond resonance” (Figure 3.10. ⟨a⟩) while in molecular orbital theory it is described as the interaction between electronic orbitals through stabilization of a filled low energy orbital and an empty high energy orbital (Figure 3.9 ⟨b⟩).

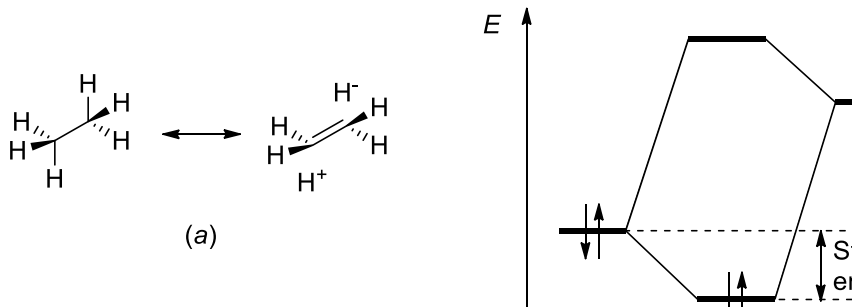


Figure 3.9. Hyperconjugation as described by VB theory (a) and MO theory (b).

Using computational methods, hyperconjugation can be described and quantified by evaluating the energy penalty that occurs when such an interaction shown in Figure 3.10 (b) is absent. Natural bond orbital (NBO) analysis is one of the methods that has been used successfully to quantify hyperconjugative effects by transforming the canonical delocalized Hartree-Fock (HF) molecular orbitals and non-orthogonal atomic orbitals into sets of localized “natural” atomic orbitals, hybrid orbitals and NBOs. Filled NBOs describe the hypothetical, strictly localized Lewis structure. Natural population analysis (NPA) charge assignments based on NBO analysis correlate well with empirical measures.⁹⁶

Interactions between filled (*e.g.* σ , π and lone pairs) and unfilled orbitals (antibonding) represent the deviation from the Lewis structure and can therefore be used as a measure of delocalization. The two ways to do this are; (i) estimate the energy contribution [$E(2)$] of delocalization from the second order perturbation approach as shown in eq. 59,⁹⁷ and (ii) delete the corresponding off-diagonal elements of the Fock matrix in the NBO basis and recalculate the energy (E_{del}).⁹⁸ Usually there is a good linear correlation between the deletion (E_{del}) and perturbation [$E(2)$] energies.⁹⁹

[59]
$$E(2) = -n_{\sigma} \frac{\langle \sigma | F | \sigma^* \rangle^2}{\varepsilon_{\sigma^*} - \varepsilon_{\sigma}} = -n_{\sigma} \frac{(F_{i,j})^2}{\Delta E}$$

where: $\langle \sigma | F | \sigma^* \rangle$ or $F_{i,j}$ = Fock matrix element between the NBO orbitals i and j

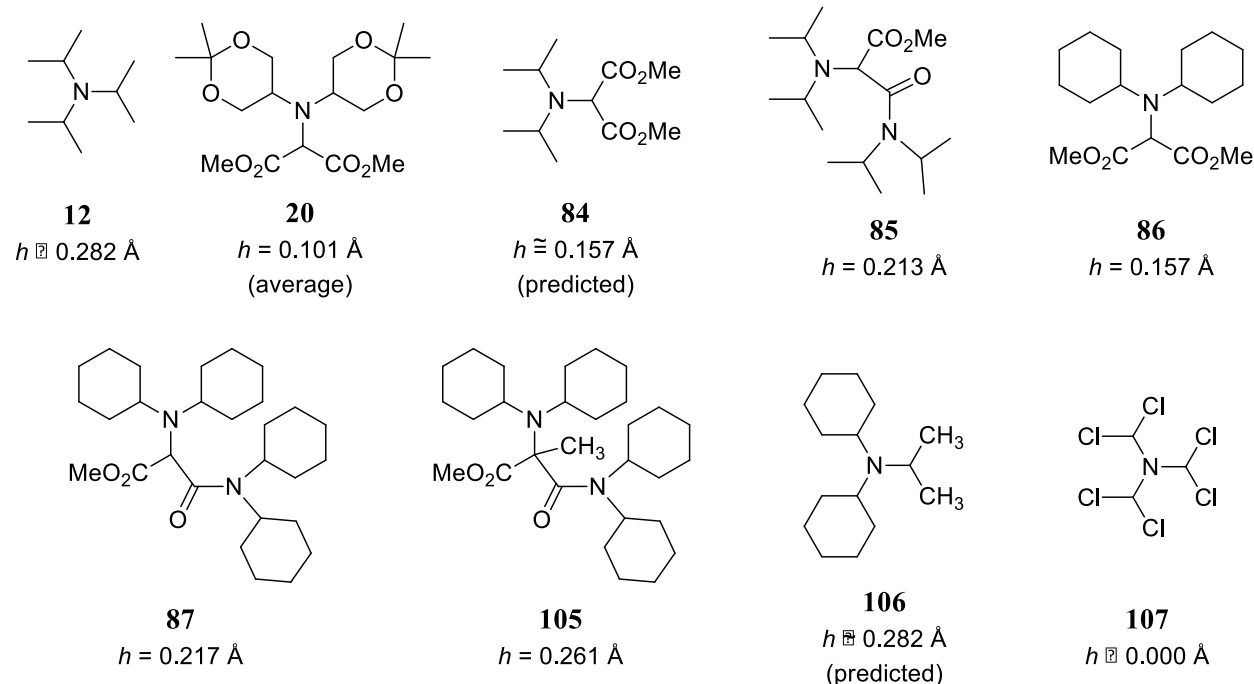
ε_{σ} and ε_{σ^*} = energies of σ and σ^* NBOs

n_{σ} = population of the donor σ orbital

3.2.4. Computational analysis.

The molecular structures of compounds **12**, **20**, **84-87** and **107** shown in Chart 3.2 were analyzed through *ab initio* molecular orbital calculations.

Chart 3.2. Computationally analyzed structures.



Both DFT and HF calculations were performed for compounds illustrated in Chart 3.2 and after various trials with different basis sets, 6-311 G (d, p) basis set gave the optimized structures whose geometrical parameters had the best correlation, at least for most, with the experimental (x-ray crystal data) as shown in Table 3.4. DFT calculations gave low energy optimized

structures than HF calculations. Comparison of the geometrical parameters was mainly focused around nitrogen of the trialkylamines, though careful analysis of other parts of the molecular structures was done to match those of x-ray structures. The HF method was done because later on we also wanted to perform NBO energetic analysis which is usually done by deleting the corresponding off-diagonal elements, of the NBO Fock matrix and recalculating the energy by a single pass through the SCF evaluator of the modified density matrix to obtain E_{del} which is also known to describe and quantify hyperconjugation. DFT functional methods are often poorly parameterized to evaluate the energetics of such NBO deletions and may lead to unrealistic DFT methods.¹⁰³

Comparison of optimized structures with solid state structures (Table 3.4).

The following geometrical parameters were compared between DFT, HF optimized structures and experimental x-ray data of trialkylamines of **12**, **20**, **84-87** and **107**:

i. Average bond length N-C of the three carbons around nitrogen.

The average bond lengths of the three C-N bonds around nitrogen lie in the range 1.418-1.467 Å (± 0.01 Å experimental data) of structures optimized by either DFT or HF method, which is relatively short compared to the average $\text{C}(\text{sp}^3)-\text{N}(\text{sp}^3)$ bond length 1.469 ± 0.014 Å, a value determined by systematic searching of the Cambridge crystallographic database.⁶¹

ii. Sum of the three bond angles C-N-C around nitrogen ($\sum\phi_{\text{C}-\text{N}-\text{C}}$).

For both DFT and HF optimized structures, $\sum\phi_{\text{C}-\text{N}-\text{C}}$ was comparable with the experimental x-ray structure data for all compounds in Chart 3.2. with the exception of compounds **12** and **86** which were at least greater than 5° with experimental data.

iii. Parameter “h”, defined as the perpendicular distance from nitrogen to the plane define by its three ipso carbons in a trialkylamine.

Comparing the two methods used, DFT gave lower “h” for the trialkylamines than HF calculation. For compounds **20**, **85**, **87**, **105** and **107**, both DFT and HF method gave “h” parameter in close agreement with experimental x-ray crystal data. In both DFT and HF methods compounds **12**, **84**, **86** and **106** “h” was exceedingly lower than experimental values, this make them more planar. This increase in nitrogen planarity in these compounds can be suggested to be as a consequence of performing the calculations in gaseous phase relative to experimental that is in solid state where crystal packing forces do exist. One wonders how crystal packing forces alter the planarization of nitrogen in solid state; increase or reduced.

Table 3.4. Comparison of calculated and exptl geometrical parameters of trialkylamines; **12**, **47**, **130-133**, **153-155**.

Cmpd	DFT			HF			Exptl.		
	av. N-C ^a	$\sum \phi_{C-N-C}^b$	h^a	av. N-C ^a	$\sum \phi_{C-N-C}^b$	h^a	av. N-C ^a	$\sum \phi_{C-N-C}^b$	h^a
20	1.457	358.486	0.104	1.450	358.463	0.104	1.451	358.320	0.101
84	1.459	359.057	0.082	1.452	358.572	0.101	-	-	0.157 ^c
85	1.468	354.569	0.199	1.461	354.442	0.200	1.460	353.745	0.213
86	1.457	359.804	0.037	1.451	358.919	0.087	1.460	353.745	0.157
87	1.467	354.956	0.192	1.460	355.041	0.190	1.461	353.500	0.217
12	1.467	355.583	0.179	1.457	356.676	0.154	1.469	349.200	0.282
105	1.489	351.589	0.251	1.480	352.214	0.240	1.474	350.780	0.261
106	1.456	356.896	0.150	1.464	357.405	0.136	-	-	0.282 ^c
107	1.418	360.000	0.000	1.415	360.000	0.000	1.418 ^d	360.000 ^d	0.000 ^d

^a Å ^b ° ^c Approximate values of h as determined by comparing A-values of isopropyl and dicyclohexyl groups. ^d geometrical parameters obtained from ref 100.

NBO calculations illustrating hyperconjugation effect.

As stated in (3.2.3) NBO method can be used to describe and quantify hyperconjugation. The two ways to do this are:

i. To estimate the energy contribution [$E(2)$] of delocalization from the second order perturbation approach as shown in eq. [59].⁹⁷ NBO analysis using both DFT and HF methods of the optimized trialkylamines **12**, **20**, **84-87**, **107** was performed and from second order perturbation theory analysis of fock matrix in NBO basis $E(2)$ values were obtained as shown in Table 3.5. These $E(2)$ values are used to describe interactions between filled (*e.g.* σ , π and lone pairs) and unfilled orbitals (antibonding) that represents deviation from the Lewis structure and hence used as a measure of delocalization (hyperconjugation).

For trialkylamines **12**, **20**, **84-87**, **107**, the focus was around nitrogen and its adjacent groups around it as shown in Figure 3.10. We mainly wanted to see the interactions between filled orbital-empty orbital interactions between the occupied N_{2p} orbital (*i.e.*, the nitrogen lone pair orbital) and an adjacent unoccupied ($C-A$) σ^* orbital on each of the alkyl groups to which nitrogen is bonded.

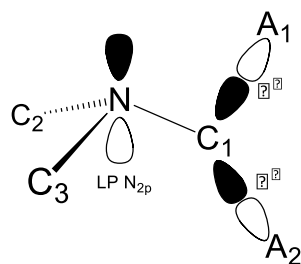


Figure 3.10. N_{2p} - ($C-A$) σ^* orbitals interaction. For clarity the interaction orbitals on C_2 and C_3 are not shown but have been designated as $A_3-C_2-A_4$ and $A_5-C_3-A_6$ respectively. Nitrogen is drawn in trigonal pyramidal geometry, lying above the plane defined by the three ipso carbons around it *i.e.* on the same side as C_1-A_1 substituent.

Table 3.5. NBO $E(2)$ energies associated with $N_{2p}-(C_{1-3}-A_{1-6})\sigma^*$ interactions.

Cmpd	$E(2)$ (Kcal/mol)					
	N-(C ₁ -A ₁)	N-(C ₁ -A ₂)	N-(C ₂ -A ₃)	N-(C ₂ -A ₄)	N-(C ₃ -A ₅)	N-(C ₃ -A ₆)
20	5.80 (7.84)	6.42 (8.36)	7.76 (10.2)	5.68 (7.16)	6.37 (8.09)	9.69 (13.9)
84	5.83 (7.87)	6.10 (7.98)	7.13 (9.65)	5.61 (7.24)	6.98 (8.68)	10.4 (14.7)
85	6.28 (8.04)	4.69 (6.49)	7.73 (10.1)	4.50 (6.04)	3.40 (4.87)	12.3 (16.2)
86	6.24 (7.89)	5.78 (7.79)	6.67 (9.46)	6.16 (7.30)	7.67 (8.95)	9.86 (14.6)
87	4.72 (6.46)	6.22 (7.93)	7.58 (9.89)	4.58 (6.11)	3.40 (4.86)	12.4 (16.3)
12	4.94 (7.16)	8.37 (10.9)	8.37 (10.9)	4.94 (7.16)	4.94 (7.16)	8.37 (10.9)
105	1.89 (2.64)	9.61 (12.5)	7.44 (9.58)	4.31 (5.87)	3.98 (5.91)	8.74 (11.8)
106	8.18 (10.6)	5.22 (7.32)	5.27 (7.33)	8.14 (10.6)	5.36 (7.45)	8.10 (10.6)
107	13.2 (16.3)	13.2 (16.3)	13.2 (16.3)	13.2 (16.3)	13.2 (16.3)	13.2 (16.3)

The values in parentheses are $E(2)$ energies obtained from HF NBO analysis. The values in italics are $E(2)$ energies associated with the bond to the carbon bearing an ester or amide group. The values in red are $E(2)$ energies associated with σ^* bonding orbitals of substituents (C₁-A₁ in Fig. 3.10) that are on the same side of the plane (defined by the three ipso carbons around nitrogen) with nitrogen.

From NBO analysis of DFT calculations of trialkylamines **12**, **20**, **84-87**, **107**, the orbital occupancy for the lone pair, of electrons, on nitrogen ranged from 1.72 (for planar **107**) to 1.87 (for nearly planar **105**). This deviation is unusual from the normally expected value 2, *i.e.* two electrons. The same was noted in the HF calculation, ranged from 1.81 (for **107**) to 1.90 (for **105**) though slightly higher occupancy than in DFT, see Appendix 10. In both levels of theory this substantial deviation from the expected two-electron occupancy for the lone pair on nitrogen was observed and this further describes and quantifies hyperconjugation effect on these planar and nearly planar trialkylamines.

ii. To delete the corresponding off-diagonal elements of the Fock matrix in the NBO basis and recalculate the energy by a single pass through the SCF evaluator of the modified density matrix to obtain E_{del} .⁹⁸ Usually there is a good linear correlation between the deletion (E_{del}) and perturbation [$E(2)$] energies.⁹⁹ E_{del} energies of trialkylamines **12**, **20**, **84-87**, **107** shown in Table 3.6 were obtained through deleting all six interacting off-diagonal elements associated with N_{2p} - (C₁₋₃-A₁₋₆) σ* interactions shown in Figure 3.10.

Table 3.6. NBO analysis E_{del} and $\sum E(2)$ energies.

Cmpd	E_{del} (kcal/mol)	$\sum E(2)$ (kcal/mol)	N _{LP} Occupancy
20	40.9	54.9	1.97
84	42.5	56.1	1.98
85	39.7	51.7	1.98
86	41.9	56.0	1.97
87	39.1	51.6	1.98
12	42.3	54.2	1.98
105	39.1	48.4	1.98
106	41.6	53.9	1.98
107	67.3	98.0	1.99

Comparison of the calculated E_{del} energies with sum of the six $E(2)$ energies associated with $\text{N}_{2\text{p}}\text{-}(\text{C}_{1-3}\text{-}\text{A}_{1-6})$ σ^* interaction [$\sum E(2)$] in Table 3.5 showed a good correlation as anticipated, further describing hyperconjugation. We also noted that the occupancy of the lone pair of electrons on nitrogen was raised to approximately 2, as normally expected, by this deletion.

4. EXPERIMENTAL

General. THF was distilled over sodium benzophenone ketyl. Ethyl ether, THF and benzene were passed down a column of basic alumina and stored over 4A molecular sieves before use. Methylene chloride and acetonitrile were used as received from a MBRAUN MB SPS-800 solvent purification system. $\text{Rh}_2(\text{OAc})_4$ and $[\text{RuCl}_2(\text{p-cymene})]_2$ were purchased from Strem Chemical Co., Newport, MA and used without further treatment. All other reagents were purchased from Aldrich Chemical Company or Fisher Scientific and used as received.

Melting points were recorded on a capillary Mel-temp[®] apparatus and are uncorrected.

NMR spectra were obtained, usually at ambient temperature, on one of three Bruker NMR spectrometers: (a) Avance II microbay AV-250 operating at 250 MHz for ^1H and 62.9 MHz for ^{13}C , (b) Avance single-bay AV-400 operating at 400 MHz for ^1H and 100 MHz for ^{13}C , with z-axis gradient capability, or (c) Avance II dual bay AV-600 operating at 600 MHz for ^1H and 150 MHz for ^{13}C , with triple-axes gradient capability. TMS was used as an internal chemical shift standard for all solvents except D_2O for ^1H spectra while the center line of CDCl_3 , C_6D_6 , Acetone- d_6 or DMSO was used as the chemical shift standard for ^{13}C spectra. In D_2O , dioxane or acetone- d_6 was used as the internal standard. NMR chemical shifts are reported as parts per million (ppm or δ) and coupling constants are reported in Hz. DEPT experiments were conducted at $\theta = 135^\circ$, which corresponded to a pulse width of 21.4 μsec , generally. Gradient COSY and HSQC experiments were done using standard settings provided by Bruker. We acknowledge and appreciate assistance received from Dr. Mike Meadows, NMR Laboratory Manager.

Mass spectral (MS) data were obtained using either Waters Micromass GCT Premier gc/ms, or Waters Micromass Q-ToF Premier. Dr. Yonnie Wu, Manager of the Mass Spectrometry Laboratory provided essential assistance in obtaining MS results, including GC-MS data, and high-resolution (HRMS) data. The results are presented in terms of intensity percentage relative to the base peak and probable fragmentation product.

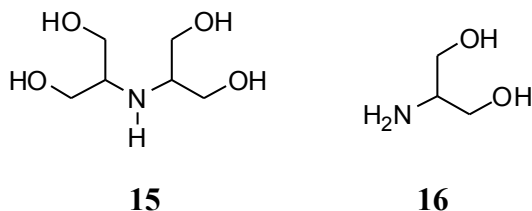
Elemental analyses were performed by Atlantic Microlab, Inc., Norcross, GA.

Single crystal X-ray crystallography was performed on a Bruker SMART APEX CCD X-ray diffractometer with Oxford cryostream low-temperature device, by Drs. Thomas Albrecht-Schmitt, Anna-Gay D. Nelson, Andrea N. Alsobrook, John Gorden, or Mr. Branson Maynard.

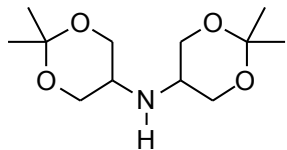
Some reactions were followed by thin-layer chromatography (TLC) using Sorbent Technologies pre-coated silica gel glass plates and visualized using a Mineralight UVGL-25 lamp or by allowing the plate to be covered by a mixture of iodine and silica gel in a closed jar. Column chromatography was performed on Scientific Adsorbents, Inc. silica gel. Gravity columns contained 63 – 200 μ m particle size, 60 Å pore size silica gel. Flash columns contained 32 – 63 μ m particle size, 60 Å pore size silica gel.

Ion exchange column was prepared by soaking the resin (Amberlite, IR-120, H⁺) in 7% HCl solution for 4 h twice. The ion exchange column was set up as an ordinary chromatography column and the column flushed with deionized water until the eluate was neutral, at which time the column was ready for use.³⁵

Gas Chromatography was performed on a Thermo Scientific Trace GC Ultra.



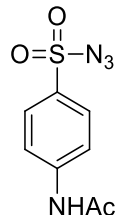
Bis(1,3-dihydroxy-2-propyl)amine, 15 and 1,3-dihydroxy-2-propylamine, 16.³² Under N₂, sodium cyanoborohydride (17.2 g, 274 mmol, 2.93 eq) in 100 mL methanol was added dropwise to a stirred solution of dihydroxyacetone dimer (50.0 g, 278 mmol, 2.97 eq) and ammonium chloride (5.00g, 93.5 mmol) in a mixture of methanol (690 mL) and acetic acid (80.0 mL). The mixture was stirred for 24 h, aqueous hydrochloric acid (2.00 M, 200 mL) was added and stirred for an additional 4 h. The reaction mixture was concentrated on the rotary evaporator and the residue dissolved in methanol (200 mL). Precipitate was filtered off and solvent removed in vacuo. The viscous residue was dissolved in water and applied to an ion-exchange resin (Amberlite, IR-120, H⁺). The column was eluted with water first, and then a solution of aqueous ammonia (1.00 M). The solvent was removed on the rotary evaporator to give brown oil 14.38 g. From the ¹H-NMR spectrum a mixture of two compounds **15** and **16** were observed with a distribution of 81.0% and 19.0% by integration respectively, hence through calculation; **15** (11.6 g, 75.4%). ¹H-NMR (400 MHz, D₂O): δ_H 2.88 (quintet, *J* = 5.4 Hz, 2H), 3.61 (m, 8H). ¹³C-NMR (100 MHz, D₂O): δ_C 57.5 (CH), 61.2 (CH₂); **16** (2.73 g, 17.7 %). ¹H-NMR (400 MHz, D₂O): δ_H 2.98 (quintet, *J* = 6.2 Hz, 1H), 3.55 (m, 4H). ¹³C-NMR (100 MHz, D₂O): δ_C 53.3 (CH), 62.5 (CH₂). HRMS (ESI+): *m/z* Calcd. for C₃H₁₀NO₂ (M⁺ + H) 92.0712; found 92.0686.



17

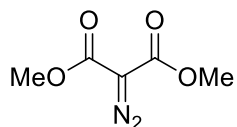
Bis(4, 4-dimethyl-3,5-dioxanyl)amine, 17. Mixture of **15** and **16** (15.1 g) was dissolved in methanol (240 mL), conc. hydrochloric acid (40 mL) was added and stirred for 2 h at rt. The solvent was removed on the rotary evaporator. The residue (16.5 g, 0.142 mol) was dissolved in DMF (30 mL). Under N₂, camphorsulfonic acid (1.63 g) and 2,2-dimethoxypropane (41.7 g, 0.400 mol) were added to the solution. The reaction mixture was stirred at rt for 24 h at which time triethylamine (1.00 mL, 6.67 mmol) was added and stirred for an additional 30 min. Precipitate was filtered off and solvent removed on a rotary evaporator. The residue was treated with ethyl acetate (100 mL) and triethylamine (22.7 mL, 0.151 mol) and the precipitate filtered off. Solvent was removed using the rotary evaporator and the residue extracted using hot hexanes. Crystallization from hexanes gave a colorless solid, **17** (10.1 g, 29.0%). Vacuum sublimation of compound **17** at < 1 mm Hg, 35.0 °C gave colorless needle crystals mp 61.1 °C.
¹H-NMR (400 MHz, D₂O): δ_H 1.50 (s, 12H), 2.92 (tt, *J* = 6.3, 3.9 Hz, 2H), 3.79 (dd, *J* = 12.1, 6.4 Hz), 4.12 (dd, *J* = 12.1, 3.9 Hz). ¹³C-NMR (100 MHz, D₂O): δ_C 22.9, 23.0, 47.5, 63.2, 99.5. ¹H-NMR (250 MHz, CDCl₃) δ_H 1.42 (s, 12H), 2.75 (tt, *J* = 6.8, 4.0 Hz, 2H), 3.63 (dd, *J* = 11.8, 6.8 Hz, 4H), 3.94 (dd, *J* = 11.5, 4.0 Hz, 4H). ¹³C-NMR (100 MHz, CDCl₃) δ_C 23.1 (CH₃), 24.4 (CH₃), 48.7 (CH), 64.5 (CH₂), 98.2 (quat). A crystal 0.292 mm x 0.242 mm x 0.078 mm was selected for X-ray crystallography with 0.71073 Å (Mo Kα) radiation: monoclinic *a* = 5.5325(11) Å, *b* = 12.496(3) Å, *c* = 9.6140(19) Å, α = 90°, β = 102.61(3)°, γ = 90°; *Z* = 2; 2173 reflections were collected, 1582 independent, -7 ≤ *h* ≤ 7, -15 ≤ *k* ≤ 15, -12 < *l* < 10. Crystal

structure determination was performed by Dr. Anna-Gay D. Nelson. Full-matrix least-squares refinement on F^2 , data-to-parameter ratio = 10.3, goodness-of-fit = 0.997, R1 = 0.0506, wR2 = 0.1213 ($I > 2\sigma(I)$), R1 = 0.0569, wR2 = 0.1247 (all data). Full details are given in Appendix 2.



23

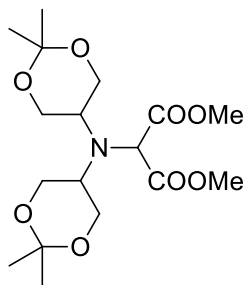
p-Acetamidobenzenesulfonyl azide, 23.³³ To a suspension of *p*-Acetamidobenzenesulfonyl chloride (50.0 g, 0.214 mol) in CH₂Cl₂ (500 mL) containing tetrabutylammonium iodide (0.600 g, 1.62 mmol) at 0 °C, a solution of sodium azide (16.2 g, 0.249 mmol, 1.16 eq) in water (50 mL) was added dropwise and stirred for 24 h at rt. The organic layer was separated, washed twice with water (75 mL), brine (100 mL) and dried over anhydrous Na₂SO₄. Solvent was removed on the rotary evaporator to yield a colorless crystalline solid **23** (48.6 g, 96.3%) mp 109-110 °C (Lit.^{ref} m. p. 106-108 °C).



19

Dimethyl diazomalonate (DDM), 19.³⁵ Under N₂, a stirred solution of dimethyl malonate (14.6 g, 0.111 mol) and *p*-acetamidobenzenesulfonyl azide (29.4 g, 0.122 mol) in acetonitrile (600 mL) at 0 °C, triethylamine (22.2 g, 0.220 mol) was added dropwise. The mixture was allowed to reach rt and stirred for 16 h. The mixture was filtered and the filtrate was evaporated under reduced pressure. The residue was washed with ethyl acetate/hexanes (1:1), filtered, and the solvent was removed on the rotary evaporator. Further purification by silica gel flash column

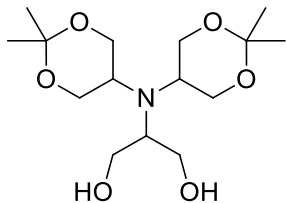
chromatography (ethyl acetate /hexanes 1:4) gave a light yellow oil, **19** (15.6 g, 89.5%). ¹H-NMR (400 MHz, CDCl₃) δ_H 3.85 (s) ¹³C-NMR (100 MHz, CDCl₃) δ_C 52.2 (CH₃), 65.5 (quat), 161.2 (quat). Stored in a freezer (-15 °C), **19** solidified but melted shortly on return to rt. A crystal 0.100 mm x 0.100 mm x 0.080 mm was selected from the solid **19** for X-ray crystallography with 0.71073 Å (Mo Kα) radiation: orthorhombic *a* = 6.3203(7) Å, *b* = 20.753(2) Å, *c* = 11.0951(12) Å, α = 90°, β = 90°, γ = 90°; Z = 8; 7096 reflections were collected, 988 independent, -8 ≤ *h* ≤ 8, -27 ≤ *k* ≤ 27, -14 ≤ *l* ≤ 14. Full-matrix least-squares refinement on F², data-to-parameter ratio = 14.3, goodness-of-fit = 1.165, R1 = 0.0475, wR2 = 0.1272 (*I* > 2σ(*I*)), R1 = 0.0486, wR2 = 0.1283 (all data). Crystal structure determination was performed by Mr. Branson Maynard. Full details are given in Appendix 9.



20

Dimethyl 2-(N,N-bis(4,4-dimethyl-3,5-dioxanyl)amino) malonate, 20.³⁵ Under N₂, a solution of diacetonide amine **17** (7.61 g, 31.1 mmol), dimethyl diazomalonate **19** (5.45 g, 34.2 mmol, 1.10 eq) and Rh₂(OAc)₄ (137 mg, 0.310 mmol, 0.998 mol%) in benzene (62 mL) was refluxed for 4 h, at which time TLC showed absence of diazo compound **19**. The solvent was removed on the rotary evaporator and the residue purified by silica gel flash column chromatography (ethyl acetate/hexanes 1:4) to give a colorless oil that crystallized to give **20** (8.03 g, 68.8%) mp 64-65 °C. ¹H-NMR (400 MHz, CDCl₃) δ_H 1.36(s, 6H), 1.39 (s, 6H), 3.34 (quintet, *J* = 6.5 Hz, 2H), 3.72 (dd, *J* = 12.0, 7.0 Hz, 4H), 3.77 (s, 6H), 3.96 (dd, *J* = 11.9, 5.4 Hz,

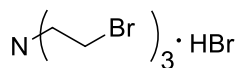
4H), 4.99 (s, 1H). ^{13}C -NMR (100 MHz, CDCl_3) δ_{C} 23.0 (CH_3), 24.3 (CH_3), 51.5 (CH), 52.6 (CH_3), 63.5 (CH_2), 64.3 (CH), 98.2 (quat), 170.3 (quat). A crystal 0.260 mm x 0.184 mm x 0.052 mm was selected for X-ray crystallography with 0.71073 Å (Mo K α) radiation: monoclinic a = 16.6797(12) Å, b = 13.2875(9) Å, c = 18.6656(13) Å, α = 90°, β = 111.3150(10)°, γ = 90°; Z = 1; 39032 reflections were collected, 9600 independent, $-22 \leq h \leq 22$, $-17 \leq k \leq 17$, $-24 \leq l \leq 24$. Full-matrix least-squares refinement on F^2 , data-to-parameter ratio = 20.7, goodness-of-fit = 0.910, R_1 = 0.0667, wR_2 = 0.1553 ($I > 2\sigma(I)$), R_1 = 0.1390, wR_2 = 0.1758 (all data). Crystal structure determination was performed by Dr. Andrea N. Alsobrook. Full details are given in Appendix 1.



21

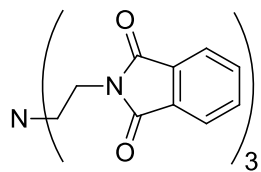
2-(N,N-bis(4,4-dimethyl-3,5-dioxanyl)amino)-1,3-propanediol, 21. Under N_2 , a solution of diacetonideamine-diester **20** (2.20 g, 5.86 mmol) in 5 mL THF was added dropwise to a suspension of LiAlH_4 (1.37 g, 36.1 mmol, 6.16 eq) in 50 mL ice-cooled THF. The reaction was stirred for 12 h and quenched by careful addition of water (1.38 mL), 15% NaOH (1.38 mL) and water (3×1.38 mL) sequentially. The mixture was filtered and filtrate was evaporated on the rotary evaporator. The residue was purified by silica gel flash column chromatography (ethyl acetate) to give a colorless sticky oil **21** (1.75 g, 93.6 %). ^1H -NMR (400 MHz, CDCl_3) δ_{H} 1.38 (s, 6H), 1.44, (s, 6H), 3.15 (m, 2H), 3.27 (m, 1H), 3.47 (dd, J = 10.7, 7.4 Hz, 2H), 3.59 (dd, J = 10.9, 6.05 Hz, 4H), 3.71 (dd, J = 12.0, 5.5 Hz, 4H), 3.82 (dd, J = 12.0, 9.54 Hz, 4H). ^{13}C -NMR (100 MHz, CDCl_3) δ_{C} 20.5 (CH_3), 27.0 (CH_3), 49.2 (CH), 58.9 (CH), 62.4 (CH_2), 63.8 (CH_2),

97.8 (quat). A prism 0.100 mm x 0.100 mm x 0.100 mm was selected from a semi-solid residue of an attempted recrystallization of **21** from ethanol for X-ray crystallography with 0.71073 Å (Mo K α) radiation: monoclinic, $a = 13.6163(12)$ Å, $b = 11.7563(10)$ Å, $c = 10.4340(9)$ Å, $\alpha = 90^\circ$, $\beta = 104.094(2)^\circ$, $\gamma = 90^\circ$; $Z = 4$; 16261 reflections were collected, 4059 independent, $-18 \leq h \leq 18$, $-15 \leq k \leq 14$, $-13 < l < 13$. Full-matrix least-squares refinement on F^2 , data-to-parameter ratio = 19.2, goodness-of-fit = 1.286, $R_1 = 0.1373$, $wR_2 = 0.2327$ ($I > 2\sigma(I)$), $R_1 = 0.1709$, $wR_2 = 0.2467$ (all data). Crystal structure determination was performed by Mr. Branson Maynard. Full details are given in Appendix 7.



25

Tris(2-bromoethyl)amine hydrobromide, 25.³⁷ Triethanolamine (2.00 g, 13.4 mmol) was added dropwise to 48% w/w aqueous hydrobromic acid (6.80 g, 40.2 mmol) at 0 °C. The reaction mixture was refluxed for 4 h, cooled and solvent removed by distillation. Further drying on the vacuum line (< 1 mm Hg) afforded a light brown salt **25** (3.35 g, 60.1%) mp 175-177 °C (lit.³⁷ 214 °C). ¹H-NMR (400 MHz, D₂O, Acetone-d₆ as internal standard δ_H 2.23) δ_H 3.54 (t, $J = 5.3$ Hz, 2H), 4.01 (t, $J = 5.3$ Hz). ¹³C-NMR (100 MHz, D₂O, acetone-d₆ as internal standard δ_C 20.5) δ_C 46.1, 46.4.



27

Tris(2-(N-phthalimidyl)ethyl)amine, 27.³⁸ Under N₂, salt **25** (3.35 g, 8.06 mmol) was dissolved in anhydrous DMF (18 mL) and excess potassium phthalimide (9.95 g, 50.0 mmol)

was added at once. The reaction was heated to 80 °C for 24 h, quenched by cooling in 100 mL mixture of ice and 1% aqueous w/v Na₂CO₃ and stirred for an additional 1 h. Precipitate was filtered, washed with boiling ethanol, and air dried to give a white fluffy solid **27** (1.16 g, 28.9%) mp 225-227 °C. This material did not dissolve in any deuterated solvent for NMR. It was used as it was obtained in the synthesis of **28**.

A. ATTEMPTED MITSUNOBU REACTIONS ON TRIETHANOLAMINE.

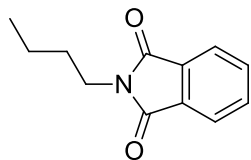
A1. Phthalimide 32. Under N₂ at 0 °C, DIAD (2.02 g, 9.99 mmol, 4.52 eq) was added dropwise over 10 min to a solution of triethanolamine (330 mg, 2.21 mmol, 1.00 eq), triphenylphosphine (2.62 g, 9.99 mmol, 4.52 eq) and phthalimide **32** (980 mg, 6.66 mmol, 3.01 eq) in THF (50 mL). After the addition the mixture was warmed to rt and stirred for 12 h at which time TLC (EtOAc/hexanes 1:1) indicated the presence of triethanolamine and phthalimide. Temperature was raised to 50 °C and stirred for 12 h. Solvent was removed on the rotary evaporator and the residue dissolved in diethyl ether. Precipitate formed (triphenylphosphine oxide) was filtered off, the filtrate concentrated and TLC indicated an inseparable mixture. Purification of the mixture with silica gel flash column chromatography (EtOAc/hexanes 1:1) yielded only DIAD-H₂.

A2. Amine 33, DIAD. Under N₂ at 0 °C, DIAD (3.005 g, 15.1 mmol, 4.51 eq) was added dropwise to a solution of triethanolamine (500 mg, 3.35 mmol, 1.00 eq), **33** (2.05 g, 11.8 mmol, 3.52 eq) and triphenylphosphine (3.96 g, 15.1 mmol, 4.51 eq) in THF (50 mL). After the addition, the mixture was warmed to rt and stirred overnight. The reaction was quenched by addition of conc HCl (15 mL) and stirred for 30 min. The mixture was partitioned between water and CH₂Cl₂. Aqueous phase was concentrated, vacuum pumped (< 1 mm Hg) to dryness and the

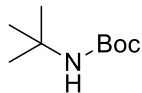
residue dissolved in D₂O for NMR analysis (inconclusive, need to check old 250 NMR files).

KOH treatment of the aqueous phase gave DIAD-H₂.³⁶

A3. Amine 33, DTBAD. Under N₂ at 0 °C, a solution of di-*tert*-butyl azodicarboxylate (DTBAD)⁹ (3.48 g, 15.1 mmol, eq) in THF (10 mL) was added dropwise to a solution of triethanolamine (500 mg, 3.35 mmol, 1.00 eq), **33** (2.05 g, 11.8 mmol, eq) and triphenylphosphine (3.96 g, 15.1 mmol, eq) in THF (50 mL). After the addition, the mixture was warmed to rt and stirred overnight. Reaction was quenched by addition of conc HCl (15 mL), stirred for 2 h and partitioned between water and CH₂Cl₂. The aqueous phase was lyophilized, treated with 50% KOH and the organic phase extracted with CH₂Cl₂. Solvent was removed on the rotary evaporator to give an inseparable mixture.



2-Butylisoindole-1,3-dione.³⁶ To a stirred solution of 1-butanol (1.20 mL, 13.5 mmol) and triphenylphosphine (5.31 g, 20.4 mmol, 1.50 eq) in 50 mL THF under N₂, phthalimide (1.98 g, 13.5 mmol) was added and the mixture cooled to 0 °C. DIAD (4.12 mL, 20.2 mmol) was added dropwise and upon completion the reaction mixture was warmed to rt. The reaction mixture was stirred for 12 h at rt and a further 12 h at 50 °C. Solvent was removed on the rotary evaporator and the residue purified by silica gel flash column chromatography (EtOAc/hexanes 1:1(v/v)) to give a colorless solid (2.44 g, 89.1%) mp 103-104 °C (Lit. 105-107 °C).^{36b} ¹H-NMR (400 MHz, CDCl₃) δ_H 0.91 (t, *J* = 7.3 Hz, 3H), 1.33 (sextet, *J* = 7.7 Hz, 2H), 3.65 (t, *J* = 7.2 Hz, 2H), 7.67 (dd, *J* = 5.4, 3.1 Hz, 2H), 7.80 (dd, *J* = 5.5, 3.0 Hz). ¹³C-NMR (100 MHz, CDCl₃) δ_C 13.6 (CH₃), 20.0 (CH₂), 30.6 (CH₂), 37.7 (CH₂), 123.1 (CH), 132.1 (quat), 133.8 (CH), 168.4 (quat). ¹H and ¹³C NMR shifts are in agreement with published values.

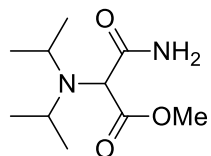


33

tert-Butylcarbamic acid *tert*-butyl ester, 33.⁴⁰ Under N₂, in an oven dried round bottom flask Boc-anhydride (15.0 g, 68.7 mmol) was cooled to 0 °C on an ice-bath and *tert*-butylamine (5.03 g, 68.8 mmol) was added dropwise for 30 min. The reaction was allowed to warm to rt and stirred for 1 h. The flask was vacuum pumped (< 1 mm Hg) to remove volatiles to yield a white solid 33 (11.9 g, 99.8%) mp 46-48 °C. ¹H-NMR (400 MHz, CDCl₃) δ_H 1.53 (s). ¹³C-NMR (100 MHz, CDCl₃) δ_C 27.4, 85.2, 146.8.

B. [RuCl₂(*p*-cymene)]₂-catalyzed “hydrogen borrowing” methodology conversion of alcohols to secondary amines.^{ref}

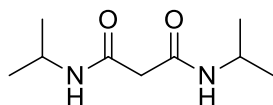
Reaction of triethanolamine with *tert*-butylamine. To an oven-dried, N₂-purged 20 mL screw-capped vial (fitted with a teflon-silicone septum) containing [RuCl₂(*p*-cymene)]₂ (7.70 mg, 0.0125 mmol, 3.81 mol%) and dppf (13.9 mg, 0.0238 mmol, 7.26 mol%) was added *tert*-butylamine (105 μL, 1.00 mmol), triethanolamine (49.0 mg, 0.328 mmol) and DMF (1.00 mL). The reaction mixture was stirred in the closed vial at rt for 10 min and the reflux for 24 h. Solvent was removed on the rotary evaporator and vacuum pumped (< 1 mm Hg) to give an inseparable mixture.



41

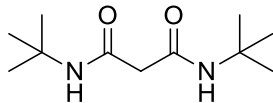
2-(Diisopropylamino)malonamic acid methyl ester, 41. An oven dried three-necked flask was charged with 40 (236 mg, 1.02 mmol) and 10 mL anhydrous methanol and cooled to 0 °C in

an ice-bath. Anhydrous ammonia was bubbled through the stirred solution for 3 h, at which time TLC showed loss of amine **40**. The solvent was removed on the rotary evaporator yielding colorless oil, which consisted of **41** (65% relative to starting material by NMR integration). ¹H-NMR (250 MHz, CDCl₃) δ_H 0.98 (d, *J* = 6.5 Hz, 6H), 1.03 (d, *J* = 6.5 Hz, 6H), 3.32 (quintet, *J* = 6.5, 2H), 3.68 (s, 3H), 4.08 (s, 1H). ¹³C-NMR (63 MHz, CDCl₃) δ_C 20.8, 23.6, 46.9, 52.1, 62.3, 171.3, 174.3.



44

N,N'-Diisopropylmalonamide 44.³⁹ A sealed tube flushed with N₂, and charged with a mixture of dimethyl malonate (9.07 g, 68.6 mmol) and isopropylamine (8.50 g, 0.144 mol, 2.10 eq) was heated at 120 °C for 2 h. The temperature was raised to 160 °C for 7 h. The crude mixture was placed under vacuum (< 1 mm Hg) to remove any volatiles. Recrystallization of the residue from EtOAc gave a white solid **70** (8.73 g, 68.3%) mp 115-117 °C. ¹H-NMR (400 MHz, CDCl₃) δ_H 1.16 (d, *J* = 6.4 Hz, 12H), 3.36 (s, 2H), 4.24 (m, 2H), 8.17 (br d, *J* = 7.2 Hz, 2H). ¹³C-NMR (100 MHz, CDCl₃) δ_C 22.7 (CH₃), 42.1 (CH), 42.3 (CH₂), 167.7 (quat). ¹H and ¹³C NMR shifts are in agreement with published values.³⁹



45

N,N'-Di-*tert*-butylmalonamide 45.³⁹ A sealed tube flushed with N₂, and charged with a mixture of dimethyl malonate (10.0 g, 75.7 mmol) and *tert*-butylamine (12.2 g, 167 mmol, 2.21 eq) was heated at 120 °C for 2 h, then at 160 °C for 7 h. The crude mixture was cooled and vacuum pumped (< 1 mm Hg) to remove any volatiles, affording a pale yellow solid **45** (12.0 g,

73.8%) mp 67-69 °C. ^1H -NMR (400 MHz, CDCl_3) δ_{H} 1.35 (s, 18H), 3.03 (s, 2H), 7.04 (2H). ^{13}C -NMR (100 MHz, CDCl_3) δ_{C} 28.7, 45.1, 51.4, 167.3. ^1H and ^{13}C NMR shifts are in agreement with published values.³⁹

C. Attempted reactions of *p*-acetamidobenzenesulfonyl azide with **44**, **45** and **DDDU**.^{ref}

C1. Under N_2 at 0 °C, triethylamine (1.08 g, 10.7 mmol, 1.99 eq) was added dropwise to the chilled solution of **44** (1.00 g, 5.37 mmol, 1.00 eq) and *p*-acetamidobenzenesulfonyl azide (1.44 g, 6.00 mmol, 1.12 eq) in acetonitrile (30 mL). The reaction was warmed to rt and stirred for 16 h. Precipitate formed was filtered off, solvent was removed on the rotary evaporator and the residue dissolved in EtOAc/hexanes (1:1). Precipitate was filtered off, filtrate was concentrated and purified by silica gel flash column chromatography (EtOAc/hexanes 1:1) to recover **44** and *p*-acetamidobenzenesulfonyl azide.

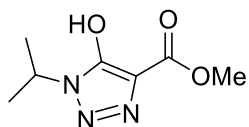
C2. Under N_2 at 0 °C, triethylamine (2.36 g, 23.3 mmol, 4.99 eq) was added dropwise to the chilled solution of **45** (1.00 g, 4.67 mmol, 1.00 eq) and *p*-acetamidobenzenesulfonyl azide (1.15 g, 4.79 mmol, 1.03 eq) in acetonitrile (25 mL). The reaction was warmed to rt and stirred overnight. Precipitate formed was filtered off, solvent was removed on the rotary evaporator and the residue dissolved in EtOAc/hexanes (1:1). Precipitate was filtered off, filtrate was concentrated and purified by silica gel flash column chromatography (EtOAc/hexanes 1:1) to recover **45** and *p*-acetamidobenzenesulfonyl azide.

C3. Under N_2 at 0 °C, DABCO (1.20 g, 10.7 mmol, 1.99 eq) was added dropwise to the chilled solution of **44** (1.00 g, 5.37 mmol, 1.00 eq) and *p*-acetamidobenzenesulfonyl azide (1.44 g, 6.00 mmol, 1.12 eq) in acetonitrile (30 mL). The reaction was warmed to rt and stirred for 12 h at which time TLC (EtOAc/hexanes 1:1) indicated presence of **44** and *p*-acetamido-benzenesulfonyl azide.

C4. Under N₂ at 0 °C, DABCO (1.20 g, 10.7 mmol, 1.99 eq) was added dropwise to the chilled solution of **44** (1.00 g, 5.37 mmol, 1.00 eq) and *p*-acetamidobenzenesulfonyl azide (1.44 g, 6.00 mmol, 1.12 eq) in acetonitrile (30 mL). The reaction was warmed to rt and stirred for 3 weeks at which time TLC (EtOAc/hexanes 1:1) indicated presence of **70** and *p*-acetamido-benzenesulfonyl azide.

C5. Under N₂ at 0 °C, a solution of DMAP (2.38 g, 19.5 mmol, 1.99 eq) in acetonitrile (15 mL) was added dropwise to the stirred chilled solution of **75** (1.46 g, 4.97 mmol, 1.00 eq) and *p*-acetamidobenzenesulfonyl azide (1.55 g, 6.45 mmol, 1.12 eq) in acetonitrile (25 mL). The reaction was warmed to rt and reaction progress followed by TLC (EtOAc/hexanes 1:1) which indicated presence of **75** and *p*-acetamidobenzenesulfonyl azide after 12 h.

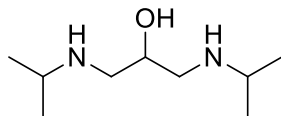
C6. Under N₂, in an oven dried round bottom flask a stirred solution of **75** (508 mg, 1.72 mmol, 1.00 eq) and DBU (1.30 g, 8.54 mmol, eq) in acetonitrile (10 mL) was chilled in an ice-bath (0 °C) for 10 min and *p*-acetamidobenzenesulfonyl azide (615 mg, 2.56 mmol, eq) was added at once. The reaction was warmed to rt and reaction progress followed by TLC (EtOAc/hexanes 1:1) which indicated presence of **75** and *p*-acetamidobenzenesulfonyl azide after 24 h.



48

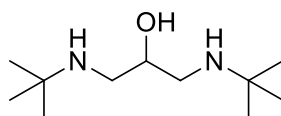
5-Hydroxy-1-isopropyl-1H-[1,2,3]triazole-4-carboxylic acid methyl ester, 48.⁴³ In a round bottom flask a mixture of dimethyl diazomalonate (7.44 g, 47.1 mmol) and isopropyl-amine (16.7 g, 282 mmol, 5.99 eq) was stirred at rt for 12 h. Precipitate formed was filtered and air-dried to give a yellow solid (8.51 g, 97.6%) mp 163-165 °C. ¹H-NMR (600 MHz, DMSO-d₆)

δ_{H} 1.18 (d, J = 6.6 Hz, 6H), 1.30 (d, J = 6.6 Hz, 6H), 3.26 (m, 1H), 3.41 (br s), 3.61 (s, 3H), 4.32 (m, 1H). ^{13}C -NMR (151 MHz, DMSO-d₆) δ_{C} 20.9, 22.3, 43.2, 44.6, 49.9, 116.9, 159.32, 163.7. HRMS (ESI+): *m/z* Calcd for C₇H₁₂N₃O₃ (M⁺+H) 186.0879; found 186.0890.



50

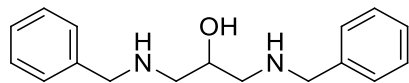
1,3-Bis(isopropylamino)propan-2-ol, 50.⁴² In a sealed tube flushed with N₂, a mixture of epichlorohydrin (9.25 g, 0.100 mol) and isopropylamine (11.8 g, 0.200 mol) was heated at 120 °C for 2 hr and the temperature raised to 160 °C for 16 h. The reaction mixture was cooled, dissolved in 50 mL CH₂Cl₂, washed twice with 2 M NaOH and once with 50 mL satd brine. The CH₂Cl₂ layer was dried over anhydrous MgSO₄ and the solvent removed on the rotary evaporator to yield a brown oil **50** (11.5 g, 65.8%). ^1H -NMR (400 MHz, CDCl₃) δ_{H} 1.06 (d, J = 6.3 Hz), 2.51 (dd, J = 11.8, 8.4 Hz, 2H), 2.71 (dd, J = 11.8, 3.48 Hz, 2H), 2.78 (septet, 2H), 3.69 (tt, J = 8.4, 3.5 Hz, 1H). ^{13}C -NMR (100 MHz, CDCl₃) δ_{C} 23.0 (CH₃), 23.0 (CH₃), 48.8 (CH), 51.3 (CH₂), 69.9 (CH).



51

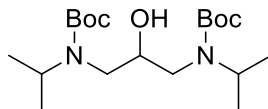
1,3-Bis(tert-butylamino)propan-2-ol, 51.⁴² In a sealed tube flushed with N₂, a mixture of epichlorohydrin (9.25 g, 0.100 mol), 50% aqueous KOH (10.0 mL) and isopropylamine (14.6 g, 0.200 mol) was heated at 120 °C for 12 h. The crude mixture was dissolved in 200 mL CH₂Cl₂ and salt filtered off. The solvent was removed on the rotary evaporator and residue recrystallized from hexanes to yield a white solid **51** (18.7 g, 92.6%) mp 59-60 °C (Lit.^{42d} 59-61 °C). ^1H -NMR

(400 MHz, CDCl₃) δ_H 1.03 (s, 18H), 2.43 (dd, *J* = 11.4, 8.3 Hz, 2H), 2.55 (dd, *J* = 11.4, 3.6 Hz, 2H), 3.39 (br s), 3.57 (m, 1H). ¹³C-NMR (100 MHz, CDCl₃) δ_C 28.9 (CH₃), 46.8 (CH₂), 50.3 (quat), 69.7 (CH).



52

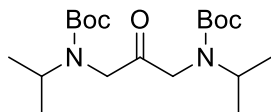
1,3-Bis(benzylamino)propan-2-ol, 52.⁴⁵ At 0 °C, benzylamine (40.6 g, 379 mmol, 3.51 eq) was added slowly to epichlorohydrin (10.0 g, 108 mmol) and stirred at rt for 5 h. Under N₂, the reaction mixture was refluxed for 12 h. On cooling a colorless solid precipitated. Aqueous 2 N NaOH solution was added until precipitate disappeared and the organic layer was extracted with CH₂Cl₂. Solvent and residual benzylamine were removed by vacuum distillation (47 °C, 0.3 mm Hg). The residue was dissolved in ethanol and recrystallized as HCl salt by addition of conc. HCl. The white solid was stirred with 50% aqueous NaOH, extracted with diethyl ether, dried over anhydrous Mg₂SO₄ and solvent removed on the rotary evaporator to yield a colorless oil **52** (13.8 g, 47.3%). ¹H-NMR (400 MHz, CDCl₃) δ_H 2.56 (dd, *J* = 12.0, 8.4 Hz, 2H), 2.67 (dd, *J* = 12.0, 3.5 Hz, 2H), 3.76 (AB quartets, *J* = 13.2 Hz, Δv = 1.03 Hz, 4H), 7.29-7.37 (m, 10H). ¹³C-NMR (100 MHz, CDCl₃) δ_C 53.0 (CH₂), 53.9 (CH₂), 68.5 (CH), 127.3 (CH), 128.4 (CH), 128.6 (CH), 139.7 (quat). ¹H and ¹³C NMR shifts are in agreement with published values.⁴⁵



53

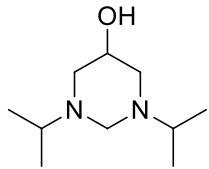
[3-(tert-Butoxycarbonylisopropylamino)-2-hydroxypropyl]isopropylcarbamic acid *tert*-butyl ester, 53.⁴⁰ Under N₂, a round-bottomed flask with Boc-anhydride (11.3 g, 30.1 mmol, 3.00 eq) was cooled in an ice-bath and aminoalcohol **50** (3.00 g, 17.2 mmol) was added slowly.

The reaction was warmed to room temperature, stirred for 1 h and vacuum pumped (< 1 mm Hg). The residue was purified by silica gel flash column chromatography (EtOAc/hexanes) to give a yellow oil **53** (6.23 g, 96.7%). It was used without further characterization to synthesize **54**.



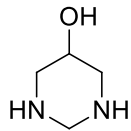
54

[3-(tert-Butoxycarbonylisopropylamino)-2-oxopropyl]isopropylcarbamic acid tert-butyl ester, 54. Under N₂, oxalyl chloride (2.00 g, 15.8 mmol, 1.83 eq) in 20 mL CH₂Cl₂ was chilled to -78 °C and anhydrous DMSO (1.60 g, 17.0 mmol, 1.97 eq) in 4 mL CH₂Cl₂ was added slowly over 5 min. Amino alcohol **53** (3.00 g, 8.63 mmol, 1.00 eq) in 8 mL CH₂Cl₂ was added dropwise over 10 min with temperature below -50 °C. The turbid reaction mixture was stirred for 15 min at which time triethylamine (3.44 g, 34.0 mmol, 3.94 eq) was added and stirred for an additional 5 min at rt. The reaction mixture was diluted with 50 mL CH₂Cl₂ and washed with 50 mL water twice. The organic layer was dried over anhydrous Na₂SO₄, filtered and solvent removed on the rotary evaporator to yield a white powder **54** (2.82 g, 94.6%) mp 114-116 °C. ¹H-NMR (400 MHz, CDCl₃, 323 K) δ_H 1.10 (d, *J* = 6.7 Hz, 12H), 1.44 (s, 18H), 3.88 (br s, 4H), 4.30 (br s, 2H). ¹³C-NMR (100 MHz, CDCl₃ 323 K) δ_C 20.8, 28.6, 46.2, 46.8, 49.7, 80.2, 155.3, 203.2. HRMS (ESI+): *m/z* Calcd for C₁₉H₃₇N₂O₅ (M⁺+H): 373.2702, found 373.2654.



59

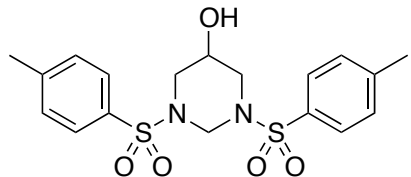
1,3-Diisopropyl-2,4,6-hexahydropyrimidin-5-ol, 59.⁴⁴ 37% aqueous formaldehyde (0.610 mL, 9.06 mmol, 0.981 eq) was added dropwise to a stirred solution of diamino alcohol **50** (1.61 g, 9.24 mmol) in water (2 mL). The reaction mixture was stirred at rt for 12 h. Solvent was removed on the rotary evaporator and vacuum pumped (< 1 mm Hg) at rt for 2 h to yield a brown oil **59** (1.71 g, 99.4%). ¹H-NMR (400 MHz, CDCl₃) δ_H 1.03 (d, *J* = Hz, 6H), 1.05 (d, *J* = Hz, 6H), 2.44 (br d, *J* = 11.0 Hz, 2H), 2.72 (br d, *J* = 9.04, 2H), 2.78 (quintet, *J* = 6.6 2H), 3.02 (br d, *J* = 8.3 Hz, 1H), 3.49 (br d, *J* = 7.7 Hz, 1H), 3.80 (br s, 1H). ¹³C-NMR (100 MHz, CDCl₃) δ_C 18.2 (CH₃), 19.3 (CH₃), 52.7 (CH), 53.7 (CH₂), 64.3 (CH), 70.6 (CH₂). HRMS (ESI+): *m/z* Calcd for C₁₀H₂₃N₂O (M⁺+H): 187.1810, found 187.1808.



61

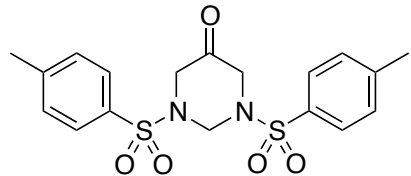
5-Hydroxy-2,4,6-hexahydropyrimidine, 61.⁴⁴ 37% aqueous formaldehyde (5.29 mL, 66.7 mmol) was added dropwise to a stirred solution of 1,3-diamino-2-propanol (6.00 g, 66.7 mmol) in water (12 mL). The reaction mixture was stirred at rt for 48 h and then lyophilized. The crude residue was purified by vacuum sublimation (100 °C/0.5 mm Hg) to yield a white solid **61** (4.44 g, 65.2%) mp 101-103 °C. ¹H-NMR (400 MHz, CDCl₃) δ_H 2.08 (br s, 3H), 2.89 (dd, *J* = 13.3, 4.7 Hz, 2H), 3.08 (dd, *J* = 13.3, 2.5 Hz, 2H), 3.55 (septet, *J* = 2.6, 1H), 3.73 (d, *J* = 12.3 Hz, 1H),

3.79 (d, $J = 12.4$ Hz, 1H). ^{13}C -NMR (100 MHz, CDCl_3) δ_{C} 51.6, 62.1, 64.3. ^1H and ^{13}C NMR shifts are in agreement with published values.⁴⁴



63

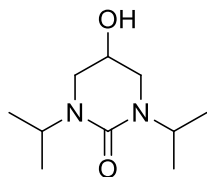
1,3-Bis(tosyl)-2,4,6-hexahydropyrimidin-5-ol, 63.^{44a} To a stirred solution of **61** (1.00 g, 9.79 mmol) in water (10 mL) containing potassium carbonate (2.70 g, 19.5 mmol) was added a solution of tosyl chloride (3.74 g, 19.6 mmol) in THF (10 mL). The reaction mixture was stirred at rt for 3 h and the solvent removed *in vacuo*. The residue was dissolved in chloroform (100 mL), washed with satd NaHCO_3 and dried over anhydrous MgSO_4 . Solvent was removed on the rotary evaporator and the residue recrystallized from ethanol to afford a white solid **63** (2.16 g, 53.7%) mp 176-178 °C (Lit.^{44a} 182-183 °C). ^1H -NMR (400 MHz, CDCl_3) δ_{H} 1.83 (br s, 1H), 2.44 (s, 6H), 3.11 (dd, $J = 13.1, 6.3$ Hz, 2H), 3.30 (dd, $J = 13.2, 3.4$ Hz, 2H), 3.54 (m, 1H), 4.62 (AB quartets, $J = 12.4$ Hz, $\Delta\nu = 26.1$ Hz, 2H), 7.34 (d, $J = 8.0$ Hz, 4H), 7.73 (d, $J = 8.3$ Hz, 4H). ^{13}C -NMR (100 MHz, CDCl_3) δ_{C} 21.6, 50.8, 60.7, 61.8, 127.6, 130.0, 134.8, 144.4. ^1H and ^{13}C NMR shifts are in agreement with published values.^{44a}



64

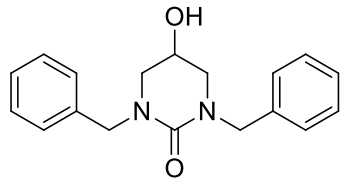
1,3-Bis(tosyl)-2,4,6-hexahydropyrimidin-5-one, 64.^{44a} A stirred solution of **63** (13.3 g, 32.4 mmol) in acetone (300 mL) at 0 °C was added dropwise to a mixture of CrO_3 (7.40 g, 74.0

mmol) in water (18.5 mL) containing concentrated sulfuric acid (9.25 mL). After addition was complete, the reaction mixture was stirred vigorously at rt for 12 h. Water was added to dissolve precipitated salts and the solution was extracted with CH₂Cl₂ (3 x 100 mL). The combined organic layers were washed with satd aq NaHCO₃ solution, water and dried over magnesium sulfate. Solvent was removed using a rotary evaporator and the residue recrystallized from acetone-hexanes to yield a colorless solid **64** (3.33 g, 25.2%) mp 146-148 °C (Lit. 148 °C). ¹H-NMR (400 MHz, CDCl₃) δ_H 2.44 (s, 6H), 3.65 (s, 4H), 4.89 (s, 2H), 7.34 (d, *J* = 7.9 Hz, 4H), 7.68 (d, *J* = 8.5 Hz, 4H). ¹³C-NMR (100 MHz, CDCl₃) δ_C 21.6, 50.8, 60.7, 61.9, 127.6, 130.0, 134.8, 144.4, 197.0. ¹H and ¹³C NMR shifts are in agreement with published values.^{44a}



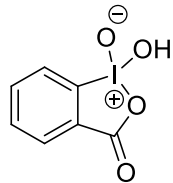
65

5-Hydroxy-1,3-diisopropyl-4,6-tetrahydropyrimidin-2-one, 65.^{45a} Under N₂, bis(4-nitrophenyl) carbonate (4.27 g, 14.0 mmol) and diamino alcohol **50** (4.00 g, 23.0 mmol), were refluxed in methylene chloride (250 mL) for 24 h. The cooled reaction mixture was washed with satd. citric acid and five times with 2 M NaOH. Solvent was removed on the rotary evaporator and the residue purified by vacuum filtration through a plug of silica gel (EtOAc/hexanes 1:1) to yield a yellow oil **65** (391 mg, 14.0%). ¹H-NMR (400 MHz, CDCl₃) δ_H 1.09 (d, *J* = 6.8 Hz, 6H), 1.08 (d, *J* = 6.8 Hz, 6H), 3.08 (dd, *J* = 11.6, 5.1 Hz, 2H), 3.24 (dd, *J* = 11.6, 3.5 Hz, 2H), 4.11 (m, 1H), 4.74 (septet, 2H). ¹³C-NMR (100 MHz, CDCl₃) δ_C 19.6 (CH₃), 19.7 (CH₃), 44.6 (CH), 44.7 (CH₂), 61.9 (CH), 154.8 (quat). HRMS (ESI+): *m/z* Calcd for C₁₀H₂₁N₂O₂ (M⁺ + H) 201.1603; found 201.1581.



66

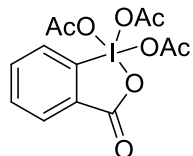
1,3-Dibenzyl-5-hydroxy-4,6-tetrahydropyrimidin-2-one, 66.⁴⁵ Under N₂, bis(4-nitrophenyl) carbonate (9.13 g, 30.0 mmol) and diamino alcohol **52** (13.8 g, 51.0 mmol), were refluxed in CH₂Cl₂ (1 L) for 24 h. The reaction mixture was washed once with satd citric acid and five times with 2 M NaOH. Solvent was removed on the rotary evaporator and the residue was recrystallized from diethyl ether/CH₂Cl₂ to yield a white solid **66** (8.17 g, 92.0%) mp 114-115 °C (Lit. 115 °C).⁴⁵ ¹H-NMR (400 MHz, CDCl₃) δ_H 3.03 (dd, *J* = 11.9, 4.8 Hz, 2H), 3.22 (d, *J* = 12.0 Hz, 2H), 3.90 (br s, 1H), 4.38 (d, *J* = 15.2 Hz, 2H), 4.57 (d, *J* = 14.8 Hz, 4H), 7.16-7.20 (m, 10H). ¹³C-NMR (100 MHz, CDCl₃) δ_C 50.5, 50.6, 60.7, 126.3, 126.9, 127.6, 136.9, 154.8. ¹H and ¹³C NMR shifts are in agreement with published values.^{45a}



DMP-1

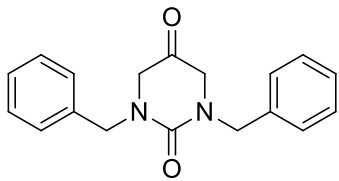
1-Hydroxy-1,2-benziodoxol-3(1H)-one 1-oxide, DMP-1.⁴⁷ To a three-necked round bottom flask fitted with a thermometer, was charged with potassium bromate (20.0 g, 120 mmol) and 2 M sulfuric acid (95 mL), the resulting clear solution was heated in a 60 °C oil bath. To this solution 2-iodobenzoic acid (10.0 g, 80.6 mmol) was added in two portions over 20 min. The internal temperature was maintained at 65 °C for 2.5 h. The reaction was cooled to 2-3 °C in an ice-water bath. The resulting precipitate was collected by vacuum filtration, washed successively

with cold water (100 mL), ethanol (2 x 20 mL) and finally cold water (100 mL). The resulting wet solid was **DMP-1** (22.6 g, 99.6%) mp 232-233 °C (Lit. 233 °C). ^{47b} ¹H-NMR (400 MHz, DMSO-d₆) δ_H 7.71 (t, J = 7.6 Hz, 1H), 7.92 (t, J = 7.2 Hz, 1H), 8.03 (t, J = 8.4 Hz, 1H), 8.15 (d, J = 8.0 Hz, 2H). ¹H NMR shifts are in agreement with published values.⁴⁷ Iodinane oxide **DMP-1** was used immediately to synthesis Dess-Martin periodinane **DMP**.



DMP

1,1,1-Triacetoxy-1,1-dihydro-1,2-benziodoxol-3(1H)-one, DMP.⁴⁷ To a three-necked round bottom flask fitted with a thermometer and a N₂ inlet, iodinane oxide **DMP-1** (22.6 g, 80.6 mmol), glacial acetic acid (40 mL) and acetic anhydride (80 mL) were added. The temperature of the stirred reaction mixture was raised to 85 °C over 30 min and maintained at this temperature until all solids dissolved to afford a clear yellow solution. Heating and stirring were discontinued and reaction mixture allowed to cool slowly to rt for 24 h. Colorless crystals formed, which were filtered under vacuum and washed with anhydrous diethyl ether (3 x 20 mL) to yield a white solid **DMP** (27.6 g, 80.8%) mp 134-135 °C (Lit. 134-135 °C). ^{47c} ¹H-NMR (250 MHz, CDCl₃) δ_H 2.01 (s, 6H), 2.23 (s, 3H), 7.92 (td, J = 7.4, 1.0 Hz, 1H), 8.10 (td, J = 8.0, 1.8 Hz, 1H), 8.28-8.34 (m, 2H). ¹³C-NMR (63 MHz, CDCl₃) δ_C 20.3, 20.4, 126.0, 126.5, 131.8, 133.8, 135.8, 142.3, 166.1, 174.0, 175.7. ¹H and ¹³C NMR shifts are in agreement with published values.^{47c}



67

1,3-Dibenzyl-4,6-tetrahydropyrimidine-2,5-dione, 67.⁴⁵ Under N₂, a mixture of alcohol **66** (1.33 g, 4.49 mmol) and freshly prepared Dess-Martin periodinane **DMP** (2.86, 6.74 mmol, 1.50 eq) was stirred in CH₂Cl₂ (12 mL) saturated with water for 12 h. The reaction was quenched by addition of satd aq NaHCO₃ (10 mL) followed by satd aq Na₂S₂O₃ (10 mL) and stirred until the precipitate completely dissolved. The organic layer was extracted with CH₂Cl₂, dried over anhydrous MgSO₄, filtered, and solvent removed on the rotary evaporator. The residue was purified by vacuum filtration through a short plug of silica gel (diethyl ether/hexanes 1:1) to yield a yellow oil that solidified upon standing **67** (1.11 g, 84.1%) mp 72-73 °C (Lit. 73 °C).^{45a} ¹H-NMR (250 MHz, CDCl₃) δ_H 3.73 (s, 4H), 4.64 (s, 4H), 7.36 (m, 10H). ¹³C-NMR (100 MHz, CDCl₃) δ_C 51.2, 55.0, 127.8, 128.4, 128.8, 136.6, 158.1, 201.4. ¹H and ¹³C NMR shifts are in agreement with published values.^{45a}

D. ATTEMPTED REDUCTIVE AMINATION REACTIONS OF KETONE **54, **64** AND **67**.**⁶⁰

D1. Ketone **80, NaBH₃CN, NH₄Cl, no added acid.** Under N₂, a solution of sodium cyanoborohydride (51.5 mg, 0.820 mmol, 3.05 eq) in methanol (2.00 mL) was added dropwise to a solution of **54** (306 mg, 0.821 mmol, 3.05 eq) and ammonium chloride (14.4 mg, 0.269 mmol, 1.00 eq) in methanol (5.00 mL) and the mixture stirred for 3 days. Solvent was removed on the rotary evaporator and the residue purified by silica gel flash column chromatography (EtOAc/hexanes 1:1) to give a white solid **54** (249 mg).

D2. Ketone 80, NaBH₃CN, NH₄Cl, acetic acid. Under N₂, a solution of sodium cyanoborohydride (105 mg, 1.67 mmol, 2.98 eq) in methanol (5.00 mL) was added dropwise to a solution of **54** (623 mg, 1.67 mmol, 2.98 eq) and ammonium chloride (30.0 mg, 0.561 mmol, 1.00 eq) in methanol (5.00 mL) and acetic acid (0.500 mL). The mixture was stirred at rt for 20 h, quenched with 5% aq NaOH (5 mL) and extracted with CH₂Cl₂ (2 x 10 mL). Combined organic phase was washed with water (10 mL), satd brine (10 mL) and dried over anhydrous Na₂SO₄. Solvent was removed on the rotary evaporator to give a white solid **54** (452 mg).

D3. Ketone 80, NaBH(OAc)₃, NH₄Cl, 3 days. Under N₂, sodium triacetoxyborohydride (174 mg, 0.821 mmol, 3.05 eq) was added at once to a solution of **54** (306 mg, 0.821 mmol, 3.05 eq) and ammonium chloride (14.4 mg, 0.269 mmol, 1.00 eq) in acetonitrile (5.00 mL) and the mixture stirred at rt for 3 days. Solvent was removed on the rotary evaporator to give an intractable mixture.

D4. Ketone 80, NaBH(OAc)₃, NH₄OAc, 2 days. Under N₂, sodium triacetoxyborohydride (407 mg, 1.92 mmol, 1.50 eq) was added at once to a solution of **54** (477 mg, 1.28 mmol, 1.00 eq) and ammonium acetate (97.7 mg, 1.28 mmol, 1.00 eq) in acetonitrile (5.00 mL) and the cloudy mixture stirred at rt for 48 h. The reaction mixture was quenched with 2 M NaOH until cloudiness disappeared and extracted with diethyl ether (2 x 10 mL). The combined organic phase was washed with water (10 mL), brine (10 mL), dried over anhydrous Na₂SO₄ and the solvent removed to give a white solid **54** (374 mg).

D5. Ketone 90, NaBH(OAc)₃, NH₄OAc. Under N₂, sodium triacetoxyborohydride (420 mg, 1.98 mmol, 1.50 eq) was added at once to a solution of **64** (540 mg, 1.32 mmol, 1.00 eq) and ammonium acetate (102 mg, 1.28 mmol, 1.00 eq) in acetonitrile (5.00 mL) and the cloudy mixture stirred at rt for 20 h. The reaction mixture was quenched with 2 M NaOH until

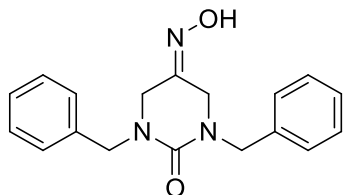
cloudiness disappeared and extracted with diethyl ether (2 x 10 mL). The combined organic phase was washed with water (10 mL), brine (10 mL), dried over anhydrous Na₂SO₄ and the solvent removed to give a colorless oil **64** (337 mg).

D6. Ketone 90, NaBH(OAc)₃, PhCH₂NH₂. Under N₂, sodium triacetoxyborohydride (391 mg, 1.85 mmol, 1.50 eq) was added at once to a solution of **64** (500 mg, 1.23 mmol, 1.00 eq) and benzylamine (144 mg, 1.35 mmol, 1.10 eq) in acetonitrile (5.00 mL) and the cloudy mixture stirred at rt for 12 h. The reaction mixture was quenched with 2 M NaOH until cloudiness disappeared and extracted with diethyl ether (2 x 10 mL). The combined organic phase was washed with water (10 mL), brine (10 mL), dried over anhydrous MgSO₄ and the solvent removed to give a yellow oil (460 mg) a mixture of **64** and benzylamine.

D7. Ketone 93, NaBH(OAc)₃, NH₄OAc. Under N₂, sodium triacetoxyborohydride (248 mg, 1.17 mmol, 1.50 eq) was added at once to a stirred solution of **67** (230 mg, 0.782 mmol, 1.00 eq) and ammonium acetate (60.3 mg, 0.782 mmol, 1.00 eq) in acetonitrile (3.00 mL) and the cloudy mixture stirred at rt for 20 h. The reaction mixture was quenched with satd NaHCO₃ until cloudiness disappeared and extracted with diethyl ether (2 x 10 mL). The combined organic phase was washed with water (10 mL), brine (10 mL), dried over anhydrous MgSO₄ and the solvent removed to give a yellow oil, **67** (195 mg).

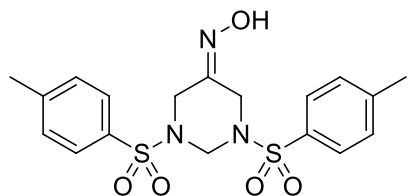
D8. Ketone 93, NaBH(OAc)₃, PhCH₂NH₂. Under N₂, sodium triacetoxyborohydride (130 mg, 0.612 mmol, 1.50 eq) was added at once to a stirred solution of **67** (180 mg, 0.612 mmol, 1.00 eq) and benzylamine (72.1 mg, 0.673 mmol, 1.00 eq) in acetonitrile (5.00 mL) and the cloudy mixture stirred at rt for 12 h. The reaction mixture was quenched with 2 M NaOH until cloudiness disappeared and extracted with diethyl ether (2 x 10 mL). The combined organic

phase was washed with water (10 mL), brine (10 mL), dried over anhydrous MgSO₄ and the solvent removed to give a yellow oil (157 mg) a mixture of **67** and benzylamine.



68

1,3-Dibenzyl-4,6-tetrahydropyrimidin-2,5-dione monooxime, 68.⁴⁸ Into a stirred solution of hydroxylamine hydrochloride (3.77 g, 54.6 mmol) in 4% NaOH (35 mL), ketone **67** (1.10 g, 3.74 mmol) in ethanol (20 mL) was added and the mixture refluxed for 15 min. The reaction mixture was extracted with CH₂Cl₂, the organic phase dried over anhydrous MgSO₄, filtered, and solvent removed on the rotary evaporator to give a colorless oil **68** (0.840 g, 72.4%). ¹H-NMR (400 MHz, CDCl₃) δ_H 3.72 (s, 2H), 3.97 (s, 2H), 4.60 (s, 4H), 7.29-7.33 (m, 10H). ¹³C-NMR (100 MHz, CDCl₃) δ_C 41.5, 46.8, 51.3, 51.5, 127.55, 127.57, 128.2, 128.3, 128.66, 128.68, 137.02, 137.04, 150.5, 158.5.



69

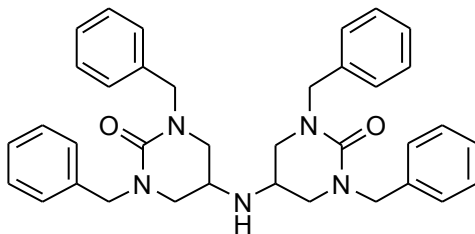
1,3-Bis(tosyl)-2,4,6-hexahydropyrimidin-5-one oxime, 69.⁴⁸ Into a stirred solution of hydroxylamine hydrochloride (1.00 g, 14.5 mmol) in 4% NaOH (10 mL), ketone **64** (1.00 g, 2.45 mmol) in ethanol (5 mL) was added and the mixture refluxed for 15 min. The reaction mixture was extracted with CH₂Cl₂, dried over anhydrous MgSO₄, filtered and solvent removed on the rotary evaporator to give a colorless oil **69** (0.860 g, 82.7%). ¹H-NMR (400 MHz, CDCl₃) δ_H

2.42 (s, 3H), 2.43 (s, 3H), 3.69 (s, 2H), 4.05 (s, 2H), 4.76 (s, 2H), 7.32 (dd, $J = 7.8, 7.1$ Hz, 4H), 7.70 (dd, $J = 12.9, 8.3$, 4H). ^{13}C -NMR (100 MHz, CDCl_3) δ_{C} 21.7 (CH_3), 41.3 (CH_2), 47.0 (CH_2), 60.8 (CH_2), 127.9 (CH), 127.9 (CH), 129.8 (CH), 130.0 (CH), 133.6 (quat), 134.1 (quat), 144.6 (quat), 153.0 (quat).

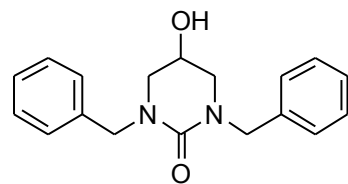
E. ATTEMPTED REDUCTION OF OXIMES **68** AND **69**.⁵⁹

E1. Compound 68. Under N_2 , a solution of **68** (840 mg, 2.72 mmol, 1.00 eq), ammonium formate (3.43 g, 54.4 mmol, 20.0 eq) and prewashed (with 1% HCl) zinc dust (1.78 mg, 27.2 mmol, 10.0 eq) in methanol (6 mL) was refluxed. The reaction was followed by TLC (EtOAc) and stopped after 24 h with **68** present.

E2. Compound 95. Under N_2 , a solution of **69** (161 mg, 0.380 mmol, 1.00 eq), ammonium formate (95.9 mg, 1.52 mmol, 4.00 eq) and prewashed zinc dust (49.7 mg, 0.760 mmol, 2.00 eq) in methanol (10 mL) was refluxed. The reaction was followed by TLC (EtOAc) and stopped after 24 h with **69** present.



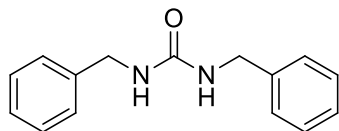
70



65

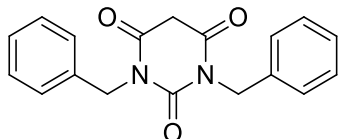
Bis(1,3-dibenzyl-2-oxo-4,6-tetrahydro-5-pyrimidinonyl)amine, 70.⁵² Under N_2 in an oven-dried round bottom flask, a mixture of ketone **67** (2.00 g, 6.80 mmol, 2.00 eq), ammonium acetate (262 mg, 3.40 mmol, 1.00 eq) and glacial acetic acid (1.00 mL, 17.3 mmol, 5.09 eq) in methanol (5 mL) were stirred at 55 °C for 20 min at which time TLC (EtOAc/hexanes 1:1) indicated a new spot. 5-Ethyl-2-methylpyridine borane (PEMB) (460 mg, 3.41 mmol, 1.00 eq)

was added slowly for over 1 h and the reaction stirred for an additional 2 h. The reaction was quenched by refluxing for 8 h, concentrated and purified by silica gel flash column chromatography (EtOAc/hexanes 1:1) to yield a colorless oil **65** (1.35 g, 67.1%) and a yellow oil **70** (100 mg, 5.13%). The following data refer to **70**. ^1H -NMR (400 MHz, CDCl_3) δ_{H} 2.58 (m, 2H), 2.72 (dd, $J = 11.6, 5.8$ Hz, 4H), 3.02 (dd, $J = 11.7, 3.8$ Hz, 4H), 4.46 (AB quartet, $J = 14.9$ Hz, $\Delta\nu = 77.3$ Hz, 8H), 7.18-7.27 (m, 20H). ^{13}C -NMR (100 MHz, CDCl_3) δ_{C} 46.4, 49.8, 51.4, 127.4, 128.0, 128.6, 138.2, 155.7. HRMS (ESI+): m/z Calcd for $\text{C}_{36}\text{H}_{40}\text{N}_5\text{O}_2$ ($\text{M}^+ + \text{H}$) 574.3182; found 574.3188.



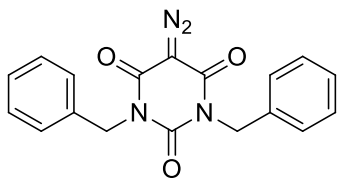
71

1,3-Dibenzylurea, 71.⁴⁹ Under N_2 , triphosgene (2.00 g, 6.81 mmol, 1.00 eq) was added to an ice-cooled stirred solution of benzylamine (4.12 g, 38.4 mmol, 5.64 eq) and triethylamine (4.12 g, 40.3 mmol, 5.92 eq) in CH_2Cl_2 (40 mL), and the reaction mixture stirred for 24 h at rt. Reaction was quenched with 1 M HCl (40 mL) and extracted twice with CH_2Cl_2 (40 mL). Combined organic layers were washed with water (40 mL), satd brine (40 mL), dried over anhydrous MgSO_4 and filtered. Solvent was removed on the rotary evaporator to yield a fluffy white solid **71** (4.43 g, 96.1%) mp 170-172 °C. ^1H -NMR (400 MHz, CDCl_3) δ_{H} 4.33 (s, 2H), 4.34 (s, 2H), 7.23-7.32 (m, 10H). ^{13}C -NMR (100 MHz, CDCl_3) δ_{C} 44.8, 127.6, 127.6, 128.9, 139.3, 158.2.



72

1,3-Dibenzylpyrimidin-2,4,6-trione, 72.⁵⁰ Under N₂ at 65-70 °C, acetic anhydride (30 mL) was added dropwise for 3 h to a stirred solution of dibenzylurea **71** (7.96 g, 33.1 mmol, 1.11 eq) and malonic acid (3.10 g, 29.8 mmol) in glacial acetic acid (20 mL). The reaction mixture was stirred for 30 min after the addition and then temperature was raised to 90 °C for 4 h. The reaction mixture was concentrated, dissolved in ethanol (40 mL) and refluxed for 15 min. Slow cooling at room temperature under N₂, gave a solid precipitate that was filtered, washed with cold ethanol to yield a cream-colored solid **72** (7.10 g, 72.7%) mp 137-138 °C. ¹H-NMR (400 MHz, CDCl₃) δ_H 3.67 (s, 2H), 5.03 (s, 4H), 7.27-7.33 (m, 6H), 7.42 (dd, *J* = 7.8, 1.7 Hz, 4H). ¹³C-NMR (100 MHz, CDCl₃) δ_C 39.7 (CH₂), 44.5 (CH₂), 45.1 (CH₂), 128.1 (CH), 128.6 (CH), 129.2 (CH), 136.0 (quat), 151.5 (quat), 164.4 (quat).



73

1,3-Dibenzyl-5-diazopyrimidin-2,4,6-trione, 73.⁵¹ At 0 °C, a solution of DMAP (1.00 g, 8.19 mmol, 4.96 eq) in acetonitrile (6 mL) was added dropwise to a stirred mixture of **72** (500 mg, 1.65 mmol) and *p*-acetamidobenzenesulfonyl azide **23** (400 mg, 1.67 mmol, 1.01 eq) in acetonitrile (6 mL). The reaction was stirred for 2.5 h at rt at which time TLC (EtOAc/hexanes 1:1) indicated loss of **72**. Reaction mixture was concentrated, residue dissolved in EtOAc/hexanes (1:1) and precipitate filtered off. Solvent was removed on the rotary evaporator

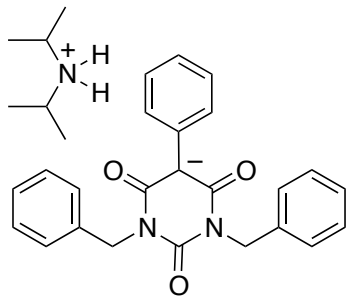
and residue purified by filtering through a plug of silica gel (EtOAc/hexanes 1:1) to furnish a yellow-white solid **73** (388 mg, 70.3%) mp 107.5-108.5 °C. ¹H-NMR (400 MHz, CDCl₃) δ_H 5.06 (s, 4H), 7.27-7.33 (m, 6H), 7.43 (dd, *J* = 7.8, 1.7 Hz, 4H). ¹³C-NMR (100 MHz, CDCl₃) δ_C 44.3, 72.0, 128.1, 128.6, 129.1, 136.0, 150.2, 158.1. HRMS (ESI+): *m/z* Calcd for C₁₈H₁₄N₄O₃Na (M⁺ + Na) 357.0964, found 357.0988. Anal. Calcd for C₁₈H₁₄N₄O₃: C, 64.66; H, 4.22; N, 16.76. Found: C, 64.57; H, 4.34; N, 16.48.

F. ATTEMPTED RHODIUM ACETATE-CATALYZED REACTION OF AMINE **70 WITH DIAZOMALONATE **19**.**

Under N₂, a mixture of amine **70** (100 mg, 0.174 mmol, 0.833 eq), **19** (33.1 mg, 0.209 mmol, 1.00 eq) and Rh₂(OAc)₄ (1.54 mg, 0.00384 mmol, 1.84 mol%) in benzene-*d*₆ (1.00 mL) was refluxed for 3 h. Solution turns red. Solvent was removed on the rotary evaporator and the residue purified by silica gel flash column chromatography (EtOAc/hexanes 1:1) to give brown oil **70** (89 mg).

G. ATTEMPTED RHODIUM ACETATE-CATALYZED N-H INSERTION REACTIONS WITH DIAZOBARBITURATE **79.**

G1. Reaction of diazobarbiturate **79 with diisopropylamine.** Under N₂, a mixture of diisopropylamine (15.0 mg, 0.148 mmol, 1.17 eq), **73** (42.0 mg, 0.126 mmol, 1.00 eq) and Rh₂(OAc)₄ (2.23 mg, 0.00504 mmol, 4 mol%) in benzene (10.0 mL) was refluxed for 3 h. The solvent was removed on the rotary evaporator to give red residue from which a colorless solid precipitated from a solution of CDCl₃ in a NMR tube. The precipitate was filtered off to give **74** (4.23 mg, 6.73%). ¹H-NMR (400 MHz, acetone-*d*₆) δ_H 0.99 (br s, 12H), 3.01 (br s, 2H), 5.13 (s, 4H), 6.94 (t, *J* = 7.3 Hz, 1H), 7.16 (t, *J* = 7.0 Hz, 3H), 7.25 (t, *J* = 7.2 Hz, 4H), 7.37 (t, *J* = 7.6 Hz, 4H), 7.60 (br s, 2H). ¹³C-NMR (100 MHz, acetone-*d*₆) δ_C 19.0, 44.3, 47.8, 79.2, 90.3, 124.3, 127.2, 127.6, 128.5, 128.8, 132.4, 139.7, 141.0, 153.6, 163.2.



74

G2. Reaction of diazobarbiturate 73 with amine 17.

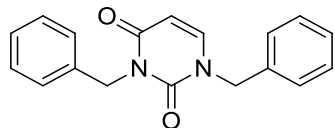
G2(a). Under N₂, a mixture of **17** (87.8 mg, 0.357 mmol, 1.10 eq), **73** (108 mg, 0.325 mmol, 1.00 eq) and Rh₂(OAc)₄ (7.35 mg, 0.0166 mmol, 5.11 mol%) in benzene-*d*₆ (1.00 mL) was refluxed for 1 h. NMR experiments were performed on the crude reaction mixture.

G2(b). *No solvent.* Under N₂ in a round bottom flask, **17** (205 mg, 0.835 mmol, 2.37 eq) was melted at 65 °C. **73** (118 mg, 0.353 mmol, 1.00 eq) and Rh₂(OAc)₄ (18.5 mg, 0.0419 mmol, 11.9 mol%) were added sequentially, then temperature was raised to 90 °C and the mixture stirred for 45 min. The crude reaction mixture was dissolved in CDCl₃ and NMR experiments were performed. Starting materials **17** and **73** were recovered.

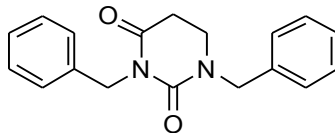
G2(c). *No solvent, long reaction time.* Under N₂ in a round bottom flask, **17** (226 mg, 0.921 mmol, 2.00 eq) was melted at 65 °C. Compound **73** (154 mg, 0.461 mmol, 1.00 eq) and Rh₂(OAc)₄ (4.08 mg, 0.00923 mmol, 2.00 mol%) were added sequentially, then temperature was raised to 90 °C and the mixture stirred for 12 h. The crude reaction mixture was purified by silica gel flash column chromatography (EtOAc/hexanes 1:1 and EtOAc; step gradient) to recover **17** and **73**.

G3. Reaction of diazobarbiturate 73 with amine 70. Under N₂, a mixture of amine **70** (486 mg, 0.847 mmol, 0.909 eq), **73** (311 mg, 0.932 mmol, 1.00 eq) and Rh₂(OAc)₄ (7.47 mg, 0.0169 mmol, 1.81 mol%) in benzene-*d*₆ (1.20 mL) was refluxed for 3 h. Solution turns red. Solvent was

removed on the rotary evaporator and the residue purified by silica gel flash column chromatography (EtOAc/hexanes 1:1) to recover **70** and **73**.



1,3-Dibenzyl-1H-pyrimidine-2,4-dione.⁵³ Under N₂, benzyl bromide (11.4 g, 66.9 mmol, 2.50 eq) was added at once to a stirred mixture of uracil (3.00 g, 26.8 mmol) and potassium carbonate (9.25 g, 66.9 mmol, 2.50 eq) in DMF (28 mL), and stirred for 2 days at rt. The reaction mixture was concentrated nearly to dryness and the oily residue was partitioned between diethyl ether and water (1:1). The organic phase was washed with water (2 x 60 mL), satd brine (50 mL) and dried over anhydrous Na₂SO₄. Solvent was removed on the rotary evaporator and the residue vacuum pumped (< 1 mm Hg) to yield a yellow oil (7.67 g, 98.1%). ¹H-NMR (400 MHz, CDCl₃) δ_H 4.87 (s, 2H), 5.13 (s, 2H), 5.71 (d, *J* = 7.9 Hz, 1H), 7.08 (d, *J* = 7.9 Hz, 1H), 7.23-7.35 (m, 8H), 7.46 (d, *J* = 6.9 Hz, 2H). ¹³C-NMR (100 MHz, CDCl₃) δ_C 44.4 (CH₂), 52.3 (CH₂), 102.1 (CH), 127.6 (CH), 128.0 (CH), 128.4 (CH), 128.5 (CH), 128.9 (CH), 129.1(CH), 135.3 (quat), 136.9 (quat), 141.9 (CH), 151.8 (quat), 162.9 (quat). ¹H and ¹³C NMR shifts are in agreement with published values.⁵³



75

1,3-Dibenzylidihydropyrimidine-2,4-dione, 75.^{53(a)} Under N₂, benzyl bromide (11.2 g, 65.7 mmol, 2.38 eq) was added at once to a stirred mixture of dihydrouracil (3.15 g, 27.6 mmol) and potassium carbonate (9.55 g, 67.7 mmol, 2.45 eq) in DMF (25 mL) and stirred for 2 days. The reaction mixture was concentrated and the residue partitioned between equal volumes of diethyl

ether and water. The organic phase was washed with water (2 x 60 mL), satd brine (50 mL) and dried over anhydrous Na₂SO₄. Solvent was removed on the rotary evaporator and vacuum pumped (< 1 mm Hg) to yield a colorless solid, **75** (5.88 g, 72.4%) mp 76-78 °C. ¹H-NMR (400 MHz, CDCl₃) δ_H 2.66 (t, *J* = 6.8 Hz, 2H), 3.25 (t, *J* = 6.8 Hz, 2H), 4.62 (s, 2H), 5.01 (s, 2H), 7.23-7.42 (m, 10H). ¹³C-NMR (100 MHz, CDCl₃) δ_C 31.7, 44.0, 51.7, 136.4, 127.4, 128.0, 128.4, 128.6, 128.9, 129.5, 137.9, 153.9, 169.0. ¹H and ¹³C NMR shifts are in agreement with published values.^{53(b)}

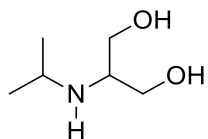
H. ATTEMPTED [RuCl₂(*p*-CYMENE)]₂-CATALYZED N-H INSERTION REACTIONS.⁵⁸

H1. Reaction of amine 17 with diazomalonate 19. Under N₂, a mixture of amine **17** (118 mg, 0.481 mmol), **19** (76 mg, 0.481 mmol) and [RuCl₂(*p*-cymene)]₂ (2.94 mg, 0.00480 mmol, 0.998 mol%) in acetonitrile (10 mL) was refluxed. Progress of the reaction was followed by TLC (EtOAc/hexanes 1:1) and stopped after 24 h. Solvent was removed on the rotary evaporator to give a mixture of **17** and **19**.

H2. Reaction of amine 76 with diazomalonate 19. Under N₂, a mixture of amine **76** (204 mg, 1.53 mmol), **19** (242 mg, 1.53 mmol) and [RuCl₂(*p*-cymene)]₂ (9.37 mg, 0.0153 mmol) in acetonitrile (30 mL) was refluxed. Progress of the reaction was followed by TLC (EtOAc/hexanes 1:1) and stopped after 24 h. Solvent was removed on the rotary evaporator to give an intractable mixture.

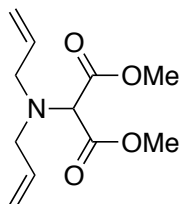
H3. Reaction of amine 15 with diazomalonate 19. Under N₂, a mixture of amine **15** (126 mg, 0.763 mmol), **19** (121 mg, 0.763 mmol) and [RuCl₂(*p*-cymene)]₂ (4.67 mg, 0.00763 mmol, 1.00 mol%) in acetonitrile (15 mL) was refluxed. Progress of the reaction was followed by TLC (EtOAc/hexanes 1:1) and stopped after 24 h. Solvent was removed on the rotary evaporator to give an intractable mixture.

H4. Reaction of diallylamine with diazobarbiturate 73. Under N₂, a mixture of diallylamine (23.0 mg, 0.237 mmol, 1.10 eq), **73** (72.0 mg, 0.215 mmol, 1.00 mmol) and [RuCl₂(*p*-cymene)]₂ (3.22 mg, 0.00523 mmol, 2.43 mol%) in acetonitrile (4.00 mL) was refluxed for 48 h. The solvent was removed on the rotary evaporator to give an intractable mixture.



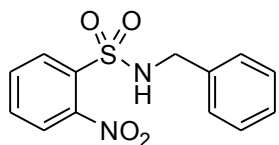
76

2-Isopropylamino-1,3-diol, 76. Under N₂, a solution of sodium cyanoborohydride (5.24 g, 83.4 mol, 1.99 eq) dissolved in 30 mL methanol was added dropwise to a stirred solution of dihydroxyacetone dimer (15.0 g, 83.3 mmol, 1.98 eq) and isopropylamine (2.48 g, 42.0 mmol) in a mixture of methanol (105 mL) and acetic acid (10.5 mL). After stirring at rt for 14 h, aq HCl (25 mL, 2 M) was added and stirred for an additional 3 h. The solvent was removed on the rotary evaporator and the resulting residue was re-dissolved in 80 mL methanol. Precipitate was filtered off and solvent removed in vacuo to give a light yellow oil residue. The residue was dissolved in water and applied to an ion-exchange resin column (Amberlite, IR-120, H⁺). The column was eluted with water first, and then a solution of aqueous ammonia (1.00 M). The solvent was removed in vacuo to yield a brown oil **76** (4.75 g, 85.5%). ¹H-NMR (400 MHz, D₂O, dioxane used as an internal reference δ_H 3.53^{ref}) δ_H 0.83 (d, *J* = 6.3 Hz, 6H), 2.62 (quintet, *J* = 5.4 Hz, 1H), 2.76 (septet, *J* = 6.3 Hz, 1H), 3.38 (m, 4H). ¹³C-NMR (100 MHz, D₂O, dioxane used as an internal reference δ_C 66.7^{ref}) δ_C 21.6 (CH₃), 45.5 (CH), 56.5 (CH), 60.9 (CH₂). HRMS (ESI+): *m/z* Calcd for C₆H₁₇NO₂ (M⁺ + H) 134.1181; found 134.1199.



77

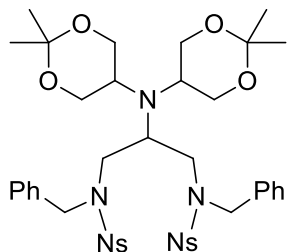
Dimethyl 2-(N,N-diallylamino)malonate, 77.⁵⁸ To a mixture of diallylamine (109 mg, 1.12 mmol, 1.08 eq), **19** (164 mg, 1.04 mmol) and [Ru(*p*-cymene)Cl₂]₂ (6.36 mg, 0.010 mmol, 0.962 mol%) in 4 mL acetonitrile was refluxed under N₂ for 48 h. Solvent was removed with on a rotary evaporator and the residue purified by silica gel flash column chromatography (EtOAc/hexanes 1:3) to yield a colorless oil, **77** (160 mg, 67.8%). ¹H (400 MHz, CDCl₃) δ_H 3.42 (d, *J* = 6.4 Hz, 4H), 3.67 (s, 6H), 4.26 (s, 1H), 5.22-5.10 (m, 4H), 5.84-5.74 (m, 2H). ¹³C (100 MHz, CDCl₃) δ_C 52.0 (CH₃), 54.3 (CH₂), 65.5 (CH), 117.8 (CH₂), 135.5 (CH), 168.5 (quat). HRMS (ESI+): *m/z* Calcd for C₁₁H₁₈NO₄ (M⁺+H) 228.1236; found 228.1251.



78

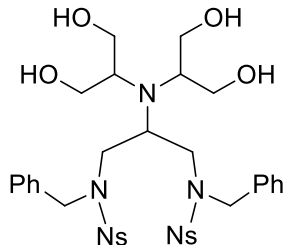
N-Benzyl-2-nitrobenzenesulfonamide, 78.⁵⁴ Under N₂ at 0 °C, a mixture of benzylamine (5.08 g, 47.4 mmol, 1.18 eq) and triethylamine (5.67 g, 56.0 mmol) in CH₂Cl₂ (70 mL) was added dropwise to a stirred solution of 2-nitrobenzenesulfonyl chloride (12.4 g, 56.1 mmol, 1.18 eq) in CH₂Cl₂ (30 mL). The mixture was warmed to rt and stirred for an additional 4 h. The reaction mixture was washed with water (2 x 50 mL), 10% aq NaHCO₃ (2 x 50 mL), 1 M HCl (2 x 50 mL), satd brine (100 mL) and dried over anhydrous Na₂SO₄. After filtration, solvent was removed on the rotary evaporator and the residue recrystallized from CH₂Cl₂/hexanes to yield a

colorless solid, **78** (8.22 g, 59.3%) mp 96.5-97.5 °C. ¹H and ¹³C NMR shifts are in agreement with published values.⁵⁴



79

2-(N,N-bis(4,4-dimethyl-3,5-dioxanyl)amino)-N,N-bis(2-nitrobenzenesulfonyl)-N,N-dibenzyl-1,3-propanediamine, 79. To a stirred solution of diacetonide amine diol, **21** (1.16 g, 3.63 mmol) in 10 mL toluene was added, in sequence, triphenylphosphine (1.91 g, 7.26 mmol, 2.00 eq), NsNHBn **78** (2.13 g, 7.26 mmol, 2.00 eq) and DTBAD (1.69 g, 7.26 mmol, 2.00 eq) at -15 °C under N₂. After stirring at -15 °C for 10 min the reaction mixture was warmed to rt and stirred for an additional 30 min. Solvent was removed on the rotary evaporator and the residue purified by silica gel flash column chromatography (diethyl ether, EtOAc: step gradient elution) to afford **79**, (2.17 g, 68.8%) as a pale yellow foam mp 142-144 °C. ¹H-NMR (250 MHz, CDCl₃) δ_H 1.36 (s, 3H), 1.39 (s, 3H), 3.13-3.22 (m, 4H), 3.50-3.78 (m, 11H), 4.58 (AB quartet, *J* = 16.4 Hz, Δ*v* = 66.6 Hz, 4H), 7.01-7.21 (m, 10H), 7.51-7.87 (m, 8H). ¹³C-NMR (62.9 MHz, CDCl₃) δ_C 22.0 (br, CH₃), 25.7 (br, CH₃), 49.1 (CH₂), 49.1 (CH), 51.4 (CH₂), 54.3 (CH), 63.7 (CH₂), 98.1 (q), 124.1 (CH), 127.8 (CH), 127.9 (CH), 128.8 (CH), 131.0 (CH), 131.5 (CH), 133.3 (q), 133.8 (CH), 134.6 (quat), 147.9 (quat). HRMS (ESI+): *m/z* Calcd for C₄₁H₄₉N₅O₁₂S₂Na (M⁺+Na) 890.2713, found 890.2717. Anal. Calcd for C₄₁H₄₉N₅O₁₂S₂: C, 56.73; H, 5.69; N, 8.07; S, 7.39. Found : C, 56.49; H, 5.79; N, 8.00; S, 7.18.



106

2-(N,N-bis(1,3-dihydroxy-2-propyl)amino)-N,N-bis(2-nitrobenzenesulfonyl)-N,N-dibenzyl-1,3-propanediamine, 80.³⁰ A mixture of compound **79** (171 mg, 0.197 mmol) and 1.00% w/v solution of I₂ in methanol (5.00 mL, 0.196 mmol) in an oven-dried round bottomed flask was stirred at rt overnight. The reaction was quenched with 5 mL 10% aq sodium thiosulfate solution, and the organic layer extracted twice with 10 mL CH₂Cl₂. The organic layer was washed with 5 mL 5% aq NaOH, 5 mL water, 5 mL satd brine and dried with anhydrous Na₂SO₄. After filtration, the solvent was removed on the rotary evaporator. The residue was further dried under vacuum (< 1 mm Hg) to yield a foamy yellow solid **80** (131 mg, 95.8%), mp 119-121 °C. ¹H-NMR (400 MHz, CDCl₃) δ_H 3.16-3.76 (m, 14H), 7.07-7.29 (m, 10H), 7.45-7.71 (m, 6H), 7.71 (d, *J* = 7.68 Hz, 2H). ¹³C-NMR (100 MHz, CDCl₃) δ_C 50.4 (CH₂), 51.9 (CH₂), 52.6 (CH), 58.1 (CH), 62.3 (CH₂), 123.9 (CH), 127.9 (CH), 128.2 (CH), 128.8 (CH), 130.8 (CH), 131.7 (CH), 133.1 (quat), 133.5 (CH), 134.9 (quat), 147.9 (quat). HRMS (ESI+): *m/z* Calcd for C₃₅H₄₃N₅O₁₂S₂ (M⁺+H): 788.2271, found 788.2284. A crystal 0.100 mm x 0.100 mm x 0.100 mm was selected for X-ray crystallography with 0.71073 Å (Mo Kα) radiation: triclinic *a* = 9.6989(9) Å, *b* = 11.7340(11) Å, *c* = 17.0649(17) Å, *α* = 80.749(2)°, *β* = 78.860(2)°, *γ* = 78.027(2)°; *Z* = 2; 19038 reflections were collected, 9173 independent, -12 ≤ *h* ≤ 12, -15 ≤ *k* ≤ 15, -22 < *l* < 22. Full-matrix least-squares refinement on F², data-to-parameter ratio = 17.8, goodness-of-fit = 0.838, R1 = 0.0505, wR2 = 0.0969 (*I*>2σ(*I*)), R1 = 0.1069, wR2 =

0.1056 (all data). Crystal structure determination was performed by Mr. Branson Maynard. Full details are given in Appendix 8.

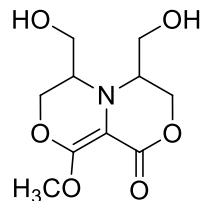
I. ATTEMPTED FUKUYAMA-MITSUNOBU REACTIONS ON TETRAOL **80 WITH SULFONAMIDE **78**.³¹**

11. To a stirred solution of **80** (130 mg, 0.165 mmol, 1.00 eq) in toluene (10 mL) at -15 °C was added, in sequence, **78** (196 mg, 0.671 mmol, 4.07 eq), triphenylphosphine (180 mg, 0.686 mmol, 4.16 eq) and DTBAP (155 mg, 0.671 mmol, 4.07 eq) under N₂. After stirring at -15 °C for 10 min the reaction mixture was warmed to rt and stirred for an additional 2 h at which point TLC (Et₂O/hexanes 1:1) indicated loss of **80**. An aliquot taken for ¹H-NMR and ³¹P-NMR. Solvent was removed on the rotary evaporator to give an intractable mixture (670 mg) that couldn't be purified by silica gel column chromatography. Attempts to purify via prep-TLC were unsuccessful as well.

12. Polymer-bound triphenylphosphine. To a stirred solution of **80** (305 mg, 0.387 mmol, 1.00 eq) in toluene (10 mL) at -15 °C was added, in sequence, **78** (452 mg, 1.55 mmol, 4.01 eq), triphenylphosphine, polymer bound resin (542 mg, 1.63 mmol, 4.21 eq) and DTBAP (375 mg, 1.63 mmol, 4.21 eq) under N₂. After stirring at -15 °C for 10 min the reaction mixture was warmed to rt and stirred for an additional 12 h at which point TLC (diethyl ether/hexanes 1:1) indicated presence of **80** and DTBAP-H₂. The resin was filtered off and solvent removed on the rotary evaporator give an intractable mixture.

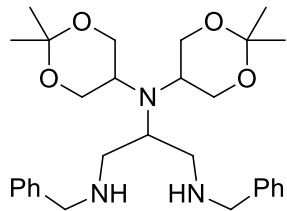
13. Excess polymer-bound triphenylphosphine and temperature effect. To a stirred solution of **80** (371 mg, 0.471 mmol, 1.00 eq) in toluene (10 mL) at -15 °C was added, in sequence, **78** (578 mg, 1.98 mmol, 4.20 eq), triphenylphosphine, polymer bound resin ²⁷⁻²⁹ (1.57 g, 4.71 mmol, 10.0 eq) and DTBAP (521 mg, 2.26 mmol, 4.80 eq) under N₂. After stirring at -15 °C for 10 min the reaction mixture was warmed to rt and stirred for an additional 12 h at which

point TLC (diethyl ether/hexanes 1:1) indicated presence of **80** and DTBAD-H₂. The mixture was refluxed for 12 h, cooled, the resin was filtered off and solvent removed on the rotary evaporator give an intractable mixture.



81

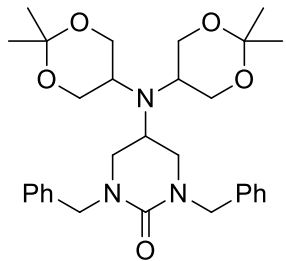
9-Hydroxy-4,6-dihydroxymethyl-9-methoxyhexahydro-[1,4]oxazino[3,4-c][1,4]oxazin-1-one, 81.³⁰ In an oven-dried round bottomed flask, compound **20** (39.1 mg, 0.104 mmol) was stirred in 1.00% w/v solution of I₂ in methanol (5.00 mL, 0.196 mmol) at rt for 1 h. The reaction was quenched with 5 mL 10% aq Na₂S₂O₃ solution, and extracted twice with 10 mL CH₂Cl₂. The organic phase was washed with 5 mL 5% aq NaOH, 5 mL water, 5 mL satd. brine and dried with anhydrous Na₂SO₄. Solvent was removed on the rotary evaporator and the residue was further dried under vacuum (< 1 mm Hg) to a brown oil **81** (25.2 mg, 92.0%). ¹H-NMR (400 MHz, CDCl₃) δ_H 3.14-3.19 (m, 1H), 3.54-3.58 (m, 1H), 3.65 (dd, *J* = 12.2, 2.8 Hz, 1H), 3.69-3.71 (m, 2H), 3.82-3.86 (m, 2H), 3.87 (s, 3H), 3.98-4.05 (m, 2H), 4.37 (dd, *J* = 12.0, 3.4 Hz, 1H), 4.47 (dd, *J* = 12.0, 10.7 Hz, 1H). ¹³C-NMR (100 MHz, CDCl₃) δ_C 53.9 (CH₃), 59.5 (CH), 61.5 (CH₂), 63.8 (CH₂), 64.4 (CH), 67.5 (CH₂), 68.2 (CH₂), 92.x (quat), 165.7 (quat), 169.2 (quat). HRMS (ESI+): *m/z* Calcd for C₁₀H₁₈NO₇ (M⁺ + H₂O + H⁺) 264.1083, found 264.1082.



82

2-(N,N-bis(4,4-dimethyl-3,5-dioxanyl)amino) N,N-dibenzyl-1,3-propanediamine, **82.**³¹ A

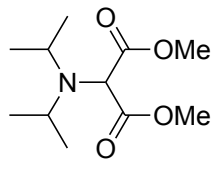
100 mL three-necked round bottomed flask under N₂, was charged with thiophenol (2.04 g, 17.3 mmol) and 25 mL acetonitrile. It was cooled in an ice-bath before adding 3.03 M aq KOH (5.71 mL, 17.3 mmol) dropwise over a period of 10 min while stirring. The ice-bath was removed after an additional 5 min and a solution of compound **79** (3.07 mg, 3.46 mmol) in 25 mL acetonitrile was added dropwise over a period of 10 min. The reaction was heated at 50 °C in an oil bath for 30 min until TLC showed no traces of compound **79**. Solvent was removed on the rotary evaporator and the residue purified by vacuum filtration through a plug of silica gel (1:1 EtOAc/hexanes, EtOAc and MeCN sequentially) to afford a brown oil **82**, 661 mg, 38.4%. ¹H-NMR (400 MHz, CDCl₃) δ_H 1.39 (s, 3H), 1.45 (s, 3H), 2.52 (dd, *J* = 11.8, 6.8 Hz, 2H), 2.74 (dd, *J* = 11.8, 6.7 Hz, 2H), 3.12 (m, 3H), 3.57 (dd, *J* = 11.5, 5.4 Hz, 4H), 3.74-3.82 (m, 8H), 7.25-7.36 (m, 10H). ¹³C-NMR (100 MHz, CDCl₃) δ_C 19.6 (CH₃), 28.2 (CH₃), 49.1 (CH), 52.3 (CH₂), 54.2 (CH₂), 56.7 (CH), 63.8 (CH₂), 97.5 (quat), 127.1 (CH), 127.9 (CH), 128.5 (CH), 140.2 (quat). HRMS (ESI+) Calcd for C₂₉H₄₅N₃O₄ (M⁺ + H): 498.3292, found 498.3311.



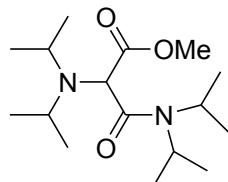
109

1,3-Dibenzyl-5-[bis-(2,2-dimethyl-[1,3]dioxan-5-yl)-amino]-tetrahydropyrimidin-2-one,

83. Under N₂, bis(4-nitrophenyl) carbonate (66.1 mg, 0.217 mmol) and **82** (181 mg, 0.364 mmol, 1.68 eq), were refluxed in methylene chloride (15 mL) for 24 h. The reaction mixture was washed with satd. citric acid (15 mL), 2 M NaOH (5 x 15 ml), water (15 mL), brine (15 mL) and dried over anhydrous MgSO₄. Solvent was removed on the rotary evaporator and vacuum pumped (< 1 mm Hg) to yield a yellow oil **83** (120 mg, 62.9%). ¹H-NMR (400 MHz, CDCl₃) δ_H 1.33 (s, 6H), 1.36 (s, 6H), 2.85 (dd, *J* = 11.2, 5.0 Hz, 2H), 2.97 (tt, *J* = 9.7, 5.7 Hz, 2H), 3.19 (t, *J* = 11.0 Hz, 2H), 3.34 (m, 1H), 3.45 (dd, *J* = 11.6, 5.6 Hz, 4H), 3.51 (t, *J* = 10.7 Hz, 4H), 4.60 (AB quartet, *J* = 15.0 Hz, Δv = 84.1 Hz, 4H), 7.27-7.38 (m, 10H). ¹³C-NMR (100 MHz, CDCl₃) δ_C 20.0 (CH₃), 27.5 (CH₃), 49.5 (CH), 49.5 (CH), 49.8 (CH₂), 51.6 (CH₂), 63.4 (CH₂), 97.6 (quat), 127.5 (CH), 127.8 (CH), 128.7 (CH), 129.1 (CH), 138.0 (quat), 155.6 (quat). HRMS (ESI+) Calcd for C₃₀H₄₂N₃O₅ (M⁺ + H): 524.3124, found 524.3118.



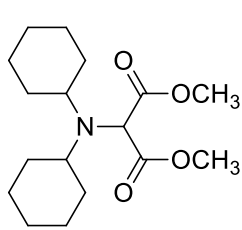
84



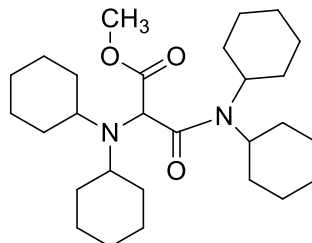
85

Dimethyl 2-(diisopropylamino)propanedioate, 84 and 2-Diisopropylamino-N,N-diisopropylmalonic acid methyl ester, 85.³⁴ Under N₂, a solution of diisopropylamine (500 mg,

4.94 mmol), dimethyl diazomalonate **19** (630 mg, 3.98 mmol) and Rh₂(OAc)₄ (16.0 mg, 0.036 mmol, 0.905 mol%) in benzene (20 mL) was refluxed for 3 h. Solvent was removed on the rotary evaporator and residue purified by silica gel flash column chromatography (EtOAc/hexanes 1:3) to yield two fractions; a non-polar colorless oil **84**, (662 mg, 72.0%) and a more polar colorless crystalline solid **85** (142 mg, 11.9%) mp 96-97 °C. **84**: ¹H-NMR (400 MHz, CDCl₃) δ_H 1.05 (d, *J* = 6.7 Hz, 12 H), 3.31 (quintet, *J* = 6.7 Hz, 2H), 3.74 (s, 6H), 4.31 (s, 1H). ¹³C-NMR (100 MHz, CDCl₃) δ_C 22.2, 46.8, 52.1, 61.4, 171.3. **85**: ¹H-NMR (250 MHz, CDCl₃) δ_H 1.06 (d, *J* = 6.7, 6H), 1.13 (d, *J* = 6.7, 6H), 1.21 (d, *J* = 7.0 Hz, 3H), 1.23 (d, *J* = 6.8 Hz, 3H), 1.38 (d, *J* = 6.8 Hz, 3H), 1.42 (d, *J* = 6.8 Hz, 6H), 3.41 (m, 3H), 3.71 (s, 3H), 4.30 (quintet, *J* = 6.6 Hz, 1H), 4.38 (s, 1H). ¹³C-NMR (63 MHz, CDCl₃) δ_C 20.0, 20.0, 20.6, 21.3, 23.5, 46.1, 46.8, 47.9, 51.6, 62.8, 168.3, 173.3. A crystal 0.660 mm x 0.422 mm x 0.124 mm was selected for X-ray crystallography with 0.71073 Å (Mo Kα) radiation: orthorhombic *a* = 28.629(2) Å, *b* = 10.2423(8) Å, *c* = 12.7234(10) Å, α = 90°, β = 90°, γ = 90°; Z = 8; 35254 reflections were collected, 4644 independent, -38 ≤ *h* ≤ 37, -13 ≤ *k* ≤ 13, -16 ≤ *l* ≤ 16. Full-matrix least-squares refinement on F², data-to-parameter ratio = 24.3, goodness-of-fit = 1.040, R1 = 0.0578, wR2 = 0.1468 (*I* > 2σ(*I*)), R1 = 0.0721, wR2 = 0.1543 (all data). Crystal structure determination was performed by Dr. Anna-Gay D. Nelson. Full details are given in Appendix 3.



86



87

Dimethyl 2-dicyclohexylaminopropan-1,3-dioate, 86, and N,N-Dicyclohexyl-2-dicyclohexylaminomalonamic acid methyl ester, 87. Under N₂, a mixture of dicyclohexylamine (2.71

g, 14.9 mmol, 1.18 eq), dimethyl diazomalonate **19** (2.00 g, 12.6 mmol) and Rh₂(OAc)₄ (60.0 mg, 0.136 mmol, 1.08 mol%) in 20 mL benzene was refluxed for 3 h. Solvent was removed on the rotary evaporator and the residue purified by silica gel flash column chromatography to yield 2.01 g of a yellow solid. It was a mixture of **86** and **87** by NMR, with a distribution of 72.0% and 28.0%. Sublimation of the ground mixture at 65 °C, 0.25 mm Hg gave two compounds; white crystals of **86** (1.22 g, 31.2%) mp 57-58 °C (Lit.⁴¹ 51-52 °C) that condensed on the cold finger and the residue, yellow crystals of **87** (473 mg, 8.41%) mp 172-174 °C. **86**: ¹H-NMR (400 MHz, C₆D₆) δ_H 0.88-0.97 (m, 2H), 1.25 (m, 8H), 1.46-1.50 (m, 2H), 1.67-1.70 (m, 4H), 1.93 (m, 4H), 2.99 (m, 2H), 3.35 (s, 6H), 4.46 (s, 1H). ¹³C-NMR (100 MHz, C₆D₆) δ_C 25.8 (CH₂), 26.6 (CH₂), 33.5 (CH₂), 51.3 (CH), 56.1 (CH₃), 62.3 (CH), 170.7 (quat). A crystal 0.230 mm x 0.200 mm x 0.150 mm was selected for X-ray crystallography with 0.71073 Å (Mo Kα) radiation: orthorhombic *a* = 8.5308(7) Å, *b* = 16.5190(12) Å, *c* = 24.783(2) Å, α = 90°, β = 90°, γ = 90°; Z = 8; 24404 reflections were collected, 4358 independent, -7 ≤ *h* ≤ 11, -22 ≤ *k* ≤ 15, -33 ≤ *l* ≤ 33. Full-matrix least-squares refinement on F², data-to-parameter ratio = 13.1, goodness-of-fit = 1.061, R1 = 0.0550, wR2 = 0.1500 (*I* > 2σ(*I*)), R1 = 0.0781, wR2 = 0.1613 (all data). Crystal structure determination was performed by Mr. Branson Maynard. Full details are given in Appendix 4. **87**: ¹H-NMR (400 MHz, C₆D₆) δ_H 0.77-1.84 (m, 38 H), 2.85 (m, 2H), 3.02 (m, 1H), 3.20 (m, 2H), 3.48 (s, 3H), 3.93 (m, 1H), 4.65 (s, 1H). ¹³C-NMR (100 MHz, C₆D₆) δ_C 25.3, 25.5, 25.7, 25.9, 26.0, 26.6, 26.7, 29.4, 29.8, 30.6, 32.1, 33.1, 35.3, 51.1, 56.0, 56.1, 56.3, 64.1, 168.1, 172.7. HRMS (ESI+): *m/z* Calcd for C₂₈H₄₉N₂O₃ (M⁺+H): 461.3743, found 461.3748. A crystal 0.270 mm x 0.266 mm x 0.190 mm was selected for X-ray crystallography with 0.71073 Å (Mo Kα) radiation: monoclinic *a* = 9.5207(5) Å, *b* = 17.1439(9) Å, *c* = 16.6718(9) Å, α = 90°, β = 96.6190(10)°, γ = 90°; Z = 4; 27406 reflections were collected, 6735 independent, -12 ≤ *h* ≤ 12,

$-22 \leq k \leq 22$, $-22 \leq l \leq 22$. Full-matrix least-squares refinement on F^2 , data-to-parameter ratio = 22.6, goodness-of-fit = 1.046, R1 = 0.0624, wR2 = 0.1445 ($I > 2\sigma(I)$), R1 = 0.0872, wR2 = 0.1554 (all data). Crystal structure determination was performed by Dr. Andrea N. Alsobrook. Full details are given in Appendix 5.

**J. INVESTIGATIONS OF THE REACTION OF DICYCLOHEXYLAMINE WITH DIAZOMALONATE 19,
AND RELATED EXPERIMENTS.**

J1. Rhodium acetate-catalyzed reaction of excess diazomalonate 19 with dicyclohexylamine. Under N_2 , a mixture of dicyclohexylamine (190 mg, 1.05 mmol, 0.761 eq), **19** (218 mg, 1.38 mmol, 1.00 eq) and $Rh_2(OAc)_4$ (18.0 mg, 0.0407 mmol, 3.88 mol%) in benzene (10 mL) was refluxed for 3 h. Solvent was removed on the rotary evaporator and the residue dissolved in $CDCl_3$ for NMR experiments.

J2. Uncatalyzed reaction of diazomalonate 19 with dicyclohexylamine. Under N_2 , a mixture of dicyclohexylamine (226 mg, 1.25 mmol, 1.23 eq) and **19** (161 mg, 1.02 mmol, 1.00 eq) in benzene (10 mL) was refluxed for 3 h. Solvent was removed on the rotary evaporator, the residue was dissolved in $CDCl_3$ and NMR experiments were performed.

J3. Reactions of dicyclohexylamine with diester 86.

J3(a) *3-hour reaction, uncatalyzed.* Under N_2 , a mixture of diester **86** (21.7 mg, 0.0697 mmol, 1.00 eq) and dicyclohexylamine (32.0 mg, 0.176 mmol, 2.53 eq) in benzene (1.00 mL) was refluxed for 3 h. Solvent was removed on the rotary evaporator and the residue dissolved in $CDCl_3$ for NMR experiments.

J3(b) *48-hour reaction, uncatalyzed.* Under N_2 , a mixture of diester **86** (43.3 mg, 0.139 mmol, 1.00 eq) and dicyclohexylamine (66.3 mg, 0.366 mmol, 2.63 eq) in benzene- d_6 (2.00 mL) was refluxed for 48 h and NMR experiments were performed.

J3(c) *3-hour reaction, catalyzed.* Under N₂, a mixture of diester **86** (50.1 mg, 0.161 mmol, 1.00 eq), dicyclohexylamine (75.2 mg, 0.415 mmol, 2.58 eq) and Rh₂(OAc)₄ (1.74 mg, 0.00394 mmol, 2.45 mol%) in benzene-*d*₆ (2.00 mL) was refluxed for 3 h and NMR experiments were performed.

J4. Rhodium acetate-catalyzed reaction of dimethyl diazomalonate **19 with dicyclohexylamine followed by NMR over time.**

J4(a) *Long timescale.* Under N₂, a mixture of dicyclohexylamine (1.39 g, 7.67 mmol, 1.17 eq), **19** (1.04 g, 6.58 mmol, 1.00 eq) and Rh₂(OAc)₄ (40.1 mg, 0.091 mmol, 1.32 mol%) in benzene-*d*₆ (10 mL) was refluxed. NMR experiments were performed for aliquots (~ 0.6 mL of the unfiltered crude reaction mixture) taken at *t* = 30, 60, 120, 180, 240 and 2880 min. Figure 4.1 shows the ¹H-NMR spectrum at *t* = 120 min.

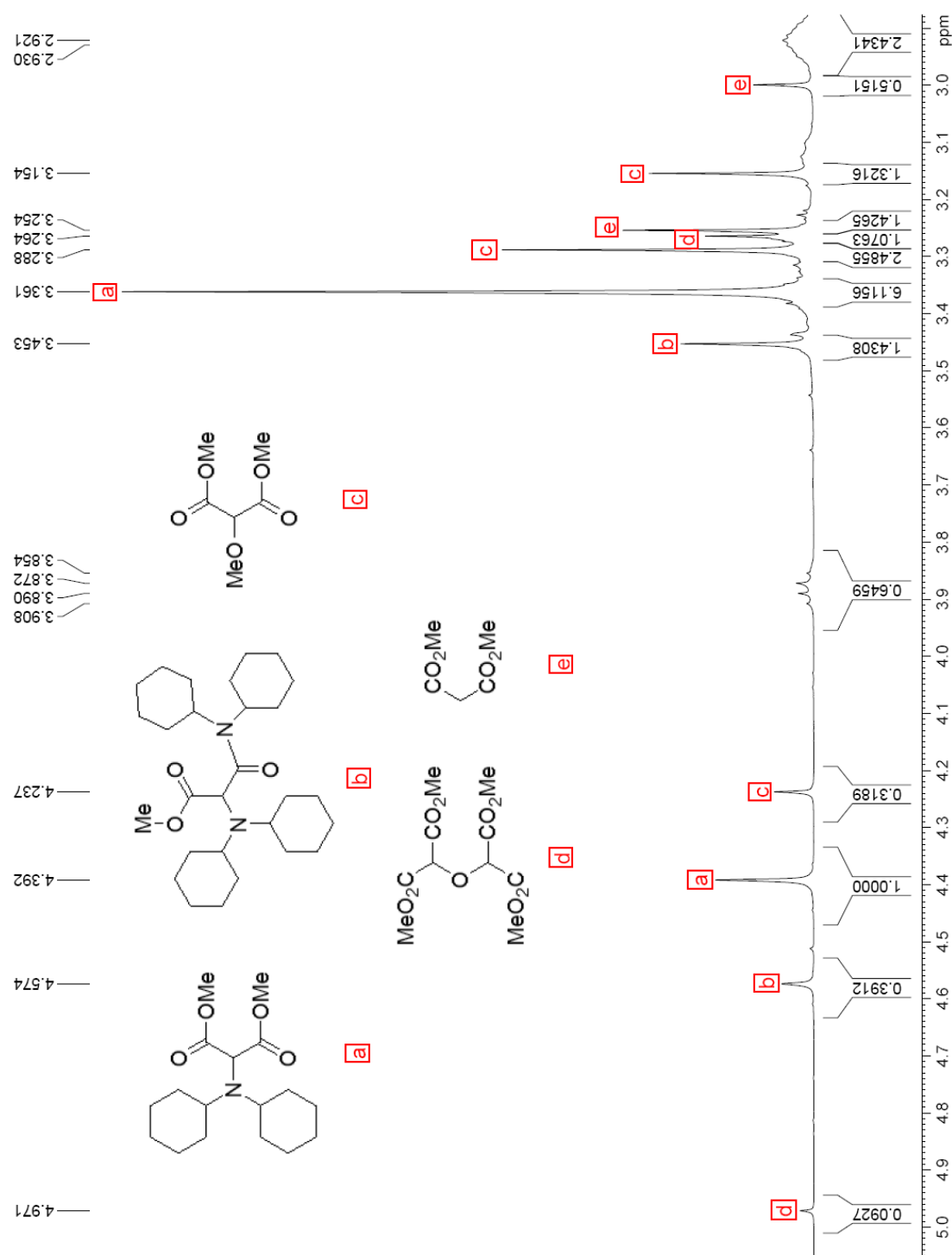
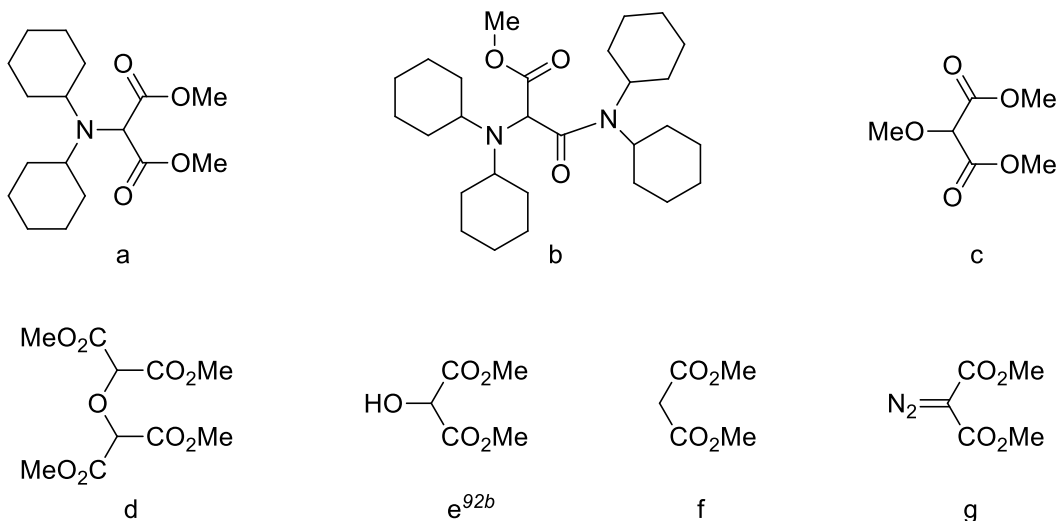


Figure 4.1. Partial 400 MHz ^1H -NMR spectrum (*ca.* 2.90 - 5.10 ppm) of the crude reaction mixture (experiment **J4(a)**) at $t = 120$ min.

J4(b) *Short timescale*. An NMR tube flushed with N₂, ~0.60 mL of a mixture of dicyclohexylamine (207 mg, 1.14 mmol, 1.13 eq), **19** (159 mg, 1.01 mmol) and Rh₂(OAc)₄ (5.08 mg, 0.011 mmol, 1.09 mol%) in benzene-*d*₆ (1.00 mL) was heated in a pre-heated oil bath at 85 °C for 3 min, quickly immersed into liquid N₂ to halt the reaction, warmed to rt and NMR experiments performed. The tube was returned to the oil bath for further heating. This was done for reaction times of 0, 3, 6, 9 and 12 min. Figures 4.2 and 4.3 show the results. Structures of products identified in the figures are shown below.



Compounds a – g identified in Figures 4.2 and 4.3.

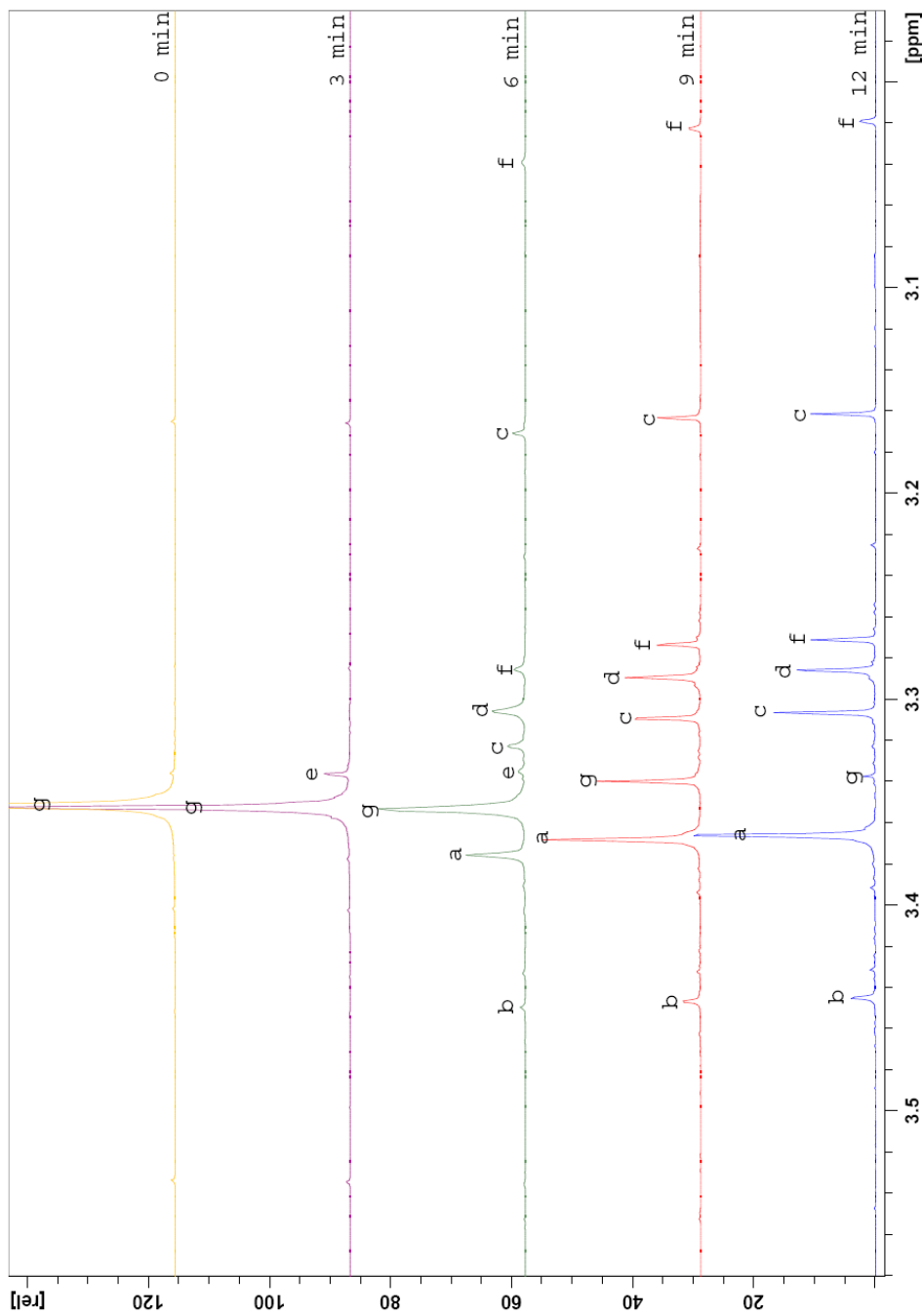


Figure 4.2. Partial 400 MHz ¹H-NMR spectrum (*ca.* 2.96 – 3.58 ppm) of the crude reaction mixture (experiment **J4(b)**) at *t* = 0, 3, 6, 9, & 12 min. Ester methoxy signals appear in the range 3.2 – 3.6 ppm. The peak at 3.16 ppm is due to the ether methoxy group of compound c. The peak at 3.02 ppm is due the CH₂ group of compound f.

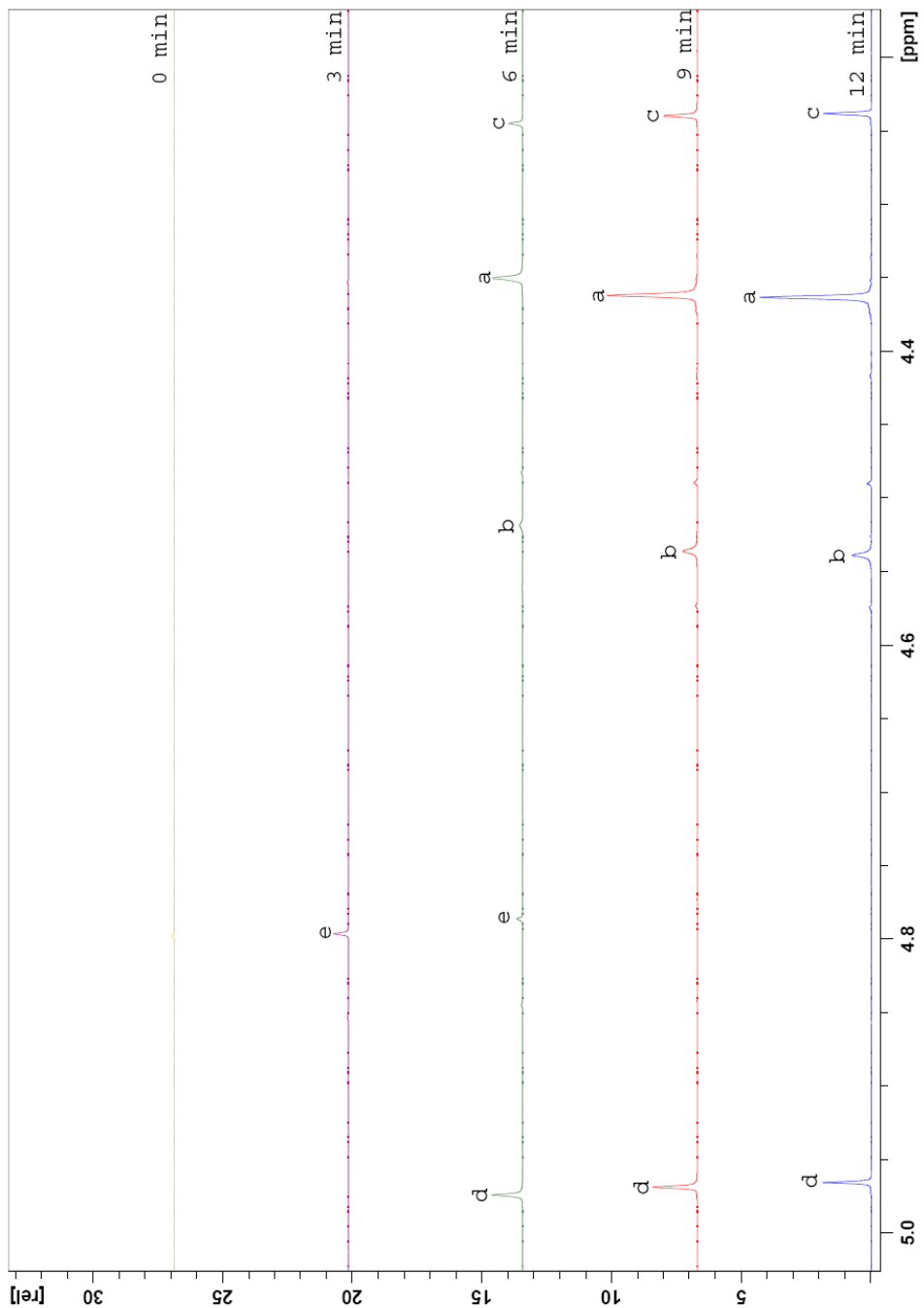


Figure 4.3. Partial 400 MHz ^1H -NMR spectrum (*ca.* 4.20 – 5.00 ppm) of the crude reaction mixture (experiment **J4(b)**) at $t = 0, 3, 6, 9$, & 12 min. All peaks in this region are due to methine protons adjacent to two carbonyl groups.

J5. Rhodium acetate-catalyzed reaction of dicyclohexylamine with the slow addition of diazomalonate 19. Under N₂, **19** (250 mg, 1.58 mmol, 1.26 eq) was added slowly via a syringe (~15 min) to a refluxing mixture of dicyclohexylamine (227 mg, 1.25 mmol, 1.00 eq) and Rh₂(OAc)₄ (12.2 mg, 0.0276 mmol, 2.21 mol%) in benzene-*d*₆ (1.00 mL) and then refluxed for 3 h. NMR experiments were performed on the crude reaction mixture.

J6. Rhodium acetate-catalyzed reaction of diazomalonate 19 with dicyclohexylamine where the temperature was gradually raised from rt to reflux. Under N₂, a mixture of dicyclohexylamine (173 mg, 0.954 mmol, 1.58 eq), **19** (95.6 mg, 0.605 mmol, 1.00 eq) and Rh₂(OAc)₄ (2.90 mg, 0.00656 mmol, 1.08 mol%) in benzene-*d*₆ (2.00 mL) was heated in an oil-bath whose temperature was raised slowly from rt to 80 °C (ca. 40 min) and then refluxed for 3 h. NMR experiments were performed on the crude reaction mixture.

K. INVESTIGATIONS OF THE REACTION OF DIISOPROPYLAMINE WITH DIAZOMALONATE 19.

K1. Uncatalyzed reaction of diazomalonate 19 with diisopropylamine. Under N₂, a mixture of diisopropylamine (253 mg, 2.50 mmol, 1.25 eq) and **19** (316 mg, 2.00 mmol, 1.00 eq) in benzene (10 mL) was refluxed for 3 h. Solvent was removed on the rotary evaporator, the residue was dissolved in CDCl₃ and NMR experiments were performed.

K2. Rhodium acetate-catalyzed reaction of diazomalonate 19 with diisopropylamine followed by NMR over time. Under N₂, a mixture of diisopropylamine (889 mg, 8.88 mmol, 1.20 eq), **19** (1.17 g, 7.40 mmol, 1.00 eq) and Rh₂(OAc)₄ (42.1 mg, 0.095 mmol, 1.28 mol%) in benzene-*d*₆ (10 mL) was refluxed. NMR experiments were conducted for aliquots (~0.6 mL) taken at *t* = 15, 45, 105, 165 and 1440 min. The ¹H-NMR spectrum at *t* = 105 min is shown in Figure 4.4.

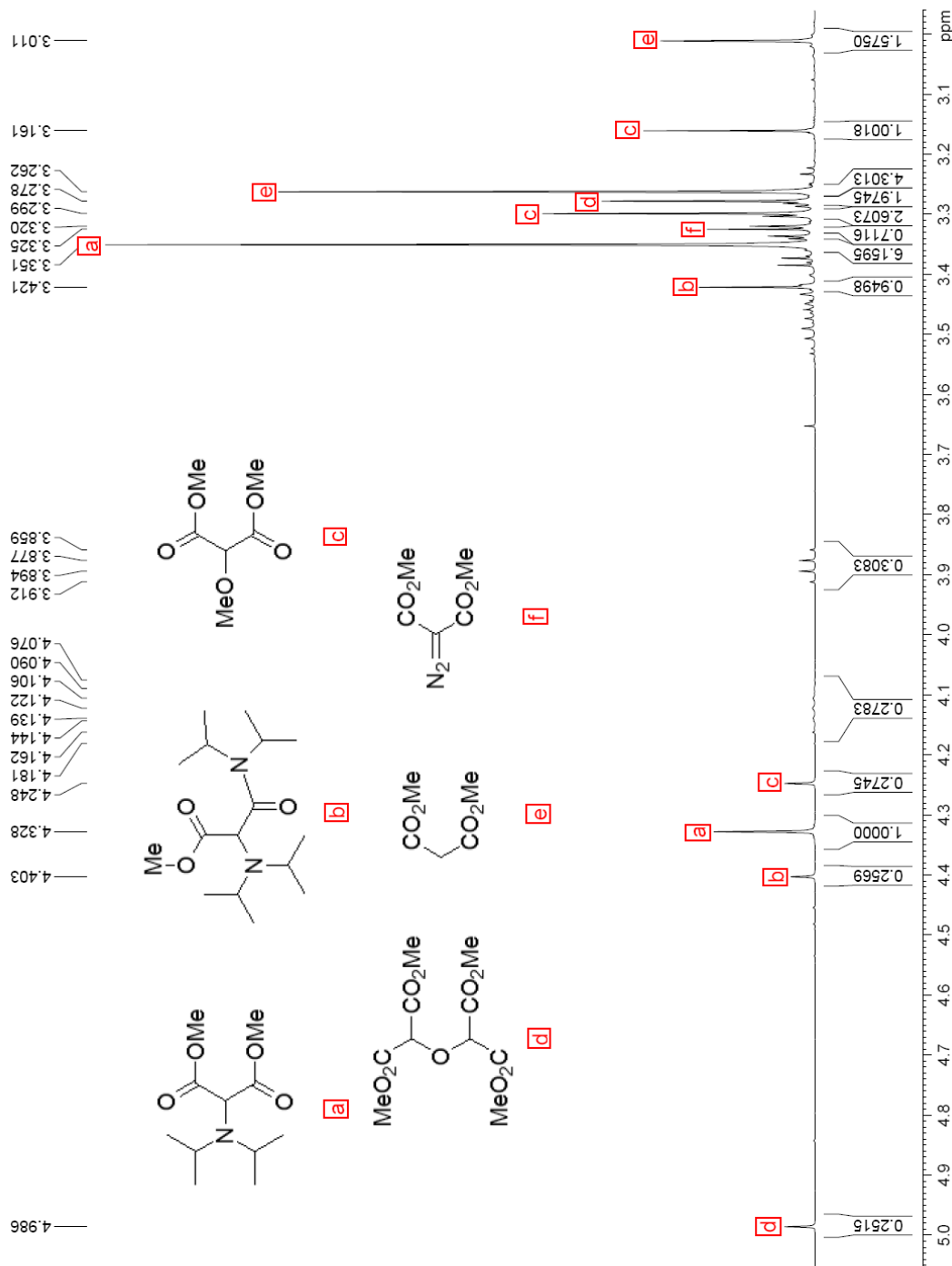
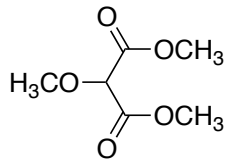
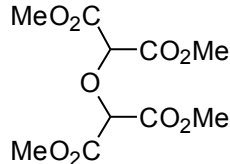


Figure 4.4. Partial 400 MHz ^1H -NMR spectrum (*ca.* 2.96 – 5.05 ppm) of the crude reaction mixture (experiment **K2**) at $t = 105$ min (Compounds were identified as indicated above).



88

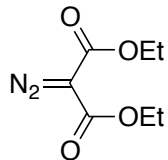
2-Methoxydimethylmalonate, 88. To an oven-dried round bottomed flask under N₂, a mixture of methanol (142 mg, 4.44 mmol, 1.20 eq), dimethyl diazomalonate **19** (585 mg, 3.70 mmol) and Rh₂(OAc)₄ (22.1 mg, 0.0500 mmol, 1.35 mol%) in 5 mL benzene-d₆ was refluxed for 15 min, at which time NMR indicated loss of starting materials. Solvent was removed on the rotary evaporator and the residual oil was purified using silica gel chromatography (EtOAc/hexanes 1:4 v/v) to give a colorless oil **88**, 462 mg, 77.0%. ¹H NMR (250 MHz, C₆D₆) δ_H 3.18 (s, 3H), 3.32 (s, 6H), 4.56 (s, 1H). ¹³C (62 MHz, C₆D₆) δ_C: 51.7 (CH₃), 57.9 (CH₃), 80.2 (CH), 166.2 (quat). HRMS (CI+): *m/z* Calcd for C₆H₁₁O₅ (M⁺ + H) 163.0606, found 163.0590. ¹H and ¹³C NMR shifts are agreement with published values.⁵⁵



89

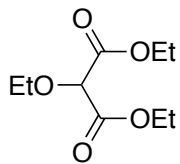
2,2'-Oxybis(malonic acid) tetramethyl ester, 89. Under N₂, a mixture of amine **108** (161 mg, 0.929 mmol, 1.00 eq), dimethyl diazomalonate **19** (189 mg, 1.20 mmol, 1.07 eq) and Rh₂(OAc)₄ (9.10 mg, 0.0206 mmol, 2.22 mol%) in benzene-d₆ (5 mL) was refluxed for 3 h. Solvent was removed on the rotary evaporator and the residue purified by silica gel flash column chromatography (EtOAc/hexanes 1:4) to yield two fractions; a non-polar inseparable mixture 135 mg and a polar colorless oil **89** (55.0 mg, 16.5%). ¹H (400 MHz, CDCl₃) δ_H 3.84 (s, 12H),

4.98 (s, 2H). ^{13}C (100 MHz, CDCl_3) δ_{C} 53.2 (CH_3), 77.2 (CH), 165.0 (quat). HRMS (ESI+): m/z Calcd for $\text{C}_{10}\text{H}_{15}\text{O}_9$ (M^++H) 279.0716; found 279.0746.



93

Diethyl diazomalonate, 93.³⁵ Under N_2 , a stirred solution of diethyl malonate (3.00 g, 18.7 mmol) and *p*-acetamidobenzenesulfonyl azide (6.76 g, 28.2 mmol, 1.51 eq) in 50 mL acetonitrile at 0 °C was added dropwise triethylamine (4.17 g, 41.2 mmol, 2.20 eq). The mixture was allowed to reach rt and was stirred for 12 h. The mixture was filtered and the filtrate concentrated on a rotary evaporator. The residue was purified by silica gel flash column chromatography (EtOAc/hexanes 1:4) to yield a pale yellow oil, **93** (2.35 g, 67.3%). ^1H (400 MHz, CDCl_3) δ_{H} : 1.32 (t, $J = 7.1$ Hz, 6H), 4.31 (quartet, $J = 7.1$ Hz, 4H). ^{13}C (100 MHz, CDCl_3) δ_{C} 14.3 (CH_3), 61.5 (CH_2), 161.0 (quat). ^1H and ^{13}C NMR shifts are in agreement with published values.⁵⁷



98

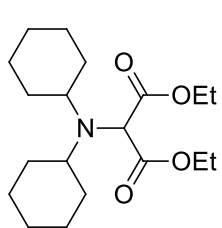
2-Ethoxydiethylmalonate, 98. To an oven-dried round bottomed flask a mixture of diethyl diazomalonate **99** (274 mg, 1.48 mmol), absolute ethanol (74.8 mg, 1.62 mmol, 1.09 eq) and $\text{Rh}_2(\text{OAc})_4$ (8.03 mg, 0.0182 mmol, 1.23 mol%) in 1 mL C_6D_6 was refluxed under N_2 for 45 min. ^1H NMR (400 MHz, C_6D_6) δ_{H} 0.92 (t, $J = 7.1$ Hz, 6H), 1.04 (t, $J = 7.0$ Hz, 3H), 3.42 (quartet, $J = 7.1$ Hz, 2H), 4.01-3.89 (m, 4H), 4.40 (s, 1H). ^{13}C (100 MHz, C_6D_6) δ_{C} 13.6 (CH_3), 14.7 (CH_3), 61.1 (CH_2), 66.4 (CH_2), 79.2 (CH), 166.4 (quat). HRMS (ESI+): m/z Calcd for $\text{C}_9\text{H}_{17}\text{O}_5$ ($\text{M}^+ + \text{H}$) 196.1136; found 196.1136.

H) 205.1076, found 205.1072. $^1\text{H-NMR}$ chemical shifts are in agreement with published values.⁵⁶

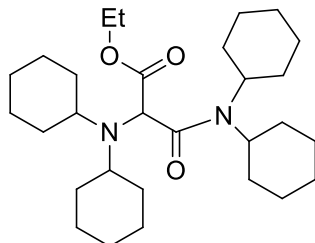
L. INVESTIGATIONS OF RHODIUM ACETATE-CATALYZED N-H INSERTION REACTIONS OF DIETHYL DIAZOMALONATE **89 WITH DICYCLOHEXYLAMINE, AND WITH DIISOPROPYLAMINE.**

L1. Rhodium acetate-catalyzed reaction of diazomalonate **93 with dicyclohexylamine.**

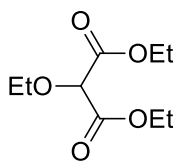
Under N_2 , a mixture of dicyclohexylamine (226 mg, 1.25 mmol, 1.15 eq), diethyl diazomalonate **139** (202 mg, 1.09 mmol, 1.00 eq) and $\text{Rh}_2(\text{OAc})_4$ (4.40 mg, 0.00995 mmol, 0.913 mol%) in benzene- d_6 (1.00 mL) was refluxed for 45 min and NMR experiments performed. Figures 4.5 and 4.6 show the results. HRMS (ESI+) of the crude mixture gave **94** m/z Calcd for $\text{C}_{19}\text{H}_{34}\text{NO}_4$ ($\text{M}^+ + \text{H}$) 340.2488; found 340.2487, **96** m/z Calcd for $\text{C}_{29}\text{H}_{51}\text{N}_2\text{O}_3$ ($\text{M}^+ + \text{H}$) 475.3900; found 475.3890.



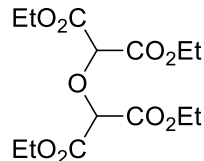
94



96



98



99

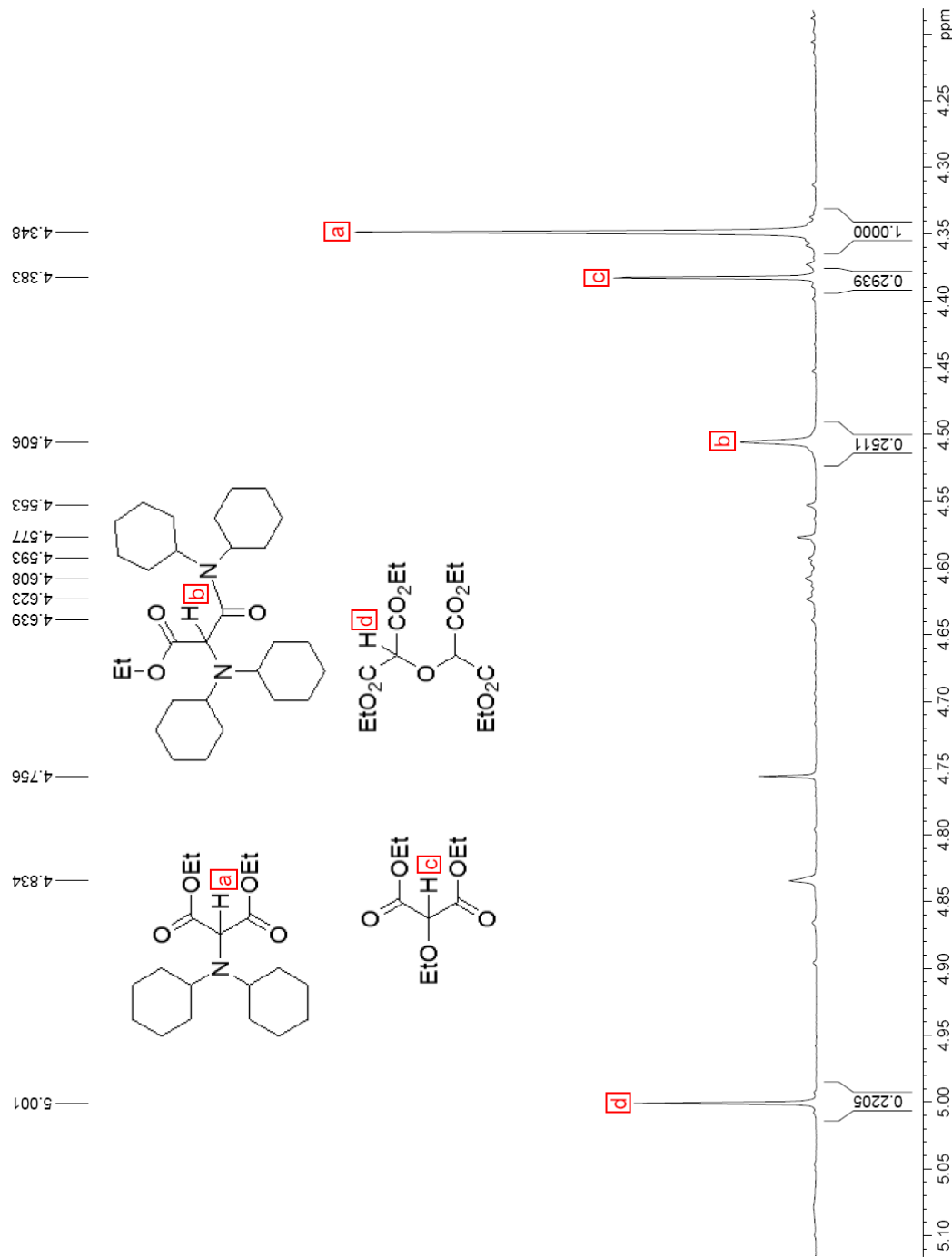


Figure 4.5. Partial 400 MHz ^1H -NMR spectrum (*ca.* 4.20 – 5.10 ppm) of the crude reaction mixture (experiment L1). All peaks in this region are due to methine protons adjacent two carbonyl groups.

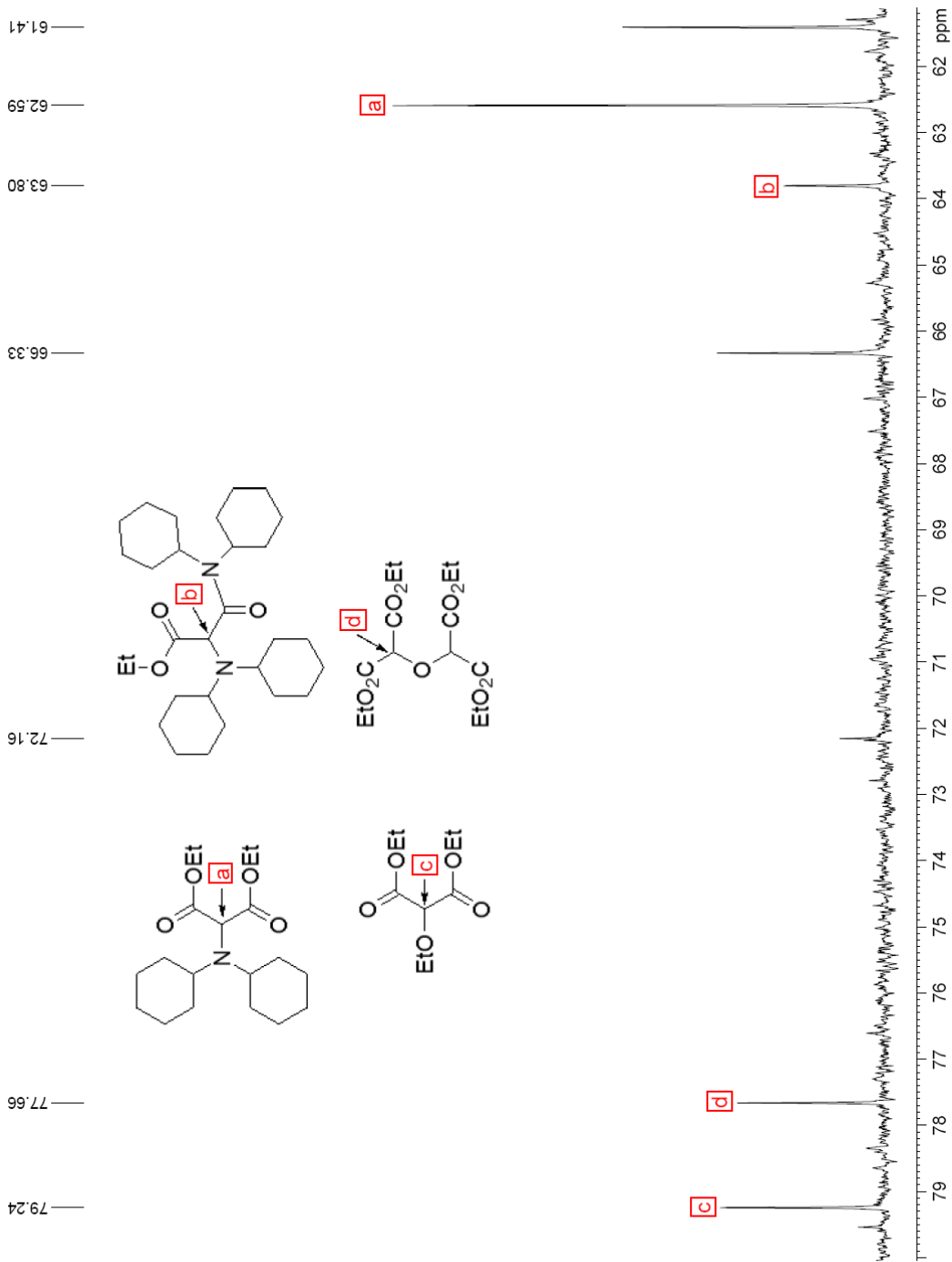
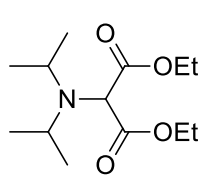


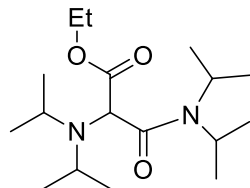
Figure 4.6. Partial 100 MHz ^{13}C -NMR spectrum (*ca.* 61.0 – 80.0 ppm) of the crude reaction mixture (experiment L1). All peaks in this region are due to methine carbons adjacent two carbonyl groups.

L2. Rhodium acetate-catalyzed reaction of diazomalonate 93 with diisopropylamine.

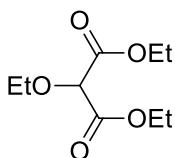
Under N₂, a mixture of diisopropylamine (127 mg, 1.26 mmol, 1.25 eq), diethyl diazomalonate **93** (188 mg, 1.01 mmol, 1.00 eq) and Rh₂(OAc)₄ (4.46 mg, 0.0101 mmol, 1.00 mol%) in benzene-*d*₆ (1.00 mL) was refluxed for 45 min and NMR experiments performed. Figure 4.7 and 4.8 show the results. HRMS (ESI+) of the crude mixture gave **95** *m/z* Calcd for C₁₃H₂₆NO₄ (M⁺ + H) 260.1862; found 260.1862, **97** *m/z* Calcd for C₁₇H₃₅N₂O₃ (M⁺ + H) 315.2648; found 315.2630 and **99** *m/z* Calcd for C₁₄H₂₃O₉ (M⁺ + H) 335.1342; found 335.1285.



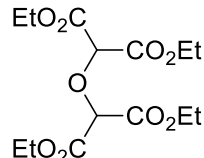
95



97



98



99

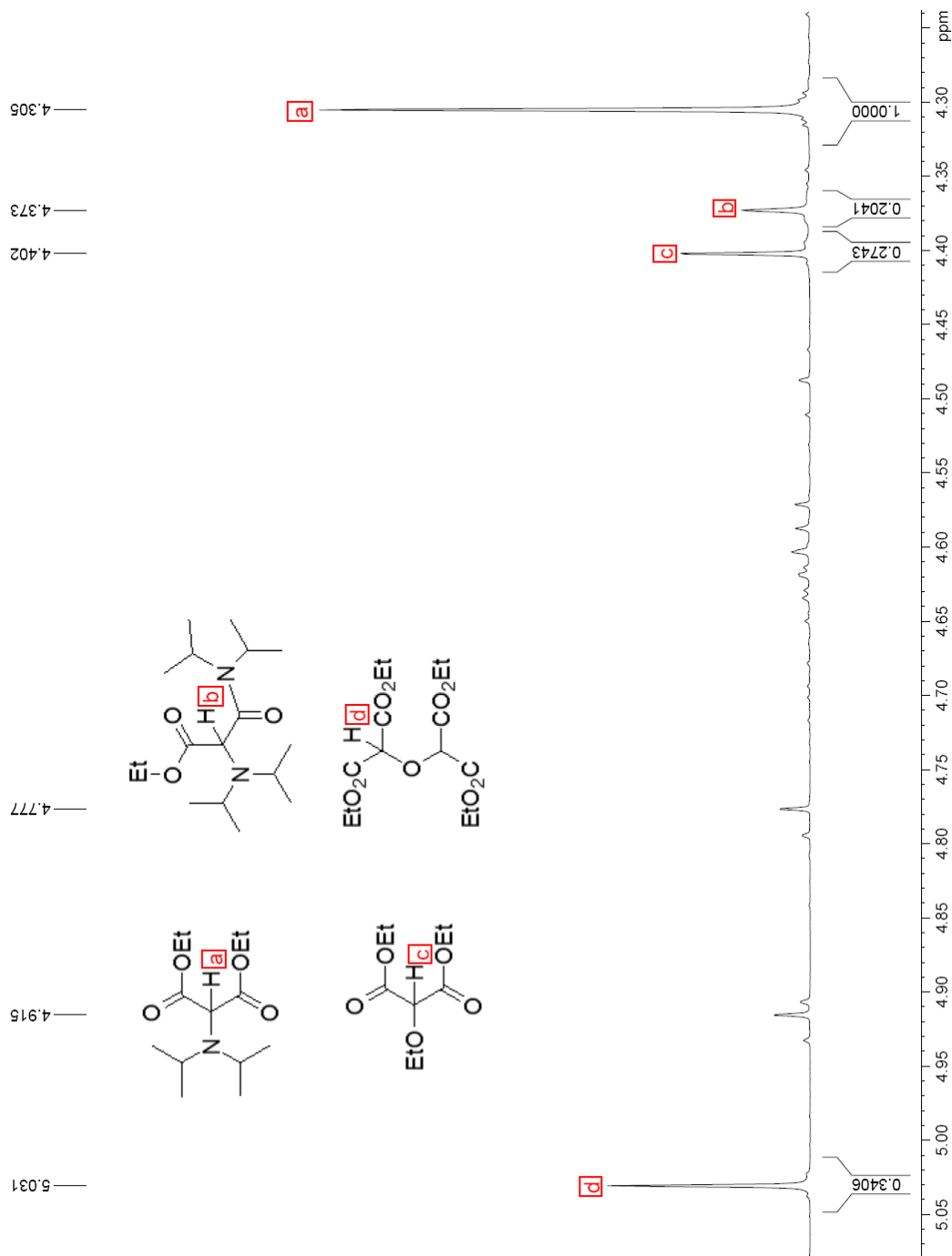


Figure 4.7. Partial 400 MHz ^1H -NMR spectrum (ca. 4.24 – 5.07 ppm) of the crude reaction mixture (experiment **L2**). All peaks in this region are due to methine protons adjacent two carbonyl groups.

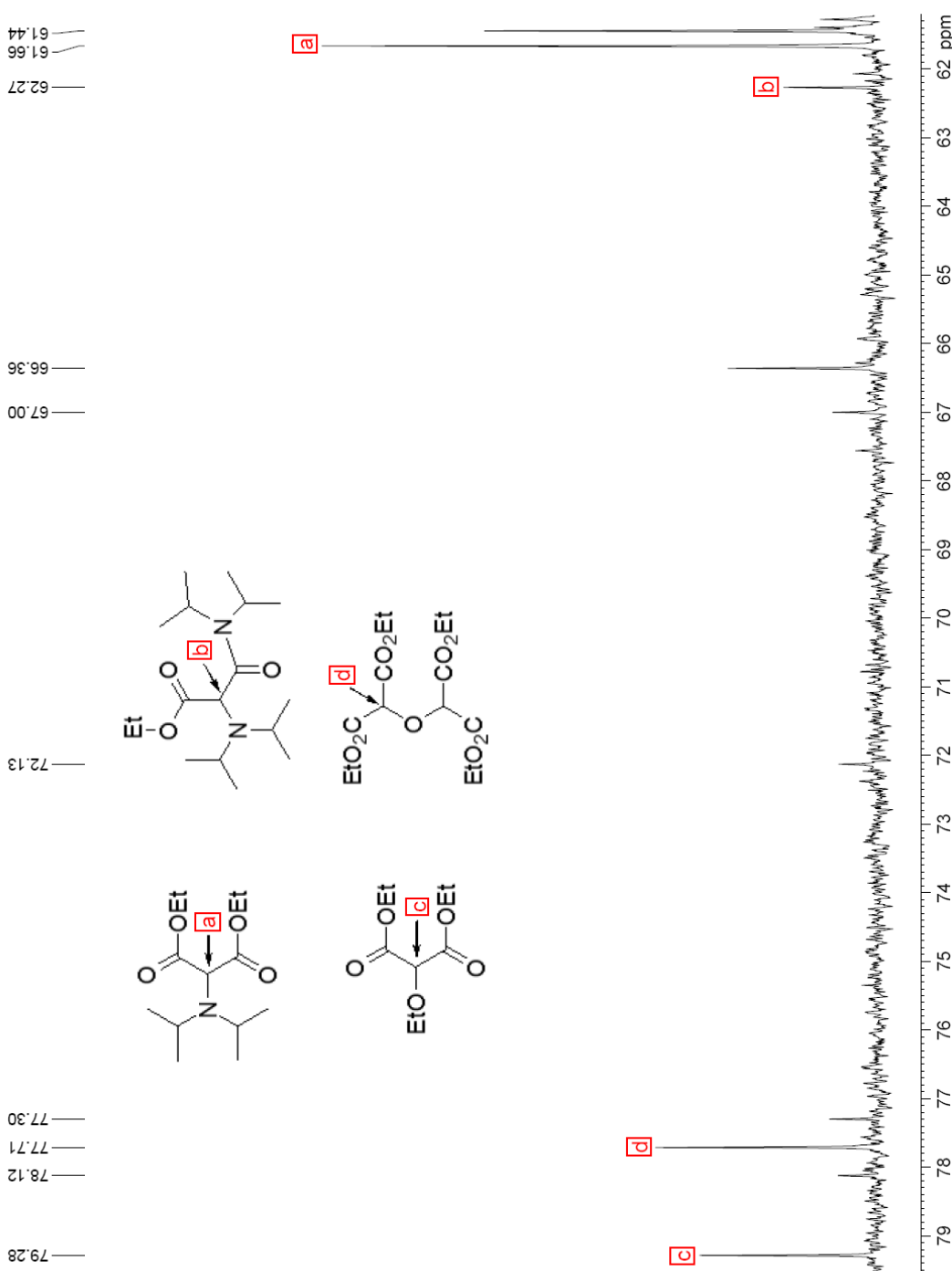


Figure 4.8. Partial 100 MHz ^{13}C -NMR spectrum (ca. 61.3 – 79.5 ppm) of the crude reaction mixture (experiment **L2**). All peaks in this region are due to methine carbons adjacent two carbonyl groups.

**M. INVESTIGATION OF RHODIUM ACETATE-CATALYZED REACTION OF
DIMETHYL DIAZOMALONATE **19** WITH 2,2,2-TRIFLUOROETHANOL.**

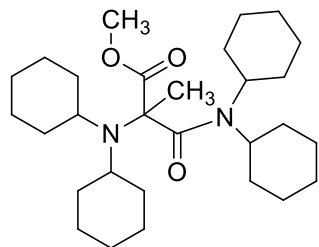
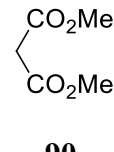
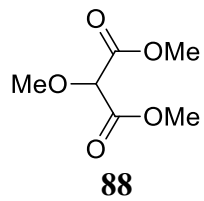
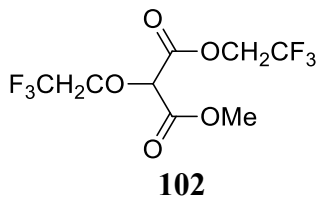
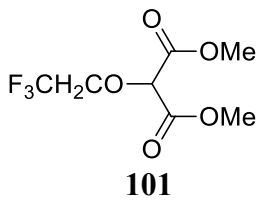
Under N₂, a mixture of trifluoroethanol (340 mg, 3.39 mmol, 1.18 eq), dimethyl diazomalonate **19** (454 mg, 2.87 mmol, 1.00 eq) and Rh₂(OAc)₄ (19.1 mg, 0.0432 mmol, 1.51 mol%) in benzene-d₆ (5.60 mL) was heated in a 70 °C oil bath. Aliquots (~ 0.60 mL) were taken at *t* = 15, 45, 105, 165 and 1440 min, quickly immersed in liquid N₂ to halt the reaction, warmed to rt and NMR experiments performed. The aliquot at *t* = 1440 min was used for GC and GC-MS experiments.

GC conditions. Column: Fisher Scientific, TG-WAXMS, 30 m x 0.25 mm, film size 0.255 μm. Carrier gas: He, 1 mL/min. Temperature program: 1 min at 50 °C, 50 °C to 250 °C at 20 °C/min, 1 min at 250 °C. Peaks were observed at the following retention times (min): 7.85, 8.36, 8.85.

GC-MS conditions. GC conditions same as above except for the temperature program: 3 min at 50 °C, 50 °C to 250 °C at 8 °C /min, 1 min at 250 °C. MS detector: CI+, CH₄ ionization gas. Compound, retention time (min), base peak (*m/z*): **90**, 12.1, 100; **102**, 14.2, 171; **101**, 15.1, 103; **88**, 16.0, 103.

Compound **101**. ¹H-NMR (400 MHz, C₆D₆) δ_H 3.24 (s, 6H), 3.66 (quartet, *J* = 8.8 Hz, 2H), 4.39 (s, 1H). ¹³C-NMR (100 MHz, C₆D₆) δ_C 52.0, 67.0 (quartet, *J* = 34.9 Hz), 123.7 (quartet, *J* = 278.5 Hz), 165.5. HRMS (CI+): *m/z* Calcd for C₇H₁₀F₃O₅ (M⁺ + H) 231.0480; found 231.0441.

Compound **102**. ¹H-NMR (400 MHz, C₆D₆) δ_H 3.28 (s, 3H), 3.63 (quartet, *J* = 8.6 Hz, 2H), 3.97 (m, 2H), 4.35 (s, 1H). ¹³C-NMR (100 MHz, C₆D₆) δ_C 52.2, 60.5 (quartet, *J* = 37.3 Hz), 67.3 (quartet, *J* = 35.0 Hz), 78.3, 122.7 (quartet, *J* = 277.5 Hz), 123.5 (quartet, *J* = 276.3 Hz), 163.8, 164.7. HRMS (CI+): *m/z* Calcd for C₈H₉F₆O₅ (M⁺ + H) 299.0354; found 299.0363.

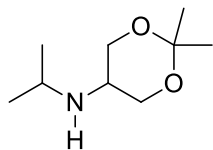


105

N,N-Dicyclohexyl-2-dicyclohexylamino-2-methylmalonic acid methyl ester, 105.

Under N₂, 50% NaH dispersion in mineral oil was added to dry THF and filtered. The solid was transferred quickly to a tared flask and weighed.³⁴ Dry THF (10 mL) was added to the pre-weighed NaH (420 mg, 17.5 mmol) followed by a 72:28 mixture of **86** and **87** (640 mg, **87**; 0.389 mmol) and the mixture stirred at rt for 30 min. Iodomethane (1.99 g, 14.0 mmol) was added dropwise to the mixture and stirred for 14 h. The reaction was quenched by addition of water (10 mL) and extracted with CH₂Cl₂ (2 x 10 mL). The combined organic phase was dried over anhydrous Na₂SO₄, filtered and solvent removed on the rotary evaporator. A CDCl₃ solution of the residue in a NMR tube precipitated a solid that was filtered and recrystallized from CHCl₃ to yield a colorless crystalline solid **105** (5.21 mg, 2.82%) mp 169-171 °C. ¹H-NMR (400 MHz, CDCl₃) δ_H 1.03-1.88 (m, 38H), 1.67 (s, 3H), 2.13 (m, 2H), 2.52 (m, 2H), 2.85 (m, 3H), 3.66 (s, 3H), 4.49 (m, 1H). ¹³C-NMR (100 MHz, CDCl₃) δ_C 24.5, 25.5, 25.7, 25.8, 26.3, 26.6, 26.6, 27.7, 27.9, 28.9, 29.3, 31.1, 31.4, 35.7, 35.9, 51.6, 55.3, 56.7, 60.6, 174.3. HRMS (ESI+): *m/z* Calcd for C₂₉H₅₁N₂O₃ (M⁺+H): 475.3900, found 475.3859. A crystal 0.434 mm x 0.268 mm x 0.184 mm was selected for X-ray crystallography with 0.71073 Å (Mo Kα)

radiation: monoclinic $a = 10.2512(5)$ Å, $b = 10.1475(5)$ Å, $c = 15.4702(8)$ Å, $\alpha = 90^\circ$, $\beta = 103.9230(10)^\circ$, $\gamma = 90^\circ$; $Z = 2$; 14124 reflections were collected, 7392 independent, $-13 \leq h \leq 13$, $-13 \leq k \leq 13$, $-22 \leq l \leq 20$. Full-matrix least-squares refinement on F^2 , data-to-parameter ratio = 21.4, goodness-of-fit = 1.092, $R_1 = 0.0449$, $wR_2 = 0.1034$ ($I > 2\sigma(I)$), $R_1 = 0.0638$, $wR_2 = 0.1275$ (all data). Crystal structure determination was performed by Dr. Anna-Gay D. Nelson. Full details are given in Appendix dms-1-67.



108

5-Isopropylamino-2,2-dimethyl-1,3-dioxane, 108. To a stirred solution of 2-isopropylamino-1,3-propanediol **102** (1.02 g, 7.68 mmol) in 5 mL methanol, 10 mL of conc. HCl was added slowly and stirred for 2 h. Solvent was removed on a rotary evaporator and the residue was vacuum pumped < 1 mm Hg overnight to give a brown semisolid (1.36 g). This was dissolved in 3 mL dry DMF, and 2,2-dimethoxypropane (4.23 g, 40.6 mmol, 5.29 eq) and camphorsulfonic acid (168 mg, 0.723 mmol, 9.41 mol%) were added, and the mixture stirred for 12 h. Triethylamine (71.8 mg, 0.709 mmol) was added and the mixture further stirred for 2 h. The solvent was removed *in vacuo*. The residue was dissolved in EtOAc and treated with additional triethylamine (1.03 g, 10.2 mmol). The precipitate that resulted was filtered off, solvent removed *in vacuo* and the residue extracted with hot hexanes to give a colorless oil (211 mg, 15.7 %). $^1\text{H-NMR}$ (400 MHz, CDCl_3) δ_{H} 1.02 (d, $J = 6.4$ Hz, 6H), 1.40 (s, 3H), 1.39 (s, 3H), 2.72 (tt, $J = 6.2, 3.9$ Hz, 1H), 2.91 (septet, $J = 6.3$ Hz, 1H), 3.61 (dd, $J = 11.6, 6.0$ Hz, 2H), 3.93 (dd, $J = 11.6, 4.0$ Hz, 2H). $^{13}\text{C-NMR}$ (100 MHz, CDCl_3) δ_{C} 23.2 (CH_3), 23.6 (CH_3), 23.8 (CH_3),

45.1 (CH), 48.1 (CH), 64.1 (CH₂), 98.0 (quat). HRMS (ESI+): *m/z* Calcd for C₉H₂₀NO₂ (M⁺ + H) 174.1494; found 174.1491.

Computational details.

Density functional theory (DFT) and Hartree Fock (HF) calculations were carried out using GAUSSIAN 09^{ref} package on High Performance Computing systems at Alabama SuperComputer (ASC). Optimizations were done using B3LYP method with the 6-311 G (d, p) basis set. Frequencies were computed analytically for all optimized structures to characterize each stationary point as a minimum (no negative, imaginary frequencies). NBO 3.1 and 5.9 programs were used as implemented in GAUSSIAN 09 package. NBO energetic analysis was performed by deleting; (*i*) the corresponding NBO σ* orbitals and (*ii*) the corresponding off-diagonal Fock matrix elements in the NBO basis, at HF theory (DFT method is poorly parameterized).¹⁰³

5. REFERENCES

1. Jie, Y. "Tris(1,3-dihydroxy-2-propyl)amine, A Planar Trialkylamine: Synthesis, Structure, And Properties. A Potential Precursor To Hypervalent Nitrogen" Ph. D Dissertation, Auburn University, **2006**.
2. (a) Pinkas, J.; Gaul, B.; Verkade, J. G. *J. Am. Chem. Soc.* **1993**, *115*, 3925-3931 (b)
Pinkas, J.; Wang, T.; Jacobson, R. A.; Verkade, J. G. *Inorg. Chem.* **1994**, *33*, 4202-4210.
3. Milbrath, D. S.; Verkade, J. G. *J. Am. Chem. Soc.* **1977**, *99*, 6607-6613.
4. (a) Pinkas, J.; Tang, J.; Wan, Y.; Verkade, J. G. *Phos. Sulf. Silicon* **1994**, *87*, 193-207. (b)
Raders, S. M.; Verkade, J. G. *Tetrahedron Lett.* **2008**, *49*, 3507-3511.
5. (a) Pinkas, J.; Gaul, B.; Verkade, J. G. *J. Am. Chem. Soc.* **1993**, *115*, 3925-3931 (b)
Pinkas, J.; Wang, T.; Jacobson, R. A.; Verkade, J. G. *Inorg. Chem.* **1994**, *33*, 4202-4210.
6. Jie, Y. P.; Livant, P.; Li, H.; Yang, M. M.; Zhu, W.; Cammarata, V.; Almond, P.; Sullens, T.; Qin, Y.; Bakker, E. *J. Org. Chem.* **2010**, *75*, 4472-4479.
7. Yang, M.; Albrecht-Schmitt, T.; Cammarata, V.; Livant, P.; Makhanu, D. S.; Sykora, R.; Zhu, W. *J. Org. Chem.* **2009**, *74*, 2671-2678.
8. Hegedus, L. S.; Holden, M. S.; McKearin, J. M. *Org. Syn.* **1990**, *7*, 501; *1984*, *62*, 48.
9. Kiankarimi, M.; Lowe, R.; McCarthy, J. R.; Whitten, J. P. *Tet. Lett.* **1999**, *40*, 4497-4500.
10. Blackman, A. G. *Australian. J. Chem.* **2002**, *55*, 263-266.
11. Schiemenz, G. P. Z. *Naturforsch.* **2007**, *62b*, 235-243.
12. Baeg, J-O.; Holm, R. H. *Chem. Commun.* **1998**, 571-572.

13. Mizzoni, R. H.; Hennessey, M. A.; Scholz, C. R. *J. Chem. Soc.* **1953**, 76, 2414-2417.
14. Schiemenz, G. P.; Petersen, S.; Porksen, S. *Z. Naturforsch.* **2003**, 58b, 715-724.
15. Henry, J. R.; Marcin, L. R.; McIntosh, M. C.; Scola, P. M.; Harris, G. D.; Weinreb, S. M. *Tet. Lett.* **1989**, 30, 5709-5712.
16. Jia, X.; Huang, Q.; Li, J.; Li, S.; Yang, Q. *Synlett.* **2007**, 5, 806-808.
17. Rew, Y.; Goodman, M. *J. Org. Chem.* **2002**, 67, 8820-8826.
18. Rowland, R. S.; Taylor, R. *J. Phys. Chem.* 1996, 100, 7384-7391.
19. Sugimura, T.; Hagiya, K. *Chem. Lett.* **2007**, 36, 566-567.
20. Lipshutz, B. H.; Chung, D. W.; Rich, B.; Corral, R. *Org. Lett.* **2006**, 8, 5069-5072.
21. Kan, T.; Fukuyama, T. *Chem. Commun.* **2004**, 353-359.
22. But, T. Y. S.; Toy, P. H. *Chem. Asian J.* **2007**, 2, 1340-1355.
23. Barnett, C. J.; Grubb, L. M. *Tetrahedron* **2000**, 56, 9221-9225.
24. Brooks, A. F.; Garcia, G. A.; Showalter, H. D. H. *Tet. Lett.* **2010**, 51, 4163-4165.
25. (a) Tunoori, A.; Dutta, D.; Georg, G.; *Tetrahedron Lett.* **1998**, 39, 8751. (b) Barret, A. G. M.; Roberts, R. S.; Schroder, J. *Org. Lett.* **2000**, 2, 2999.
26. Swamy, K. C. K.; Kumar, N. N. B.; Balaraman, E.; Kumar, K. V. P. P. *Chem. Rev.* **2009**, 109, 2551-2651.
27. Dembinski, R. *Eur. J. Org. Chem.* **2004**, 2763-2772.
28. Reynolds, A. J.; Kassiou, M. *Curr. Org. Chem.* **2009**, 13, 1610-1632.
29. Golantsov, N. E.; Karchava, A. V.; Yurovskaya, M. A. *Chem. Het. Compounds* **2008**, 44, 263-294.
30. (a) Szarek, W. A.; Zamojski, A.; Tiwari, K. N.; Ison, E. R. *Tetrahedron Lett.* **1986**, 27, 3827-3830. (b) Feldman, K. S.; Lawlor, M. D. *J. Am. Chem. Soc.* **2000**, 122, 7396-7397.

31. (a) Kurosawa, W.; Kan, T.; Fukuyama, T. *Org. Syn.* **2002**, *79*, 186-195. (b) Guisado, C.; Waterhouse, J. E.; Price, W. S.; Jorgensen, M. R.; Miller, A. D. *Org. Biomol. Chem.* **2005**, *3*, 1049-1057.
32. Scott, D. A.; Krulle, T. M.; Finn, M.; Nash, R. J.; Winters, A. L.; Asano, N.; Butters, T. D.; Fleet, G. W. *J. Tetrahedron Lett.* **1999**, *40*, 7581-7584.
33. Baum, J. S.; Shook, D. A.; Davies, H. M. L.; Smith, H. D. *Synth. Commun.* **1987**, *17*, 1709-1714.
34. (a) Yang, M. “Studies in Carbenoid Chemistry: N-H Insertion Reactions Leading to Hindered Tertiary amines, and Double Cyclopropanations of Aromatic Compounds” Ph. D. Dissertation, Auburn University, **2001**. (b) Yang, M.; Wang, X.; Li, H.; Livant, P. J. *Org. Chem.* **2001**, *45*, 4472-4479.
35. (a) Jie, Y. “Tris(1,3-dihydroxy-2-propyl)amine, A Planar Trialkylamine:Synthesis, Structure, And Properties. A Potential Precursor To Hypervalent Nitrogen” Ph. D Dissertation, Auburn University, **2006**. (b) Jie, Y. P.; Livant, P.; Li, H.; Yang, M. M.; Zhu, W.; Cammarata, V.; Almond, P.; Sullens, T.; Qin, Y.; Bakker, E. *J. Org. Chem.* **2010**, *75*, 4472-4479.
36. (a) Hsieh, J-C.; Cheng, C-H. *Chem. Comm.* 2005, *36*, 4554-4556. (b) Yang, M.; Zhou, J.; Schneller, S. W. *Tetrahedron* **2006**, *62*, 1295-1300.
37. (a) Hopkins, C. E.; O’Connor, P. B.; Allen, K. N.; Costello, C. E.; Tollan, D. R. *Prot. Sci.* **2002**, *11*, 1591-1599. (b) Childs, A. F.; Goldsworthy, L. J.; Harding, G. F.; King, F. E.; Nineham, A. W.; Norris, W. L.; Plant, S. G. P.; Selton, B.; Tompsett, A. L. L. *J. Chem. Soc.* **1948**, 2174-2177.

38. (a) Barrett, D. M. Y.; Kahwa, I. A.; Mague, J. T.; McPherson, G. L. *J. Org. Chem.* **1995**, *60*, 5946 “recrystallized from ethanol/CHCl₃ to form brown crystals mp 183 °C”. (b) Kimura, E.; Young, S.; Collman, J. P. *Inorg. Chem.* **1970**, *9*, 1183-1191. “Tren ligand synthesis through tris(2-chloroethyl)amine”
39. Backes, J. V.; West, R. W.; Whiteley, M. A. *J. Chem. Soc.* **1921**, *119*, 359-
40. Jia, X.; Huang, Q.; Li, J.; Li, S.; Yang, Q. *SynLett.* **2007**, *5*, 0806-0808.
41. Yang, M.; Wang, X.; Li, H.; Livant, P. *J. Org. Chem.*, **2001**, *66*, 6729–6733.
42. (a) Ludwig, B. J.; West, W.A.; Farnsworth, D.W. *J. Am. Chem. Soc.* **1954**, *76*, 2891-2893. (b) Leclerc, G.; Bieth, N.; Schwartz, J. *J. Med. Chem.* **1980**, *23*, 620-624. (c) Hollingsworth, N.; Kociok-Kohn, G.; Molloy, K. C.; Sudlow, A. L. *Dalt. Trans.* **2010**, *39*, 5446-5452. (d) Gaertner, V. R. *Tetrahedron* **1967**, *23*, 2123-2136.
43. (a) Murray-Rust, P.; McManus, J.; Lennon, S. P.; Porter, A. E. A.; Rechka, J. A. *J. Chem. Soc. Perkin Trans. 1* **1984**, 783. (b) Morzherin, Y.; Subbotina, O.; Nein, I.; Kolobov, M.; Bakulev, V. A. *Russ. Chem. Bull., In. Ed.* **2004**, *53*, 1305-1310.
44. (a) Axenrod, T.; Sun, J.; Das, K. K.; Dave, P.R.; Forohar, F.; Kaselj, M.; Trivedi, N. J.; Gilardi, R. D.; Flippen-Anderson, J. L. *J. Org. Chem.* **2000**, *65*, 1200. (b) Locke, J. M.; Crumbie, R. L.; Griffith, R.; Bailey, T. D.; Boyd, S.; Roberts, J. D. *J. Org. Chem.* **2007**, *72*, 4156-4162.
45. (a) Enders, D.; Wortmann, L.; Dücker, B.; Raabe, G. *Helv. Chim. Act.* **1999**, *82*, 1195-1201. (b) Enders, D.; Wortmann, L.; Dücker, B.; Raabe, G. *Heterocycles*, **2004**, *62*, 559-581. (c) Medou, M.; Priem, G.; Quelever, G.; Camplo, M.; Kraus, J. L. *Tetrahedron Lett.* **1998**, *39*, 4021-4024. (d) Stork, G.; Leong, A.; Touzin, A. *J. Org. Chem.* **1976**, *41*, 3491-3493.

46. Rosowsky, A.; Chen, K. K. N.; Papathanasopoulos, N. *J. Heterocycl. Chem.* **1976**, *13*, 727-732. (b) Rao, J.; Saxena, A. K. *Ind. J. Chem.* **1989**, *28B*, 620-625.
47. (a) Boeckman, Jr, R. K.; Shao, P.; Mullins, J. J. *Org. Syn. Coll.* **2004**, *10*, 696. (b) *Org. Syn.* **2000**, *77*, 141. (c) Dess, D. B.; Martin, J. C. *J. Am. Chem. Soc.* **1991**, *113*, 7277-7287.
48. Shriner, R. L.; Fuson, R. C.; Curtin, D. C. *The Systematic Identification of Organic Compounds. A laboratory manual*; 5th ed. John Wiley & Sons Inc.: New York. London. Sydney, **1967**, p 290.
49. Grotjahn, D.; Joubran, C. *Tetrahedron Asym.* **1995**, *6*, 745-752.
50. Clark-Lewis, J. W.; Thompson, M. J. *J. Chem. Soc.* **1959**, 1628-1629.
51. Ramachary, D. B.; Narayana, V.V.; Ramakumar, K. *Tetrahedron Lett.* **2008**, *49*, 2704-2709.
52. Burkhardt, E. R.; Coleridge, B. M. *Tetrahedron Lett.* **2008**, *49*, 5152-5155.
53. (a) Hannon, S. J.; Kundu, N. G.; Hertzberg, R. P.; Bhatt, R. S.; Heidelberger, C. *Tetrahedron Lett.* **1980**, *21*, 1105-1108. (b) Ulgheri, F.; Basca, J.; Nassimbeni, L.; Spanu, P. *Tetrahedron Lett.* **2003**, *44*, 671-675.
54. Baslé, E.; Jean, M.; Gouault, N.; Renault, J.; Uriac, P. *Tetrahedron Lett.* **2007**, *48*, 8138-8140.
55. (a) Shevchenko, V. V.; *Russ. J. Org. Chem.* **2006**, *42*, 1741-1744. (b) Shevchenko, V. *Helv. Chim. Act.* **2008**, *91*, 501-509. (c) Pellicciari, R.; Cogolli, P. *J. Chem. Soc., Perkin I* **1976**, 2483-2484.
56. Pellicciari, R.; Cogolli, P. *Synthesis* **1975**, *4*, 269-270.

57. (a) Schulze, B.; Russ. J. Org. Chem. 2004, 40, 740-746. (b) Albright, T. A.; Freeman, W. J. Org. Mag. Res. 1977, 9, 75-79. (b) Kitamura, M.; Tashiro, N.; Miyagawa, S.; Okauchi, T. Synthesis 2011, 7, 1037-1044. (c) Goddard-Borger, E. D. Org. Lett. 2007, 9, 3797-3800. (d) Ranielli, R. de S.; de Souza, M. C. B. V.; Ferreira, V. F. Synth. Commun. 2004, 34, 951-959. (e) Chen, Y-J.; Hung, H-C.; Sha, C-K.; Chung, W-S. Tetrahedron 2010, 66, 176-182.
58. Deng, Q.; Xu, H. ; Yuen, A. W. ; Xu, Z. ; Che, C. *Org. Lett.* **2008**, *10*, 1529-1532.
59. Abiraj, K.; Gowda, D. C. *J. Chem. Res.* **2003**, *6*, 332-334.
60. (a) Abdel-Magid, A. F.; Carson, K. G.; Harris, B. D.; Maryanoff, C. A.; Shah, R. D. *J. Org. Chem.* **1996**, *61*, 3849-3862. (b) Baxter, E. W.; Reitz, A. B. *Organic Reactions*, **2002**, *59*, 1-715 Chapter 1. (c) Abdel-Magid, A. F.; Mehrman, S. *J. Org. Proc. Res. Dev.* **2006**, *10*, 971-1031.
61. Murase, I. *Inorganica Chim. Acta* **1984**, 155-157.
62. Vaswani, R. G.; Chaberlain, A. R. *J. Org. Chem.* **2008**, *73*, 1661-1681.
63. (a) Dobereine, G. E.; Crabtree, R. H. *Chem. Rev.* **2010**, *110*, 681-703. (b) Guillena, G.; Ramon, D. J.; Yus, M. *Angew. Chem. Int. Ed.* **2007**, *46*, 2358-2364. (c) Hamid, M. H. S.A.; Slatford, P. A.; Williams, J. M. *J. Adv. Synth. Catal.* **2007**, *349*, 1555-1575.
64. (a) Hamid, M. H. S. A.; Allen, C. L.; Lamb, G. W.; Maxwell, A. C.; Maytum, H. C.; Watson, J. A. A.; Williams, J. M. *J. Am. Chem. Soc.* **2009**, *131*, 1766-1774. (b) Saidi, O.; Blacker, A. J.; Lamb, G. W.; Marsden, S. P.; Taylor, J. E.; Williams, J. M. *J. Org. Proc. Res. Devel.* **2010**, *14*, 1046-1049.

65. (a) Husinec, S.; Juranic, I.; Llobera, A.; Porter, A. E. A. *Synthesis*, **1988**, 721-723. (b) Murray-Rust, P.; McManus, J.; Lennon, S. P.; Porter, A. E. A.; Rechka, J. A. *J. Chem Soc. Perkin Trans. I* **1984**, 713.
66. Ganem, B. *Acc. Chem. Res.* **1982**, *15*, 290-298.
67. Doyle, M. P.; McKervey, M. A.; Ye, T. *Modern Catalytic Methods for Organic Synthesis with Diazo Compounds*; Wiley & Sons: New York, 1998; (a) Chapter 2 pg 65. (b) 449-450.
68. (a) Cama, L. D.; Christensen, B. G. *Tetrahedron Lett.* **1978**, 4233-4236. (b) Salzmann, T. N.; Ratcliffe, R. W.; Christensen, B. G.; Bouffard, F. A. *J. Am. Chem. Soc.* **1980**, *102*, 6161-6163. (c) Garcia, C. F.; McKervey, M. A.; Ye, T. *J. Chem. Soc., Chem. Commun.* **1996**, 1465-1466.
69. Backes, J. V.; West, R. W.; Whately, M. A. *J. Chem. Soc.* **1921**, *119*, 359-379.
70. (a) Ludwig, B. J.; West, W. A.; Farnsworth, D. W. *J. Am. Chem. Soc.* **1954**, *76*, 2891-2893. (b) Leclerc, G.; Bieth, N.; Schwartz, J. *J. Med. Chem.* **1980**, *23*, 624-627.
71. (a) Allen, F. H. *Acta Cryst. Sec. B* **1995**, *B51*, 378-381. (b) Kawano, M.; Hirai, K.; Tomioka, H.; Ohashi, Y. *J. Am. Chem. Soc.* **2007**, *129*, 2383-2391. (c) Allen, F. H.; Kennard, O.; Watson, D. G.; Brammer, L.; Orpen, A. G.; Taylor, R. *J. Chem. Soc., Perkin Trans. II*, **1987**, pp. S1-S19.
72. (a) Bogdanova, A.; Popik, V. V. *J. Am. Chem. Soc.* **2004**, *126*, 11293-11302. (b) Nikolaev, V. A.; Popik, V. V.; Korobitsyna, I. K. *Zh. Org. Khim.* **1991**, *27*, 505.
73. Lommerse, J. P. P.; Price, S. L.; Taylor, R. *J. Comput. Chem.* **1997**, *18*, 757-774.
74. Bondi, A. *J. Phys. Chem.* **1964**, *68*, 441-451.

75. (a) Booth, H.; Everett, J. R. *J. Chem. Soc., Perkin Trans. 2* **1980**, 255-259. (b) Booth, H.; Everett, J. R. *J. Chem. Soc., Chem. Commun.* **1976**, 278-279.
76. Anet, F. A. L.; Bradley, C. H.; Buchanan, G. W. *J. Am. Chem. Soc.* **1971**, 93, 258-259.
77. Booth, H.; Dixon, J. M.; Khedhair, K. A. *Tetrahedron* **1992**, 48, 6161-6174.
78. Eliel, E. L.; Reece, M. C. *J. Am. Chem. Soc.* **1968**, 90, 1560-1566.
79. Jensen, F. R.; Bushweller, C. H.; Beck, B. H. *J. Am. Chem. Soc.* **1969**, 91, 344-351.
80. Booth, H. J.; Jozefowicz, M. L. *J. Chem. Soc., Perkin Trans. 2* **1976**, 895-901.
81. Sicher, J.; Jonáš, J.; Tichý, M. *Tetrahedron Lett.* **1963**, 825-830.
82. Schneider, H.-J.; Hoppen, V. *J. Org. Chem.* **1978**, 43, 3866-3873.
83. (a) Meir, H.; Zeller, K. P. *Angew. Chem., Int. Ed. Engl.* **1975**, 14, 32. (b) Popik, V. V.; Bogdanova, A. *J. Am. Chem. Soc.* **2003**, 125, 14153-14162. (c) Tomioka, H.; Okuno, H.; Izawa, Y. *J. Org. Chem.* **1980**, 45, 5278-5283.
84. Brady, S. F.; Singh, M. P.; Janso, J. E.; Clardy, J. *Org. Lett.* **2000**, 2, 4047-4049.
85. Boese, R.; Bläser, D.; Antipin, M. Y.; Chaplinski, V.; de Meijere, A. *Chem. Commun. (Cambridge)* **1998**, 781-782.
86. Yang, M.; Albrecht-Schmitt, T.; Cammarata, V.; Livant, P.; Makhanu, D. S.; Sykora, R.; Zhu, W. *J. Org. Chem.* **2009**, 74, 2671-2678.
87. Reisse, J.; Celotti, J. C.; Zimmerman, D.; Chiurdoglu, G. *Tetrahedron Lett.* **1964**, 2145-2150.
88. (a) Albright, T. A.; Burdett, J. K.; Whangbo, M.-H. *Orbital Interactions in Chemistry*; Wiley & Sons: New York, **1985**; pp 140-148. (b) Anh, N. T. *Frontier Orbitals. A practical Manual*; Wiley & Sons: West Sussex, **2007**; 28 ff.

89. a) Baum, J. S.; Shook, D. A.; Davies, H. M. L.; Smith, H. D. *Synth. Commun.* **1987**, *17*, 1709. b) Regitz, M. *Angew. Chem. Int. Ed. Engl.* **1967**, *6*, 733. c) Regitz, M. *Synthesis* **1972**, 351. d) Regitz, M.; Maas, G. *Diazo Compounds: Properties and Synthesis*; Academic Press, Orlando, **1986** Chapter 13.
90. (a) Hovinen, J.; Sillanpää, R. *Tetrahedron Lett.* **2005**, *46*, 4387-4389. (b) Cluzeau, J.; Oishi, S.; Ohno, H.; Wang, Z.; Evans, B.; Pieper, S. C.; Fujii, N. *Org. Biomol. Chem.* **2007**, *5*, 1915-1923. (c) Bhandari, M. R.; Sivappa, R.; Lovely, C. J. *J. Org. Lett.* **2009**, *11*, 1535-1538.
91. (a) Fernández, J. M. G.; Mellet, C. O.; Marín, A. M.; Fuentes, J *Carbohydrate Research* **1995**, *274*, 263-268. (b) Chen, L-Y.; Li, S-R.; Chen, P-Y.; Chang, H-C.; Wang, T-P.; Tsai, I-L.; Wang, E-C *ARKIVOC* **2010**, *xi*, 64-76.
92. (a) L'Esperance, R. P.; Ford, T. M.; Jones Jr, M. *J. Am. Chem. Soc.* **1988**, *110*, 209-213. (b) Nikolaev, V. V.; Heimgartner, H.; Linden, A.; Krylov, I. S.; Nikolaev, V. A. *Eur. J. Org. Chem.* **2006**, 4737-4746.
93. (a) Bien, S.; Segal, Y. *J. Org. Chem.* **1977**, *42*, 1685-1688. (b) Marsden, S. P.; Pang, W-K. *Chem. Commun.* **1990**, 1199-1200.
94. Cossy, J.; Belotti, D.; Thelland, A.; Pete, J. P. *Synthesis*, **1988**, 721-723.
95. (a) Alabugin, I. V.; Gilmore, K. M.; Peterson, P. W. *Wiley Interdisciplinary Reviews: Computational Molecular Science*: John Wiley & Sons. **2011**, *1*, 109-141. (b) Alabugin, I. V.; Manoharan, M.; Zeidan, T. A. *J. Am. Chem. Soc.* **2003**, *125*, 14014-14031.
96. Gross, K. C.; Seybold, P. C. *Int. J. Quantum Chem.* **2001**, *85*, 569-579.
97. Reed, A. E.; Curtiss, L. A.; Weinhold, F. *Chem. Rev.* **1988**, *88*, 899-926.

98. (a) Weinhold, F.; Schleyer, P. V. R. eds. *Encyclopedia of Computational Chemistry*. New York: John Wiley & Sons **1998**, 3, 1792. (b) Reed, A. D.; Weinhold, F. *J. Chem. Phys.* **1985**, 83, 1736-1740.
99. Alabugin, I. V.; Zeidan, T. A. *J. Am. Chem. Soc.* **2002**, 124, 3175-3185.
100. Allenstein, E.; Schwarz, W.; Schrempf, E. *Z. Anorg. Allg. Chem.* **1987**, 546, 107-112.
101. (a) Muller, E.; Burgi, H. B. *Helv. Chim. Acta* **1987**, 70, 520-533. (b) Pinkas, J.; Verkade, J. G. *Inorg. Chem.* **1993**, 32, 2711-2716. (c) Pinkas, J.; Gaul, B.; Verkade, J. G. *J. Am. Chem. Soc.* **1993**, 115, 3925-3931. (d) Pinkas, J.; Wang, T.; Jacobson, R. A.; Verkade, J. G. *Inorg. Chem.* **1994**, 33, 4202-4210.
102. (a) Milbrath, D. S.; Verkade, J. G. *J. Am. Chem. Soc.* **1977**, 99, 6607-6613. (b) Verkade, J. G. *Acc. Chem. Res.* **1993**, 26, 483-489. (c) Pinkas, J.; Tang, J.; Wan, Y.; Verkade, J. G. *Phos. Sulf. Silicon* **1994**, 87, 193-207.
103. Natural Bond Orbital Analysis Programs. NBO 5.0/5.G Program manual.

6. APPENDICES

APPENDIX 1
CRYSTAL STRUCTURE DATA FOR **20**



```

data_p21n (diacetonideamine_diester)

_audit_creation_method      SHELXL-97
_chemical_name_systematic
_chemical_name_common        ?
_chemical_melting_point     ?
_chemical_formula_moiety    ?
_chemical_formula_sum        'C136 H232 N8 O64'
_chemical_formula_weight     3003.30
loop_
_atom_type_symbol
_atom_type_description
_atom_type_scat_dispersion_real
_atom_type_scat_dispersion_imag
_atom_type_scat_source
'C' 'C' 0.0033 0.0016
'International Tables Vol C Tables 4.2.6.8 and 6.1.1.4'
'N' 'N' 0.0061 0.0033
'International Tables Vol C Tables 4.2.6.8 and 6.1.1.4'
'O' 'O' 0.0106 0.0060
'International Tables Vol C Tables 4.2.6.8 and 6.1.1.4'
'H' 'H' 0.0000 0.0000
'International Tables Vol C Tables 4.2.6.8 and 6.1.1.4'

_symmetry_cell_setting      'Monoclinic'
_symmetry_space_group_name_H-M  'P2(1)/n'

loop_
_symmetry_equiv_pos_as_xyz
'x, y, z'
'x+1/2, y+1/2, -z+1/2'
'-x, -y, -z'
'x-1/2, -y-1/2, z-1/2'

_cell_length_a              16.6797(12)
_cell_length_b              13.2875(9)
_cell_length_c              18.6656(13)
_cell_angle_alpha            90.00
_cell_angle_beta             111.3150(10)
_cell_angle_gamma            90.00
_cell_volume                 3853.9(5)
_cell_formula_units_Z        1
_cell_measurement_temperature 193(2)
_cell_measurement_reflns_used 4592
_cell_measurement_theta_min   1.40
_cell_measurement_theta_max    28.38

_exptl_crystal_description  'Plate'
_exptl_crystal_colour        'Colorless'
_exptl_crystal_size_max      0.260
_exptl_crystal_size_mid      0.184
_exptl_crystal_size_min      0.052
_exptl_crystal_density_meas   'nm'
_exptl_crystal_density_diffrn 1.294
_exptl_crystal_density_method 'not measured'
_exptl_crystal_F_000          1616
_exptl_absorpt_coefficient_mu 0.102
_exptl_absorpt_correction_type ?
_exptl_absorpt_correction_T_min ?
_exptl_absorpt_correction_T_max ?
_exptl_absorpt_process_details ?
_exptl_special_details
_diffrn_ambient_temperature   193(2)
_diffrn_radiation_wavelength  0.71073
_diffrn_radiation_type        MoK\alpha
_diffrn_radiation_source      'fine-focus sealed tube'
_diffrn_radiation_monochromator graphite
_diffrn_measurement_device_type 'Bruker APEX'
_diffrn_measurement_method     '0.3 widew/ exposures'
_diffrn_detector_area_resol_mean 0
_diffrn_standards_number       39032
_diffrn_standards_interval_count 0.0807
_diffrn_standards_interval_time 0.0937
_diffrn_standards_decay_%      0
_diffrn_reflns_number         39032
_diffrn_reflns_av_R_equivalents 0.0807
_diffrn_reflns_av_sigma/netl  0.0937
_diffrn_reflns_limit_h_min     -22
_diffrn_reflns_limit_h_max     22
_diffrn_reflns_limit_k_min     -17
_diffrn_reflns_limit_k_max     17
_diffrn_reflns_limit_l_min     -24
_diffrn_reflns_limit_l_max     24
_diffrn_reflns_theta_min       1.40
_diffrn_reflns_theta_max       28.38
_reflns_number_total          9600
_reflns_number_gt              4592
_reflns_threshold_expression  >2sigma(I)
_computing_data_collection    'SMART'
_computing_cell_refinement    'SMART'
_computing_data_reduction     'SAINT'
_computing_structure_solution  'SHELXS-97 (Sheldrick, 1990)'
_computing_structure_refinement 'SHELXL-97 (Sheldrick, 1997)'
_computing_molecular_graphics  'SHELXL-97 (Sheldrick, 1997)'
_computing_publication_material 'SHELXCIF-97 (Sheldrick, 2000)'
_refine_special_details
Refinement of F^2 against ALL reflections. The weighted R-factor wR and
goodness of fit S are based on F^2, conventional R-factors R are
based
on F, with F set to zero for negative F^2. The threshold expression of
F^2 > 2sigma(F^2) is used only for calculating R-factors(gt) etc. and
is
not relevant to the choice of reflections for refinement. R-factors
based
on F^2 are statistically about twice as large as those based on F, and
R-
factors based on ALL data will be even larger.
_refine_ls_structure_factor_coef Fsqd
_refine_ls_matrix_type        full
_refine_ls_weighting_scheme   calc
_refine_ls_weighting_details
'calc      w=1/[s^2*(Fo^2)+(0.0893P)^2+0.0000P]      where
P=(Fo^2+2Fc^2)/3'
_atom_sites_solution_primary   direct
_atom_sites_solution_secondary difmap
_atom_sites_solution_hydrogens geom
_refine_ls_hydrogen_treatment  mixed
_refine_ls_extinction_method   none
_refine_ls_extinction_coef     ?
_refine_ls_number_reflns       9600
_refine_ls_number_parameters   464
_refine_ls_number_restraints   0
_refine_ls_R_factor_all        0.1390
_refine_ls_R_factor_gt         0.0667
_refine_ls_wR_factor_ref       0.1758
_refine_ls_wR_factor_gt        0.1553
_refine_ls_goodness_of_fit_ref  0.910
_refine_ls_restrained_S_all    0.910
_refine_ls_shift/su_max        0.000

```

`_refine_ls_shift/su_mean` 0.000
`loop_`
`_atom_site_label`
`_atom_site_type_symbol`
`_atom_site_fract_x`
`_atom_site_fract_y`
`_atom_site_fract_z`
`_atom_site_U_iso_or_equiv`
`_atom_site_adp_type`
`_atom_site_occupancy`
`_atom_site_symmetry_multiplicity`
`_atom_site_calc_flag`
`_atom_site_refinement_flags`
`_atom_site_disorder_assembly`
`_atom_site_disorder_group`
N1 N 0.29856(12) -0.31145(15) 0.23872(12) 0.0359(5) Uani 1 1 d ...
O1 O 0.1910(3) -0.42978(18) 0.2918(2) 0.1502(17) Uani 1 1 d ...
O2 O 0.13638(16) -0.29998(17) 0.32241(14) 0.0795(7) Uani 1 1 d ...
O3 O 0.08746(14) -0.2467(2) 0.15281(14) 0.0951(9) Uani 1 1 d ...
O4 O 0.19769(13) -0.15925(14) 0.14932(11) 0.0541(5) Uani 1 1 d ...
O5 O 0.29977(11) -0.56360(12) 0.15255(10) 0.0416(4) Uani 1 1 d ...
O6 O 0.29715(11) -0.44145(13) 0.06232(9) 0.0431(5) Uani 1 1 d ...
O7 O 0.48696(11) -0.14709(13) 0.33625(10) 0.0414(4) Uani 1 1 d ...
O8 O 0.48814(11) -0.27605(13) 0.41955(10) 0.0453(5) Uani 1 1 d ...
C1 C 0.22585(14) -0.27044(17) 0.25268(13) 0.0327(6) Uani 1 1 d ...
H1A H 0.2480 -0.2139 0.2901 0.039 Uiso 1 1 calc R ...
C2 C 0.18261(17) -0.3448(2) 0.28942(17) 0.0432(7) Uani 1 1 d ...
C3 C 0.0951(2) -0.3634(3) 0.3618(2) 0.0763(10) Uiso 1 1 d ...
H3A H 0.0608 -0.3216 0.3831 0.114 Uiso 1 1 calc R ...
H3B H 0.1391 -0.3995 0.4035 0.114 Uiso 1 1 calc R ...
H3C H 0.0576 -0.4119 0.3254 0.114 Uiso 1 1 calc R ...
C4 C 0.16080(17) -0.22483(18) 0.17949(14) 0.0362(6) Uani 1 1 d ...
C5 C 0.1457(2) -0.1080(2) 0.07976(16) 0.0583(8) Uani 1 1 d ...
H5A H 0.1815 -0.0603 0.0647 0.087 Uiso 1 1 calc R ...
H5B H 0.0991 -0.0716 0.0888 0.087 Uiso 1 1 calc R ...
H5C H 0.1211 -0.1574 0.0386 0.087 Uiso 1 1 calc R ...
C6 C 0.28283(15) -0.39001(17) 0.18108(13) 0.0322(6) Uani 1 1 d ...
H6 H 0.2190 -0.3981 0.1568 0.039 Uiso 1 1 calc R ...
C7 C 0.31895(17) -0.49166(17) 0.21357(13) 0.0384(6) Uani 1 1 d ...
H7A H 0.3821 -0.4866 0.2405 0.046 Uiso 1 1 calc R ...
H7B H 0.2934 -0.5137 0.2512 0.046 Uiso 1 1 calc R ...
C8 C 0.31442(17) -0.36181(19) 0.11722(14) 0.0410(6) Uani 1 1 d ...
H8A H 0.2852 -0.2996 0.0916 0.049 Uiso 1 1 calc R ...
H8B H 0.3771 -0.3485 0.1391 0.049 Uiso 1 1 calc R ...
C9 C 0.33106(16) -0.53678(19) 0.09400(14) 0.0400(6) Uani 1 1 d ...
C10 C 0.42816(18) -0.5369(3) 0.12229(18) 0.0633(9) Uani 1 1 d ...
H10A H 0.4509 -0.4871 0.1635 0.095 Uiso 1 1 calc R ...
H10B H 0.4469 -0.5198 0.0797 0.095 Uiso 1 1 calc R ...
H10C H 0.4498 -0.6038 0.1420 0.095 Uiso 1 1 calc R ...
C11 C 0.2919(2) -0.6117(2) 0.02973(16) 0.0574(8) Uani 1 1 d ...
H11A H 0.2290 -0.6084 0.0125 0.086 Uiso 1 1 calc R ...
H11B H 0.3113 -0.6797 0.0484 0.086 Uiso 1 1 calc R ...
H11C H 0.3100 -0.5955 -0.0133 0.086 Uiso 1 1 calc R ...
C12 C 0.38557(14) -0.28360(17) 0.28824(13) 0.0321(6) Uani 1 1 d ...
H12A H 0.4262 -0.3223 0.2704 0.039 Uiso 1 1 calc R ...
C13 C 0.40523(17) -0.31135(19) 0.37167(14) 0.0415(6) Uani 1 1 d ...
H13A H 0.3610 -0.2817 0.3891 0.050 Uiso 1 1 calc R ...
H13B H 0.4029 -0.3854 0.3764 0.050 Uiso 1 1 calc R ...
C14 C 0.40347(16) -0.17259(18) 0.28186(14) 0.0377(6) Uani 1 1 d ...
H14A H 0.4009 -0.1575 0.2291 0.045 Uiso 1 1 calc R ...
H14B H 0.3591 -0.1317 0.2919 0.045 Uiso 1 1 calc R ...
C15 C 0.49903(16) -0.17064(18) 0.41308(14) 0.0384(6) Uani 1 1 d ...
C16 C 0.59254(17) -0.1490(2) 0.45930(16) 0.0522(8) Uani 1 1 d ...
H16A H 0.6290 -0.1886 0.4389 0.078 Uiso 1 1 calc R ...
H16B H 0.6053 -0.1671 0.5132 0.078 Uiso 1 1 calc R ...
H16C H 0.6040 -0.0772 0.4558 0.078 Uiso 1 1 calc R ...
C17 C 0.43973(19) -0.1099(2) 0.44182(18) 0.0629(9) Uani 1 1 d ...
H17A H 0.3797 -0.1254 0.4106 0.094 Uiso 1 1 calc R ...
H17C H 0.4503 -0.0379 0.4378 0.094 Uiso 1 1 calc R ...
N2 N 0.71166(12) 0.67873(14) 0.27447(11) 0.0313(5) Uani 1 1 d ...
O9 O 0.90832(11) 0.68393(13) 0.37884(10) 0.0450(5) Uani 1 1 d ...
O10 O 0.84075(12) 0.83296(12) 0.35424(10) 0.0448(5) Uani 1 1 d ...
O11 O 0.78109(12) 0.55932(13) 0.18505(10) 0.0468(5) Uani 1 1 d ...
O12 O 0.89673(11) 0.65923(12) 0.21560(10) 0.0411(4) Uani 1 1 d ...
O13 O 0.70924(11) 0.51813(12) 0.43608(9) 0.0384(4) Uani 1 1 d ...
O14 O 0.67316(11) 0.41646(11) 0.32719(9) 0.0383(4) Uani 1 1 d ...
O15 O 0.52163(10) 0.73840(11) 0.09838(9) 0.0380(4) Uani 1 1 d ...
O16 O 0.54006(10) 0.86774(12) 0.18671(9) 0.0360(4) Uani 1 1 d ...
C18 C 0.78771(14) 0.70939(17) 0.25976(13) 0.0294(5) Uani 1 1 d ...
H18A H 0.7724 0.7714 0.2272 0.035 Uiso 1 1 calc R ...
C19 C 0.85505(15) 0.73922(19) 0.33719(14) 0.0322(6) Uani 1 1 d ...
C20 C 0.8862(2) 0.8668(2) 0.43154(15) 0.0567(8) Uani 1 1 d ...
H20A H 0.8703 0.9367 0.4367 0.085 Uiso 1 1 calc R ...
H20B H 0.9483 0.8626 0.4432 0.085 Uiso 1 1 calc R ...
H20C H 0.8708 0.8242 0.4675 0.085 Uiso 1 1 calc R ...
C21 C 0.82083(16) 0.63189(18) 0.21683(13) 0.0323(6) Uani 1 1 d ...
C22 C 0.93340(18) 0.5916(2) 0.17449(16) 0.0510(7) Uani 1 1 d ...
H22A H 0.9898 0.6169 0.1778 0.076 Uiso 1 1 calc R ...
H22B H 0.8952 0.5879 0.1204 0.076 Uiso 1 1 calc R ...
H22C H 0.9399 0.5244 0.1975 0.076 Uiso 1 1 calc R ...
C23 C 0.71846(15) 0.58694(16) 0.31938(13) 0.0288(5) Uani 1 1 d ...
H23A H 0.7794 0.5633 0.3354 0.035 Uiso 1 1 calc R ...
C24 C 0.70140(16) 0.60829(17) 0.39256(13) 0.0352(6) Uani 1 1 d ...
H24A H 0.7431 0.6589 0.4238 0.042 Uiso 1 1 calc R ...
H24B H 0.6427 0.6362 0.3793 0.042 Uiso 1 1 calc R ...
C25 C 0.66203(16) 0.50106(17) 0.27667(13) 0.0359(6) Uani 1 1 d ...
H25A H 0.6010 0.5225 0.2571 0.043 Uiso 1 1 calc R ...
H25B H 0.6775 0.4817 0.2321 0.043 Uiso 1 1 calc R ...
C26 C 0.65577(16) 0.43790(19) 0.39462(15) 0.0379(6) Uani 1 1 d ...
C27 C 0.6847(2) 0.3461(2) 0.44496(17) 0.0571(8) Uani 1 1 d ...
H27A H 0.7457 0.3334 0.4550 0.086 Uiso 1 1 calc R ...
H27B H 0.6506 0.2878 0.4188 0.086 Uiso 1 1 calc R ...
H27C H 0.6765 0.3575 0.4937 0.086 Uiso 1 1 calc R ...
C28 C 0.56174(18) 0.4613(2) 0.37690(18) 0.0576(8) Uani 1 1 d ...
H28A H 0.5457 0.5219 0.3450 0.086 Uiso 1 1 calc R ...
H28B H 0.5521 0.4725 0.4250 0.086 Uiso 1 1 calc R ...
H28C H 0.5265 0.4046 0.3492 0.086 Uiso 1 1 calc R ...
C29 C 0.62833(14) 0.71850(17) 0.22654(13) 0.0300(5) Uani 1 1 d ...
H29A H 0.5846 0.6864 0.2443 0.036 Uiso 1 1 calc R ...
C30 C 0.60242(16) 0.69384(18) 0.14135(13) 0.0356(6) Uani 1 1 d ...
H30A H 0.6468 0.7193 0.1224 0.043 Uiso 1 1 calc R ...
H30B H 0.5986 0.6199 0.1341 0.043 Uiso 1 1 calc R ...
C31 C 0.62198(15) 0.83121(17) 0.23620(13) 0.0334(6) Uani 1 1 d ...
H31A H 0.6301 0.8465 0.2903 0.040 Uiso 1 1 calc R ...
H31B H 0.6681 0.8656 0.2239 0.040 Uiso 1 1 calc R ...
C32 C 0.51933(15) 0.84522(17) 0.10751(13) 0.0324(6) Uani 1 1 d ...
C33 C 0.57689(17) 0.8998(2) 0.07421(15) 0.0450(7) Uani 1 1 d ...
H33A H 0.6367 0.8792 0.1015 0.067 Uiso 1 1 calc R ...
H33B H 0.5716 0.9725 0.0800 0.067 Uiso 1 1 calc R ...
H33C H 0.5598 0.8831 0.0195 0.067 Uiso 1 1 calc R ...
C34 C 0.42654(16) 0.8751(2) 0.06731(15) 0.0446(7) Uani 1 1 d ...
H34A H 0.3905 0.8381 0.0897 0.067 Uiso 1 1 calc R ...
H34B H 0.4084 0.8590 0.0125 0.067 Uiso 1 1 calc R ...
H34C H 0.4203 0.9475 0.0736 0.067 Uiso 1 1 calc R ...

`loop_`
`_atom_site_aniso_label`
`_atom_site_aniso_U_11`
`_atom_site_aniso_U_22`
`_atom_site_aniso_U_33`
`_atom_site_aniso_U_23`

_atom_site_aniso_U_13
 _atom_site_aniso_U_12
 N1 0.0275(11) 0.0362(12) 0.0430(12) -0.0144(10) 0.0116(10) -0.0034(9)
 O1 0.247(4) 0.0394(15) 0.277(5) 0.008(2) 0.229(4) 0.0030(19)
 O2 0.0999(18) 0.0671(15) 0.108(2) 0.0051(14) 0.0809(17) -0.0132(13)
 O3 0.0360(13) 0.147(2) 0.0859(18) 0.0606(17) 0.0032(12) -0.0102(14)
 O4 0.0645(13) 0.0459(11) 0.0462(12) 0.0110(9) 0.0132(10) -0.0126(10)
 O5 0.0572(12) 0.0308(9) 0.0399(10) -0.0077(8) 0.0215(9) -0.0049(8)
 O6 0.0552(12) 0.0432(11) 0.0335(10) -0.0058(8) 0.0193(9) -0.0019(9)
 O7 0.0375(10) 0.0451(11) 0.0393(11) -0.0021(8) 0.0113(9) -0.0148(8)
 O8 0.0439(11) 0.0399(11) 0.0400(10) 0.0027(8) 0.0007(8) -0.0071(8)
 C1 0.0322(14) 0.0306(13) 0.0359(14) -0.0043(11) 0.0131(11) -0.0016(11)
 C2 0.0403(16) 0.0348(16) 0.0592(18) -0.0017(13) 0.0239(14) -0.0006(12)
 C4 0.0388(15) 0.0334(14) 0.0395(15) 0.0008(12) 0.0179(12) 0.0032(12)
 C5 0.082(2) 0.0470(17) 0.0457(17) 0.0131(14) 0.0229(17) 0.0127(16)
 C6 0.0317(13) 0.0316(13) 0.0328(13) -0.0050(11) 0.0110(11) -0.0040(10)
 C7 0.0537(17) 0.0300(14) 0.0302(14) -0.0027(11) 0.0140(12) 0.0040(12)
 C8 0.0505(17) 0.0360(14) 0.0394(15) -0.0016(12) 0.0198(13) -0.0009(12)
 C9 0.0437(16) 0.0423(15) 0.0351(15) -0.0094(12) 0.0157(13) -0.0022(12)
 C10 0.0448(18) 0.073(2) 0.071(2) -0.0177(18) 0.0200(16) 0.0070(16)
 C11 0.070(2) 0.0552(19) 0.0493(18) -0.0210(15) 0.0250(16) -0.0103(16)
 C12 0.0278(13) 0.0332(13) 0.0344(14) -0.0069(11) 0.0102(11) -0.0020(10)
 C13 0.0428(16) 0.0325(14) 0.0409(16) 0.0052(11) 0.0055(13) -0.0081(12)
 C14 0.0356(14) 0.0386(15) 0.0343(14) 0.0009(11) 0.0073(12) -0.0114(11)
 C15 0.0391(15) 0.0367(15) 0.0368(15) -0.0088(11) 0.0105(12) -0.0063(12)
 C16 0.0452(17) 0.0516(17) 0.0507(18) -0.0115(14) 0.0064(14) -0.0088(14)
 C17 0.0547(19) 0.073(2) 0.062(2) -0.0313(17) 0.0226(16) -0.0063(16)
 N2 0.0285(11) 0.0300(11) 0.0339(11) 0.0081(9) 0.0096(9) 0.0020(8)
 O9 0.0393(11) 0.0487(11) 0.0401(11) -0.0017(9) 0.0060(9) 0.0080(9)
 O10 0.0648(13) 0.0314(10) 0.0355(10) -0.0032(8) 0.0149(9) -0.0006(9)
 O11 0.0510(12) 0.0452(11) 0.0497(11) -0.0142(9) 0.0250(9) -0.0090(9)
 O12 0.0381(10) 0.0418(10) 0.0495(11) -0.0088(8) 0.0231(9) -0.0016(8)
 O13 0.0462(11) 0.0385(10) 0.0311(9) 0.0061(8) 0.0149(8) -0.0032(8)
 O14 0.0537(11) 0.0261(9) 0.0384(10) 0.0038(7) 0.0207(9) -0.0007(8)

O5 C7 1.431(3) . ?

loop_
 _geom_bond_atom_site_label_1
 _geom_bond_atom_site_label_2
 _geom_bond_distance
 _geom_bond_site_symmetry_2
 _geom_bond_publ_flag
 N1 C1 1.437(3) . ?
 N1 C6 1.453(3) . ?
 N1 C12 1.457(3) . ?
 O1 C2 1.136(3) . ?
 O2 C2 1.294(3) . ?
 O2 C3 1.446(4) . ?
 O3 C4 1.177(3) . ?
 O4 C4 1.307(3) . ?
 O4 C5 1.443(3) . ?
 O5 C9 1.417(3) . ?

O6 C9 1.425(3) . ?

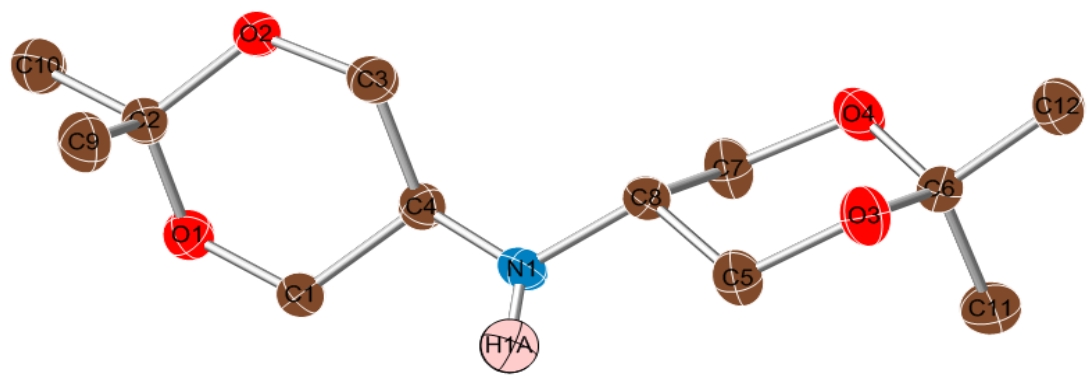
C6 C8 1.515(3) . ?
 C6 H6 1.0000 . ?
 C7 H7A 0.9900 . ?
 C7 H7B 0.9900 . ?
 C8 H8A 0.9900 . ?
 C8 H8B 0.9900 . ?
 C9 C10 1.510(4) . ?
 C9 C11 1.512(3) . ?
 C10 H10A 0.9800 . ?
 C10 H10B 0.9800 . ?
 C10 H10C 0.9800 . ?
 C11 H11A 0.9800 . ?
 C11 H11B 0.9800 . ?
 C11 H11C 0.9800 . ?
 C12 C13 1.516(3) . ?
 C12 C14 1.518(3) . ?
 C12 H12A 1.0000 . ?
 C13 H13A 0.9900 . ?

C13 H13B 0.9900 . ?	C34 H34C 0.9800 . ?	C10 C9 C11 112.1(2) . . ?
C14 H14A 0.9900 . ?		C9 C10 H10A 109.5 . . ?
C14 H14B 0.9900 . ?		C9 C10 H10B 109.5 . . ?
C15 C16 1.511(4) . ?		H10A C10 H10B 109.5 . . ?
C15 C17 1.518(4) . ?		C9 C10 H10C 109.5 . . ?
C16 H16A 0.9800 . ?		H10A C10 H10C 109.5 . . ?
C16 H16B 0.9800 . ?		H10B C10 H10C 109.5 . . ?
C16 H16C 0.9800 . ?		C9 C11 H11A 109.5 . . ?
C17 H17A 0.9800 . ?		C9 C11 H11B 109.5 . . ?
C17 H17B 0.9800 . ?		H11A C11 H11B 109.5 . . ?
C17 H17C 0.9800 . ?		C9 C11 H11C 109.5 . . ?
N2 C18 1.450(3) . ?		H11A C11 H11C 109.5 . . ?
N2 C29 1.452(3) . ?		H11B C11 H11C 109.5 . . ?
N2 C23 1.461(3) . ?		N1 C12 C13 112.56(19) . . ?
O9 C19 1.196(3) . ?		N1 C12 C14 112.1(2) . . ?
O10 C19 1.328(3) . ?		C13 C12 C14 109.98(19) . . ?
O10 C20 1.436(3) . ?		N1 C12 H12A 107.3 . . ?
O11 C21 1.198(3) . ?		C13 C12 H12A 107.3 . . ?
O12 C21 1.325(3) . ?		C14 C12 H12A 107.3 . . ?
O12 C22 1.453(3) . ?		O8 C13 C12 111.23(19) . . ?
O13 C26 1.424(3) . ?		O8 C13 H13A 109.4 . . ?
O13 C24 1.426(3) . ?		C12 C13 H13A 109.4 . . ?
O14 C26 1.419(3) . ?		O8 C13 H13B 109.4 . . ?
O14 C25 1.435(3) . ?		C12 C13 H13B 109.4 . . ?
O15 C30 1.423(3) . ?		H13A C13 H13B 108.0 . . ?
O15 C32 1.432(3) . ?		O7 C14 C12 110.00(19) . . ?
O16 C32 1.422(3) . ?		O7 C14 H14A 109.7 . . ?
O16 C31 1.428(3) . ?		C12 C14 H14A 109.7 . . ?
C18 C19 1.525(3) . ?		O7 C14 H14B 109.7 . . ?
C18 C21 1.526(3) . ?		C12 C14 H14B 109.7 . . ?
C18 H18A 1.0000 . ?		H14A C14 H14B 108.2 . . ?
C20 H20A 0.9800 . ?		O7 C15 O8 109.24(19) . . ?
C20 H20B 0.9800 . ?		O7 C15 C16 106.0(2) . . ?
C20 H20C 0.9800 . ?		O8 C15 C16 106.0(2) . . ?
C22 H22A 0.9800 . ?		O7 C15 C17 111.8(2) . . ?
C22 H22B 0.9800 . ?		O8 C15 C17 112.0(2) . . ?
C22 H22C 0.9800 . ?		C16 C15 C17 111.5(2) . . ?
C23 C25 1.509(3) . ?		C15 C16 H16A 109.5 . . ?
C23 C24 1.520(3) . ?		C15 C16 H16B 109.5 . . ?
C23 H23A 1.0000 . ?		H16A C16 H16B 109.5 . . ?
C24 H24A 0.9900 . ?		C15 C16 H16C 109.5 . . ?
C24 H24B 0.9900 . ?		H16A C16 H16C 109.5 . . ?
C25 H25A 0.9900 . ?		H16B C16 H16C 109.5 . . ?
C25 H25B 0.9900 . ?		C15 C17 H17A 109.5 . . ?
C26 C27 1.508(3) . ?		C15 C17 H17B 109.5 . . ?
C26 C28 1.513(4) . ?		H17A C17 H17B 109.5 . . ?
C27 H27A 0.9800 . ?		C15 C17 H17C 109.5 . . ?
C27 H27B 0.9800 . ?		H17A C17 H17C 109.5 . . ?
C27 H27C 0.9800 . ?		H17B C17 H17C 109.5 . . ?
C28 H28A 0.9800 . ?		C18 N2 C29 119.24(18) . . ?
C28 H28B 0.9800 . ?		C18 N2 C23 116.89(18) . . ?
C28 H28C 0.9800 . ?		C29 N2 C23 120.98(18) . . ?
C29 C31 1.517(3) . ?		C19 O10 C20 117.3(2) . . ?
C29 C30 1.524(3) . ?		C21 O12 C22 115.32(19) . . ?
C29 H29A 1.0000 . ?		C26 O13 C24 114.17(17) . . ?
C30 H30A 0.9900 . ?		C26 O14 C25 113.95(17) . . ?
C30 H30B 0.9900 . ?		C30 O15 C32 113.97(17) . . ?
C31 H31A 0.9900 . ?		C32 O16 C31 114.51(17) . . ?
C31 H31B 0.9900 . ?		N2 C18 C19 106.69(18) . . ?
C32 C33 1.506(3) . ?		N2 C18 C21 114.72(19) . . ?
C32 C34 1.507(3) . ?		C19 C18 C21 112.98(19) . . ?
C33 H33A 0.9800 . ?		N2 C18 H18A 107.4 . . ?
C33 H33B 0.9800 . ?		C19 C18 H18A 107.4 . . ?
C33 H33C 0.9800 . ?		C21 C18 H18A 107.4 . . ?
C34 H34A 0.9800 . ?		O9 C19 O10 125.1(2) . . ?
C34 H34B 0.9800 . ?		O9 C19 C18 125.0(2) . . ?

O10 C19 C18 109.6(2) . . ?	C29 C31 H31A 109.5 . . ?	C1 N1 C12 C13 59.6(3) . . . ?
O10 C20 H20A 109.5 . . ?	O16 C31 H31B 109.5 . . ?	C6 N1 C12 C13 -112.3(2) . . . ?
O10 C20 H20B 109.5 . . ?	C29 C31 H31B 109.5 . . ?	C1 N1 C12 C14 -65.0(3) . . . ?
H20A C20 H20B 109.5 . . ?	H31A C31 H31B 108.1 . . ?	C6 N1 C12 C14 123.1(2) . . . ?
O10 C20 H20C 109.5 . . ?	O16 C32 O15 108.98(18) . . ?	C15 O8 C13 C12 55.6(3) . . . ?
H20A C20 H20C 109.5 . . ?	O16 C32 C33 112.2(2) . . ?	N1 C12 C13 O8 -175.34(19) . . . ?
H20B C20 H20C 109.5 . . ?	O15 C32 C33 112.3(2) . . ?	C14 C12 C13 O8 -49.6(3) . . . ?
O11 C21 O12 124.9(2) . . ?	O16 C32 C34 106.24(19) . . ?	C15 O7 C14 C12 -56.2(3) . . . ?
O11 C21 C18 124.2(2) . . ?	O15 C32 C34 105.59(19) . . ?	N1 C12 C14 O7 175.10(18) . . . ?
O12 C21 C18 110.8(2) . . ?	C33 C32 C34 111.2(2) . . ?	C13 C12 C14 O7 49.1(3) . . . ?
O12 C22 H22A 109.5 . . ?	C32 C33 H33A 109.5 . . ?	C14 O7 C15 O8 60.1(3) . . . ?
O12 C22 H22B 109.5 . . ?	C32 C33 H33B 109.5 . . ?	C14 O7 C15 C16 174.0(2) . . . ?
H22A C22 H22B 109.5 . . ?	H33A C33 H33B 109.5 . . ?	C14 O7 C15 C17 -64.3(3) . . . ?
O12 C22 H22C 109.5 . . ?	C32 C33 H33C 109.5 . . ?	C13 O8 C15 O7 -59.3(3) . . . ?
H22A C22 H22C 109.5 . . ?	H33A C33 H33C 109.5 . . ?	C13 O8 C15 C16 -173.1(2) . . . ?
H22B C22 H22C 109.5 . . ?	H33B C33 H33C 109.5 . . ?	C13 O8 C15 C17 65.0(3) . . . ?
N2 C23 C25 115.13(18) . . ?	C32 C34 H34A 109.5 . . ?	C29 N2 C18 C19 132.0(2) . . . ?
N2 C23 C24 111.05(18) . . ?	C32 C34 H34B 109.5 . . ?	C23 N2 C18 C19 -67.0(2) . . . ?
C25 C23 C24 109.34(19) . . ?	H34A C34 H34B 109.5 . . ?	C29 N2 C18 C21 -102.1(2) . . . ?
N2 C23 H23A 107.0 . . ?	C32 C34 H34C 109.5 . . ?	C23 N2 C18 C21 58.9(3) . . . ?
C25 C23 H23A 107.0 . . ?	H34A C34 H34C 109.5 . . ?	C20 O10 C19 O9 -7.2(4) . . . ?
C24 C23 H23A 107.0 . . ?	H34B C34 H34C 109.5 . . ?	C20 O10 C19 C18 167.4(2) . . . ?
O13 C24 C23 110.29(18) . . ?	loop_	N2 C18 C19 O9 92.5(3) . . . ?
O13 C24 H24A 109.6 . . ?	_geom_torsion_atom_site_label_1	C21 C18 C19 O9 -34.5(3) . . . ?
C23 C24 H24A 109.6 . . ?	_geom_torsion_atom_site_label_2	N2 C18 C19 O10 -82.1(2) . . . ?
O13 C24 H24B 109.6 . . ?	_geom_torsion_atom_site_label_3	C21 C18 C19 O10 150.9(2) . . . ?
C23 C24 H24B 109.6 . . ?	_geom_torsion_atom_site_label_4	C22 O12 C21 O11 -2.6(3) . . . ?
H24A C24 H24B 108.1 . . ?	_geom_torsion	C22 O12 C21 C18 -178.7(2) . . . ?
O14 C25 C23 109.76(18) . . ?	_geom_torsion_site_symmetry_1	N2 C18 C21 O11 12.9(3) . . . ?
O14 C25 H25A 109.7 . . ?	_geom_torsion_site_symmetry_2	C19 C18 C21 O11 135.5(2) . . . ?
C23 C25 H25A 109.7 . . ?	_geom_torsion_site_symmetry_3	N2 C18 C21 O12 -170.93(18) . . . ?
O14 C25 H25B 109.7 . . ?	_geom_torsion_site_symmetry_4	C19 C18 C21 O12 -48.3(3) . . . ?
C23 C25 H25B 109.7 . . ?	_geom_torsion_publ_flag	C18 N2 C23 C25 -115.0(2) . . . ?
H25A C25 H25B 108.2 . . ?	C6 N1 C1 C2 67.4(3) . . . ?	C29 N2 C23 C25 45.7(3) . . . ?
O14 C26 O13 110.04(18) . . ?	C12 N1 C1 C2 -104.8(2) . . . ?	C18 N2 C23 C24 120.1(2) . . . ?
O14 C26 C27 105.5(2) . . ?	C6 N1 C1 C4 -59.0(3) . . . ?	C29 N2 C23 C24 -79.3(2) . . . ?
O13 C26 C27 105.8(2) . . ?	C12 N1 C1 C4 128.8(2) . . . ?	C26 O13 C24 C23 -55.5(3) . . . ?
O14 C26 C28 112.2(2) . . ?	C3 O2 C2 O1 -0.6(5) . . . ?	N2 C23 C24 O13 -179.36(18) . . . ?
O13 C26 C28 111.1(2) . . ?	C3 O2 C2 C1 -177.6(3) . . . ?	C25 C23 C24 O13 52.5(2) . . . ?
C27 C26 C28 111.9(2) . . ?	N1 C1 C2 O1 -16.7(5) . . . ?	C26 O14 C25 C23 57.0(3) . . . ?
C26 C27 H27A 109.5 . . ?	C4 C1 C2 O1 109.7(4) . . . ?	N2 C23 C25 O14 -178.79(18) . . . ?
C26 C27 H27B 109.5 . . ?	N1 C1 C2 O2 160.1(2) . . . ?	C24 C23 C25 O14 -53.0(3) . . . ?
H27A C27 H27B 109.5 . . ?	C4 C1 C2 O2 -73.5(3) . . . ?	C25 O14 C26 O13 -57.4(2) . . . ?
C26 C27 H27C 109.5 . . ?	C5 O4 C4 O3 1.5(4) . . . ?	C25 O14 C26 C27 -171.1(2) . . . ?
H27A C27 H27C 109.5 . . ?	C5 O4 C4 C1 -179.7(2) . . . ?	C25 O14 C26 C28 66.8(3) . . . ?
H27B C27 H27C 109.5 . . ?	N1 C1 C4 O3 125.0(3) . . . ?	C24 O13 C26 C27 170.2(2) . . . ?
C26 C28 H28A 109.5 . . ?	C2 C1 C4 O3 -2.8(4) . . . ?	C24 O13 C26 C28 -68.1(3) . . . ?
C26 C28 H28B 109.5 . . ?	N1 C1 C4 O4 -53.8(3) . . . ?	C18 N2 C29 C31 -65.4(3) . . . ?
H28A C28 H28B 109.5 . . ?	C2 C1 C4 O4 178.4(2) . . . ?	C23 N2 C29 C31 134.4(2) . . . ?
C26 C28 H28C 109.5 . . ?	C1 N1 C6 C7 -112.9(2) . . . ?	C18 N2 C29 C30 59.7(3) . . . ?
H28A C28 H28C 109.5 . . ?	C12 N1 C6 C7 59.2(3) . . . ?	C23 N2 C29 C30 -100.5(2) . . . ?
H28B C28 H28C 109.5 . . ?	C1 N1 C6 C8 121.5(2) . . . ?	C32 O15 C30 C29 56.7(3) . . . ?
N2 C29 C31 112.26(19) . . ?	C12 N1 C6 C8 -66.4(3) . . . ?	N2 C29 C30 O15 -178.00(18) . . . ?
N2 C29 C30 114.17(19) . . ?	C9 O5 C7 C6 57.2(3) . . . ?	C31 C29 C30 O15 -51.3(3) . . . ?
C31 C29 C30 109.31(18) . . ?	N1 C6 C7 O5 179.70(19) . . . ?	C32 O16 C31 C29 -56.1(3) . . . ?
N2 C29 H29A 106.9 . . ?	C8 C6 C7 O5 -53.2(3) . . . ?	N2 C29 C31 O16 178.48(18) . . . ?
C31 C29 H29A 106.9 . . ?	C9 O6 C8 C6 -55.0(3) . . . ?	C30 C29 C31 O16 50.7(3) . . . ?
C30 C29 H29A 106.9 . . ?	N1 C6 C8 O6 -179.87(19) . . . ?	C31 O16 C32 O15 58.0(2) . . . ?
O15 C30 C29 110.48(19) . . ?	C7 C6 C8 O6 52.2(3) . . . ?	C31 O16 C32 C33 -67.0(2) . . . ?
O15 C30 H30A 109.6 . . ?	C7 O5 C9 O6 -57.4(3) . . . ?	C31 O16 C32 C34 171.37(19) . . . ?
C29 C30 H30A 109.6 . . ?	C7 O5 C9 C10 66.8(3) . . . ?	C30 O15 C32 O16 -58.4(2) . . . ?
O15 C30 H30B 109.6 . . ?	C7 O5 C9 C11 -170.7(2) . . . ?	C30 O15 C32 C33 66.5(3) . . . ?
C29 C30 H30B 109.6 . . ?	C8 O6 C9 O5 56.3(3) . . . ?	C30 O15 C32 C34 -172.15(19) . . . ?
H30A C30 H30B 108.1 . . ?	C8 O6 C9 C10 -68.6(3) . . . ?	
O16 C31 C29 110.52(19) . . ?	C8 O6 C9 C11 169.9(2) . . . ?	
O16 C31 H31A 109.5 . . ?		

```
_diffrn_measured_fraction_theta_max  
0.995  
_diffrn_reflns_theta_full      28.38  
_diffrn_measured_fraction_theta_full 0.995  
_refine_diff_density_max 0.538  
_refine_diff_density_min -0.482  
_refine_diff_density_rms 0.051
```

APPENDIX 2
CRYSTAL STRUCTURE DATA FOR **15**



```

data_face (diacetonideamine)

_audit_creation_method      SHELXL-97
_chemical_name_systematic
;
?
;
_chemical_name_common      ?
_chemical_melting_point    ?
_chemical_formula_moiety   'C12 H23 N O4'
_chemical_formula_sum       'C12 H23 N O4'
_chemical_formula_weight    245.31

loop_
_atom_type_symbol
_atom_type_description
_atom_type_scat_dispersion_real
_atom_type_scat_dispersion_imag
_atom_type_scat_source
'C' 'C' 0.0033 0.0016
'International Tables Vol C Tables 4.2.6.8 and 6.1.1.4'
'H' 'H' 0.0000 0.0000
'International Tables Vol C Tables 4.2.6.8 and 6.1.1.4'
'N' 'N' 0.0061 0.0033
'International Tables Vol C Tables 4.2.6.8 and 6.1.1.4'
'O' 'O' 0.0106 0.0060
'International Tables Vol C Tables 4.2.6.8 and 6.1.1.4'

_symmetry_cell_setting     'monoclinic'
_symmetry_space_group_name_H-M  'P n'
_symmetry_space_group_name_Hall 'P -2yac'

loop_
_symmetry_equiv_pos_as_xyz
'x, y, z'
'x+1/2, -y, z+1/2'

_cell_length_a              5.5325(11)
_cell_length_b              12.496(3)
_cell_length_c              9.6140(19)
_cell_angle_alpha            90.00
_cell_angle_beta             102.61(3)
_cell_angle_gamma            90.00
_cell_volume                 648.6(2)
_cell_formula_units_Z        2
_cell_measurement_temperature 193(2)
_cell_measurement_reflns_used 1351
_cell_measurement_theta_min  2.71
_cell_measurement_theta_max  28.30

_exptl_crystal_description  'block'
_exptl_crystal_colour       'colorless'
_exptl_crystal_size_max     0.292
_exptl_crystal_size_mid     0.242
_exptl_crystal_size_min     0.078
_exptl_crystal_density_meas 'nm'
_exptl_crystal_density_diffrn 1.256
_exptl_crystal_density_method 'not measured'
_exptl_crystal_F_000         268
_exptl_absorpt_coefficient_mu 0.093
_exptl_absorpt_correction_type 'numerical'
_exptl_absorpt_correction_T_min 0.9755
_exptl_absorpt_correction_T_max 0.9914
_exptl_absorpt_process_details 'SHELXPREP'

_exptl_special_details
;

_diffrn_ambient_temperature 193(2)
_diffrn_radiation_wavelength 0.71073
_diffrn_radiation_type      MoK\alpha
_diffrn_radiation_source    'fine-focus sealed tube'
_diffrn_radiation_monochromator graphite
_diffrn_measurement_device_type 'Bruker APEX'
_diffrn_measurement_method   '0.3 wide /w exposure'
_diffrn_detector_area_resol_mean ?
_diffrn_stands_number      'na'
_diffrn_stands_interval_count 'na'
_diffrn_stands_interval_time 'na'
_diffrn_stands_decay_%      0
_diffrn_reflns_number       2173
_diffrn_reflns_av_R_equivalents 0.0278
_diffrn_reflns_av_sigmaI/netI 0.0428
_diffrn_reflns_limit_h_min  -7
_diffrn_reflns_limit_h_max  4
_diffrn_reflns_limit_k_min  -15
_diffrn_reflns_limit_k_max  15
_diffrn_reflns_limit_l_min  -12
_diffrn_reflns_limit_l_max  10
_diffrn_reflns_theta_min    2.71
_diffrn_reflns_theta_max    28.30
_reflns_number_total       1582
_reflns_number_gt           1351
_reflns_threshold_expression >2sigma(I)

_computing_data_collection  'SMART'
_computing_cell_refinement   'SMART, SAINT'
_computing_data_reduction    'SAINT'
_computing_structure_solution 'SHELXS-97 (Sheldrick, 1990)'
_computing_structure_refinement 'SHELXL-97 (Sheldrick, 1997)'
_computing_molecular_graphics 'SHELXP-97 (Sheldrick, 1997)'
_computing_publication_material 'SHELXCIF-97 (Sheldrick, 2000)'

_refine_special_details
;
Refinement of F^2 against ALL reflections. The weighted R-factor wR and
goodness of fit S are based on F^2, conventional R-factors R are
based
on F, with F set to zero for negative F^2. The threshold expression of
F^2 > 2sigma(F^2) is used only for calculating R-factors(gt) etc. and is
not relevant to the choice of reflections for refinement. R-factors
based
on F^2 are statistically about twice as large as those based on F, and
R-
factors based on ALL data will be even larger.
;

_refine_ls_structure_factor_coef Fsqd
_refine_ls_matrix_type      full
_refine_ls_weighting_scheme calc
_refine_ls_weighting_details
'calc      w=1/[s^2*(Fo^2)+(0.0768P)^2+0.0000P]      where
P=(Fo^2+2Fc^2)/3'
_atom_sites_solution_primary direct
_atom_sites_solution_secondary difmap
_atom_sites_solution_hydrogens geom
_refine_ls_hydrogen_treatment constr
_refine_ls_extinction_method none

```

```

_refine_ls_extinction_coef      0
_refine_ls_abs_structure_details
'Flack H D (1983), Acta Cryst. A39, 876-881'
_refine_ls_abs_structure_Flack  0
_refine_ls_number_reflns       1582
_refine_ls_number_parameters   154
_refine_ls_number_restraints   2
_refine_ls_R_factor_all        0.0569
_refine_ls_R_factor_gt         0.0506
_refine_ls_wR_factor_ref       0.1247
_refine_ls_wR_factor_gt        0.1213
_refine_ls_goodness_of_fit_ref 0.997
_refine_ls_restrained_S_all    0.996
_refine_ls_shift/su_max        0.000
_refine_ls_shift/su_mean       0.000

loop_
_atom_site_label
_atom_site_type_symbol
_atom_site_fract_x
_atom_site_fract_y
_atom_site_fract_z
_atom_site_U_iso_or_equiv
_atom_site_adp_type
_atom_site_occupancy
_atom_site_symmetry_multiplicity
_atom_site_calc_flag
_atom_site_refinement_flags
_atom_site_disorder_assembly
_atom_site_disorder_group
O1 O 0.1799(4) 0.55757(16) 0.5447(2) 0.0301(5) Uani 1 1 d ...
O4 O -0.3059(4) 0.13720(18) 0.8258(2) 0.0350(6) Uani 1 1 d ...
N1 N -0.2376(4) 0.3288(2) 0.5426(2) 0.0286(6) Uani 1 1 d ...
H1A H -0.2626 0.3153 0.4508 0.034 Uiso 1 1 calc R ..
O2 O -0.0204(4) 0.58411(15) 0.7308(2) 0.0306(5) Uani 1 1 d ...
O3 O -0.6457(3) 0.12084(16) 0.6367(2) 0.0321(5) Uani 1 1 d ...
C2 C 0.0548(6) 0.6336(2) 0.6132(3) 0.0279(7) Uani 1 1 d ...
C8 C -0.3655(5) 0.2688(2) 0.6353(3) 0.0260(6) Uani 1 1 d ...
H8A H -0.4629 0.3189 0.6830 0.031 Uiso 1 1 calc R ..
C4 C -0.0672(5) 0.4117(2) 0.6088(3) 0.0259(6) Uani 1 1 d ...
H4A H 0.0737 0.3770 0.6767 0.031 Uiso 1 1 calc R ..
C6 C -0.4695(6) 0.0643(2) 0.7404(3) 0.0276(6) Uani 1 1 d ...
C5 C -0.5381(6) 0.1872(3) 0.5469(3) 0.0326(7) Uani 1 1 d ...
H5A H -0.6704 0.2248 0.4784 0.039 Uiso 1 1 calc R ..
H5B H -0.4440 0.1426 0.4920 0.039 Uiso 1 1 calc R ..
C10 C 0.2469(7) 0.7168(3) 0.6744(4) 0.0400(8) Uani 1 1 d ...
H10A H 0.3861 0.6822 0.7394 0.060 Uiso 1 1 calc R ..
H10B H 0.1727 0.7705 0.7266 0.060 Uiso 1 1 calc R ..
H10C H 0.3063 0.7516 0.5968 0.060 Uiso 1 1 calc R ..
C1 C 0.0337(6) 0.4657(2) 0.4923(3) 0.0290(7) Uani 1 1 d ...
H1B H 0.1365 0.4141 0.4526 0.035 Uiso 1 1 calc R ..
H1C H -0.1058 0.4878 0.4144 0.035 Uiso 1 1 calc R ..
C7 C -0.1807(6) 0.2072(3) 0.7470(3) 0.0345(8) Uani 1 1 d ...
H7A H -0.0706 0.1647 0.6997 0.041 Uiso 1 1 calc R ..
H7B H -0.0769 0.2581 0.8131 0.041 Uiso 1 1 calc R ..
C3 C -0.1823(6) 0.4952(2) 0.6906(3) 0.0296(7) Uani 1 1 d ...
H3A H -0.3403 0.5206 0.6302 0.035 Uiso 1 1 calc R ..
H3B H -0.2191 0.4620 0.7771 0.035 Uiso 1 1 calc R ..
C9 C -0.1620(6) 0.6842(3) 0.5109(4) 0.0397(8) Uani 1 1 d ...
H9A H -0.2837 0.6288 0.4723 0.060 Uiso 1 1 calc R ..

loop_
_geom_bond_publ_flag
O1 C2 1.419(4) . ?
O1 C1 1.431(3) . ?
O4 C6 1.414(3) . ?
O4 C7 1.431(4) . ?
N1 C4 1.451(4) . ?

loop_
_atom_site_aniso_label
_atom_site_aniso_U_11
_atom_site_aniso_U_22
_atom_site_aniso_U_33
_atom_site_aniso_U_23
_atom_site_aniso_U_13
_atom_site_aniso_U_12
O1 0.0290(10) 0.0296(11) 0.0335(11) 0.0011(10) 0.0106(8) -0.0009(10)
O4 0.0418(13) 0.0374(13) 0.0247(10) 0.0057(9) 0.0050(9) -0.0079(11)
N1 0.0361(14) 0.0303(13) 0.0203(11) -0.0002(10) 0.0079(11) -
0.0059(11)
O2 0.0406(13) 0.0271(11) 0.0249(9) -0.0023(9) 0.0089(9) -0.0077(10)
O3 0.0252(11) 0.0321(12) 0.0381(12) 0.0065(10) 0.0046(9) -0.0050(10)
C2 0.0344(16) 0.0253(16) 0.0241(14) 0.0010(12) 0.0063(12) -
0.0046(13)
C8 0.0288(15) 0.0247(15) 0.0263(13) 0.0005(12) 0.0097(12)
0.0002(12)
C4 0.0278(15) 0.0243(15) 0.0250(14) 0.0028(12) 0.0043(12) -
0.0005(12)
C6 0.0319(15) 0.0227(14) 0.0293(14) -0.0001(12) 0.0090(12) -
0.0012(13)
C5 0.0341(16) 0.0332(17) 0.0275(14) 0.0044(13) 0.0002(12) -
0.0082(14)
C10 0.047(2) 0.0378(18) 0.0367(17) -0.0022(15) 0.0114(15) -
0.0134(17)
C1 0.0352(16) 0.0255(16) 0.0293(14) -0.0016(12) 0.0136(13) -
0.0034(14)
C7 0.0335(16) 0.0353(18) 0.0308(15) 0.0082(13) -0.0016(13) -
0.0099(14)
C3 0.0316(15) 0.0313(16) 0.0262(14) -0.0006(12) 0.0072(12) -
0.0045(14)
C9 0.0408(19) 0.0375(18) 0.0402(17) 0.0107(15) 0.0077(15)
0.0043(15)
C11 0.054(2) 0.0344(19) 0.045(2) -0.0009(16) 0.0232(17) 0.0054(17)
C12 0.0455(19) 0.0322(18) 0.048(2) 0.0045(16) 0.0224(16) -0.0017(16)

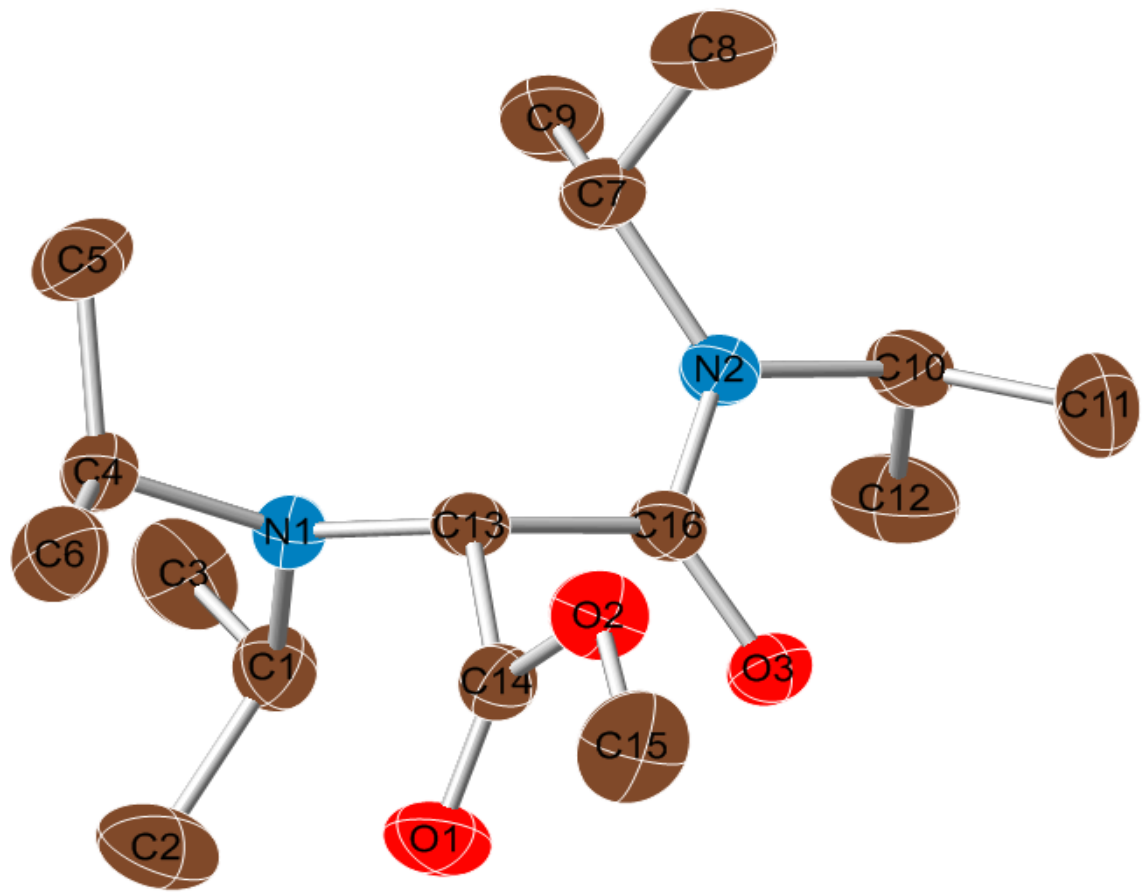
_geom_special_details
;
All esds (except the esd in the dihedral angle between two l.s. planes)
are estimated using the full covariance matrix. The cell esds are taken
into account individually in the estimation of esds in distances, angles
and torsion angles; correlations between esds in cell parameters are
only
used when they are defined by crystal symmetry. An approximate
(isotropic)
treatment of cell esds is used for estimating esds involving l.s. planes.
;

```

<p>_geom_bond_publ_flag</p> <p>loop_</p> <p>_geom_bond_atom_site_label_1</p> <p>_geom_bond_atom_site_label_2</p> <p>_geom_bond_distance</p> <p>_geom_bond_site_symmetry_2</p>	<p>N1 C8 1.461(4) . ?</p> <p>N1 H1A 0.8800 . ?</p> <p>O2 C3 1.426(3) . ?</p> <p>O2 C2 1.428(4) . ?</p> <p>O3 C5 1.418(4) . ?</p> <p>O3 C6 1.421(3) . ?</p>
---	--

C2 C10 1.511(4) . ?	O4 C6 O3 109.9(2) . . ?
C2 C9 1.513(4) . ?	O4 C6 C12 105.7(3) . . ?
C8 C7 1.520(4) . ?	O3 C6 C12 106.0(3) . . ?
C8 C5 1.523(4) . ?	O4 C6 C11 111.9(3) . . ?
C8 H8A 1.0000 . ?	O3 C6 C11 111.8(3) . . ?
C4 C1 1.515(4) . ?	C12 C6 C11 111.1(2) . . ?
C4 C3 1.526(4) . ?	O3 C5 C8 110.3(2) . . ?
C4 H4A 1.0000 . ?	O3 C5 H5A 109.6 . . ?
C6 C12 1.505(4) . ?	C8 C5 H5A 109.6 . . ?
C6 C11 1.519(4) . ?	O3 C5 H5B 109.6 . . ?
C5 H5A 0.9900 . ?	C8 C5 H5B 109.6 . . ?
C5 H5B 0.9900 . ?	H5A C5 H5B 108.1 . . ?
C10 H10A 0.9800 . ?	C2 C10 H10A 109.5 . . ?
C10 H10B 0.9800 . ?	C2 C10 H10B 109.5 . . ?
C10 H10C 0.9800 . ?	H10A C10 H10B 109.5 . . ?
C1 H1B 0.9900 . ?	C2 C10 H10C 109.5 . . ?
C1 H1C 0.9900 . ?	H10B C10 H10C 109.5 . . ?
C7 H7A 0.9900 . ?	O1 C1 C4 111.6(2) . . ?
C7 H7B 0.9900 . ?	O1 C1 H1B 109.3 . . ?
C3 H3A 0.9900 . ?	C4 C1 H1B 109.3 . . ?
C3 H3B 0.9900 . ?	O1 C1 H1C 109.3 . . ?
C9 H9A 0.9800 . ?	C4 C1 H1C 109.3 . . ?
C9 H9B 0.9800 . ?	H1B C1 H1C 108.0 . . ?
C9 H9C 0.9800 . ?	O4 C7 C8 110.8(2) . . ?
C11 H11A 0.9800 . ?	O4 C7 H7A 109.5 . . ?
C11 H11B 0.9800 . ?	C8 C7 H7A 109.5 . . ?
C11 H11C 0.9800 . ?	O4 C7 H7B 109.5 . . ?
C12 H12A 0.9800 . ?	C8 C7 H7B 109.5 . . ?
C12 H12B 0.9800 . ?	H7A C7 H7B 108.1 . . ?
C12 H12C 0.9800 . ?	O2 C3 C4 111.4(2) . . ?
loop_	O2 C3 H3A 109.4 . . ?
_geom_angle_atom_site_label_1	C4 C3 H3A 109.4 . . ?
_geom_angle_atom_site_label_2	H3A C3 H3B 108.0 . . ?
_geom_angle_atom_site_label_3	C2 C9 H9A 109.5 . . ?
_geom_angle	C2 C9 H9B 109.5 . . ?
_geom_angle_site_symmetry_1	H9A C9 H9B 109.5 . . ?
_geom_angle_site_symmetry_3	C2 C9 H9C 109.5 . . ?
_geom_angle_publ_flag	H9A C9 H9C 109.5 . . ?
C2 O1 C1 113.9(2) . . ?	H9B C9 H9C 109.5 . . ?
C6 O4 C7 114.1(2) . . ?	C6 C11 H11A 109.5 . . ?
C4 N1 C8 117.0(2) . . ?	C6 C11 H11B 109.5 . . ?
C4 N1 H1A 121.5 . . ?	H11A C11 H11B 109.5 . . ?
C8 N1 H1A 121.5 . . ?	C6 C11 H11C 109.5 . . ?
C3 O2 C2 113.4(2) . . ?	H11A C11 H11C 109.5 . . ?
C5 O3 C6 113.8(2) . . ?	H11B C11 H11C 109.5 . . ?
O1 C2 O2 109.4(2) . . ?	C6 C12 H12A 109.5 . . ?
O1 C2 C10 105.6(3) . . ?	C6 C12 H12B 109.5 . . ?
O2 C2 C10 106.9(2) . . ?	H12A C12 H12B 109.5 . . ?
O1 C2 C9 112.1(2) . . ?	C6 C12 H12C 109.5 . . ?
O2 C2 C9 111.6(3) . . ?	H12A C12 H12C 109.5 . . ?
C10 C2 C9 110.9(3) . . ?	H12B C12 H12C 109.5 . . ?
N1 C8 C7 110.5(2) . . ?	
N1 C8 C5 109.3(2) . . ?	_diffrn_measured_fraction_theta_max
C7 C8 C5 107.3(2) . . ?	0.933
N1 C8 H8A 109.9 . . ?	_diffrn_reflins_theta_full 28.30
C7 C8 H8A 109.9 . . ?	_diffrn_measured_fraction_theta_full 0.933
C5 C8 H8A 109.9 . . ?	_refine_diff_density_max 0.382
N1 C4 C1 107.6(2) . . ?	_refine_diff_density_min -0.287
N1 C4 C3 114.2(2) . . ?	_refine_diff_density_rms 0.049
C1 C4 C3 109.8(2) . . ?	
N1 C4 H4A 108.4 . . ?	
C1 C4 H4A 108.4 . . ?	
C3 C4 H4A 108.4 . . ?	

APPENDIX 3
CRYSTAL STRUCTURE DATA FOR **85**



```

data_pccn (diisopropylamine_ester-amide)

_audit_creation_method      SHELXL-97
_chemical_name_systematic
;
?
;
_chemical_name_common      ?
_chemical_melting_point    ?
_chemical_formula_moiety   'C16 H32 N2 O3'
_chemical_formula_sum       'C16 H32 N2 O3'
_chemical_formula_weight    300.44

loop_
_atom_type_symbol
_atom_type_description
_atom_type_scat_dispersion_real
_atom_type_scat_dispersion_imag
_atom_type_scat_source
'C' 'C' 0.0033 0.0016
'International Tables Vol C Tables 4.2.6.8 and 6.1.1.4'
'H' 'H' 0.0000 0.0000
'International Tables Vol C Tables 4.2.6.8 and 6.1.1.4'
'N' 'N' 0.0061 0.0033
'International Tables Vol C Tables 4.2.6.8 and 6.1.1.4'
'O' 'O' 0.0106 0.0060
'International Tables Vol C Tables 4.2.6.8 and 6.1.1.4'

_symmetry_cell_setting     'Orthorhombic'
_symmetry_space_group_name_H-M  'P c c n'
_symmetry_space_group_name_Hall '-P 2ab 2ac'
loop_
_symmetry_equiv_pos_as_xyz
'x, y, z'
'-x+1/2, -y+1/2, z'
'-x, y+1/2, -z+1/2'
'x+1/2, -y, -z+1/2'
'-x, -y, -z'
'x-1/2, y-1/2, -z'
'x, -y-1/2, z-1/2'
'-x-1/2, y, z-1/2'

_cell_length_a              28.629(2)
_cell_length_b              10.2423(8)
_cell_length_c              12.7234(10)
_cell_angle_alpha            90.00
_cell_angle_beta             90.00
_cell_angle_gamma            90.00
_cell_volume                 3730.8(5)
_cell_formula_units_Z        8
_cell_measurement_temperature 193(2)
_cell_measurement_reflns_used 3607
_cell_measurement_theta_min   1.42
_cell_measurement_theta_max    28.33

_exptl_crystal_description  'rectangular block'
_exptl_crystal_colour       'colorless'
_exptl_crystal_size_max      0.660
_exptl_crystal_size_mid      0.422
_exptl_crystal_size_min      0.124
_exptl_crystal_density_meas   'nm'
_exptl_crystal_density_diffn  1.070
_exptl_crystal_density_method  'not measured'
_exptl_crystal_F_000          1328
_exptl_absorpt_coefficient_mu 0.073
_exptl_absorpt_correction_type 'numerical'

_exptl_absorpt_correction_T_min  0.9621
_exptl_absorpt_correction_T_max  0.9891
_exptl_absorpt_process_details  'SHELXPREP'

_exptl_special_details
;
?
;
_diffrn_ambient_temperature   193(2)
_diffrn_radiation_wavelength  0.71073
_diffrn_radiation_type        MoK\alpha
_diffrn_radiation_source      'fine-focus sealed tube'
_diffrn_radiation_monochromator 'graphite'
_diffrn_measurement_device_type 'Bruker APEX'
_diffrn_measurement_method    '0.3 wide /w exposures'
_diffrn_detector_area_resol_mean ?
_diffrn_standards_number      'na'
_diffrn_standards_interval_count 'na'
_diffrn_standards_interval_time 'na'
_diffrn_standards_decay_%      0
_diffrn_reflns_number         35254
_diffrn_reflns_av_R_equivalents 0.0458
_diffrn_reflns_av_sigmaI/netI 0.0293
_diffrn_reflns_limit_h_min    -38
_diffrn_reflns_limit_h_max    37
_diffrn_reflns_limit_k_min    -13
_diffrn_reflns_limit_k_max    13
_diffrn_reflns_limit_l_min    -16
_diffrn_reflns_limit_l_max    16
_diffrn_reflns_theta_min      1.42
_diffrn_reflns_theta_max      28.33
_reflns_number_total          4644
_reflns_number_gt              3607
_reflns_threshold_expression  >2sigma(I)

_computing_data_collection    'SMART'
_computing_cell_refinement    'SMART, SAINT'
_computing_data_reduction      'SAINT'
_computing_structure_solution  'SHELXS-97 (Sheldrick, 1990)'
_computing_structure_refinement 'SHELXL-97 (Sheldrick, 1997)'
_computing_molecular_graphics   'SHELXP-97 (Sheldrick, 1990)'
_computing_publication_material 'SHELXS-97 (Sheldrick, 2000)'

_refine_special_details
;
Refinement of F^2^ against ALL reflections. The weighted R-factor wR and
goodness of fit S are based on F^2^, conventional R-factors R are
based
on F, with F set to zero for negative F^2^. The threshold expression of
F^2^ > 2sigma(F^2^) is used only for calculating R-factors(gt) etc. and
is
not relevant to the choice of reflections for refinement. R-factors
based
on F^2^ are statistically about twice as large as those based on F, and
R-
factors based on ALL data will be even larger.
;

_refine_ls_structure_factor_coef Fsqd
_refine_ls_matrix_type        full
_refine_ls_weighting_scheme    calc
_refine_ls_weighting_details
'calc      w=1/[s^2^(Fo^2^)+(0.0793P)^2^+0.8135P]      where
P=(Fo^2^+2Fc^2^)/3'
_atom_sites_solution_primary    direct

```

```

_atom_sites_solution_secondary difmap
_atom_sites_solution_hydrogens geom
_refine_ls_hydrogen_treatment constr
_refine_ls_extinction_method SHELXL
_refine_ls_extinction_coeff 0.0009(5)
_refine_ls_extinction_expression
'Fc^*^=kFc[1+0.001xFc^2^/\|3^/sin(2\q)]^-1/4^'
_refine_ls_number_refns 4644
_refine_ls_number_parameters 191
_refine_ls_number_restraints 0
_refine_ls_R_factor_all 0.0721
_refine_ls_R_factor_gt 0.0578
_refine_ls_wR_factor_ref 0.1543
_refine_ls_wR_factor_gt 0.1468
_refine_ls_goodness_of_fit_ref 1.040
_refine_ls_restrained_S_all 1.040
_refine_ls_shift/su_max 0.001
_refine_ls_shift/su_mean 0.000

loop_
_atom_site_label
_atom_site_type_symbol
_atom_site_fract_x
_atom_site_fract_y
_atom_site_fract_z
_atom_site_U_iso_or_equiv
_atom_site_adp_type
_atom_site_occupancy
_atom_site_symmetry_multiplicity
_atom_site_calc_flag
_atom_site_refinement_flags
_atom_site_disorder_assembly
_atom_site_disorder_group
C1 C 0.69791(5) 0.03758(15) 0.40591(12) 0.0385(3) Uani 1 1 d...
H1A H 0.6799 0.1199 0.4180 0.046 Uiso 1 1 calc R ..
C2 C 0.71588(6) -0.0080(2) 0.51305(14) 0.0570(5) Uani 1 1 d...
H2A H 0.6893 -0.0303 0.5582 0.086 Uiso 1 1 calc R ..
H2B H 0.7341 0.0621 0.5458 0.086 Uiso 1 1 calc R ..
H2C H 0.7358 -0.0851 0.5037 0.086 Uiso 1 1 calc R ..
C3 C 0.73881(6) 0.07189(19) 0.33469(15) 0.0534(5) Uani 1 1 d...
H3A H 0.7270 0.1014 0.2664 0.080 Uiso 1 1 calc R ..
H3B H 0.7585 -0.0054 0.3248 0.080 Uiso 1 1 calc R ..
H3C H 0.7573 0.1417 0.3670 0.080 Uiso 1 1 calc R ..
C4 C 0.68303(5) -0.18794(14) 0.33618(11) 0.0367(3) Uani 1 1 d...
H4A H 0.7171 -0.1877 0.3532 0.044 Uiso 1 1 calc R ..
C5 C 0.67899(8) -0.22972(17) 0.22145(13) 0.0553(5) Uani 1 1 d...
H5A H 0.6935 -0.1635 0.1764 0.083 Uiso 1 1 calc R ..
H5B H 0.6460 -0.2390 0.2027 0.083 Uiso 1 1 calc R ..
H5C H 0.6949 -0.3135 0.2115 0.083 Uiso 1 1 calc R ..
C6 C 0.66066(7) -0.28968(16) 0.40760(13) 0.0491(4) Uani 1 1 d...
H6A H 0.6638 -0.2621 0.4810 0.074 Uiso 1 1 calc R ..
H6B H 0.6763 -0.3739 0.3978 0.074 Uiso 1 1 calc R ..
H6C H 0.6275 -0.2985 0.3899 0.074 Uiso 1 1 calc R ..
N1 N 0.66652(4) -0.05329(11) 0.35119(9) 0.0298(3) Uani 1 1 d...
C7 C 0.61768(6) 0.07442(16) 0.14560(11) 0.0413(4) Uani 1 1 d...
H7A H 0.6306 -0.0095 0.1733 0.050 Uiso 1 1 calc R ..
C8 C 0.57536(7) 0.04093(19) 0.07899(14) 0.0568(5) Uani 1 1 d...
H8A H 0.5517 -0.0016 0.1229 0.085 Uiso 1 1 calc R ..
H8B H 0.5847 -0.0183 0.0223 0.085 Uiso 1 1 calc R ..
H8C H 0.5623 0.1211 0.0488 0.085 Uiso 1 1 calc R ..
C9 C 0.65576(6) 0.1388(2) 0.08052(13) 0.0547(5) Uani 1 1 d...
H9A H 0.6826 0.1587 0.1256 0.082 Uiso 1 1 calc R ..
H9B H 0.6437 0.2198 0.0497 0.082 Uiso 1 1 calc R ..
H9C H 0.6655 0.0794 0.0242 0.082 Uiso 1 1 calc R ..

C10 C 0.58940(5) 0.29172(14) 0.21598(12) 0.0385(3) Uani 1 1 d...
H10A H 0.5915 0.3044 0.1382 0.046 Uiso 1 1 calc R ..
C11 C 0.53888(7) 0.31721(19) 0.24612(15) 0.0566(5) Uani 1 1 d...
H11A H 0.5187 0.2526 0.2120 0.085 Uiso 1 1 calc R ..
H11B H 0.5299 0.4050 0.2232 0.085 Uiso 1 1 calc R ..
H11C H 0.5355 0.3105 0.3226 0.085 Uiso 1 1 calc R ..
C12 C 0.62295(8) 0.38901(17) 0.26532(14) 0.0568(5) Uani 1 1 d...
H12A H 0.6550 0.3681 0.2439 0.085 Uiso 1 1 calc R ..
H12B H 0.6205 0.3842 0.3420 0.085 Uiso 1 1 calc R ..
H12C H 0.6150 0.4774 0.2418 0.085 Uiso 1 1 calc R ..
N2 N 0.60406(4) 0.15505(11) 0.23729(9) 0.0329(3) Uani 1 1 d...
C13 C 0.61667(4) -0.03488(13) 0.35732(10) 0.0276(3) Uani 1 1 d...
H13A H 0.6023 -0.0897 0.3009 0.033 Uiso 1 1 calc R ..
C14 C 0.59286(5) -0.07207(13) 0.46128(11) 0.0313(3) Uani 1 1 d...
O1 O 0.60945(4) -0.06910(12) 0.54736(8) 0.0463(3) Uani 1 1 d...
O2 O 0.54940(4) -0.11364(11) 0.44115(8) 0.0413(3) Uani 1 1 d...
C15 C 0.52279(7) -0.15522(19) 0.53186(15) 0.0553(5) Uani 1 1 d...
H15A H 0.4917 -0.1836 0.5094 0.083 Uiso 1 1 calc R ..
H15B H 0.5198 -0.0823 0.5812 0.083 Uiso 1 1 calc R ..
H15C H 0.5389 -0.2279 0.5664 0.083 Uiso 1 1 calc R ..
C16 C 0.60201(4) 0.10857(13) 0.33629(10) 0.0286(3) Uani 1 1 d...
O3 O 0.58892(3) 0.17460(10) 0.41126(7) 0.0349(2) Uani 1 1 d...

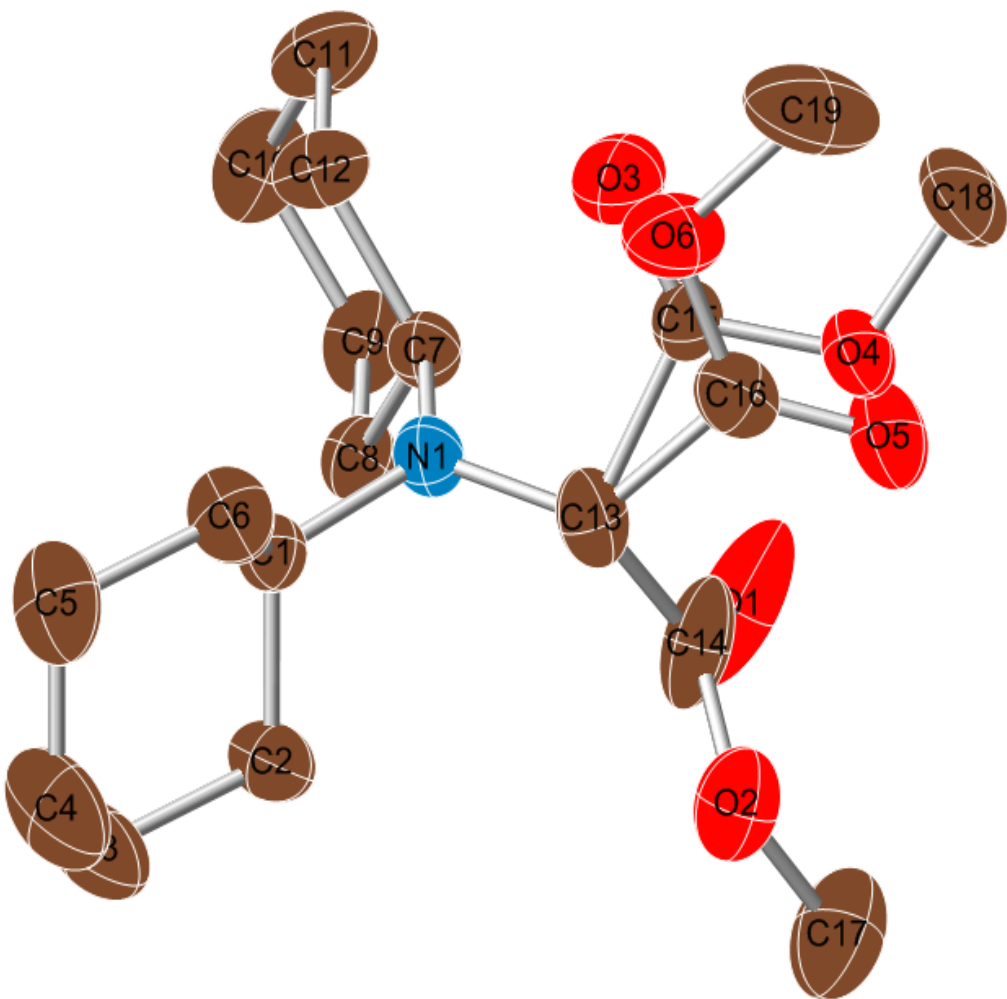
loop_
_atom_site_aniso_label
_atom_site_aniso_U_11
_atom_site_aniso_U_22
_atom_site_aniso_U_33
_atom_site_aniso_U_23
_atom_site_aniso_U_13
_atom_site_aniso_U_12
C1 0.0316(7) 0.0385(8) 0.0454(8) -0.0041(6) -0.0041(6) -0.0006(6)
C2 0.0423(9) 0.0857(14) 0.0430(9) -0.0026(9) -0.0103(7) -0.0106(9)
C3 0.0387(9) 0.0568(10) 0.0649(11) 0.0148(9) -0.0032(8) -0.0085(8)
C4 0.0419(8) 0.0328(7) 0.0354(7) -0.0003(6) 0.0015(6) 0.0087(6)
C5 0.0838(13) 0.0438(9) 0.0384(8) -0.0069(7) 0.0057(8) 0.0185(9)
C6 0.0667(11) 0.0323(8) 0.0482(9) 0.0057(7) 0.0062(8) 0.0084(7)
N1 0.0285(6) 0.0298(6) 0.0311(6) -0.0010(4) 0.0002(4) 0.0029(4)
C7 0.0568(10) 0.0415(8) 0.0254(7) 0.0024(6) 0.0041(6) 0.0140(7)
C8 0.0777(13) 0.0531(10) 0.0396(9) -0.0085(8) -0.0006(8) -0.0085(9)
C9 0.0521(10) 0.0776(13) 0.0343(8) 0.0081(8) 0.0081(7) 0.0137(9)
C10 0.0496(9) 0.0344(7) 0.0315(7) 0.0061(6) -0.0018(6) 0.0050(7)
C11 0.0579(11) 0.0556(11) 0.0564(10) 0.0099(8) 0.0002(9) 0.0230(9)
C12 0.0835(14) 0.0431(9) 0.0439(9) 0.0070(7) -0.0079(9) -0.0141(9)
N2 0.0388(6) 0.0336(6) 0.0263(6) 0.0034(4) 0.0014(5) 0.0057(5)
C13 0.0290(6) 0.0304(6) 0.0233(6) 0.0003(5) -0.0004(5) -0.0001(5)
C14 0.0321(7) 0.0303(7) 0.0315(7) 0.0018(5) 0.0025(5) 0.0018(5)
O1 0.0448(6) 0.0669(8) 0.0272(5) 0.0043(5) 0.0017(4) -0.0002(5)
O2 0.0338(6) 0.0474(6) 0.0425(6) 0.0039(5) 0.0050(4) -0.0080(5)
C15 0.0481(10) 0.0559(10) 0.0619(11) 0.0101(9) 0.0206(8) -0.0069(8)
C16 0.0256(6) 0.0325(7) 0.0276(6) 0.0013(5) -0.0007(5) -0.0004(5)
O3 0.0401(6) 0.0358(5) 0.0288(5) -0.0014(4) 0.0041(4) 0.0036(4)

_geom_special_details
;

All esds (except the esd in the dihedral angle between two l.s. planes) are estimated using the full covariance matrix. The cell esds are taken into account individually in the estimation of esds in distances, angles and torsion angles; correlations between esds in cell parameters are only used when they are defined by crystal symmetry. An approximate isotropic treatment of cell esds is used for estimating esds involving l.s. planes.
;
```

loop_	loop_	H8A C8 H8C 109.5 . . ?
_geom_bond_atom_site_label_1	_geom_angle_atom_site_label_1	H8B C8 H8C 109.5 . . ?
_geom_bond_atom_site_label_2	_geom_angle_atom_site_label_2	C7 C9 H9A 109.5 . . ?
_geom_bond_distance	_geom_angle_atom_site_label_3	C7 C9 H9B 109.5 . . ?
_geom_bond_site_symmetry_2	_geom_angle	H9A C9 H9B 109.5 . . ?
_geom_bond_publ_flag	_geom_angle_site_symmetry_1	C7 C9 H9C 109.5 . . ?
C1 N1 1.4692(18) . ?	_geom_angle_site_symmetry_3	H9A C9 H9C 109.5 . . ?
C1 C3 1.522(2) . ?	_geom_angle_publ_flag	H9B C9 H9C 109.5 . . ?
C1 C2 1.530(2) . ?	N1 C1 C3 109.55(13) . . ?	N2 C10 C11 112.63(13) . . ?
C1 H1A 1.0000 . ?	N1 C1 C2 115.75(13) . . ?	N2 C10 C12 111.32(13) . . ?
C2 H2A 0.9800 . ?	C3 C1 C2 110.02(13) . . ?	C11 C10 C12 112.63(15) . . ?
C2 H2B 0.9800 . ?	N1 C1 H1A 107.0 . . ?	N2 C10 H10A 106.6 . . ?
C2 H2C 0.9800 . ?	C3 C1 H1A 107.0 . . ?	C11 C10 H10A 106.6 . . ?
C3 H3A 0.9800 . ?	C2 C1 H1A 107.0 . . ?	C12 C10 H10A 106.6 . . ?
C3 H3B 0.9800 . ?	C1 C2 H2A 109.5 . . ?	C10 C11 H11A 109.5 . . ?
C3 H3C 0.9800 . ?	C1 C2 H2B 109.5 . . ?	C10 C11 H11B 109.5 . . ?
C4 N1 1.4703(18) . ?	H2A C2 H2B 109.5 . . ?	H11A C11 H11B 109.5 . . ?
C4 C6 1.524(2) . ?	C1 C2 H2C 109.5 . . ?	C10 C11 H11C 109.5 . . ?
C4 C5 1.525(2) . ?	H2A C2 H2C 109.5 . . ?	H11A C11 H11C 109.5 . . ?
C4 H4A 1.0000 . ?	H2B C2 H2C 109.5 . . ?	H11B C11 H11C 109.5 . . ?
C5 H5A 0.9800 . ?	C1 C3 H3A 109.5 . . ?	C10 C12 H12A 109.5 . . ?
C5 H5B 0.9800 . ?	C1 C3 H3B 109.5 . . ?	C10 C12 H12B 109.5 . . ?
C5 H5C 0.9800 . ?	C1 C3 H3C 109.5 . . ?	H12A C12 H12B 109.5 . . ?
C6 H6A 0.9800 . ?	H3A C3 H3B 109.5 . . ?	C10 C12 H12C 109.5 . . ?
C6 H6B 0.9800 . ?	C1 C3 H3C 109.5 . . ?	H12A C12 H12C 109.5 . . ?
C6 H6C 0.9800 . ?	H3A C3 H3C 109.5 . . ?	H12B C12 H12C 109.5 . . ?
N1 C13 1.4418(17) . ?	H3B C3 H3C 109.5 . . ?	C16 N2 C7 123.40(12) . . ?
C7 N2 1.4814(18) . ?	N1 C4 C6 115.39(12) . . ?	C16 N2 C10 119.39(12) . . ?
C7 C8 1.518(3) . ?	N1 C4 C5 111.29(12) . . ?	C7 N2 C10 117.11(11) . . ?
C7 C9 1.520(2) . ?	C6 C4 C5 110.30(14) . . ?	N1 C13 C14 116.96(11) . . ?
C7 H7A 1.0000 . ?	N1 C4 H4A 106.4 . . ?	N1 C13 C16 112.48(11) . . ?
C8 H8A 0.9800 . ?	C6 C4 H4A 106.4 . . ?	C14 C13 C16 105.27(10) . . ?
C8 H8B 0.9800 . ?	C5 C4 H4A 106.4 . . ?	N1 C13 H13A 107.2 . . ?
C8 H8C 0.9800 . ?	C4 C5 H5A 109.5 . . ?	C14 C13 H13A 107.2 . . ?
C9 H9A 0.9800 . ?	C4 C5 H5B 109.5 . . ?	C16 C13 H13A 107.2 . . ?
C9 H9B 0.9800 . ?	H5A C5 H5B 109.5 . . ?	O1 C14 O2 123.56(13) . . ?
C9 H9C 0.9800 . ?	C4 C5 H5C 109.5 . . ?	O1 C14 C13 127.38(13) . . ?
C10 N2 1.4863(18) . ?	H5A C5 H5C 109.5 . . ?	O2 C14 C13 109.04(11) . . ?
C10 C11 1.519(2) . ?	H5B C5 H5C 109.5 . . ?	C14 O2 C15 115.47(13) . . ?
C10 C12 1.520(2) . ?	C4 C6 H6A 109.5 . . ?	O2 C15 H15A 109.5 . . ?
C10 H10A 1.0000 . ?	C4 C6 H6B 109.5 . . ?	O2 C15 H15B 109.5 . . ?
C11 H11A 0.9800 . ?	H6A C6 H6B 109.5 . . ?	H15A C15 H15B 109.5 . . ?
C11 H11B 0.9800 . ?	C4 C6 H6C 109.5 . . ?	O2 C15 H15C 109.5 . . ?
C11 H11C 0.9800 . ?	H6A C6 H6C 109.5 . . ?	H15A C15 H15C 109.5 . . ?
C12 H12A 0.9800 . ?	H6B C6 H6C 109.5 . . ?	H15B C15 H15C 109.5 . . ?
C12 H12B 0.9800 . ?	C13 N1 C1 119.80(11) . . ?	O3 C16 N2 123.01(12) . . ?
C12 H12C 0.9800 . ?	C13 N1 C4 116.61(11) . . ?	O3 C16 C13 118.05(11) . . ?
N2 C16 1.3479(16) . ?	C1 N1 C4 117.34(11) . . ?	N2 C16 C13 118.94(11) . . ?
C13 C14 1.5360(18) . ?	N2 C7 C8 110.84(13) . . ?	
C13 C16 1.5512(18) . ?	N2 C7 C9 112.08(14) . . ?	_diffrrn_measured_fraction_theta_max
C13 H13A 1.0000 . ?	C8 C7 C9 111.50(13) . . ?	0.999
C14 O1 1.1942(17) . ?	N2 C7 H7A 107.4 . . ?	_diffrrn_reflns_theta_full
C14 O2 1.3397(17) . ?	C8 C7 H7A 107.4 . . ?	28.33
O2 C15 1.4471(19) . ?	C9 C7 H7A 107.4 . . ?	_diffrrn_measured_fraction_theta_full
C15 H15A 0.9800 . ?	C7 C8 H8A 109.5 . . ?	0.999
C15 H15B 0.9800 . ?	C7 C8 H8B 109.5 . . ?	_refine_diff_density_max
C15 H15C 0.9800 . ?	H8A C8 H8B 109.5 . . ?	0.342
C16 O3 1.2279(16) . ?	C7 C8 H8C 109.5 . . ?	_refine_diff_density_min
		-0.195
		_refine_diff_density_rms
		0.045

APPENDIX 4
CRYSTAL STRUCTURE DATA FOR **86**



```

data_pbca (dicyclohexylamine_diester)

_audit_creation_method      SHELXL-97
_chemical_name_systematic
;
?
;
_chemical_name_common      ?
_chemical_melting_point    ?
_chemical_formula_moiety
;
C17 H29 N O4
;

_chemical_formula_sum
'C17 H29 N O4'
_chemical_formula_weight    311.41

loop_
_atom_type_symbol
_atom_type_description
_atom_type_scat_dispersion_real
_atom_type_scat_dispersion_imag
_atom_type_scat_source
'C' 'C' 0.0033 0.0016
'International Tables Vol C Tables 4.2.6.8 and 6.1.1.4'
'H' 'H' 0.0000 0.0000
'International Tables Vol C Tables 4.2.6.8 and 6.1.1.4'
'N' 'N' 0.0061 0.0033
'International Tables Vol C Tables 4.2.6.8 and 6.1.1.4'
'O' 'O' 0.0106 0.0060
'International Tables Vol C Tables 4.2.6.8 and 6.1.1.4'

_symmetry_cell_setting     'Orthorhombic'
_symmetry_space_group_name_H-M 'P b c a'
_symmetry_space_group_name_Hall      '-P 2ac 2ab'

loop_
_symmetry_equiv_pos_as_xyz
'x, y, z'
'-x+1/2, -y, z+1/2'
'-x, y+1/2, -z+1/2'
'x+1/2, -y+1/2, -z'
'-x, -y, -z'
'x-1/2, y, -z-1/2'
'x, -y-1/2, z-1/2'
'-x-1/2, y-1/2, z'

_cell_length_a              8.5308(7)
_cell_length_b              16.5190(12)
_cell_length_c              24.783(2)
_cell_angle_alpha            90.00
_cell_angle_beta             90.00
_cell_angle_gamma            90.00
_cell_volume                 3492.5(5)
_cell_formula_units_Z        8
_cell_measurement_temperature 153(2)
_cell_measurement_reflins_used ?
_cell_measurement_theta_min   2.46
_cell_measurement_theta_max   27.92

_exptl_crystal_description  'fragment'
_exptl_crystal_colour       'colorless'
_exptl_crystal_size_max     .23
_exptl_crystal_size_mid     .20
_exptl_crystal_size_min     .15

_exptl_crystal_density_meas  ?
_exptl_crystal_density_diffn  1.185
_exptl_crystal_density_method 'not measured'
_exptl_crystal_F_000          1360
_exptl_absorpt_coefficient_mu 0.083
_exptl_absorpt_correction_type 'empirical'
_exptl_absorpt_correction_T_min 0.981
_exptl_absorpt_correction_T_max 0.988
_exptl_absorpt_process_details sadabs

_exptl_special_details
;
?
;

_diffrn_ambient_temperature  153(2)
_diffrn_radiation_wavelength 0.71073
_diffrn_radiation_type       MoK\alpha
_diffrn_radiation_source     'fine-focus sealed tube'
_diffrn_radiation_monochromator graphite
_diffrn_measurement_device_type 'Bruker APEX CCD area detector'
_diffrn_measurement_method    'phi and omega scans'
_diffrn_detector_area_resol_mean ?

_diffrn_standards_number      ?
_diffrn_standards_interval_count ?
_diffrn_standards_interval_time ?
_diffrn_standards_decay_%     ?
_diffrn_reflins_number        24404
_diffrn_reflins_av_R_equivalents 0.0370
_diffrn_reflins_av_sigma/netl  0.0278
_diffrn_reflins_limit_h_min   -7
_diffrn_reflins_limit_h_max   11
_diffrn_reflins_limit_k_min   -22
_diffrn_reflins_limit_k_max   15
_diffrn_reflins_limit_l_min   -33
_diffrn_reflins_limit_l_max   33
_diffrn_reflins_theta_min     2.47
_diffrn_reflins_theta_max     28.37
_reflins_number_total         4358
_reflins_number_gt             2946
_reflins_threshold_expression >2sigma(l)

_computing_data_collection   'SMART (Bruker, 2000)'
_computing_cell_refinement    'SMART, SAINT (Bruker, 1999)'
_computing_data_reduction     'SAINT (Bruker, 1999)'
_computing_structure_solution 'SHELXS-97 (Sheldrick, 1990)'
_computing_structure_refinement 'SHELXL-97 (Sheldrick, 1997)'
_computing_molecular_graphics 'Bruker SHELXTL'
_computing_publication_material 'SHELXCIF-97 (Sheldrick, 1997)'

_refine_special_details
;
Refinement of F^2 against ALL reflections. The weighted R-factor wR and
goodness of fit S are based on F^2, conventional R-factors R are
based
on F, with F set to zero for negative F^2. The threshold expression of
F^2 > 2sigma(F^2) is used only for calculating R-factors(gt) etc. and
is
not relevant to the choice of reflections for refinement. R-factors
based
on F^2 are statistically about twice as large as those based on F, and
R-
factors based on ALL data will be even larger.
;
```

`_refine_ls_structure_factor_coef Fsqd`
`_refine_ls_matrix_type full`
`_refine_ls_weighting_scheme calc`
`_refine_ls_weighting_details`
`'calc w=1/[s^2^(Fo^2)+(0.0993P)^2+0.0000P]` where
`P=(Fo^2+2Fc^2)/3'`
`_atom_sites_solution_primary direct`
`_atom_sites_solution_secondary difmap`
`_atom_sites_solution_hydrogens geom`
`_refine_ls_hydrogen_treatment mixed`
`_refine_ls_extinction_method none`
`_refine_ls_extinction_coeff ?`
`_refine_ls_number_reflins 4358`
`_refine_ls_number_parameters 332`
`_refine_ls_number_restraints 0`
`_refine_ls_R_factor_all 0.0781`
`_refine_ls_R_factor_gt 0.0550`
`_refine_ls_wR_factor_ref 0.1613`
`_refine_ls_wR_factor_gt 0.1500`
`_refine_ls_goodness_of_fit_ref 1.061`
`_refine_ls_restrained_S_all 1.061`
`_refine_ls_shift/su_max 0.051`
`_refine_ls_shift/su_mean 0.008`

`loop_`
`_atom_site_label`
`_atom_site_type_symbol`
`_atom_site_fract_x`
`_atom_site_fract_y`
`_atom_site_fract_z`
`_atom_site_U_iso_or_equiv`
`_atom_site_adp_type`
`_atom_site_occupancy`
`_atom_site_symmetry_multiplicity`
`_atom_site_calc_flag`
`_atom_site_refinement_flags`
`_atom_site_disorder_assembly`
`_atom_site_disorder_group`
`N1 N 0.45356(14) 0.11560(6) 0.39158(4) 0.0363(3) Uani 1 1 d . A .`
`C7 C 0.34382(16) 0.17386(7) 0.36819(5) 0.0347(3) Uani 1 1 d . . .`
`C1 C 0.56176(14) 0.07314(8) 0.35611(5) 0.0326(3) Uani 1 1 d . . .`
`C8 C 0.24658(18) 0.14073(8) 0.32163(5) 0.0387(3) Uani 1 1 d . . .`
`C2 C 0.51541(18) -0.01347(9) 0.34300(6) 0.0431(3) Uani 1 1 d . . .`
`C13 C 0.41947(17) 0.08122(9) 0.44280(5) 0.0411(3) Uani 1 1 d . . .`
`C6 C 0.72932(17) 0.07514(11) 0.37727(6) 0.0469(4) Uani 1 1 d . . .`
`C12 C 0.42701(19) 0.25164(9) 0.35094(7) 0.0471(4) Uani 1 1 d . . .`
`C9 C 0.13117(19) 0.20325(10) 0.30071(6) 0.0479(4) Uani 1 1 d . . .`
`C5 C 0.8428(2) 0.03704(13) 0.33721(8) 0.0596(5) Uani 1 1 d . . .`
`C14 C 0.26732(19) 0.03462(12) 0.44642(6) 0.0571(5) Uani 1 1 d . A .`
`C10 C 0.2146(2) 0.27958(11) 0.28312(7) 0.0581(4) Uani 1 1 d . . .`
`C11 C 0.3108(2) 0.31352(10) 0.32886(9) 0.0582(5) Uani 1 1 d . . .`
`C3 C 0.6305(2) -0.05173(13) 0.30333(9) 0.0653(5) Uani 1 1 d . . .`
`C4 C 0.7956(2) -0.04822(12) 0.32420(9) 0.0718(6) Uani 1 1 d . . .`
`H4A H 0.8041 -0.0813 0.3564 0.086 Uiso 1 1 calc R . . .`
`H4B H 0.8663 -0.0701 0.2973 0.086 Uiso 1 1 calc R . . .`
`O2 O 0.29034(13) -0.04119(7) 0.46344(5) 0.0576(3) Uani 1 1 d . . .`
`O1 O 0.14126(14) 0.06198(10) 0.43553(6) 0.0938(6) Uani 1 1 d . . .`
`C17 C 0.1522(3) -0.09098(19) 0.46889(10) 0.0779(6) Uani 1 1 d . A .`
`O4 O 0.3602(4) 0.1408(2) 0.52922(14) 0.0470(7) Uani 0.529(5) 1 d P A 1`
`C18 C 0.3648(5) 0.2015(2) 0.57051(12) 0.0638(13) Uani 0.529(5) 1 d P A 1`
`H18A H 0.3046 0.1837 0.6010 0.096 Uiso 0.529(5) 1 calc PR A 1`
`H18B H 0.3215 0.2510 0.5568 0.096 Uiso 0.529(5) 1 calc PR A 1`
`H18C H 0.4715 0.2104 0.5814 0.096 Uiso 0.529(5) 1 calc PR A 1`

`C15 C 0.4402(5) 0.1590(3) 0.4846(2) 0.0353(11) Uani 0.529(5) 1 d P A 1`
`O3 O 0.5137(7) 0.2180(3) 0.4774(2) 0.0646(12) Uani 0.529(5) 1 d P A 1`
`O6 O 0.4872(7) 0.1923(3) 0.4907(3) 0.0539(16) Uani 0.471(5) 1 d P A 2`
`C16 C 0.3967(7) 0.1272(3) 0.4920(2) 0.0422(12) Uani 0.471(5) 1 d P A 2`
`O5 O 0.3182(7) 0.1071(3) 0.52979(17) 0.0735(13) Uani 0.471(5) 1 d P A 2`
`C19 C 0.4768(7) 0.2388(2) 0.54054(17) 0.082(2) Uani 0.471(5) 1 d P A 2`
`H19A H 0.5435 0.2855 0.5381 0.124 Uiso 0.471(5) 1 calc PR A 2`
`H19B H 0.5095 0.2057 0.5703 0.124 Uiso 0.471(5) 1 calc PR A 2`
`H19C H 0.3704 0.2559 0.5460 0.124 Uiso 0.471(5) 1 calc PR A 2`
`H1 H 0.5612(16) 0.1035(8) 0.3222(6) 0.035(4) Uiso 1 1 d . . .`
`H8A H 0.3197(19) 0.1246(9) 0.2928(6) 0.046(4) Uiso 1 1 d . . .`
`H6B H 0.7333(18) 0.0459(9) 0.4116(7) 0.049(4) Uiso 1 1 d . . .`
`H8B H 0.1844(18) 0.0905(9) 0.3330(6) 0.042(4) Uiso 1 1 d . . .`
`H9A H 0.0695(19) 0.1794(9) 0.2724(7) 0.050(4) Uiso 1 1 d . . .`
`H2A H 0.406(2) -0.0134(9) 0.3277(6) 0.046(4) Uiso 1 1 d . . .`
`H12A H 0.479(2) 0.2728(11) 0.3812(7) 0.056(5) Uiso 1 1 d . . .`
`H11A H 0.240(2) 0.3309(10) 0.3582(7) 0.055(5) Uiso 1 1 d . . .`
`H11B H 0.369(2) 0.3606(12) 0.3175(7) 0.060(5) Uiso 1 1 d . . .`
`H2B H 0.5198(18) -0.0454(9) 0.3772(7) 0.048(4) Uiso 1 1 d . . .`
`H9B H 0.058(2) 0.2154(10) 0.3295(7) 0.053(4) Uiso 1 1 d . . .`
`H13 H 0.5021(19) 0.0457(9) 0.4520(5) 0.042(4) Uiso 1 1 d . . .`
`H6A H 0.7534(19) 0.1283(11) 0.3843(7) 0.049(4) Uiso 1 1 d . . .`
`H5B H 0.846(3) 0.0736(13) 0.3020(9) 0.079(6) Uiso 1 1 d . . .`
`H3A H 0.602(2) -0.1097(13) 0.2993(8) 0.072(6) Uiso 1 1 d . . .`
`H12B H 0.508(2) 0.2387(9) 0.3232(6) 0.045(4) Uiso 1 1 d . . .`
`H10B H 0.141(2) 0.3194(11) 0.2713(7) 0.062(5) Uiso 1 1 d . . .`
`H3B H 0.623(3) -0.0207(11) 0.2679(9) 0.076(6) Uiso 1 1 d . . .`
`H7 H 0.2733(17) 0.1880(8) 0.3962(6) 0.036(4) Uiso 1 1 d . . .`
`H17C H 0.093(3) -0.0858(12) 0.4356(10) 0.084(7) Uiso 1 1 d . . .`
`H17A H 0.092(2) -0.0704(12) 0.4971(9) 0.075(6) Uiso 1 1 d . . .`
`H5A H 0.944(3) 0.0403(12) 0.3503(8) 0.080(6) Uiso 1 1 d . . .`
`H10A H 0.288(2) 0.2658(11) 0.2529(8) 0.069(5) Uiso 1 1 d . . .`
`H17B H 0.191(3) -0.1440(17) 0.4772(11) 0.103(9) Uiso 1 1 d . . .`

`loop_`
`_atom_site_aniso_label`
`_atom_site_aniso_U_11`
`_atom_site_aniso_U_22`
`_atom_site_aniso_U_33`
`_atom_site_aniso_U_23`
`_atom_site_aniso_U_13`
`_atom_site_aniso_U_12`
`N1 0.0415(6) 0.0347(6) 0.0327(5) 0.0024(4) 0.0030(4) 0.0080(5)`
`C7 0.0357(7) 0.0334(7) 0.0349(6) 0.0006(5) 0.0007(5) 0.0034(5)`
`C1 0.0299(7) 0.0350(7) 0.0328(6) -0.0001(5) 0.0011(5) -0.0010(5)`
`C8 0.0396(7) 0.0418(8) 0.0347(6) 0.0040(6) -0.0009(6) -0.0007(6)`
`C2 0.0331(7) 0.0406(8) 0.0558(8) -0.0112(7) 0.0014(6) -0.0005(6)`
`C13 0.0395(8) 0.0548(9) 0.0289(6) 0.0042(5) -0.0014(5) 0.0135(7)`
`C6 0.0346(8) 0.0563(10) 0.0499(8) -0.0095(7) -0.0025(6) -0.0077(7)`
`C12 0.0443(9) 0.0343(8) 0.0627(10) 0.0048(7) -0.0042(7) -0.0019(6)`
`C9 0.0420(8) 0.0598(10) 0.0419(7) 0.0081(7) -0.0046(7) 0.0029(7)`
`C5 0.0277(8) 0.0895(14) 0.0615(10) -0.0078(9) 0.0031(7) -0.0013(8)`
`C14 0.0412(9) 0.0913(13) 0.0388(7) 0.0301(8) 0.0026(6) 0.0042(8)`
`C10 0.0558(10) 0.0575(10) 0.0609(10) 0.0254(8) -0.0017(8) 0.0123(9)`
`C11 0.0547(10) 0.0368(8) 0.0832(12) 0.0174(8) 0.0008(9) 0.0030(8)`
`C3 0.0482(10) 0.0655(12) 0.0820(13) -0.0369(10) 0.0071(9) 0.0029(9)`
`C4 0.0438(10) 0.0825(13) 0.0891(14) -0.0283(11) 0.0081(9) 0.0182(9)`
`O2 0.0491(7) 0.0684(8) 0.0553(6) 0.0126(5) 0.0045(5) -0.0036(6)`
`O1 0.0389(7) 0.1400(14) 0.1026(11) 0.0792(10) 0.0008(7) 0.0020(8)`
`C17 0.0646(13) 0.0999(18) 0.0692(13) 0.0092(12) 0.0062(11) -0.0236(13)`

O4 0.0656(19) 0.0435(17) 0.0318(12) -0.0042(13) 0.0076(11)
 0.0031(13);
 C18 0.104(3) 0.054(2) 0.0328(14) -0.0104(13) 0.0054(16) 0.0114(18)
 C15 0.037(3) 0.038(4) 0.0313(19) 0.004(2) 0.0003(15) 0.001(2)
 O3 0.088(2) 0.055(3) 0.051(2) -0.0077(16) 0.0049(16) -0.027(2)
 O6 0.071(4) 0.043(4) 0.048(3) -0.0067(19) -0.017(2) -0.008(3)
 C16 0.052(3) 0.041(3) 0.034(2) -0.001(2) -0.0083(19) 0.006(2)
 O5 0.112(4) 0.068(3) 0.0403(15) -0.0074(19) 0.0227(18) -0.001(2)
 C19 0.138(5) 0.050(2) 0.059(3) -0.0143(18) -0.040(3) 0.005(2)

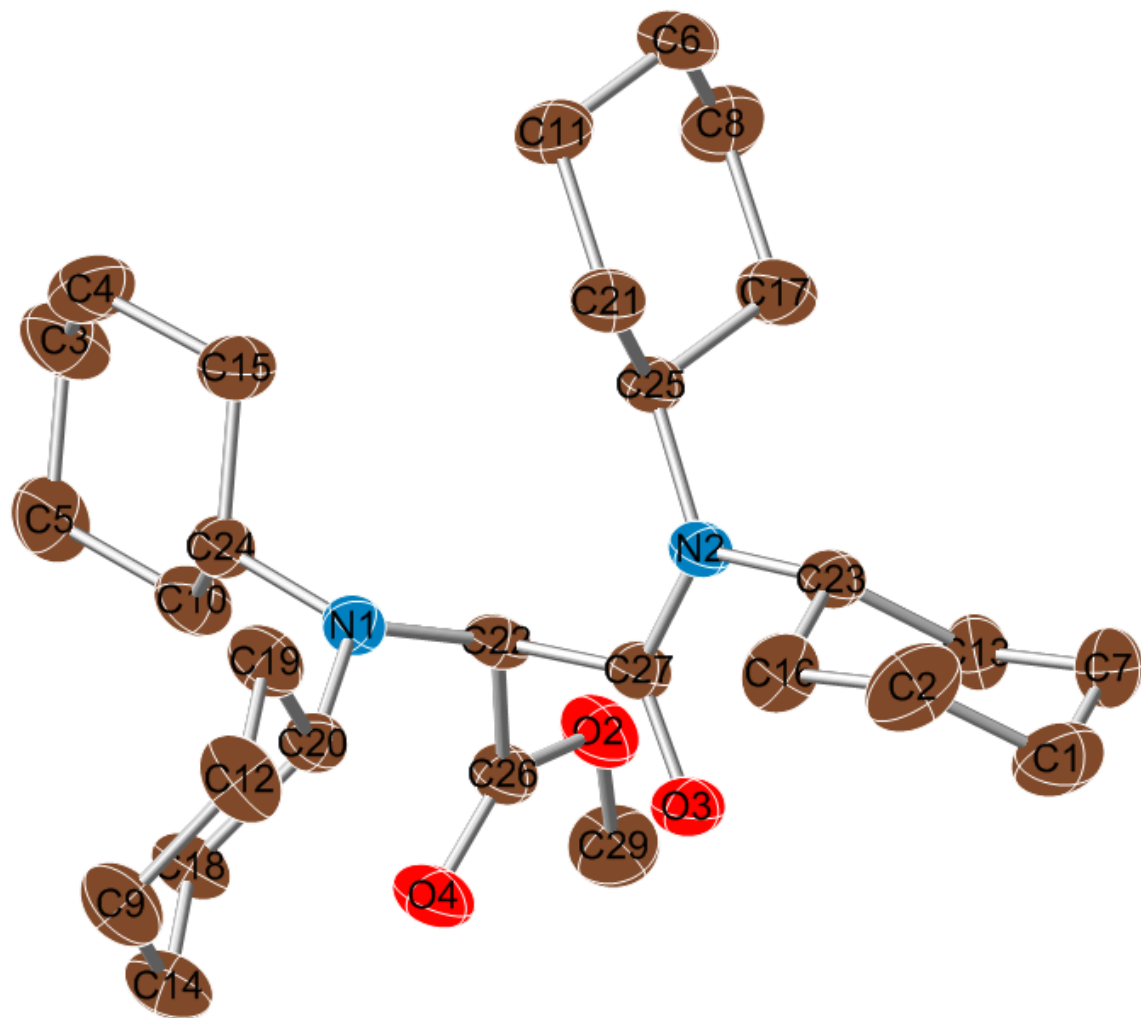
;
 All esds (except the esd in the dihedral angle between two l.s. planes)
 are estimated using the full covariance matrix. The cell esds are taken
 into account individually in the estimation of esds in distances, angles
 and torsion angles; correlations between esds in cell parameters are
 only
 used when they are defined by crystal symmetry. An approximate
 (isotropic)
 treatment of cell esds is used for estimating esds involving l.s. planes.
 ;

_geom_special_details
 loop_
_geom_bond_atom_site_label_1 C18 H18A 0.9600 . ?
_geom_bond_atom_site_label_2 C18 H18B 0.9600 . ?
_geom_bond_distance C18 H18C 0.9600 . ?
_geom_bond_site_symmetry_2 C15 O3 1.171(7) . ?
_geom_bond_publ_flag O6 C16 1.325(6) . ?
 N1 C13 1.4209(17) . ?
 N1 C1 1.4548(16) . ?
 N1 C7 1.4624(16) . ?
 C7 C8 1.5230(19) . ?
 C7 C12 1.529(2) . ?
 C7 H7 0.948(14) . ?
 C1 C2 1.5194(19) . ?
 C1 C6 1.5230(19) . ?
 C1 H1 0.979(15) . ?
 C8 C9 1.518(2) . ?
 C8 H8A 0.985(16) . ?
 C8 H8B 1.025(16) . ?
 C2 C3 1.527(2) . ?
 C2 H2A 1.006(17) . ?
 C2 H2B 1.000(17) . ?
 C13 C16 1.449(5) . ?
 C13 C14 1.512(2) . ?
 C13 C15 1.661(5) . ?
 C13 H13 0.945(16) . ?
 C6 C5 1.522(2) . ?
 C6 H6B 0.978(16) . ?
 C6 H6A 0.919(18) . ?
 C12 C11 1.525(2) . ?
 C12 H12A 0.940(18) . ?
 C12 H12B 1.001(17) . ?
 C9 C10 1.512(2) . ?
 C9 H9A 0.960(17) . ?
 C9 H9B 0.972(17) . ?
 C5 C4 1.500(3) . ?
 C5 H5B 1.06(2) . ?
 C5 H5A 0.92(2) . ?
 C14 O1 1.197(2) . ?
 C14 O2 1.336(2) . ?
 C10 C11 1.508(3) . ?
 C10 H10B 0.956(19) . ?
 C10 H10A 1.00(2) . ?
 C11 H11A 0.987(19) . ?
 C11 H11B 0.96(2) . ?
 C3 C4 1.502(3) . ?
 C3 H3A 0.99(2) . ?
 C3 H3B 1.02(2) . ?
 C4 H4A 0.9700 . ?
 C4 H4B 0.9700 . ?
 O2 C17 1.444(2) . ?
 C17 H17C 0.97(2) . ?
 C17 H17A 0.93(2) . ?
 C17 H17B 0.96(3) . ?
 O4 C15 1.334(6) . ?
 O4 C18 1.433(4) . ?

C15 C13 H13 104.5(9) . ?
 C5 C6 C1 111.29(13) . ?
 C5 C6 H6B 109.9(9) . ?
 C1 C6 H6B 108.7(9) . ?
 C5 C6 H6A 112.1(11) . ?
 C1 C6 H6A 107.2(10) . ?
 H6B C6 H6A 107.5(14) . ?
 C11 C12 C7 111.22(13) . ?
 C11 C12 H12A 110.2(11) . ?
 C7 C12 H12A 108.0(11) . ?
 C11 C12 H12B 110.3(9) . ?
 C7 C12 H12B 109.6(9) . ?
 H12A C12 H12B 107.4(14) . ?
 C10 C9 C8 111.11(13) . ?
 C10 C9 H9A 112.9(9) . ?
 C8 C9 H9A 109.0(9) . ?
 C10 C9 H9B 110.1(10) . ?
 C8 C9 H9B 108.0(10) . ?
 H9A C9 H9B 105.4(14) . ?
 C4 C5 C6 110.98(15) . ?
 C4 C5 H5B 111.4(11) . ?
 C6 C5 H5B 108.6(12) . ?
 C4 C5 H5A 112.4(13) . ?
 C6 C5 H5A 109.9(13) . ?
 H5B C5 H5A 103.2(17) . ?
 O1 C14 O2 123.85(17) . ?
 O1 C14 C13 124.44(17) . ?
 O2 C14 C13 111.71(13) . ?
 C9 C10 C11 110.47(14) . ?
 C9 C10 H10B 110.6(11) . ?
 C11 C10 H10B 109.4(11) . ?
 C9 C10 H10A 108.7(11) . ?
 C11 C10 H10A 107.8(11) . ?
 H10B C10 H10A 109.7(15) . ?
 C10 C11 C12 111.98(14) . ?
 C10 C11 H11A 109.2(10) . ?
 C12 C11 H11A 109.2(10) . ?
 C10 C11 H11B 111.0(11) . ?
 C12 C11 H11B 108.3(11) . ?
 H11A C11 H11B 107.1(14) . ?
 C4 C3 C2 111.43(15) . ?
 C4 C3 H3A 107.7(12) . ?
 C2 C3 H3A 107.7(12) . ?
 C4 C3 H3B 109.7(13) . ?
 C2 C3 H3B 107.8(12) . ?
 H3A C3 H3B 112.6(17) . ?
 C5 C4 C3 111.22(16) . ?
 C5 C4 H4A 109.4 . ?
 C3 C4 H4A 109.4 . ?
 C5 C4 H4B 109.4 . ?
 C3 C4 H4B 109.4 . ?
 H4A C4 H4B 108.0 . ?
 C14 O2 C17 116.34(17) . ?
 O2 C17 H17C 107.3(13) . ?
 O2 C17 H17A 108.3(13) . ?

H17C C17 H17A 108.4(18) . . . ?	C8 C9 C10 C11 -56.47(19) . . . ?
O2 C17 H17B 104.9(16) . . . ?	C9 C10 C11 C12 55.9(2) . . . ?
H17C C17 H17B 116(2) . . . ?	C7 C12 C11 C10 -55.4(2) . . . ?
H17A C17 H17B 111(2) . . . ?	C1 C2 C3 C4 56.0(2) . . . ?
C15 O4 C18 114.8(3) . . . ?	C6 C5 C4 C3 56.1(2) . . . ?
O4 C18 H18A 109.5 . . . ?	C2 C3 C4 C5 -55.8(2) . . . ?
O4 C18 H18B 109.5 . . . ?	O1 C14 O2 C17 -0.5(3) . . . ?
H18A C18 H18B 109.5 . . . ?	C13 C14 O2 C17 179.40(15) . . . ?
O4 C18 H18C 109.5 . . . ?	C18 O4 C15 O3 1.5(7) . . . ?
H18A C18 H18C 109.5 . . . ?	C18 O4 C15 C13 179.8(3) . . . ?
H18B C18 H18C 109.5 . . . ?	N1 C13 C15 O3 -22.8(6) . . . ?
O3 C15 O4 126.0(5) . . . ?	C16 C13 C15 O3 179.1(10) . . . ?
O3 C15 C13 127.2(4) . . . ?	C14 C13 C15 O3 -150.6(5) . . . ?
O4 C15 C13 106.7(4) . . . ?	N1 C13 C15 O4 158.9(3) . . . ?
C16 O6 C19 111.9(5) . . . ?	C16 C13 C15 O4 0.8(5) . . . ?
O5 C16 O6 124.7(5) . . . ?	C14 C13 C15 O4 31.1(4) . . . ?
O5 C16 C13 126.0(5) . . . ?	C19 O6 C16 O5 -1.7(9) . . . ?
O6 C16 C13 109.1(5) . . . ?	C19 O6 C16 C13 -176.6(3) . . . ?
O6 C19 H19A 109.5 . . . ?	N1 C13 C16 O5 152.3(4) . . . ?
O6 C19 H19B 109.5 . . . ?	C14 C13 C16 O5 25.4(5) . . . ?
H19A C19 H19B 109.5 . . . ?	C15 C13 C16 O5 178.5(11) . . . ?
O6 C19 H19C 109.5 . . . ?	N1 C13 C16 O6 -32.9(5) . . . ?
H19A C19 H19C 109.5 . . . ?	C14 C13 C16 O6 -159.8(4) . . . ?
H19B C19 H19C 109.5 . . . ?	C15 C13 C16 O6 -6.7(5) . . . ?
loop_	_diffrn_measured_fraction_theta_max
_geom_torsion_atom_site_label_1	0.998
_geom_torsion_atom_site_label_2	_diffrn_reflns_theta_full 26.30
_geom_torsion_atom_site_label_3	_diffrn_measured_fraction_theta_full 1.000
_geom_torsion_atom_site_label_4	_refine_diff_density_max 0.367
_geom_torsion	_refine_diff_density_min -0.378
_geom_torsion_site_symmetry_1	_refine_diff_density_rms 0.061
_geom_torsion_site_symmetry_2	
_geom_torsion_site_symmetry_3	
_geom_torsion_site_symmetry_4	
_geom_torsion_publ_flag	
C13 N1 C7 C8 -106.15(14) . . . ?	
C1 N1 C7 C8 52.51(16) . . . ?	
C13 N1 C7 C12 128.17(14) . . . ?	
C1 N1 C7 C12 -73.17(15) . . . ?	
C13 N1 C1 C2 56.72(16) . . . ?	
C7 N1 C1 C2 -102.06(14) . . . ?	
C13 N1 C1 C6 -69.38(16) . . . ?	
C7 N1 C1 C6 131.84(13) . . . ?	
N1 C7 C8 C9 177.86(11) . . . ?	
C12 C7 C8 C9 -55.70(16) . . . ?	
N1 C1 C2 C3 176.97(13) . . . ?	
C6 C1 C2 C3 -55.71(17) . . . ?	
C1 N1 C13 C16 142.6(3) . . . ?	
C7 N1 C13 C16 -58.6(3) . . . ?	
C1 N1 C13 C14 -99.35(16) . . . ?	
C7 N1 C13 C14 59.40(17) . . . ?	
C1 N1 C13 C15 132.16(18) . . . ?	
C7 N1 C13 C15 -69.09(19) . . . ?	
N1 C1 C6 C5 -174.92(13) . . . ?	
C2 C1 C6 C5 56.34(18) . . . ?	
N1 C7 C12 C11 -177.53(13) . . . ?	
C8 C7 C12 C11 54.45(18) . . . ?	
C7 C8 C9 C10 57.19(17) . . . ?	
C1 C6 C5 C4 -56.8(2) . . . ?	
N1 C13 C14 O1 -56.3(2) . . . ?	
C16 C13 C14 O1 76.9(3) . . . ?	
C15 C13 C14 O1 65.2(3) . . . ?	
N1 C13 C14 O2 123.86(14) . . . ?	
C16 C13 C14 O2 -103.0(2) . . . ?	
C15 C13 C14 O2 -114.7(2) . . . ?	

APPENDIX 5
CRYSTAL STRUCTURE DATA FOR **87**



```

data_p21n (dicyclohexylamine_ester-amide)

_audit_creation_method      SHEXL-97
_chemical_name_systematic
;
?
_chemical_name_common      ?
_chemical_melting_point    ?
_chemical_formula_moiety   'C28 H48 N2 O3'
_chemical_formula_sum       'C28 H48 N2 O3'
_chemical_formula_weight    460.68

loop_
_atom_type_symbol
_atom_type_description
_atom_type_scat_dispersion_real
_atom_type_scat_dispersion_imag
_atom_type_scat_source
'C' 'C' 0.0033 0.0016
'International Tables Vol C Tables 4.2.6.8 and 6.1.1.4'
'H' 'H' 0.0000 0.0000
'International Tables Vol C Tables 4.2.6.8 and 6.1.1.4'
'N' 'N' 0.0061 0.0033
'International Tables Vol C Tables 4.2.6.8 and 6.1.1.4'
'O' 'O' 0.0106 0.0060
'International Tables Vol C Tables 4.2.6.8 and 6.1.1.4'

_symmetry_cell_setting     'monoclinic'
_symmetry_space_group_name_H-M  'P 21/n'
_symmetry_space_group_name_Hall '-P 2yn'

loop_
_symmetry_equiv_pos_as_xyz
'x, y, z'
'-x+1/2, y+1/2, -z+1/2'
'-x, -y, -z'
'x-1/2, -y-1/2, z-1/2'

_cell_length_a              9.5207(5)
_cell_length_b              17.1439(9)
_cell_length_c              16.6718(9)
_cell_angle_alpha            90.00
_cell_angle_beta             96.6190(10)
_cell_angle_gamma            90.00
_cell_volume                 2703.1(2)
_cell_formula_units_Z        4
_cell_measurement_temperature 193(2)
_cell_measurement_reflns_used 4902
_cell_measurement_theta_min   1.71
_cell_measurement_theta_max    28.34

_exptl_crystal_description   'block'
_exptl_crystal_colour        'colorless'
_exptl_crystal_size_max      0.270
_exptl_crystal_size_mid      0.266
_exptl_crystal_size_min      0.190

_exptl_crystal_density_meas   'nm'
_exptl_crystal_density_diffrn 1.132
_exptl_crystal_density_method  'not measured'
_exptl_crystal_F_000          1016
_exptl_absorpt_coefficient_mu 0.072
_exptl_absorpt_correction_type 'numerical'
_exptl_absorpt_correction_T_min 0.9809
_exptl_absorpt_correction_T_max 0.9874
_exptl_absorpt_process_details 'SHELXPREP'

_exptl_special_details
;
?

_diffrn_ambient_temperature   193(2)
_diffrn_radiation_wavelength  0.71073
_diffrn_radiation_type        MoK\alpha
_diffrn_radiation_source      'fine-focus sealed tube'
_diffrn_radiation_monochromator graphite
_diffrn_measurement_device_type 'BRUKER APEX'
_diffrn_measurement_method    '0.3 wide /w exposures'
_diffrn_detector_area_resol_mean ?
_diffrn_stands_number         'na'
_diffrn_stands_interval_count 'na'
_diffrn_stands_interval_time  'na'
_diffrn_stands_decay_%        0
_diffrn_reflns_number         27406
_diffrn_reflns_av_R_equivalents 0.0434
_diffrn_reflns_av_sigmaI/netI 0.0534
_diffrn_reflns_limit_h_min    -12
_diffrn_reflns_limit_h_max    12
_diffrn_reflns_limit_k_min    -22
_diffrn_reflns_limit_k_max    22
_diffrn_reflns_limit_l_min    -22
_diffrn_reflns_limit_l_max    22
_diffrn_reflns_theta_min      1.71
_diffrn_reflns_theta_max      28.34
_reflns_number_total          6735
_reflns_number_gt              4902
_reflns_threshold_expression  >2sigma(I)

_computing_data_collection    'SMART'
_computing_cell_refinement    'SMART, SAINT'
_computing_data_reduction      'SAINT'
_computing_structure_solution  'SHELXS-97 (Sheldrick, 1990)'
_computing_structure_refinement 'SHELXL-97 (Sheldrick, 1997)'
_computing_molecular_graphics   'SHELXP-97 (Sheldrick, 1990)'
_computing_publication_material 'SHELXS-97 (Sheldrick, 2000)'

_refine_special_details
;
Refinement of F^2 against ALL reflections. The weighted R-factor wR
and
goodness of fit S are based on F^2, conventional R-factors R are
based
on F, with F set to zero for negative F^2. The threshold expression of

```

$F^2 > 2\sigma(F^2)$ is used only for calculating R-factors(gt) etc. and is not relevant to the choice of reflections for refinement. R-factors based on F^2 are statistically about twice as large as those based on F, and R-factors based on ALL data will be even larger.
;
`_refine_ls_structure_factor_coef Fsqd`
`_refine_ls_matrix_type full`
`_refine_ls_weighting_scheme calc`
`_refine_ls_weighting_details`
`'calc w=1/[s^2^(Fo^2)+(0.0653P)^2+0.6424P]` where $P=(Fo^2+2Fc^2)/3'$
`_atom_sites_solution_primary direct`
`_atom_sites_solution_secondary difmap`
`_atom_sites_solution_hydrogens geom`
`_refine_ls_hydrogen_treatment constr`
`_refine_ls_extinction_method none`
`_refine_ls_extinction_coeff 0`
`_refine_ls_number_reflns 6735`
`_refine_ls_number_parameters 298`
`_refine_ls_number_restraints 0`
`_refine_ls_R_factor_all 0.0872`
`_refine_ls_R_factor_gt 0.0624`
`_refine_ls_wR_factor_ref 0.1554`
`_refine_ls_wR_factor_gt 0.1445`
`_refine_ls_goodness_of_fit_ref 1.046`
`_refine_ls_restrained_S_all 1.046`
`_refine_ls_shift/su_max 0.000`
`_refine_ls_shift/su_mean 0.000`

`loop_`
`_atom_site_label`
`_atom_site_type_symbol`
`_atom_site_fract_x`
`_atom_site_fract_y`
`_atom_site_fract_z`
`_atom_site_U_iso_or_equiv`
`_atom_site_adp_type`
`_atom_site_occupancy`
`_atom_site_symmetry_multiplicity`
`_atom_site_calc_flag`
`_atom_site_refinement_flags`
`_atom_site_disorder_assembly`
`_atom_site_disorder_group`
C27 C 0.23815(17) -0.01483(9) 0.24378(9) 0.0317(3) Uani 1 1 d ...
C26 C 0.17726(17) -0.12436(9) 0.15195(10) 0.0338(3) Uani 1 1 d ...
C25 C 0.12219(16) 0.11447(9) 0.22369(9) 0.0325(3) Uani 1 1 d ...
H25A H 0.0474 0.0810 0.1939 0.039 Uiso 1 1 calc R ...
C24 C -0.14382(17) -0.07657(9) 0.18361(9) 0.0340(4) Uani 1 1 d ...
H24A H -0.2074 -0.1010 0.2202 0.041 Uiso 1 1 calc R ...
C23 C 0.34976(17) 0.09706(9) 0.31587(9) 0.0331(3) Uani 1 1 d ...
H23A H 0.3298 0.1543 0.3167 0.040 Uiso 1 1 calc R ...
C22 C 0.11406(17) -0.05259(8) 0.18919(9) 0.0302(3) Uani 1 1 d ...
H22A H 0.0844 -0.0152 0.1444 0.036 Uiso 1 1 calc R ...

C21 C 0.05098(19) 0.16217(10) 0.28450(11) 0.0418(4) Uani 1 1 d ...
H21A H 0.1220 0.1955 0.3162 0.050 Uiso 1 1 calc R ...
H21B H 0.0095 0.1268 0.3223 0.050 Uiso 1 1 calc R ...
C20 C 0.01469(17) -0.10444(9) 0.31173(9) 0.0311(3) Uani 1 1 d ...
H20A H 0.1183 -0.1021 0.3304 0.037 Uiso 1 1 calc R ...
C19 C -0.0593(2) -0.05872(10) 0.37266(10) 0.0404(4) Uani 1 1 d ...
H19A H -0.1627 -0.0601 0.3566 0.049 Uiso 1 1 calc R ...
H19B H -0.0284 -0.0036 0.3726 0.049 Uiso 1 1 calc R ...
C18 C -0.0280(2) -0.19041(9) 0.31373(10) 0.0399(4) Uani 1 1 d ...
H18A H -0.1307 -0.1955 0.2967 0.048 Uiso 1 1 calc R ...
H18B H 0.0229 -0.2204 0.2754 0.048 Uiso 1 1 calc R ...
C17 C 0.1797(2) 0.16712(11) 0.16135(11) 0.0462(4) Uani 1 1 d ...
H17A H 0.2211 0.1346 0.1210 0.055 Uiso 1 1 calc R ...
H17B H 0.2556 0.2006 0.1884 0.055 Uiso 1 1 calc R ...
C16 C 0.3501(2) 0.06879(12) 0.40231(10) 0.0449(4) Uani 1 1 d ...
H16A H 0.2556 0.0775 0.4201 0.054 Uiso 1 1 calc R ...
H16B H 0.3699 0.0121 0.4049 0.054 Uiso 1 1 calc R ...
C15 C -0.21139(19) 0.00145(10) 0.15708(11) 0.0439(4) Uani 1 1 d ...
H15A H -0.2157 0.0352 0.2049 0.053 Uiso 1 1 calc R ...
H15B H -0.1525 0.0281 0.1202 0.053 Uiso 1 1 calc R ...
C14 C 0.0069(2) -0.22375(11) 0.39876(11) 0.0490(5) Uani 1 1 d ...
H14A H -0.0238 -0.2789 0.3992 0.059 Uiso 1 1 calc R ...
H14B H 0.1105 -0.2223 0.4139 0.059 Uiso 1 1 calc R ...
C13 C 0.49511(18) 0.08863(11) 0.28715(11) 0.0422(4) Uani 1 1 d ...
H13A H 0.4933 0.1105 0.2321 0.051 Uiso 1 1 calc R ...
H13B H 0.5202 0.0327 0.2849 0.051 Uiso 1 1 calc R ...
C12 C -0.0268(2) -0.09212(11) 0.45747(10) 0.0485(5) Uani 1 1 d ...
H12A H 0.0752 -0.0856 0.4758 0.058 Uiso 1 1 calc R ...
H12B H -0.0805 -0.0628 0.4950 0.058 Uiso 1 1 calc R ...
C11 C -0.0654(2) 0.21344(11) 0.24059(14) 0.0512(5) Uani 1 1 d ...
H11A H -0.1405 0.1797 0.2132 0.061 Uiso 1 1 calc R ...
H11B H -0.1080 0.2458 0.2806 0.061 Uiso 1 1 calc R ...
C10 C -0.1431(2) -0.13151(10) 0.11177(11) 0.0433(4) Uani 1 1 d ...
H10A H -0.0800 -0.1102 0.0739 0.052 Uiso 1 1 calc R ...
H10B H -0.1054 -0.1829 0.1309 0.052 Uiso 1 1 calc R ...
C9 C -0.0652(2) -0.17814(11) 0.46010(11) 0.0502(5) Uani 1 1 d ...
H9A H -0.0358 -0.1990 0.5148 0.060 Uiso 1 1 calc R ...
H9B H -0.1689 -0.1842 0.4485 0.060 Uiso 1 1 calc R ...
C8 C 0.0627(2) 0.21844(13) 0.11869(14) 0.0623(6) Uani 1 1 d ...
H8A H 0.1036 0.2540 0.0807 0.075 Uiso 1 1 calc R ...
H8B H -0.0084 0.1851 0.0871 0.075 Uiso 1 1 calc R ...
C7 C 0.6060(2) 0.13145(12) 0.34461(14) 0.0562(5) Uani 1 1 d ...
H7A H 0.7007 0.1226 0.3272 0.067 Uiso 1 1 calc R ...
H7B H 0.5866 0.1882 0.3417 0.067 Uiso 1 1 calc R ...
C6 C -0.0086(2) 0.26598(11) 0.17894(15) 0.0597(6) Uani 1 1 d ...
H6A H 0.0602 0.3031 0.2068 0.072 Uiso 1 1 calc R ...
H6B H -0.0872 0.2964 0.1501 0.072 Uiso 1 1 calc R ...
C5 C -0.2910(2) -0.14190(11) 0.06777(12) 0.0538(5) Uani 1 1 d ...
H5A H -0.2860 -0.1748 0.0194 0.065 Uiso 1 1 calc R ...
H5B H -0.3510 -0.1692 0.1036 0.065 Uiso 1 1 calc R ...
C4 C -0.3601(2) -0.01060(12) 0.11431(13) 0.0560(5) Uani 1 1 d ...
H4A H -0.4209 -0.0335 0.1525 0.067 Uiso 1 1 calc R ...
H4B H -0.4008 0.0404 0.0961 0.067 Uiso 1 1 calc R ...
C3 C -0.3579(2) -0.06405(12) 0.04233(13) 0.0593(6) Uani 1 1 d ...
H3A H -0.3037 -0.0392 0.0020 0.071 Uiso 1 1 calc R ...
H3B H -0.4558 -0.0726 0.0167 0.071 Uiso 1 1 calc R ...
C2 C 0.4610(2) 0.11174(14) 0.45844(12) 0.0594(6) Uani 1 1 d ...

H2A H 0.4352 0.1676 0.4604 0.071 Uiso 1 1 calc R . .
 H2B H 0.4632 0.0902 0.5137 0.071 Uiso 1 1 calc R . .
 C1 C 0.6063(2) 0.10428(13) 0.43067(14) 0.0600(6) Uani 1 1 d . .
 H1A H 0.6747 0.1358 0.4663 0.072 Uiso 1 1 calc R . .
 H1B H 0.6370 0.0491 0.4349 0.072 Uiso 1 1 calc R . .
 C29 C 0.2946(2) -0.16600(12) 0.04353(14) 0.0583(6) Uani 1 1 d . .
 H29A H 0.3330 -0.1456 -0.0043 0.087 Uiso 1 1 calc R . .
 H29B H 0.2217 -0.2050 0.0270 0.087 Uiso 1 1 calc R . .
 H29C H 0.3707 -0.1902 0.0797 0.087 Uiso 1 1 calc R . .
 O3 O 0.33614(13) -0.05739(6) 0.27092(8) 0.0441(3) Uani 1 1 d . .
 O2 O 0.23333(14) -0.10306(7) 0.08509(8) 0.0448(3) Uani 1 1 d . .
 O4 O 0.17538(14) -0.19026(6) 0.17519(8) 0.0447(3) Uani 1 1 d . .
 N2 N 0.23304(14) 0.06176(7) 0.26106(8) 0.0307(3) Uani 1 1 d . .
 N1 N -0.00613(13) -0.06587(7) 0.23234(7) 0.0301(3) Uani 1 1 d . .

 loop_
 _atom_site_aniso_label
 _atom_site_aniso_U_11
 _atom_site_aniso_U_22
 _atom_site_aniso_U_33
 _atom_site_aniso_U_23
 _atom_site_aniso_U_13
 _atom_site_aniso_U_12
 C27 0.0343(8) 0.0258(7) 0.0351(8) 0.0013(6) 0.0049(6) 0.0005(6)
 C26 0.0371(9) 0.0265(8) 0.0376(8) -0.0029(6) 0.0030(7) -0.0010(6)
 C25 0.0326(8) 0.0242(7) 0.0391(8) -0.0012(6) -0.0021(7) 0.0008(6)
 C24 0.0361(8) 0.0307(8) 0.0334(8) 0.0016(6) -0.0042(7) -0.0019(6)
 C23 0.0348(8) 0.0257(7) 0.0376(8) -0.0031(6) -0.0007(7) -0.0004(6)
 C22 0.0372(8) 0.0212(7) 0.0318(8) 0.0005(6) 0.0019(6) 0.0012(6)
 C21 0.0429(10) 0.0326(8) 0.0502(10) -0.0013(7) 0.0075(8) 0.0068(7)
 C20 0.0343(8) 0.0297(8) 0.0283(7) 0.0017(6) -0.0006(6) -0.0002(6)
 C19 0.0527(11) 0.0317(8) 0.0377(9) -0.0029(7) 0.0087(8) -0.0025(7)
 C18 0.0562(11) 0.0277(8) 0.0362(9) 0.0019(7) 0.0066(8) -0.0009(7)
 C17 0.0470(10) 0.0463(10) 0.0454(10) 0.0128(8) 0.0053(8) 0.0060(8)
 C16 0.0441(10) 0.0543(11) 0.0359(9) -0.0021(8) 0.0024(8) 0.0017(8)
 C15 0.0429(10) 0.0368(9) 0.0490(10) -0.0017(8) -0.0079(8) 0.0049(7)
 C14 0.0669(13) 0.0367(9) 0.0439(10) 0.0108(8) 0.0089(9) 0.0035(9)
 C13 0.0377(9) 0.0396(9) 0.0497(10) 0.0002(8) 0.0072(8) -0.0067(7)
 C12 0.0674(13) 0.0456(10) 0.0341(9) -0.0028(8) 0.0122(9) -0.0100(9)

 loop_
 _geom_bond_atom_site_label_1 C24 C15 1.527(2) . ?
 _geom_bond_atom_site_label_2 C24 H24A 1.0000 . ?
 _geom_bond_distance C23 N2 1.4840(19) . ?
 _geom_bond_site_symmetry_2 C23 C16 1.520(2) . ?
 _geom_bond_publ_flag C23 C13 1.522(2) . ?
 C27 O3 1.2289(19) . ? C23 H23A 1.0000 . ?
 C27 N2 1.3463(19) . ? C22 N1 1.438(2) . ?
 C27 C22 1.548(2) . ? C22 H22A 1.0000 . ?
 C26 O4 1.1951(19) . ? C21 C11 1.533(2) . ?
 C26 O2 1.341(2) . ? C21 H21A 0.9900 . ?
 C26 C22 1.532(2) . ? C21 H21B 0.9900 . ?
 C25 N2 1.4721(19) . ? C20 N1 1.4724(19) . ?
 C25 C21 1.521(2) . ? C20 C19 1.519(2) . ?
 C25 C17 1.525(2) . ? C20 C18 1.530(2) . ?
 C25 H25A 1.0000 . ? C20 H20A 1.0000 . ?
 C24 N1 1.4720(19) . ? C19 C12 1.524(2) . ?
 C24 C10 1.524(2) . ? C19 H19A 0.9900 . ?

 C11 0.0417(10) 0.0345(9) 0.0768(14) -0.0045(9) 0.0045(9) 0.0102(8)
 C10 0.0537(11) 0.0307(8) 0.0420(9) -0.0032(7) -0.0091(8) -0.0030(7)
 C9 0.0684(13) 0.0461(10) 0.0376(10) 0.0077(8) 0.0124(9) -0.0078(9)
 C8 0.0577(13) 0.0621(13) 0.0650(14) 0.0307(11) -0.0018(11)
 0.0081(10)
 C7 0.0385(10) 0.0457(11) 0.0817(15) 0.0004(10) -0.0050(10) -0.0088(8)
 C6 0.0504(12) 0.0318(9) 0.0926(17) 0.0132(10) -0.0094(11) 0.0065(8)
 C5 0.0629(13) 0.0454(11) 0.0474(11) 0.0005(8) -0.0181(9) -0.0137(9)
 C4 0.0458(11) 0.0532(12) 0.0633(13) 0.0073(10) -0.0174(9) 0.0061(9)
 C3 0.0579(12) 0.0582(13) 0.0542(12) 0.0123(10) -0.0252(10) -0.0102(10)
 C2 0.0647(14) 0.0654(13) 0.0434(11) -0.0100(10) -0.0134(10)
 0.0090(11)
 C1 0.0491(12) 0.0557(12) 0.0688(14) -0.0069(10) -0.0203(10)
 0.0019(10)
 C29 0.0649(13) 0.0472(11) 0.0684(14) -0.0135(10) 0.0322(11)
 0.0023(10)
 O3 0.0395(7) 0.0273(6) 0.0628(8) -0.0005(5) -0.0061(6) 0.0043(5)
 O2 0.0559(8) 0.0319(6) 0.0500(7) -0.0031(5) 0.0210(6) 0.0000(5)
 O4 0.0571(8) 0.0246(6) 0.0539(8) 0.0005(5) 0.0129(6) 0.0048(5)
 N2 0.0330(7) 0.0225(6) 0.0357(7) -0.0025(5) -0.0003(5) -0.0004(5)
 N1 0.0324(7) 0.0287(6) 0.0283(6) 0.0013(5) -0.0010(5) -0.0011(5)

 _geom_special_details
;
 All esds (except the esd in the dihedral angle between two l.s. planes) are estimated using the full covariance matrix. The cell esds are taken into account individually in the estimation of esds in distances, angles and torsion angles; correlations between esds in cell parameters are only used when they are defined by crystal symmetry. An approximate (isotropic) treatment of cell esds is used for estimating esds involving l.s. planes.
;

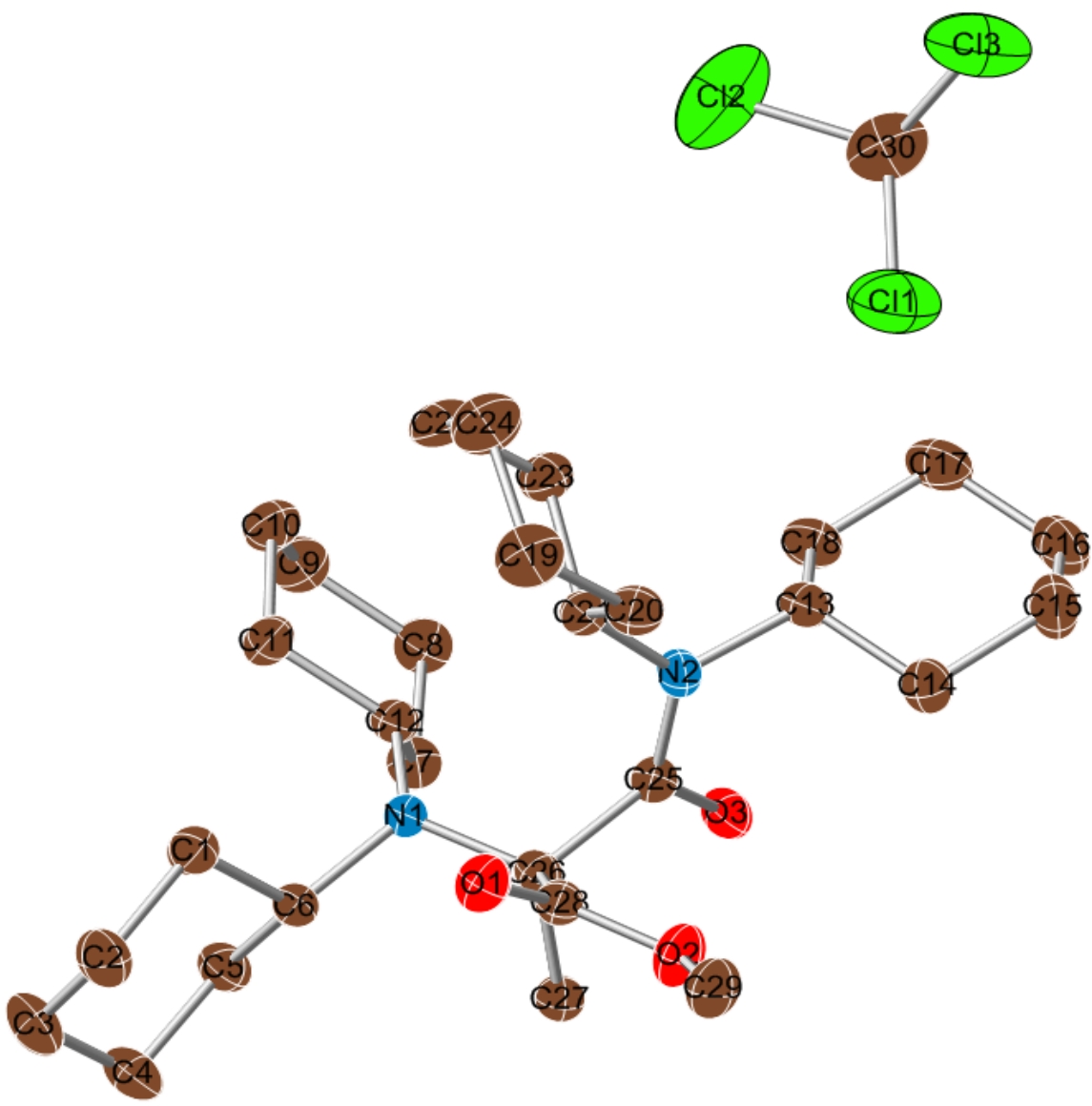
C12 C9 1.521(3) . ?	N1 C24 C10 115.23(14) . . ?	C4 C15 H15B 109.5 . . ?
C12 H12A 0.9900 . ?	N1 C24 C15 111.67(13) . . ?	C24 C15 H15B 109.5 . . ?
C12 H12B 0.9900 . ?	C10 C24 C15 110.71(13) . . ?	H15A C15 H15B 108.1 . . ?
C11 C6 1.513(3) . ?	N1 C24 H24A 106.2 . . ?	C9 C14 C18 111.49(15) . . ?
C11 H11A 0.9900 . ?	C10 C24 H24A 106.2 . . ?	C9 C14 H14A 109.3 . . ?
C11 H11B 0.9900 . ?	C15 C24 H24A 106.2 . . ?	C18 C14 H14A 109.3 . . ?
C10 C5 1.522(3) . ?	N2 C23 C16 111.91(13) . . ?	C9 C14 H14B 109.3 . . ?
C10 H10A 0.9900 . ?	N2 C23 C13 114.26(13) . . ?	C18 C14 H14B 109.3 . . ?
C10 H10B 0.9900 . ?	C16 C23 C13 111.43(14) . . ?	H14A C14 H14B 108.0 . . ?
C9 H9A 0.9900 . ?	N2 C23 H23A 106.2 . . ?	C23 C13 C7 110.15(16) . . ?
C9 H9B 0.9900 . ?	C16 C23 H23A 106.2 . . ?	C23 C13 H13A 109.6 . . ?
C8 C6 1.514(3) . ?	C13 C23 H23A 106.2 . . ?	C7 C13 H13A 109.6 . . ?
C8 H8A 0.9900 . ?	N1 C22 C26 116.61(12) . . ?	C23 C13 H13B 109.6 . . ?
C8 H8B 0.9900 . ?	N1 C22 C27 111.68(12) . . ?	C7 C13 H13B 109.6 . . ?
C7 C1 1.508(3) . ?	C26 C22 C27 105.39(12) . . ?	H13A C13 H13B 108.1 . . ?
C7 H7A 0.9900 . ?	N1 C22 H22A 107.6 . . ?	C9 C12 C19 111.55(15) . . ?
C7 H7B 0.9900 . ?	C26 C22 H22A 107.6 . . ?	C9 C12 H12A 109.3 . . ?
C6 H6A 0.9900 . ?	C27 C22 H22A 107.6 . . ?	C19 C12 H12A 109.3 . . ?
C6 H6B 0.9900 . ?	C25 C21 C11 110.06(15) . . ?	C9 C12 H12B 109.3 . . ?
C5 C3 1.518(3) . ?	C25 C21 H21A 109.6 . . ?	C19 C12 H12B 109.3 . . ?
C5 H5A 0.9900 . ?	C11 C21 H21A 109.6 . . ?	H12A C12 H12B 108.0 . . ?
C5 H5B 0.9900 . ?	C25 C21 H21B 109.6 . . ?	C6 C11 C21 111.76(16) . . ?
C4 C3 1.512(3) . ?	C11 C21 H21B 109.6 . . ?	C6 C11 H11A 109.3 . . ?
C4 H4A 0.9900 . ?	H21A C21 H21B 108.2 . . ?	C21 C11 H11A 109.3 . . ?
C4 H4B 0.9900 . ?	N1 C20 C19 110.15(13) . . ?	C6 C11 H11B 109.3 . . ?
C3 H3A 0.9900 . ?	N1 C20 C18 116.33(12) . . ?	C21 C11 H11B 109.3 . . ?
C3 H3B 0.9900 . ?	C19 C20 C18 109.72(13) . . ?	H11A C11 H11B 107.9 . . ?
C2 C1 1.514(3) . ?	N1 C20 H20A 106.7 . . ?	C5 C10 C24 111.30(16) . . ?
C2 H2A 0.9900 . ?	C19 C20 H20A 106.7 . . ?	C5 C10 H10A 109.4 . . ?
C2 H2B 0.9900 . ?	C18 C20 H20A 106.7 . . ?	C24 C10 H10A 109.4 . . ?
C1 H1A 0.9900 . ?	C20 C19 C12 111.48(15) . . ?	C5 C10 H10B 109.4 . . ?
C1 H1B 0.9900 . ?	C20 C19 H19A 109.3 . . ?	C24 C10 H10B 109.4 . . ?
C29 O2 1.441(2) . ?	C12 C19 H19A 109.3 . . ?	H10A C10 H10B 108.0 . . ?
C29 H29A 0.9800 . ?	C20 C19 H19B 109.3 . . ?	C14 C9 C12 110.62(15) . . ?
C29 H29B 0.9800 . ?	C12 C19 H19B 109.3 . . ?	C14 C9 H9A 109.5 . . ?
C29 H29C 0.9800 . ?	H19A C19 H19B 108.0 . . ?	C12 C9 H9A 109.5 . . ?
loop_	C14 C18 C20 110.50(14) . . ?	C14 C9 H9B 109.5 . . ?
_geom_angle_atom_site_label_1	C14 C18 H18A 109.5 . . ?	C12 C9 H9B 109.5 . . ?
_geom_angle_atom_site_label_2	C20 C18 H18A 109.5 . . ?	H9A C9 H9B 108.1 . . ?
_geom_angle_atom_site_label_3	C14 C18 H18B 109.5 . . ?	C6 C8 C17 111.07(18) . . ?
_geom_angle	C20 C18 H18B 109.5 . . ?	C6 C8 H8A 109.4 . . ?
_geom_angle_site_symmetry_1	H18A C18 H18B 108.1 . . ?	C17 C8 H8A 109.4 . . ?
_geom_angle_site_symmetry_3	C25 C17 C8 110.98(16) . . ?	C6 C8 H8B 109.4 . . ?
_geom_angle_publ_flag	C25 C17 H17A 109.4 . . ?	C17 C8 H8B 109.4 . . ?
O3 C27 N2 123.02(15) . . ?	C8 C17 H17A 109.4 . . ?	H8A C8 H8B 108.0 . . ?
O3 C27 C22 117.63(13) . . ?	C25 C17 H17B 109.4 . . ?	C1 C7 C13 111.89(16) . . ?
N2 C27 C22 119.33(13) . . ?	C8 C17 H17B 109.4 . . ?	C1 C7 H7A 109.2 . . ?
O4 C26 O2 123.32(15) . . ?	H17A C17 H17B 108.0 . . ?	C13 C7 H7A 109.2 . . ?
O4 C26 C22 127.33(15) . . ?	C2 C16 C23 110.78(16) . . ?	C1 C7 H7B 109.2 . . ?
O2 C26 C22 109.31(13) . . ?	C2 C16 H16A 109.5 . . ?	C13 C7 H7B 109.2 . . ?
N2 C25 C21 113.62(13) . . ?	C23 C16 H16A 109.5 . . ?	H7A C7 H7B 107.9 . . ?
N2 C25 C17 110.83(13) . . ?	C2 C16 H16B 109.5 . . ?	C11 C6 C8 110.67(16) . . ?
C21 C25 C17 111.01(14) . . ?	C23 C16 H16B 109.5 . . ?	C11 C6 H6A 109.5 . . ?
N2 C25 H25A 107.0 . . ?	H16A C16 H16B 108.1 . . ?	C8 C6 H6A 109.5 . . ?
C21 C25 H25A 107.0 . . ?	C4 C15 C24 110.75(15) . . ?	C11 C6 H6B 109.5 . . ?
C17 C25 H25A 107.0 . . ?	C4 C15 H15A 109.5 . . ?	C8 C6 H6B 109.5 . . ?
	C24 C15 H15A 109.5 . . ?	H6A C6 H6B 108.1 . . ?

C3 C5 C10 111.54(15) . . ?
 C3 C5 H5A 109.3 . . ?
 C10 C5 H5A 109.3 . . ?
 C3 C5 H5B 109.3 . . ?
 C10 C5 H5B 109.3 . . ?
 H5A C5 H5B 108.0 . . ?
 C3 C4 C15 110.89(17) . . ?
 C3 C4 H4A 109.5 . . ?
 C15 C4 H4A 109.5 . . ?
 C3 C4 H4B 109.5 . . ?
 C15 C4 H4B 109.5 . . ?
 H4A C4 H4B 108.0 . . ?
 C4 C3 C5 110.78(16) . . ?
 C4 C3 H3A 109.5 . . ?
 C5 C3 H3A 109.5 . . ?
 C4 C3 H3B 109.5 . . ?
 C5 C3 H3B 109.5 . . ?
 H3A C3 H3B 108.1 . . ?
 C1 C2 C16 111.45(17) . . ?
 C1 C2 H2A 109.3 . . ?
 C16 C2 H2A 109.3 . . ?
 C1 C2 H2B 109.3 . . ?
 C16 C2 H2B 109.3 . . ?
 H2A C2 H2B 108.0 . . ?
 C7 C1 C2 111.32(17) . . ?
 C7 C1 H1A 109.4 . . ?
 C2 C1 H1A 109.4 . . ?
 C7 C1 H1B 109.4 . . ?
 C2 C1 H1B 109.4 . . ?
 H1A C1 H1B 108.0 . . ?
 O2 C29 H29A 109.5 . . ?
 O2 C29 H29B 109.5 . . ?
 H29A C29 H29B 109.5 . . ?
 O2 C29 H29C 109.5 . . ?
 H29A C29 H29C 109.5 . . ?
 H29B C29 H29C 109.5 . . ?
 C26 O2 C29 114.68(14) . . ?
 C27 N2 C25 123.36(13) . . ?
 C27 N2 C23 119.12(13) . . ?
 C25 N2 C23 117.36(11) . . ?
 C22 N1 C24 116.93(12) . . ?
 C22 N1 C20 119.23(12) . . ?
 C24 N1 C20 117.34(12) . . ?

```

_diffrn_measured_fraction_theta_max
0.998
_diffrn_reflns_theta_full      28.34
_diffrn_measured_fraction_theta_full  0.998
_refine_diff_density_max  0.280
_refine_diff_density_min -0.192
_refine_diff_density_rms  0.042
  
```

APPENDIX 6
CRYSTAL STRUCTURE DATA FOR **105**·CHCl₃



```

data_final (dicyclohexylamine_ester-amide_methyl)

_audit_creation_method      SHELXL-97
_chemical_name_systematic
;
?
;
_chemical_name_common      ?
_chemical_melting_point    ?
_chemical_formula_moiety   ?
_chemical_formula_sum       'C30 H51 Cl3 N2 O3'
_chemical_formula_weight    594.08

loop_
_atom_type_symbol
_atom_type_description
_atom_type_scat_dispersion_real
_atom_type_scat_dispersion_imag
_atom_type_scat_source
'C' 'C' 0.0033 0.0016
'International Tables Vol C Tables 4.2.6.8 and 6.1.1.4'
'H' 'H' 0.0000 0.0000
'International Tables Vol C Tables 4.2.6.8 and 6.1.1.4'
'N' 'N' 0.0061 0.0033
'International Tables Vol C Tables 4.2.6.8 and 6.1.1.4'
'O' 'O' 0.0106 0.0060
'International Tables Vol C Tables 4.2.6.8 and 6.1.1.4'
'Cl' 'Cl' 0.1484 0.1585
'International Tables Vol C Tables 4.2.6.8 and 6.1.1.4'

_symmetry_cell_setting      ?
_symmetry_space_group_name_H-M ?

loop_
_symmetry_equiv_pos_as_xyz
'x, y, z'
'-x, y+1/2, -z'

_cell_length_a              10.2512(5)
_cell_length_b              10.1475(5)
_cell_length_c              15.4702(8)
_cell_angle_alpha            90.00
_cell_angle_beta             103.9230(10)
_cell_angle_gamma            90.00
_cell_volume                 1561.99(14)
_cell_formula_units_Z        2
_cell_measurement_temperature 193(2)
_cell_measurement_reflns_used 5685
_cell_measurement_theta_min   1.36
_cell_measurement_theta_max    28.28

_exptl_crystal_description   'rectangular prism'
_exptl_crystal_colour        'colorless'
_exptl_crystal_size_max      0.434
_exptl_crystal_size_mid      0.268
_exptl_crystal_size_min      0.184
_exptl_crystal_density_meas   'nm'
_exptl_crystal_density_diffrn 1.263
_exptl_crystal_density_method  'not measured'
_exptl_crystal_F_000          640
_exptl_absorpt_coefficient_mu 0.326
_exptl_absorpt_correction_type 'numerical'
_exptl_absorpt_correction_T_min 0.8816
_exptl_absorpt_correction_T_max 0.9446
_exptl_absorpt_process_details 'SHELXPREP'

_exptl_special_details
;
?
;
_diffrn_ambient_temperature    193(2)
_diffrn_radiation_wavelength   0.71073
_diffrn_radiation_type         MoK $\alpha$ 
_diffrn_radiation_source        'fine-focus sealed tube'
_diffrn_radiation_monochromator graphite
_diffrn_measurement_device_type 'Bruker APEX'
_diffrn_measurement_method     '0.3 wide/w exposure'
_diffrn_detector_area_resol_mean ?
_diffrn_standards_number      ?
_diffrn_standards_interval_count ?
_diffrn_standards_interval_time ?
_diffrn_standards_decay_% ?
_diffrn_reflns_number          5383
_diffrn_reflns_av_R_equivalents 0.1268
_diffrn_reflns_av_sigmaI/netI 0.0457
_diffrn_reflns_limit_h_min     -13
_diffrn_reflns_limit_h_max     13
_diffrn_reflns_limit_k_min     -13
_diffrn_reflns_limit_k_max     13
_diffrn_reflns_limit_l_min     -20
_diffrn_reflns_limit_l_max     20
_diffrn_reflns_theta_min       1.36
_diffrn_reflns_theta_max       28.28
_reflns_number_total          7392
_reflns_number_gt              5685
_reflns_threshold_expression   >2sigma(I)

_computing_data_collection    'SMART'
_computing_cell_refinement    'SMART'
_computing_data_reduction     'SAINT'
_computing_structure_solution  'SHELXS-97 (Sheldrick, 1990)'
_computing_structure_refinement 'SHELXL-97 (Sheldrick, 1997)'
_computing_molecular_graphics  'SHELXL-97 (Sheldrick, 1997)'
_computing_publication_material 'SHELXL-CIF-97 (Sheldrick, 2000)'

_refine_special_details
;
Refinement of F^2 against ALL reflections. The weighted R-factor wR and
goodness of fit S are based on F^2, conventional R-factors R are
based
on F, with F set to zero for negative F^2. The threshold expression of
F^2 > 2sigma(F^2) is used only for calculating R-factors(gt) etc. and
is
not relevant to the choice of reflections for refinement. R-factors
based
on F^2 are statistically about twice as large as those based on F, and
R-
factors based on ALL data will be even larger.
;

_refine_ls_structure_factor_coef Fsqd
_refine_ls_matrix_type        full
_refine_ls_weighting_scheme    calc
_refine_ls_weighting_details
'calc      w=1/[s^2^(Fo^2^(P)+(0.1000P)^2^(P)+0.0000P)]      where
P=(Fo^2^(P)+Fc^2^(P))/3'
_atom_sites_solution_primary   direct
_atom_sites_solution_secondary difmap
_atom_sites_solution_hydrogens geom

```

```

_refine_ls_hydrogen_treatment mixed
_refine_ls_extinction_method SHELXL
_refine_ls_extinction_coef 0.000(8)
_refine_ls_extinction_expression
'Fc^*^=kFc[1+0.001xFc^2\|^{3/\sin(2\q)}]^-1/4^'
_refine_ls_abs_structure_details
'Flack H D (1983), Acta Cryst. A39, 876-881'
_refine_ls_abs_structure_Flack 0.4(3)
_refine_ls_number_reflns 5178
_refine_ls_number_parameters 154
_refine_ls_number_restraints 1
_refine_ls_R_factor_all 0.2072
_refine_ls_R_factor_gt 0.1627
_refine_ls_wR_factor_ref 0.5053
_refine_ls_wR_factor_gt 0.3978
_refine_ls_goodness_of_fit_ref 3.493
_refine_ls_restrained_S_all 3.493
_refine_ls_shift/su_max 0.062
_refine_ls_shift/su_mean 0.000

loop_
_atom_site_label
_atom_site_type_symbol
_atom_site_fract_x
_atom_site_fract_y
_atom_site_fract_z
_atom_site_U_iso_or_equiv
_atom_site_adp_type
_atom_site_occupancy
_atom_site_symmetry_multiplicity
_atom_site_calc_flag
_atom_site_refinement_flags
_atom_site_disorder_assembly
_atom_site_disorder_group
Cl1 Cl 0.8348(4) 0.5734(5) 0.1579(3) 0.0807(13) Uiso 1 1 d ...
Cl2 Cl 0.5667(5) 0.6349(6) 0.0628(4) 0.0956(17) Uiso 1 1 d ...
Cl3 Cl 0.6830(6) 0.3876(7) 0.0358(4) 0.1103(19) Uiso 1 1 d ...
C30 C 0.6761(14) 0.5112(15) 0.1131(9) 0.055(3) Uiso 1 1 d ...
H30A H 0.6410 0.4720 0.1623 0.066 Uiso 1 1 calc R ...
O2 O 0.5455(8) 0.3612(9) 0.2478(5) 0.044(2) Uiso 1 1 d ...
O1 O 0.3090(8) 0.2459(8) 0.4494(5) 0.0434(19) Uiso 1 1 d ...
C25 C 0.3230(11) 0.2604(11) 0.3754(7) 0.036(2) Uiso 1 1 d ...
N2 N 0.2265(9) 0.3256(10) 0.3101(6) 0.037(2) Uiso 1 1 d ...
C14 C 0.0969(12) 0.2502(13) 0.1584(8) 0.042(3) Uiso 1 1 d ...
H14A H 0.0890 0.1614 0.1833 0.051 Uiso 1 1 calc R ...
H14B H 0.0162 0.3014 0.1620 0.051 Uiso 1 1 calc R ...
C1 C 0.3419(10) 0.0197(10) 0.2835(6) 0.027(2) Uiso 1 1 d ...
H1A H 0.2593 0.0743 0.2786 0.033 Uiso 1 1 calc R ...
C7 C 0.5833(10) 0.0708(12) 0.2750(7) 0.034(2) Uiso 1 1 d ...
H7A H 0.6491 0.1400 0.3037 0.041 Uiso 1 1 calc R ...
N1 N 0.4508(9) 0.1201(9) 0.2880(6) 0.0326(19) Uiso 1 1 d ...
C19 C 0.1125(11) 0.3777(12) 0.3382(7) 0.037(2) Uiso 1 1 d ...
H19A H 0.0570 0.4230 0.2844 0.044 Uiso 1 1 calc R ...
O3 O 0.5289(9) 0.4478(10) 0.3790(6) 0.056(2) Uiso 1 1 d ...
C8 C 0.6428(13) -0.0569(14) 0.3200(8) 0.047(3) Uiso 1 1 d ...
H8A H 0.6396 -0.0557 0.3835 0.056 Uiso 1 1 calc R ...
H8B H 0.5892 -0.1329 0.2910 0.056 Uiso 1 1 calc R ...
C13 C 0.2247(11) 0.3199(12) 0.2152(7) 0.036(2) Uiso 1 1 d ...
H13A H 0.3057 0.2700 0.2082 0.044 Uiso 1 1 calc R ...
C27 C 0.5603(11) 0.1950(12) 0.4456(7) 0.039(3) Uiso 1 1 d ...
H27A H 0.5281 0.1149 0.4692 0.059 Uiso 1 1 calc R ...
H27B H 0.5644 0.2672 0.4882 0.059 Uiso 1 1 calc R ...
H27C H 0.6501 0.1793 0.4360 0.059 Uiso 1 1 calc R ...
C15 C 0.1027(14) 0.2375(15) 0.0623(9) 0.053(3) Uiso 1 1 d ...
H15A H 0.0199 0.1946 0.0275 0.064 Uiso 1 1 calc R ...
H15B H 0.1807 0.1827 0.0577 0.064 Uiso 1 1 calc R ...

C18 C 0.2311(12) 0.4622(12) 0.1773(7) 0.041(3) Uiso 1 1 d ...
H18A H 0.1504 0.5118 0.1830 0.049 Uiso 1 1 calc R ...
H18B H 0.3109 0.5081 0.2137 0.049 Uiso 1 1 calc R ...
C2 C 0.3430(11) -0.0706(13) 0.3632(7) 0.040(3) Uiso 1 1 d ...
H2A H 0.4114 -0.1405 0.3666 0.048 Uiso 1 1 calc R ...
H2B H 0.3665 -0.0189 0.4191 0.048 Uiso 1 1 calc R ...
C24 C 0.0188(12) 0.2807(13) 0.3648(8) 0.043(3) Uiso 1 1 d ...
H24A H 0.0668 0.2319 0.4185 0.052 Uiso 1 1 calc R ...
H24B H -0.0124 0.2162 0.3162 0.052 Uiso 1 1 calc R ...
C20 C 0.1504(11) 0.4864(12) 0.4083(7) 0.039(3) Uiso 1 1 d ...
H20A H 0.2068 0.4481 0.4637 0.046 Uiso 1 1 calc R ...
H20B H 0.2047 0.5538 0.3867 0.046 Uiso 1 1 calc R ...
C28 C 0.5162(12) 0.3581(12) 0.3176(8) 0.042(3) Uiso 1 1 d ...
C6 C 0.3124(11) -0.0574(12) 0.1984(7) 0.038(2) Uiso 1 1 d ...
H6A H 0.3871 -0.1194 0.1990 0.046 Uiso 1 1 calc R ...
H6B H 0.3057 0.0036 0.1476 0.046 Uiso 1 1 calc R ...
C11 C 0.7334(12) 0.0626(14) 0.1691(8) 0.048(3) Uiso 1 1 d ...
H11A H 0.7852 0.1405 0.1966 0.058 Uiso 1 1 calc R ...
H11B H 0.7361 0.0598 0.1055 0.058 Uiso 1 1 calc R ...
C12 C 0.5882(10) 0.0753(12) 0.1760(7) 0.037(2) Uiso 1 1 d ...
H12A H 0.5339 0.0024 0.1432 0.045 Uiso 1 1 calc R ...
H12B H 0.5499 0.1596 0.1491 0.045 Uiso 1 1 calc R ...
C26 C 0.4632(12) 0.2322(13) 0.3565(8) 0.043(3) Uiso 1 1 d ...
C29 C 0.5772(14) 0.5718(16) 0.3504(10) 0.058(3) Uiso 1 1 d ...
H29A H 0.5872 0.6369 0.3984 0.087 Uiso 1 1 calc R ...
H29B H 0.5125 0.6043 0.2974 0.087 Uiso 1 1 calc R ...
H29C H 0.6644 0.5574 0.3364 0.087 Uiso 1 1 calc R ...
C23 C -0.1033(12) 0.3532(13) 0.3845(8) 0.045(3) Uiso 1 1 d ...
H23A H -0.1562 0.3933 0.3287 0.054 Uiso 1 1 calc R ...
H23B H -0.1615 0.2882 0.4048 0.054 Uiso 1 1 calc R ...
C5 C 0.1780(12) -0.1363(13) 0.1861(7) 0.041(3) Uiso 1 1 d ...
H5A H 0.1012 -0.0743 0.1738 0.050 Uiso 1 1 calc R ...
H5B H 0.1676 -0.1963 0.1344 0.050 Uiso 1 1 calc R ...
C9 C 0.7873(15) -0.0710(17) 0.3130(10) 0.063(4) Uiso 1 1 d ...
H9A H 0.8233 -0.1568 0.3385 0.076 Uiso 1 1 calc R ...
H9B H 0.8425 -0.0004 0.3481 0.076 Uiso 1 1 calc R ...
C10 C 0.7977(16) -0.0626(19) 0.2158(11) 0.069(4) Uiso 1 1 d ...
H10A H 0.8937 -0.0649 0.2142 0.083 Uiso 1 1 calc R ...
H10B H 0.7532 -0.1404 0.1829 0.083 Uiso 1 1 calc R ...
C16 C 0.1169(17) 0.3849(19) 0.0234(11) 0.071(4) Uiso 1 1 d ...
H16A H 0.1269 0.3773 -0.0385 0.086 Uiso 1 1 calc R ...
H16B H 0.0333 0.4347 0.0216 0.086 Uiso 1 1 calc R ...
C22 C -0.0651(13) 0.4582(14) 0.4534(8) 0.050(3) Uiso 1 1 d ...
H22A H -0.1469 0.5053 0.4596 0.060 Uiso 1 1 calc R ...
H22B H -0.0228 0.4173 0.5115 0.060 Uiso 1 1 calc R ...
C3 C 0.2095(12) -0.1304(13) 0.3528(8) 0.042(3) Uiso 1 1 d ...
H3A H 0.1409 -0.0604 0.3481 0.051 Uiso 1 1 calc R ...
H3B H 0.2082 -0.1852 0.4055 0.051 Uiso 1 1 calc R ...
C4 C 0.1771(14) -0.2158(15) 0.2687(9) 0.052(3) Uiso 1 1 d ...
H4A H 0.2441 -0.2876 0.2750 0.062 Uiso 1 1 calc R ...
H4B H 0.0874 -0.2565 0.2622 0.062 Uiso 1 1 calc R ...
C21 C 0.0285(13) 0.5522(15) 0.4294(9) 0.053(3) Uiso 1 1 d ...
H21A H 0.0592 0.6148 0.4792 0.064 Uiso 1 1 calc R ...
H21B H -0.0193 0.6034 0.3768 0.064 Uiso 1 1 calc R ...
C17 C 0.2387(15) 0.4640(17) 0.0796(9) 0.061(4) Uiso 1 1 d ...
H17B H 0.3240 0.4234 0.0737 0.073 Uiso 1 1 calc R ...
H17A H 0.2359 0.5559 0.0579 0.073 Uiso 1 1 calc R ...

_geom_special_details
;
All esds (except the esd in the dihedral angle between two l.s. planes) are estimated using the full covariance matrix. The cell esds are taken into account individually in the estimation of esds in distances, angles and torsion angles; correlations between esds in cell parameters are only

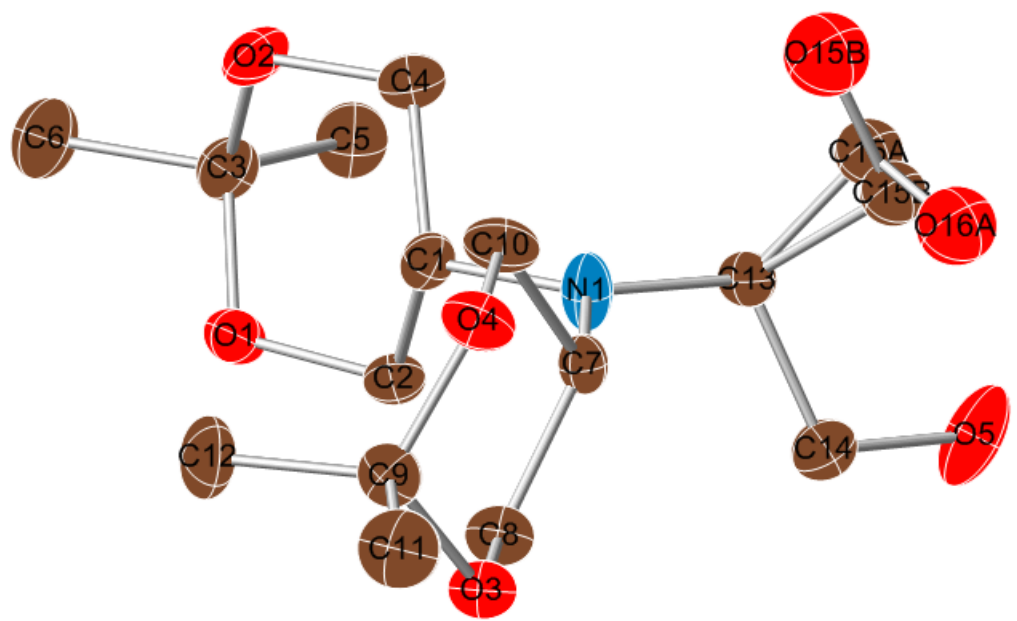
```

used when they are defined by crystal symmetry. An approximate (isotropic) treatment of cell esds is used for estimating esds involving l.s. planes.

```
;
loop_
  _geom_bond_atom_site_label_1      C11 C12 1.524(15) . ?
  _geom_bond_atom_site_label_2      C11 C10 1.53(2) . ?
  _geom_bond_distance              C11 H11A 0.9900 . ?
  _geom_bond_site_symmetry_2       C11 H11B 0.9900 . ?
  _geom_bond_publ_flag             C12 H12A 0.9900 . ?
  _geom_bond_publ_flag             C12 H12B 0.9900 . ?
  Cl1 C30 1.726(15) . ?          C29 H29A 0.9800 . ?
  Cl2 C30 1.737(16) . ?          C29 H29B 0.9800 . ?
  Cl3 C30 1.746(16) . ?          C29 H29C 0.9800 . ?
  C30 H30A 1.0000 . ?           C23 C22 1.491(18) . ?
  O2 C28 1.188(14) . ?          C23 H23A 0.9900 . ?
  O1 C25 1.197(13) . ?          C23 H23B 0.9900 . ?
  C25 N2 1.399(15) . ?          C5 C4 1.514(18) . ?
  C25 C26 1.561(16) . ?          C5 H5A 0.9900 . ?
  N2 C19 1.443(14) . ?          C5 H5B 0.9900 . ?
  N2 C13 1.465(14) . ?          C9 C10 1.54(2) . ?
  C14 C15 1.508(17) . ?          C9 H9A 0.9900 . ?
  C14 C13 1.560(16) . ?          C9 H9B 0.9900 . ?
  C14 H14A 0.9900 . ?          C10 H10A 0.9900 . ?
  C14 H14B 0.9900 . ?          C10 H10B 0.9900 . ?
  C1 C6 1.498(14) . ?          C16 C17 1.56(2) . ?
  C1 N1 1.501(13) . ?          C16 H16A 0.9900 . ?
  C1 C2 1.534(15) . ?          C16 H16B 0.9900 . ?
  C1 H1A 1.0000 . ?            C22 C21 1.463(19) . ?
  C7 N1 1.506(13) . ?          C22 H22A 0.9900 . ?
  C7 C8 1.527(18) . ?          C22 H22B 0.9900 . ?
  C7 C12 1.544(14) . ?          C3 C4 1.532(18) . ?
  C7 H7A 1.0000 . ?            C3 H3A 0.9900 . ?
  N1 C26 1.539(15) . ?          C3 H3B 0.9900 . ?
  C19 C24 1.500(17) . ?          C4 H4A 0.9900 . ?
  C19 C20 1.530(16) . ?          C4 H4B 0.9900 . ?
  C19 H19A 1.0000 . ?          C21 H21A 0.9900 . ?
  O3 C28 1.299(15) . ?          C21 H21B 0.9900 . ?
  O3 C29 1.459(19) . ?          C17 H17B 0.9900 . ?
  C8 C9 1.518(19) . ?          C17 H17A 0.9900 . ?
  C8 H8A 0.9900 . ?            loop_
  C8 H8B 0.9900 . ?            _geom_angle_atom_site_label_1
  C13 C18 1.566(16) . ?          _geom_angle_atom_site_label_2
  C13 H13A 1.0000 . ?          _geom_angle_atom_site_label_3
  C27 C26 1.540(17) . ?          _geom_angle
  C27 H27A 0.9800 . ?          _geom_angle_site_symmetry_1
  C27 H27B 0.9800 . ?          _geom_angle_site_symmetry_3
  C27 H27C 0.9800 . ?          _geom_angle_publ_flag
  C15 C16 1.63(2) . ?          Cl1 C30 Cl2 111.1(9) . ?
  C15 H15A 0.9900 . ?          Cl1 C30 Cl3 110.4(8) . ?
  C15 H15B 0.9900 . ?          Cl2 C30 Cl3 109.9(8) . ?
  C18 C17 1.533(19) . ?          Cl1 C30 H30A 108.5 . .
  C18 H18A 0.9900 . ?          Cl2 C30 H30A 108.5 . .
  C18 H18B 0.9900 . ?          Cl3 C30 H30A 108.5 . ?
  C2 C3 1.470(17) . ?          O1 C25 N2 121.5(10) . ?
  C2 H2A 0.9900 . ?            O1 C25 C26 119.0(10) . ?
  C2 H2B 0.9900 . ?            N2 C25 C26 118.4(9) . ?
  C24 C23 1.543(17) . ?          C25 N2 C19 116.0(9) . ?
  C24 H24A 0.9900 . ?          C25 N2 C13 122.8(9) . ?
  C24 H24B 0.9900 . ?          C19 N2 C13 120.1(9) . ?
  C20 C21 1.520(17) . ?          C15 C14 C13 111.5(10) . ?
  C20 H20A 0.9900 . ?          C15 C14 H14A 109.3 . ?
  C20 H20B 0.9900 . ?          C13 C14 H14A 109.3 . ?
  C28 C26 1.565(18) . ?          C15 C14 H14B 109.3 . ?
  C6 C5 1.565(17) . ?          C13 C14 H14B 109.3 . ?
  C6 H6A 0.9900 . ?            C14A C14 H14B 108.0 . ?
  C6 H6B 0.9900 . ?            C6 C1 N1 112.7(8) . ?
                                         C6 C1 C2 110.8(9) . ?
                                         N1 C1 C2 120.5(8) . ?
                                         C6 C1 H1A 103.6 . ?
                                         N1 C1 H1A 103.6 . ?
                                         C2 C1 H1A 103.6 . ?
                                         N1 C7 C8 119.7(9) . ?
                                         N1 C7 C12 111.6(8) . ?
                                         C8 C7 C12 111.9(10) . ?
                                         N1 C7 H7A 103.9 . ?
                                         C8 C7 H7A 103.9 . ?
                                         C12 C7 H7A 103.9 . ?
                                         C1 N1 C7 117.0(8) . ?
                                         C1 N1 C26 118.1(8) . ?
                                         C7 N1 C26 114.2(8) . ?
                                         N2 C19 C24 117.5(10) . ?
                                         N2 C19 C20 113.1(9) . ?
                                         C24 C19 C20 110.4(9) . ?
                                         N2 C19 H19A 104.9 . ?
                                         C24 C19 H19A 104.9 . ?
                                         C20 C19 H19A 104.9 . ?
                                         C28 O3 C29 111.3(10) . ?
                                         C9 C8 C7 109.7(11) . ?
                                         C9 C8 H8A 109.7 . ?
                                         C7 C8 H8A 109.7 . ?
                                         C9 C8 H8B 109.7 . ?
                                         C7 C8 H8B 109.7 . ?
                                         H8A C8 H8B 108.2 . ?
                                         N2 C13 C14 112.8(9) . ?
                                         N2 C13 C18 110.3(9) . ?
                                         C14 C13 C18 108.3(9) . ?
                                         N2 C13 H13A 108.5 . ?
                                         C14 C13 H13A 108.5 . ?
                                         C18 C13 H13A 108.5 . ?
                                         C26 C27 H27A 109.5 . ?
                                         C26 C27 H27B 109.5 . ?
                                         H27A C27 H27B 109.5 . ?
                                         C26 C27 H27C 109.5 . ?
                                         H27A C27 H27C 109.5 . ?
                                         H27B C27 H27C 109.5 . ?
                                         C14 C15 C16 108.3(12) . ?
                                         C14 C15 H15A 110.0 . ?
                                         C16 C15 H15A 110.0 . ?
                                         C14 C15 H15B 110.0 . ?
                                         C16 C15 H15B 110.0 . ?
                                         H15A C15 H15B 108.4 . ?
                                         C17 C18 C13 113.3(11) . ?
                                         C17 C18 H18A 108.9 . ?
                                         C13 C18 H18A 108.9 . ?
                                         C17 C18 H18B 108.9 . ?
                                         C13 C18 H18B 108.9 . ?
                                         H18A C18 H18B 107.7 . ?
                                         C3 C2 C1 109.4(9) . ?
                                         C3 C2 H2A 109.8 . ?
                                         C1 C2 H2A 109.8 . ?
                                         C3 C2 H2B 109.8 . ?
                                         C1 C2 H2B 109.8 . ?
                                         H2A C2 H2B 108.2 . ?
                                         C19 C24 C23 110.1(10) . ?
                                         C19 C24 H24A 109.6 . ?
                                         C23 C24 H24A 109.6 . ?
                                         C19 C24 H24B 109.6 . ?
```

C23 C24 H24B 109.6 .. ?	C17 C16 H16A 108.9 .. ?
H24A C24 H24B 108.2 .. ?	C15 C16 H16A 108.9 .. ?
C21 C20 C19 112.7(10) .. ?	C17 C16 H16B 108.9 .. ?
C21 C20 H20A 109.0 .. ?	C15 C16 H16B 108.9 .. ?
C19 C20 H20A 109.0 .. ?	H16A C16 H16B 107.7 .. ?
C21 C20 H20B 109.0 .. ?	C21 C22 C23 111.1(11) .. ?
C19 C20 H20B 109.0 .. ?	C21 C22 H22A 109.4 .. ?
H20A C20 H20B 107.8 .. ?	C23 C22 H22A 109.4 .. ?
O2 C28 O3 130.1(12) .. ?	C21 C22 H22B 109.4 .. ?
O2 C28 C26 123.9(11) .. ?	C23 C22 H22B 109.4 .. ?
O3 C28 C26 105.9(9) .. ?	H22A C22 H22B 108.0 .. ?
C1 C6 C5 111.2(9) .. ?	C2 C3 C4 109.5(10) .. ?
C1 C6 H6A 109.4 .. ?	C2 C3 H3A 109.8 .. ?
C5 C6 H6A 109.4 .. ?	C4 C3 H3A 109.8 .. ?
C1 C6 H6B 109.4 .. ?	C2 C3 H3B 109.8 .. ?
C5 C6 H6B 109.4 .. ?	C4 C3 H3B 109.8 .. ?
H6A C6 H6B 108.0 .. ?	H3A C3 H3B 108.2 .. ?
C12 C11 C10 110.7(11) .. ?	C5 C4 C3 111.8(11) .. ?
C12 C11 H11A 109.5 .. ?	C5 C4 H4A 109.3 .. ?
C10 C11 H11A 109.5 .. ?	C3 C4 H4A 109.3 .. ?
C12 C11 H11B 109.5 .. ?	C5 C4 H4B 109.3 .. ?
C10 C11 H11B 109.5 .. ?	C3 C4 H4B 109.3 .. ?
H11A C11 H11B 108.1 .. ?	H4A C4 H4B 107.9 .. ?
C11 C12 C7 109.4(9) .. ?	C22 C21 C20 113.0(11) .. ?
C11 C12 H12A 109.8 .. ?	C22 C21 H21A 109.0 .. ?
C7 C12 H12A 109.8 .. ?	C20 C21 H21A 109.0 .. ?
C11 C12 H12B 109.8 .. ?	C22 C21 H21B 109.0 .. ?
C7 C12 H12B 109.8 .. ?	C20 C21 H21B 109.0 .. ?
H12A C12 H12B 108.2 .. ?	H21A C21 H21B 107.8 .. ?
N1 C26 C27 111.4(10) .. ?	C18 C17 C16 108.7(12) .. ?
N1 C26 C25 109.7(9) .. ?	C18 C17 H17B 110.0 .. ?
C27 C26 C25 107.7(10) .. ?	C16 C17 H17B 110.0 .. ?
N1 C26 C28 108.5(9) .. ?	C18 C17 H17A 110.0 .. ?
C27 C26 C28 109.6(10) .. ?	C16 C17 H17A 110.0 .. ?
C25 C26 C28 110.0(10) .. ?	H17B C17 H17A 108.3 .. ?
O3 C29 H29A 109.5 .. ?	_diffrn_measured_fraction_theta_max
O3 C29 H29B 109.5 .. ?	0.901
H29A C29 H29B 109.5 .. ?	_diffrn_reflns_theta_full 28.25
O3 C29 H29C 109.5 .. ?	_diffrn_measured_fraction_theta_full 0.901
H29A C29 H29C 109.5 .. ?	_refine_diff_density_max 1.477
H29B C29 H29C 109.5 .. ?	_refine_diff_density_min -1.777
C22 C23 C24 113.3(10) .. ?	_refine_diff_density_rms 0.178
C22 C23 H23A 108.9 .. ?	
C24 C23 H23A 108.9 .. ?	
C22 C23 H23B 108.9 .. ?	
C24 C23 H23B 108.9 .. ?	
H23A C23 H23B 107.7 .. ?	
C4 C5 C6 110.7(10) .. ?	
C4 C5 H5A 109.5 .. ?	
C6 C5 H5A 109.5 .. ?	
C4 C5 H5B 109.5 .. ?	
C6 C5 H5B 109.5 .. ?	
H5A C5 H5B 108.1 .. ?	
C8 C9 C10 111.4(12) .. ?	
C8 C9 H9A 109.4 .. ?	
C10 C9 H9A 109.4 .. ?	
C8 C9 H9B 109.4 .. ?	
C10 C9 H9B 109.4 .. ?	
H9A C9 H9B 108.0 .. ?	
C11 C10 C9 112.7(14) .. ?	
C11 C10 H10A 109.1 .. ?	
C9 C10 H10A 109.1 .. ?	
C11 C10 H10B 109.1 .. ?	
C9 C10 H10B 109.1 .. ?	
H10A C10 H10B 107.8 .. ?	
C17 C16 C15 113.3(13) .. ?	

APPENDIX 7
CRYSTAL STRUCTURE DATA FOR **21**



```

data_new (amine diacetonide_diol)

_audit_creation_method      SHELXL-97
_chemical_name_systematic
;
?
;
_chemical_name_common      ?
_chemical_melting_point    ?
_chemical_formula_moiety   'C15 H29 N1 O6'
_chemical_formula_sum       'C15 H29 N O6'
_chemical_formula_weight    319.39

loop_
_atom_type_symbol
_atom_type_description
_atom_type_scat_dispersion_real
_atom_type_scat_dispersion_imag
_atom_type_scat_source
'C' 'C' 0.0033 0.0016
'International Tables Vol C Tables 4.2.6.8 and 6.1.1.4'
'H' 'H' 0.0000 0.0000
'International Tables Vol C Tables 4.2.6.8 and 6.1.1.4'
'N' 'N' 0.0061 0.0033
'International Tables Vol C Tables 4.2.6.8 and 6.1.1.4'
'O' 'O' 0.0106 0.0060
'International Tables Vol C Tables 4.2.6.8 and 6.1.1.4'

_symmetry_cell_setting      monoclinic
_symmetry_space_group_name_H-M   'P 21/c'
_symmetry_space_group_name_Hall   '-P 2ybc'
_symmetry_Int_Tables_number     14

loop_
_symmetry_equiv_pos_as_xyz
'x, y, z'
'-x, y+1/2, -z+1/2'
'-x, -y, -z'
'x, -y-1/2, z-1/2'

_cell_length_a              13.6163(12)
_cell_length_b              11.7563(10)
_cell_length_c              10.4340(9)
_cell_angle_alpha            90.00
_cell_angle_beta             104.094(2)
_cell_angle_gamma            90.00
_cell_volume                 1620.0(2)
_cell_formula_units_Z        4
_cell_measurement_temperature 193(2)
_cell_measurement_reflns_used 4059
_cell_measurement_theta_min   2.32
_cell_measurement_theta_max    28.45

_exptl_crystal_description   'prism'
_exptl_crystal_colour        'colorless'
_exptl_crystal_size_max      .1
_exptl_crystal_size_mid      .1
_exptl_crystal_size_min      .1
_exptl_crystal_density_meas  ?
_exptl_crystal_density_diffrn 1.310
_exptl_crystal_density_method 'not measured'
_exptl_crystal_F_000          696
_exptl_absorpt_coefficient_mu 0.100
_exptl_absorpt_correction_type none

_exptl_special_details
;
?
;
_diffrn_ambient_temperature   193(2)
_diffrn_radiation_wavelength  0.71073
_diffrn_radiation_type        MoK $\alpha$ 
_diffrn_radiation_source      'fine-focus sealed tube'
_diffrn_radiation_monochromator graphite
_diffrn_measurement_device_type 'CCD area detector'
_diffrn_measurement_method    'phi and omega scans'
_diffrn_detector_area_resol_mean ?
_diffrn_standards_number      ?
_diffrn_standards_interval_count ?
_diffrn_standards_interval_time ?
_diffrn_standards_decay_% ?
_diffrn_reflns_number         16261
_diffrn_reflns_av_R_equivalents 0.0907
_diffrn_reflns_av_sigmaI/netI 0.0850
_diffrn_reflns_limit_h_min    -18
_diffrn_reflns_limit_h_max    18
_diffrn_reflns_limit_k_min    -15
_diffrn_reflns_limit_k_max    14
_diffrn_reflns_limit_l_min    -13
_diffrn_reflns_limit_l_max    13
_diffrn_reflns_theta_min      2.32
_diffrn_reflns_theta_max      28.45
_reflns_number_total          4059
_reflns_number_gt             3213
_reflns_threshold_expression  >2sigma(I)

_computing_data_collection    'Bruker SMART'
_computing_cell_refinement    'Bruker SMART'
_computing_data_reduction     'Bruker SAINT'
_computing_structure_solution  'SHELXS-97 (Sheldrick, 1990)'
_computing_structure_refinement 'SHELXL-97 (Sheldrick, 1997)'
_computing_molecular_graphics  'Bruker SHELXTL'
_computing_publication_material 'Bruker SHELXTL'

_refine_special_details
;
Refinement of F2 against ALL reflections. The weighted R-factor wR and
goodness of fit S are based on F2, conventional R-factors R are
based
on F, with F set to zero for negative F2. The threshold expression of
F2 > 2sigma(F2) is used only for calculating R-factors(gt) etc. and
is
not relevant to the choice of reflections for refinement. R-factors
based
on F2 are statistically about twice as large as those based on F, and
R-
factors based on ALL data will be even larger.
;

_refine_ls_structure_factor_coef Fsqd
_refine_ls_matrix_type        full
_refine_ls_weighting_scheme   calc
_refine_ls_weighting_details
'calc      w=1/[s2(Fo2)+(0.0463P)2+3.6863P]      where
P=(Fo2+2Fc2)/3'
_atom_sites_solution_primary   direct
_atom_sites_solution_secondary difmap
_atom_sites_solution_hydrogens geom
_refine_ls_hydrogen_treatment  mixed

```

```

_refine_ls_extinction_method    none
_refine_ls_extinction_coef      ?
_refine_ls_number_reflns       4059
_refine_ls_number_parameters   211
_refine_ls_number_restraints   2
_refine_ls_R_factor_all        0.1709
_refine_ls_R_factor_gt         0.1373
_refine_ls_wR_factor_ref       0.2467
_refine_ls_wR_factor_gt         0.2327
_refine_ls_goodness_of_fit_ref 1.286
_refine_ls_restrained_S_all    1.287
_refine_ls_shift/su_max        0.000
_refine_ls_shift/su_mean        0.000

loop_
_atom_site_label
_atom_site_type_symbol
_atom_site_fract_x
_atom_site_fract_y
_atom_site_fract_z
_atom_site_U_iso_or_equiv
_atom_site_adp_type
_atom_site_occupancy
_atom_site_symmetry_multiplicity
_atom_site_calc_flag
_atom_site_refinement_flags
_atom_site_disorder_assembly
_atom_site_disorder_group
C1 C 0.6788(3) 0.8756(3) 0.0067(4) 0.0216(9) Uani 1 1 d ...
H1 H 0.6731(4) 0.8962(10) 1.095(4) 0.026 Uiso 1 1 calc R ...
C2 C 0.6992(3) 0.7476(4) 1.0079(4) 0.0250(9) Uani 1 1 d ...
H2A H 0.7086(5) 0.7251(9) 0.927(3) 0.030 Uiso 1 1 calc R ...
H2B H 0.757(2) 0.7307(7) 1.072(2) 0.030 Uiso 1 1 calc R ...
C3 C 0.5221(3) 0.7114(4) 0.9437(4) 0.0256(9) Uani 1 1 d ...
C4 C 0.5770(3) 0.8998(4) 0.9130(4) 0.0277(10) Uani 1 1 d ...
H4A H 0.5596(7) 0.977(3) 0.9207(5) 0.033 Uiso 1 1 calc R ...
H4B H 0.5813(3) 0.8873(5) 0.825(3) 0.033 Uiso 1 1 calc R ...
C5 C 0.5222(4) 0.6655(4) 0.8074(4) 0.0347(11) Uani 1 1 d ...
H5A H 0.5659 0.7131 0.7675 0.052 Uiso 1 1 calc R ...
H5B H 0.4530 0.6666 0.7514 0.052 Uiso 1 1 calc R ...
H5C H 0.5477 0.5872 0.8155 0.052 Uiso 1 1 calc R ...
C6 C 0.4405(3) 0.6555(4) 0.9976(5) 0.0370(12) Uani 1 1 d ...
H6A H 0.4497 0.5728 0.9990 0.056 Uiso 1 1 calc R ...
H6B H 0.3738 0.6747 0.9412 0.056 Uiso 1 1 calc R ...
H6C H 0.4450 0.6828 1.0876 0.056 Uiso 1 1 calc R ...
C7 C 0.8214(3) 1.0114(3) 1.0832(4) 0.0199(8) Uani 1 1 d ...
H7 H 0.869(2) 1.0468(18) 1.0481(18) 0.024 Uiso 1 1 calc R ...
C8 C 0.8790(3) 0.9417(4) 1.2000(4) 0.0239(9) Uani 1 1 d ...
H8A H 0.8340(15) 0.8943(16) 1.2294(10) 0.029 Uiso 1 1 calc R ...
H8B H 0.9266(16) 0.8960(16) 1.1737(9) 0.029 Uiso 1 1 calc R ...
C9 C 0.8630(3) 1.0920(4) 1.3484(4) 0.0251(9) Uani 1 1 d ...
C10 C 0.7602(3) 1.1047(4) 1.1285(4) 0.0276(10) Uani 1 1 d ...
H10A H 0.7374(9) 1.1583(18) 1.057(2) 0.033 Uiso 1 1 calc R ...
H10B H 0.701(2) 1.0715(11) 1.1492(8) 0.033 Uiso 1 1 calc R ...
C11 C 0.9318(4) 1.1653(4) 1.4507(5) 0.0373(12) Uani 1 1 d ...
H11A H 0.9805 1.2043 1.4106 0.056 Uiso 1 1 calc R ...
H11B H 0.9683 1.1174 1.5238 0.056 Uiso 1 1 calc R ...
H11C H 0.8913 1.2217 1.4842 0.056 Uiso 1 1 calc R ...
C12 C 0.7870(4) 1.0301(5) 1.4058(5) 0.0379(12) Uani 1 1 d ...
H12A H 0.7453 1.0854 1.4390 0.057 Uiso 1 1 calc R ...
H12B H 0.8225 0.9814 1.4786 0.057 Uiso 1 1 calc R ...
H12C H 0.7436 0.9831 1.3372 0.057 Uiso 1 1 calc R ...
C13 C 0.7871(3) 0.9300(4) 0.8542(4) 0.0214(8) Uani 1 1 d ...
H13 H 0.737(2) 0.877(3) 0.805(2) 0.026 Uiso 1 1 calc R A 1
C14 C 0.8871(3) 0.8678(4) 0.8718(4) 0.0258(9) Uani 1 1 d . B .
H14A H 0.9408(18) 0.9130(15) 0.9270(19) 0.031 Uiso 1 1 calc R ...

H14B H 0.8837(3) 0.796(2) 0.9163(15) 0.031 Uiso 1 1 calc R ..
N1 N 0.7586(3) 0.9449(3) 0.9784(3) 0.0279(8) Uani 1 1 d . B .
O1 O 0.6150(2) 0.6878(2) 1.0353(3) 0.0262(7) Uani 1 1 d ...
O2 O 0.5002(2) 0.8287(2) 0.9412(3) 0.0283(7) Uani 1 1 d ...
O3 O 0.9292(2) 1.0145(2) 1.3053(3) 0.0234(7) Uani 1 1 d ...
O4 O 0.8176(2) 1.1637(2) 1.2420(3) 0.0272(7) Uani 1 1 d ...
O5 O 0.9101(2) 0.8471(3) 0.7482(4) 0.0416(9) Uani 1 1 d ...
H5 H 0.9516 0.8960 0.7353 0.062 Uiso 1 1 calc R B .
C15A C 0.7760(6) 1.0328(6) 0.7694(7) 0.0311(18) Uiso 0.684(9) 1 d PD
B 1
H15A H 0.7710 1.0109 0.6764 0.037 Uiso 0.684(9) 1 calc PR B 1
H15B H 0.7139 1.0749 0.7736 0.037 Uiso 0.684(9) 1 calc PR B 1
O16A O 0.8630(4) 1.1017(5) 0.8173(5) 0.0428(17) Uiso 0.684(9) 1 d PD
B 1
H16A H 0.8588 1.1607 0.7708 0.064 Uiso 0.684(9) 1 calc PR B 1
C15B C 0.8134(12) 1.0549(13) 0.7994(16) 0.029(4) Uiso 0.316(9) 1 d
PD B 2
H15C H 0.8799 1.0815 0.8522 0.035 Uiso 0.316(9) 1 calc PR B 2
H15D H 0.8172 1.0480 0.7062 0.035 Uiso 0.316(9) 1 calc PR B 2
O15B O 0.7394(9) 1.1326(10) 0.8087(12) 0.049(4) Uiso 0.316(9) 1 d PD
B 2
H15E H 0.6821 1.1051 0.7745 0.073 Uiso 0.316(9) 1 calc PR B 2

loop_
_atom_site_aniso_label
_atom_site_aniso_U_11
_atom_site_aniso_U_22
_atom_site_aniso_U_33
_atom_site_aniso_U_23
_atom_site_aniso_U_13
_atom_site_aniso_U_12
C1 0.0201(19) 0.025(2) 0.020(2) -0.0042(16) 0.0055(16) -0.0029(16)
C2 0.0170(19) 0.033(2) 0.023(2) 0.0044(18) -0.0007(16) 0.0011(17)
C3 0.023(2) 0.026(2) 0.028(2) -0.0031(17) 0.0059(17) -0.0037(17)
C4 0.025(2) 0.027(2) 0.031(2) 0.0017(18) 0.0060(18) 0.0055(18)
C5 0.032(2) 0.042(3) 0.028(2) -0.007(2) 0.0031(19) -0.010(2)
C6 0.030(2) 0.038(3) 0.045(3) -0.002(2) 0.013(2) -0.011(2)
C7 0.0208(18) 0.021(2) 0.019(2) -0.0010(15) 0.0064(15) -0.0044(16)
C8 0.026(2) 0.020(2) 0.025(2) -0.0060(16) 0.0038(17) 0.0031(17)
C9 0.030(2) 0.024(2) 0.021(2) -0.0043(17) 0.0056(17) 0.0001(17)
C10 0.029(2) 0.020(2) 0.030(2) 0.0011(18) -0.0004(18) 0.0048(17)
C11 0.041(3) 0.042(3) 0.028(3) -0.015(2) 0.007(2) 0.004(2)
C12 0.041(3) 0.049(3) 0.031(3) -0.001(2) 0.021(2) -0.003(2)
C13 0.0232(19) 0.025(2) 0.0155(19) -0.0038(16) 0.0041(16) 0.0026(17)
C14 0.024(2) 0.024(2) 0.029(2) -0.0033(18) 0.0051(18) -0.0018(17)
N1 0.0271(18) 0.037(2) 0.0211(18) -0.0060(16) 0.0097(15) -0.0135(16)
O1 0.0250(15) 0.0249(15) 0.0270(16) 0.0073(13) 0.0028(12) -
0.0026(12)
O2 0.0167(13) 0.0251(16) 0.0434(19) 0.0014(14) 0.0076(13) -
0.0014(12)
O3 0.0245(14) 0.0226(15) 0.0211(15) -0.0067(12) 0.0018(12)
0.0023(12)
O4 0.0342(16) 0.0183(15) 0.0262(16) -0.0018(12) 0.0018(13)
0.0026(13)
O5 0.0317(18) 0.046(2) 0.055(2) -0.0286(18) 0.0265(17) -0.0134(16)

_geom_special_details
;
All esds (except the esd in the dihedral angle between two l.s. planes) are estimated using the full covariance matrix. The cell esds are taken into account individually in the estimation of esds in distances, angles and torsion angles; correlations between esds in cell parameters are only used when they are defined by crystal symmetry. An approximate (isotropic) treatment of cell esds is used for estimating esds involving l.s. planes.

```

```

;
loop_
    _geom_bond_atom_site_label_1
    _geom_bond_atom_site_label_2
    _geom_bond_distance
    _geom_bond_site_symmetry_2
    _geom_bond_publ_flag
    C1 N1 1.444(5) . ?
    C1 C4 1.517(5) . ?
    C1 C2 1.530(6) . ?
    C1 H1 0.9777 . ?
    C2 O1 1.432(5) . ?
    C2 H2A 0.9260 . ?
    C2 H2B 0.9260 . ?
    C3 O2 1.411(5) . ?
    C3 O1 1.414(5) . ?
    C3 C6 1.513(6) . ?
    C3 C5 1.521(6) . ?
    C4 O2 1.424(5) . ?
    C4 H4A 0.9412 . ?
    C4 H4B 0.9412 . ?
    C5 H5A 0.9800 . ?
    C5 H5B 0.9800 . ?
    C5 H5C 0.9800 . ?
    C6 H6A 0.9800 . ?
    C6 H6B 0.9800 . ?
    C6 H6C 0.9800 . ?
    C7 N1 1.443(5) . ?
    C7 C8 1.519(5) . ?
    C7 C10 1.521(6) . ?
    C7 H7 0.9158 . ?
    C8 O3 1.429(5) . ?
    C8 H8A 0.9332 . ?
    C8 H8B 0.9332 . ?
    C9 O4 1.411(5) . ?
    C9 O3 1.429(5) . ?
    C9 C12 1.505(6) . ?
    C9 C11 1.506(6) . ?
    C10 O4 1.429(5) . ?
    C10 H10A 0.9658 . ?
    C10 H10B 0.9658 . ?
    C11 H11A 0.9800 . ?
    C11 H11B 0.9800 . ?
    C11 H11C 0.9800 . ?
    C12 H12A 0.9800 . ?
    C12 H12B 0.9800 . ?
    C12 H12C 0.9800 . ?
    C13 N1 1.451(5) . ?
    C13 C15A 1.483(8) . ?
    C13 C14 1.517(6) . ?
    C13 C15B 1.646(17) . ?
    C13 H13 0.9666 . ?
    C14 O5 1.420(5) . ?
    C14 H14A 0.9714 . ?
    C14 H14B 0.9714 . ?
    O5 H5 0.8400 . ?
    C15A O16A 1.422(8) . ?
    C15A H15A 0.9900 . ?
    C15A H15B 0.9900 . ?
    O16A H16A 0.8400 . ?
    C15B O15B 1.380(14) . ?
    C15B H15C 0.9900 . ?
    C15B H15D 0.9900 . ?
    O15B H15E 0.8400 . ?

    loop_
        _geom_angle_atom_site_label_1
        _geom_angle_atom_site_label_2
        _geom_angle_atom_site_label_3
        _geom_angle
        _geom_angle_site_symmetry_1
        _geom_angle_site_symmetry_2
        _geom_angle_publ_flag
        N1 C1 C4 112.2(4) . ?
        N1 C1 C2 114.3(3) . ?
        C4 C1 C2 108.9(3) . ?
        N1 C1 H1 107.0 . ?
        C4 C1 H1 107.0 . ?
        C2 C1 H1 107.0 . ?
        O1 C2 C1 109.4(3) . ?
        O1 C2 H2A 109.8 . ?
        C1 C2 H2A 109.8 . ?
        O1 C2 H2B 109.8 . ?
        C1 C2 H2B 109.8 . ?
        H2A C2 H2B 108.2 . ?
        O2 C3 O1 110.8(3) . ?
        O2 C3 C6 105.0(4) . ?
        O1 C3 C6 106.3(4) . ?
        O2 C3 C5 112.2(4) . ?
        O1 C3 C5 111.0(4) . ?
        C6 C3 C5 111.2(4) . ?
        O2 C4 C1 111.0(3) . ?
        O2 C4 H4A 109.4 . ?
        C1 C4 H4A 109.4 . ?
        O2 C4 H4B 109.4 . ?
        C1 C4 H4B 109.4 . ?
        H4A C4 H4B 108.0 . ?
        C3 C5 H5A 109.5 . ?
        C3 C5 H5B 109.5 . ?
        H5A C5 H5B 109.5 . ?
        C3 C5 H5C 109.5 . ?
        H5A C5 H5C 109.5 . ?
        H5B C5 H5C 109.5 . ?
        C3 C6 H6A 109.5 . ?
        C3 C6 H6B 109.5 . ?
        H6A C6 H6B 109.5 . ?
        C3 C6 H6C 109.5 . ?
        H6A C6 H6C 109.5 . ?
        H6B C6 H6C 109.5 . ?
        N1 C7 C8 114.2(3) . ?
        N1 C7 C10 111.0(3) . ?
        C8 C7 C10 110.7(3) . ?
        N1 C7 H7 106.8 . ?
        C8 C7 H7 106.8 . ?
        C10 C7 H7 106.8 . ?
        O3 C8 C7 110.6(3) . ?
        O3 C8 H8A 109.5 . ?
        C7 C8 H8A 109.5 . ?
        O3 C8 H8B 109.5 . ?
        C7 C8 H8B 109.5 . ?
        H8A C8 H8B 108.1 . ?
        O4 C9 O3 108.8(3) . ?
        O4 C9 C12 112.9(4) . ?
        O3 C9 C12 111.4(4) . ?
        O4 C9 C11 107.1(4) . ?
        O3 C9 C11 104.9(3) . ?
        C12 C9 C11 111.3(4) . ?
        O4 C10 C7 112.1(3) . ?
        O4 C10 H10A 109.2 . ?
        C7 C10 H10A 109.2 . ?
        O4 C10 H10B 109.2 . ?

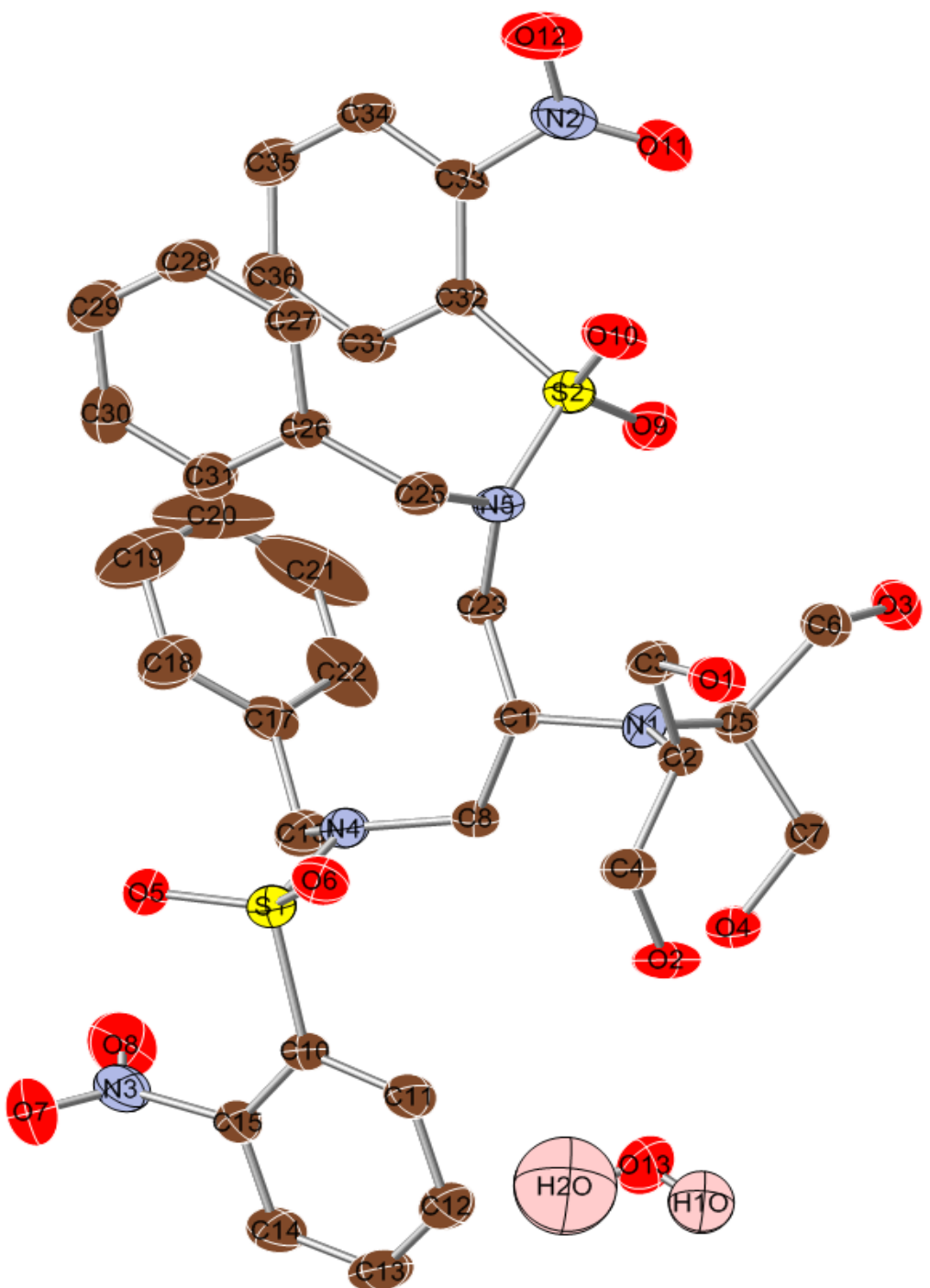
        loop_
            _geom_torsion_atom_site_label_1
            _geom_torsion_atom_site_label_2
            _geom_torsion_atom_site_label_3
            _geom_torsion_atom_site_label_4
            _geom_torsion
            _geom_torsion_site_symmetry_1
            _geom_torsion_site_symmetry_2
            _geom_torsion_site_symmetry_3
            _geom_torsion_site_symmetry_4
            _geom_torsion_publ_flag
            N1 C1 C2 O1 -179.3(3) . . . ?
            C4 C1 C2 O1 -52.9(4) . . . ?

```

N1 C1 C4 O2 178.7(3) . . . ?
 C2 C1 C4 O2 51.1(5) . . . ?
 N1 C7 C8 O3 -173.0(3) . . . ?
 C10 C7 C8 O3 -46.8(5) . . . ?
 N1 C7 C10 O4 173.4(3) . . . ?
 C8 C7 C10 O4 45.4(5) . . . ?
 N1 C13 C14 O5 175.9(3) . . . ?
 C15A C13 C14 O5 -50.1(6) . . . ?
 C15B C13 C14 O5 -67.3(7) . . . ?
 C8 C7 N1 C1 59.8(5) . . . ?
 C10 C7 N1 C1 -66.3(5) . . . ?
 C8 C7 N1 C13 -108.3(4) . . . ?
 C10 C7 N1 C13 125.6(4) . . . ?
 C4 C1 N1 C7 126.7(4) . . . ?
 C2 C1 N1 C7 -108.6(4) . . . ?
 C4 C1 N1 C13 -65.1(5) . . . ?
 C2 C1 N1 C13 59.6(5) . . . ?
 C15A C13 N1 C7 -71.5(6) . . . ?
 C14 C13 N1 C7 62.5(5) . . . ?
 C15B C13 N1 C7 -49.8(7) . . . ?
 C15A C13 N1 C1 120.5(5) . . . ?
 C14 C13 N1 C1 -105.5(4) . . . ?
 C15B C13 N1 C1 142.2(7) . . . ?
 O2 C3 O1 C2 -58.6(5) . . . ?
 C6 C3 O1 C2 -172.1(4) . . . ?
 C5 C3 O1 C2 66.8(5) . . . ?
 C1 C2 O1 C3 57.9(4) . . . ?
 O1 C3 O2 C4 56.3(5) . . . ?
 C6 C3 O2 C4 170.6(4) . . . ?
 C5 C3 O2 C4 -68.4(4) . . . ?
 C1 C4 O2 C3 -54.0(5) . . . ?
 C7 C8 O3 C9 56.3(5) . . . ?
 O4 C9 O3 C8 -61.4(4) . . . ?
 C12 C9 O3 C8 63.7(5) . . . ?
 C11 C9 O3 C8 -175.8(4) . . . ?
 O3 C9 O4 C10 59.2(4) . . . ?
 C12 C9 O4 C10 -65.0(5) . . . ?
 C11 C9 O4 C10 172.1(4) . . . ?
 C7 C10 O4 C9 -53.0(5) . . . ?
 N1 C13 C15A O16A 81.4(6) . . . ?
 C14 C13 C15A O16A -51.3(6) . . . ?
 C15B C13 C15A O16A 3.2(16) . . . ?
 N1 C13 C15B O15B -46.3(13) . . . ?
 C15A C13 C15B O15B 63.8(16) . . . ?
 C14 C13 C15B O15B -165.1(10) . . . ?

_diffrn_measured_fraction_theta_max
 0.996
 _diffrn_reflns_theta_full 28.45
 _diffrn_measured_fraction_theta_full 0.996
 _refine_diff_density_max 0.471
 _refine_diff_density_min -0.335
 _refine_diff_density_rms 0.072

APPENDIX 8
CRYSTAL STRUCTURE DATA FOR **80**·H₂O



```

data_p-1 (amine tetraalcohol_N,N-dibenzyl-N,N-dinosyldiamine)

_audit_creation_method      SHELXL-97
_chemical_name_systematic
;
?
;
_chemical_name_common      ?
_chemical_melting_point    ?
_chemical_formula_moiety   'C37 H43 N3 O12 S2, O'
_chemical_formula_sum       'C37 H43 N3 O13 S2'
_chemical_formula_weight    801.86

loop_
_atom_type_symbol
_atom_type_description
_atom_type_scat_dispersion_real
_atom_type_scat_dispersion_imag
_atom_type_scat_source
'C' 'C' 0.0033 0.0016
'International Tables Vol C Tables 4.2.6.8 and 6.1.1.4'
'H' 'H' 0.0000 0.0000
'International Tables Vol C Tables 4.2.6.8 and 6.1.1.4'
'N' 'N' 0.0061 0.0033
'International Tables Vol C Tables 4.2.6.8 and 6.1.1.4'
'O' 'O' 0.0106 0.0060
'International Tables Vol C Tables 4.2.6.8 and 6.1.1.4'
'S' 'S' 0.1246 0.1234
'International Tables Vol C Tables 4.2.6.8 and 6.1.1.4'

_symmetry_cell_setting      triclinic
_symmetry_space_group_name_H-M      'P -1'
_symmetry_space_group_name_Hall     '-P 1'
_symmetry_Int_Tables_number      2

loop_
_symmetry_equiv_pos_as_xyz
'x, y, z'
'-x, -y, -z'

_cell_length_a              9.6989(9)
_cell_length_b              11.7340(11)
_cell_length_c              17.0649(17)
_cell_angle_alpha            80.749(2)
_cell_angle_beta             78.860(2)
_cell_angle_gamma            78.027(2)
_cell_volume                 1849.3(3)
_cell_formula_units_Z        2
_cell_measurement_temperature 193(2)
_cell_measurement_reflns_used ?
_cell_measurement_theta_min  ?
_cell_measurement_theta_max  ?

_exptl_crystal_description  ?
_exptl_crystal_colour       ?
_exptl_crystal_size_max      0.10
_exptl_crystal_size_mid      0.10
_exptl_crystal_size_min      0.10
_exptl_crystal_density_meas  ?
_exptl_crystal_density_diffrn 1.440
_exptl_crystal_density_method 'not measured'
_exptl_crystal_F_000          844
_exptl_absorpt_coefficient_mu 0.216
_exptl_absorpt_correction_type ?
_exptl_absorpt_correction_T_min 0.9787

_exptl_absorpt_correction_T_max 0.9787
_exptl_absorpt_process_details  ?

_exptl_special_details
;
?
;

_diffrn_ambient_temperature 193(2)
_diffrn_radiation_wavelength 0.71073
_diffrn_radiation_type      MoK\alpha
_diffrn_radiation_source     'fine-focus sealed tube'
_diffrn_radiation_monochromator graphite
_diffrn_measurement_device_type ?
_diffrn_measurement_method   ?
_diffrn_detector_area_resol_mean ?
_diffrn_standards_number     ?
_diffrn_standards_interval_count ?
_diffrn_standards_interval_time ?
_diffrn_standards_decay_%    ?
_diffrn_reflns_number        19038
_diffrn_reflns_av_R_equivalents 0.0520
_diffrn_reflns_av_sigmaI/netI 0.1138
_diffrn_reflns_limit_h_min   -12
_diffrn_reflns_limit_h_max   12
_diffrn_reflns_limit_k_min   -15
_diffrn_reflns_limit_k_max   15
_diffrn_reflns_limit_l_min   -22
_diffrn_reflns_limit_l_max   22
_diffrn_reflns_theta_min     1.23
_diffrn_reflns_theta_max     28.29
_reflns_number_total        9067
_reflns_number_gt            4629
_reflns_threshold_expression >2sigma(I)

_computing_data_collection  'Bruker SMART'
_computing_cell_refinement   'Bruker SMART'
_computing_data_reduction    'Bruker SAINT'
_computing_structure_solution 'SHELXS-97 (Sheldrick, 1990)'
_computing_structure_refinement 'SHELXL-97 (Sheldrick, 1997)'
_computing_molecular_graphics 'Bruker SHELXTL'
_computing_publication_material 'Bruker SHELXTL'

_refine_special_details
;
Refinement of F^2 against ALL reflections. The weighted R-factor wR and
goodness of fit S are based on F^2, conventional R-factors R are
based
on F, with F set to zero for negative F^2. The threshold expression of
F^2 > 2sigma(F^2) is used only for calculating R-factors(gt) etc. and
is
not relevant to the choice of reflections for refinement. R-factors
based
on F^2 are statistically about twice as large as those based on F, and
R-
factors based on ALL data will be even larger.
;

_refine_ls_structure_factor_coef Fsqd
_refine_ls_matrix_type       full
_refine_ls_weighting_scheme   calc
_refine_ls_weighting_details
'calc      w=1/[s^2^(Fo^2^()+(0.1030P)^2^(+0.0000P)]      where
P=(Fo^2^(+2Fc^2^()/3'
_atom_sites_solution_primary   direct

```

`_atom_sites_solution_secondary difmap`
`_atom_sites_solution_hydrogens geom`
`_refine_ls_hydrogen_treatment constr`
`_refine_ls_extinction_method none`
`_refine_ls_extinction_coeff ?`
`_refine_ls_number_reflns 9067`
`_refine_ls_number_parameters 500`
`_refine_ls_number_restraints 0`
`_refine_ls_R_factor_all 0.1263`
`_refine_ls_R_factor_gt 0.0673`
`_refine_ls_wR_factor_ref 0.1916`
`_refine_ls_wR_factor_gt 0.1750`
`_refine_ls_goodness_of_fit_ref 0.927`
`_refine_ls_restrained_S_all 0.927`
`_refine_ls_shift/su_max 0.000`
`_refine_ls_shift/su_mean 0.000`

`loop_`
`_atom_site_label`
`_atom_site_type_symbol`
`_atom_site_fract_x`
`_atom_site_fract_y`
`_atom_site_fract_z`
`_atom_site_U_iso_or_equiv`
`_atom_site_adp_type`
`_atom_site_occupancy`
`_atom_site_symmetry_multiplicity`
`_atom_site_calc_flag`
`_atom_site_refinement_flags`
`_atom_site_disorder_assembly`
`_atom_site_disorder_group`

S1 S 0.35997(9) 0.27324(7) 0.29938(5) 0.0323(2) Uani 1 1 d ...
S2 S 0.12433(10) -0.20355(7) 0.21640(5) 0.0361(2) Uani 1 1 d ...
O1 O -0.1852(2) 0.2411(2) 0.10527(14) 0.0389(6) Uani 1 1 d ...
H1 H -0.2310 0.1970 0.0908 0.058 Uiso 1 1 calc R ...
O13 O 0.1841(4) 0.6014(2) 0.03352(16) 0.0689(9) Uani 1 1 d ...
O2 O 0.2046(3) 0.3668(2) 0.05242(16) 0.0466(6) Uani 1 1 d ...
H2 H 0.1890 0.4404 0.0434 0.070 Uiso 1 1 calc R ...
O3 O 0.3110(2) -0.0915(2) -0.04748(13) 0.0397(6) Uani 1 1 d ...
H3 H 0.3756 -0.1307 -0.0226 0.059 Uiso 1 1 calc R ...
O4 O 0.4393(2) 0.2133(2) -0.00898(14) 0.0402(6) Uani 1 1 d ...
H4 H 0.3881 0.2700 0.0133 0.060 Uiso 1 1 calc R ...
O5 O 0.3938(3) 0.2529(2) 0.37885(13) 0.0423(6) Uani 1 1 d ...
O6 O 0.2152(2) 0.3086(2) 0.28631(14) 0.0387(6) Uani 1 1 d ...
O7 O 0.5924(3) 0.4096(3) 0.39623(17) 0.0664(9) Uani 1 1 d ...
O8 O 0.7228(3) 0.2662(3) 0.33598(19) 0.0673(9) Uani 1 1 d ...
O9 O 0.2330(3) -0.2254(2) 0.14833(14) 0.0498(7) Uani 1 1 d ...
O10 O -0.0216(3) -0.1992(2) 0.21127(16) 0.0517(7) Uani 1 1 d ...
O11 O 0.0349(3) -0.4374(2) 0.20485(18) 0.0585(8) Uani 1 1 d ...
O12 O -0.1047(3) -0.4792(3) 0.31529(19) 0.0679(9) Uani 1 1 d ...
C1 C 0.1999(3) 0.1173(2) 0.10538(14) 0.0147(6) Uani 1 1 d ...
H1A H 0.1426 0.0530 0.1205 0.018 Uiso 1 1 calc R ...
C2 C 0.0743(3) 0.2065(3) 0.08972(18) 0.0306(7) Uani 1 1 d ...
H2A H 0.0687 0.2108 0.0314 0.037 Uiso 1 1 calc R ...
C3 C -0.0652(3) 0.1716(3) 0.1377(2) 0.0351(8) Uani 1 1 d ...
H3A H -0.0633 0.0875 0.1356 0.042 Uiso 1 1 calc R ...
H3B H -0.0738 0.1831 0.1948 0.042 Uiso 1 1 calc R ...
C4 C 0.0837(4) 0.3283(3) 0.1041(2) 0.0364(8) Uani 1 1 d ...
H4A H -0.0047 0.3836 0.0935 0.044 Uiso 1 1 calc R ...
H4B H 0.0926 0.3276 0.1610 0.044 Uiso 1 1 calc R ...
C5 C 0.2888(3) 0.0619(3) 0.03833(18) 0.0305(7) Uani 1 1 d ...
H5 H 0.3719 0.0093 0.0597 0.037 Uiso 1 1 calc R ...
C6 C 0.2121(3) -0.0165(3) 0.0044(2) 0.0344(8) Uani 1 1 d ...
H6A H 0.1621 -0.0650 0.0494 0.041 Uiso 1 1 calc R ...
H6B H 0.1396 0.0335 -0.0260 0.041 Uiso 1 1 calc R ...
C7 C 0.3507(3) 0.1462(3) -0.03162(18) 0.0323(8) Uani 1 1 d ...

H7A H 0.4069 0.1002 -0.0747 0.039 Uiso 1 1 calc R ...
H7B H 0.2709 0.2004 -0.0540 0.039 Uiso 1 1 calc R ...
C8 C 0.3812(3) 0.1478(3) 0.18017(18) 0.0310(7) Uani 1 1 d ...
H8A H 0.4608 0.0981 0.1486 0.037 Uiso 1 1 calc R ...
H8B H 0.3699 0.2280 0.1504 0.037 Uiso 1 1 calc R ...
C9 C 0.4215(3) 0.1527(2) 0.25876(15) 0.0148(6) Uani 1 1 d ...
H9 H 0.3627 0.0984 0.2948 0.018 Uiso 1 1 calc R ...
C10 C 0.4557(3) 0.3819(3) 0.24398(19) 0.0320(7) Uani 1 1 d ...
C11 C 0.4090(4) 0.4429(3) 0.1741(2) 0.0398(9) Uani 1 1 d ...
H11 H 0.3237 0.4301 0.1603 0.048 Uiso 1 1 calc R ...
C12 C 0.4852(4) 0.5218(3) 0.1247(2) 0.0484(10) Uani 1 1 d ...
H12 H 0.4515 0.5635 0.0776 0.058 Uiso 1 1 calc R ...
C13 C 0.6099(5) 0.5402(4) 0.1437(2) 0.0584(12) Uani 1 1 d ...
H13 H 0.6641 0.5921 0.1085 0.070 Uiso 1 1 calc R ...
C14 C 0.6559(4) 0.4838(3) 0.2133(2) 0.0488(10) Uani 1 1 d ...
H14 H 0.7407 0.4977 0.2271 0.059 Uiso 1 1 calc R ...
C15 C 0.5784(4) 0.4071(3) 0.26300(19) 0.0355(8) Uani 1 1 d ...
C16 C 0.5682(4) 0.0915(3) 0.2707(2) 0.0381(8) Uani 1 1 d ...
H16A H 0.6317 0.0927 0.2178 0.046 Uiso 1 1 calc R ...
H16B H 0.6048 0.1356 0.3047 0.046 Uiso 1 1 calc R ...
C17 C 0.5756(3) -0.0320(3) 0.3090(2) 0.0368(8) Uani 1 1 d ...
C18 C 0.5202(4) -0.0579(4) 0.3893(2) 0.0511(10) Uani 1 1 d ...
H18 H 0.4728 0.0030 0.4208 0.061 Uiso 1 1 calc R ...
C19 C 0.5353(5) -0.1759(5) 0.4234(3) 0.0824(18) Uani 1 1 d ...
H19 H 0.4970 -0.1965 0.4783 0.099 Uiso 1 1 calc R ...
C20 C 0.6067(6) -0.2616(5) 0.3759(6) 0.106(3) Uani 1 1 d ...
H20 H 0.6201 -0.3415 0.3992 0.128 Uiso 1 1 calc R ...
C21 C 0.6586(6) -0.2345(5) 0.2966(5) 0.102(2) Uani 1 1 d ...
H21 H 0.7048 -0.2951 0.2646 0.122 Uiso 1 1 calc R ...
C22 C 0.6439(4) -0.1219(4) 0.2639(3) 0.0609(12) Uani 1 1 d ...
H22 H 0.6811 -0.1033 0.2086 0.073 Uiso 1 1 calc R ...
C23 C 0.2670(3) -0.0307(3) 0.22263(18) 0.0295(7) Uani 1 1 d ...
H23A H 0.3367 -0.0780 0.1844 0.035 Uiso 1 1 calc R ...
H23B H 0.3086 -0.0374 0.2721 0.035 Uiso 1 1 calc R ...
C24 C 0.1338(3) -0.0791(2) 0.24288(15) 0.0144(6) Uani 1 1 d ...
H24 H 0.0910 -0.0309 0.1967 0.017 Uiso 1 1 calc R ...
C25 C 0.0186(3) -0.0285(3) 0.30499(19) 0.0342(8) Uani 1 1 d ...
H25A H -0.0747 -0.0308 0.2904 0.041 Uiso 1 1 calc R ...
H25B H 0.0242 0.0549 0.3043 0.041 Uiso 1 1 calc R ...
C26 C 0.0231(3) -0.0901(3) 0.38988(19) 0.0321(8) Uani 1 1 d ...
C27 C -0.0773(4) -0.1578(3) 0.4258(2) 0.0381(8) Uani 1 1 d ...
H27 H -0.1496 -0.1649 0.3974 0.046 Uiso 1 1 calc R ...
C28 C -0.0742(4) -0.2158(3) 0.5031(2) 0.0455(9) Uani 1 1 d ...
H28 H -0.1448 -0.2616 0.5277 0.055 Uiso 1 1 calc R ...
C29 C 0.0321(4) -0.2067(3) 0.5445(2) 0.0475(10) Uani 1 1 d ...
H29 H 0.0359 -0.2477 0.5970 0.057 Uiso 1 1 calc R ...
C30 C 0.1315(4) -0.1386(3) 0.5094(2) 0.0453(9) Uani 1 1 d ...
H30 H 0.2041 -0.1323 0.5379 0.054 Uiso 1 1 calc R ...
C31 C 0.1273(4) -0.0787(3) 0.4325(2) 0.0387(8) Uani 1 1 d ...
H31 H 0.1953 -0.0300 0.4091 0.046 Uiso 1 1 calc R ...
C32 C 0.1675(3) -0.3161(3) 0.2969(2) 0.0332(8) Uani 1 1 d ...
C33 C 0.0962(3) -0.4099(3) 0.3233(2) 0.0341(8) Uani 1 1 d ...
C34 C 0.1176(4) -0.4836(3) 0.3932(2) 0.0399(9) Uani 1 1 d ...
H34 H 0.0641 -0.5448 0.4116 0.048 Uiso 1 1 calc R ...
C35 C 0.2169(4) -0.4678(3) 0.4361(2) 0.0445(9) Uani 1 1 d ...
H35 H 0.2320 -0.5177 0.4845 0.053 Uiso 1 1 calc R ...
C36 C 0.2938(4) -0.3799(3) 0.4085(2) 0.0474(10) Uani 1 1 d ...
H36 H 0.3652 -0.3709 0.4369 0.057 Uiso 1 1 calc R ...
C37 C 0.2692(4) -0.3039(3) 0.3398(2) 0.0384(8) Uani 1 1 d ...
H37 H 0.3228 -0.2427 0.3220 0.046 Uiso 1 1 calc R ...
N1 N 0.2430(3) 0.0998(3) 0.18466(19) 0.0499(8) Uani 1 1 d ...
N2 N 0.0015(3) -0.4425(2) 0.2774(2) 0.0452(8) Uani 1 1 d ...
N3 N 0.6326(4) 0.3565(3) 0.3382(2) 0.0479(8) Uani 1 1 d ...

`loop_`
`_atom_site_aniso_label`

`_atom_site_aniso_U_11`
`_atom_site_aniso_U_22`
`_atom_site_aniso_U_33`
`_atom_site_aniso_U_23`
`_atom_site_aniso_U_13`
`_atom_site_aniso_U_12`
`S1 0.0359(5) 0.0328(5) 0.0303(4) -0.0006(3) -0.0063(3) -0.0131(4)`
`S2 0.0464(5) 0.0292(5) 0.0364(5) 0.0007(4) -0.0125(4) -0.0139(4)`
`O1 0.0362(14) 0.0349(14) 0.0489(14) -0.0017(11) -0.0140(11) -0.0100(11)`
`O13 0.118(3) 0.0396(17) 0.0532(17) 0.0039(13) -0.0243(17) -0.0217(17)`
`O2 0.0490(16) 0.0321(14) 0.0599(16) 0.0043(12) -0.0087(13) -0.0180(12)`
`O3 0.0407(14) 0.0412(15) 0.0410(14) -0.0120(11) -0.0097(11) -0.0084(11)`
`O4 0.0410(14) 0.0415(16) 0.0404(14) 0.0008(11) -0.0029(11) -0.0206(12)`
`O5 0.0587(16) 0.0451(15) 0.0284(12) 0.0007(11) -0.0089(11) -0.0240(13)`
`O6 0.0318(13) 0.0386(14) 0.0466(14) -0.0094(11) -0.0040(11) -0.0079(11)`
`O7 0.091(2) 0.075(2) 0.0454(17) -0.0103(16) -0.0266(16) -0.0283(18)`
`O8 0.076(2) 0.0503(19) 0.085(2) 0.0086(16) -0.0510(18) -0.0107(17)`
`O9 0.0794(19) 0.0335(15) 0.0356(14) -0.0054(11) -0.0018(13) -0.0148(13)`
`O10 0.0528(16) 0.0431(16) 0.0704(18) 0.0044(13) -0.0355(14) -0.0195(13)`
`O11 0.086(2) 0.0449(17) 0.0560(18) -0.0083(14) -0.0246(16) -0.0232(15)`
`O12 0.0539(18) 0.064(2) 0.094(2) 0.0135(17) -0.0256(16) -0.0356(16)`
`C1 0.0189(14) 0.0139(14) 0.0115(12) 0.0020(10) -0.0030(10) -0.0058(11)`
`C2 0.0381(19) 0.0282(18) 0.0271(16) -0.0009(13) -0.0054(14) -0.0113(15)`
`C3 0.0325(18) 0.034(2) 0.0382(19) 0.0035(15) -0.0101(15) -0.0078(15)`
`C4 0.0367(19) 0.0297(19) 0.043(2) 0.0026(15) -0.0092(16) -0.0098(16)`
`C5 0.0296(17) 0.0334(19) 0.0295(17) -0.0004(14) -0.0051(13) -0.0106(14)`
`C6 0.0368(19) 0.033(2) 0.0357(18) -0.0061(15) -0.0044(15) -0.0121(16)`
`C7 0.0345(19) 0.038(2) 0.0264(16) 0.0003(14) -0.0047(14) -0.0142(15)`
`C8 0.0321(18) 0.0292(18) 0.0331(17) 0.0001(14) -0.0049(14) -0.0124(14)`
`C9 0.0157(13) 0.0140(14) 0.0154(13) 0.0035(10) -0.0029(10) -0.0080(11)`
`C10 0.0374(19) 0.0295(19) 0.0319(17) -0.0009(14) -0.0082(14) -0.0122(15)`
`C11 0.048(2) 0.033(2) 0.043(2) 0.0048(16) -0.0207(17) -0.0139(17)`
`C12 0.069(3) 0.041(2) 0.041(2) 0.0139(17) -0.0244(19) -0.024(2)`
`loop_`
`_geom_bond_atom_site_label_1 O2 H2 0.8400 . ?`
`_geom_bond_atom_site_label_2 O3 C6 1.432(4) . ?`
`_geom_bond_distance O3 H3 0.8400 . ?`
`_geom_bond_site_symmetry_2 O4 C7 1.420(4) . ?`
`_geom_bond_publ_flag`
`S1 O5 1.428(2) . ?`
`S1 O6 1.429(2) . ?`
`S1 C9 1.626(3) . ?`
`S1 C10 1.774(3) . ?`
`S2 O10 1.425(2) . ?`
`S2 O9 1.427(3) . ?`
`S2 C24 1.621(3) . ?`
`S2 C32 1.793(3) . ?`
`O1 C3 1.428(4) . ?`
`O1 H1 0.8400 . ?`
`O2 C4 1.432(4) . ?`
`C13 0.071(3) 0.051(3) 0.059(3) 0.018(2) -0.020(2) -0.035(2)`
`C14 0.051(2) 0.048(2) 0.057(2) 0.0052(19) -0.0211(19) -0.0276(19)`
`C15 0.049(2) 0.0289(19) 0.0348(18) 0.0006(14) -0.0183(16) -0.0136(16)`
`C16 0.0351(19) 0.040(2) 0.0401(19) 0.0012(16) -0.0087(15) -0.0124(16)`
`C17 0.0307(18) 0.033(2) 0.051(2) -0.0049(17) -0.0177(16) -0.0068(15)`
`C18 0.043(2) 0.060(3) 0.048(2) 0.012(2) -0.0104(18) -0.016(2)`
`C19 0.051(3) 0.094(4) 0.100(4) 0.047(4) -0.032(3) -0.034(3)`
`C20 0.060(4) 0.045(3) 0.219(8) 0.048(5) -0.073(5) -0.025(3)`
`C21 0.075(4) 0.039(3) 0.210(8) -0.031(4) -0.069(5) 0.002(3)`
`C22 0.044(2) 0.058(3) 0.089(3) -0.029(3) -0.028(2) 0.002(2)`
`C23 0.0314(18) 0.0281(18) 0.0297(17) 0.0036(14) -0.0043(14) -0.0132(14)`
`C24 0.0169(14) 0.0111(14) 0.0148(13) 0.0045(10) -0.0019(10) -0.0070(11)`
`C25 0.0327(18) 0.035(2) 0.0351(18) 0.0028(15) -0.0055(14) -0.0125(15)`
`C26 0.0324(18) 0.0296(19) 0.0325(17) -0.0008(14) 0.0005(14) -0.0097(15)`
`C27 0.038(2) 0.035(2) 0.042(2) -0.0018(16) -0.0042(16) -0.0126(16)`
`C28 0.054(2) 0.036(2) 0.042(2) 0.0030(17) 0.0051(18) -0.0140(18)`
`C29 0.064(3) 0.039(2) 0.035(2) 0.0031(17) -0.0053(18) -0.008(2)`
`C30 0.048(2) 0.049(2) 0.038(2) -0.0066(18) -0.0115(17) -0.0029(19)`
`C31 0.039(2) 0.041(2) 0.0361(19) -0.0019(16) -0.0031(15) -0.0130(17)`
`C32 0.0371(19) 0.0244(18) 0.0390(19) -0.0022(14) -0.0067(15) -0.0084(15)`
`C33 0.0336(18) 0.0270(19) 0.044(2) -0.0047(15) -0.0087(15) -0.0092(15)`
`C34 0.045(2) 0.0259(19) 0.047(2) 0.0001(16) -0.0020(17) -0.0090(16)`
`C35 0.063(3) 0.030(2) 0.041(2) 0.0074(16) -0.0166(18) -0.0107(18)`
`C36 0.052(2) 0.040(2) 0.057(2) 0.0020(18) -0.0257(19) -0.0124(19)`
`C37 0.042(2) 0.0258(19) 0.051(2) 0.0026(16) -0.0145(17) -0.0130(16)`
`N1 0.055(2) 0.044(2) 0.055(2) 0.0085(15) -0.0163(16) -0.0233(16)`
`N2 0.052(2) 0.0277(17) 0.061(2) 0.0014(15) -0.0205(17) -0.0138(15)`
`N3 0.059(2) 0.045(2) 0.053(2) 0.0070(17) -0.0302(17) -0.0288(18)`

`_geom_special_details`
`;`

All esds (except the esd in the dihedral angle between two l.s. planes) are estimated using the full covariance matrix. The cell esds are taken into account individually in the estimation of esds in distances, angles and torsion angles; correlations between esds in cell parameters are only used when they are defined by crystal symmetry. An approximate isotropic treatment of cell esds is used for estimating esds involving l.s. planes.

`;`

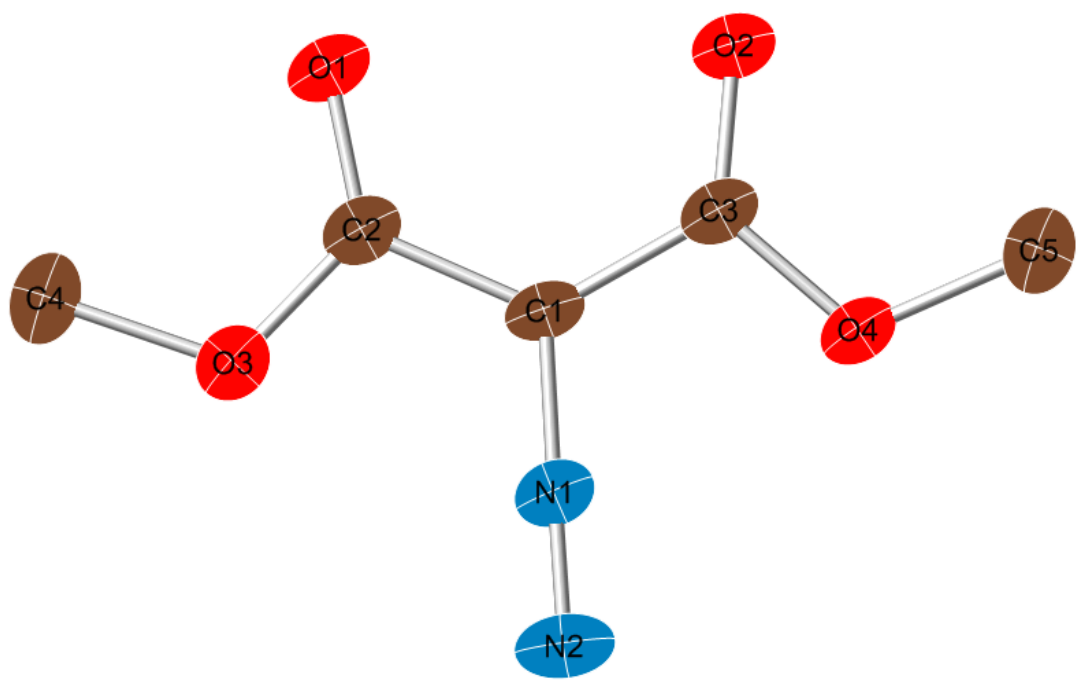
C10 C11 1.392(4) . ?	O6 S1 C9 105.99(13) . . ?	C16 C9 H9 100.7 . . ?
C11 C12 1.380(5) . ?	O5 S1 C10 107.08(14) . . ?	S1 C9 H9 100.7 . . ?
C11 H11 0.9500 . ?	O6 S1 C10 107.15(15) . . ?	C15 C10 C11 117.2(3) . . ?
C12 C13 1.377(5) . ?	C9 S1 C10 107.54(15) . . ?	C15 C10 S1 124.8(2) . . ?
C12 H12 0.9500 . ?	O10 S2 O9 120.18(16) . . ?	C11 C10 S1 117.8(2) . . ?
C13 C14 1.370(5) . ?	O10 S2 C24 106.74(15) . . ?	C12 C11 C10 120.8(3) . . ?
C13 H13 0.9500 . ?	O9 S2 C24 107.85(14) . . ?	C12 C11 H11 119.6 . . ?
C14 C15 1.372(5) . ?	O10 S2 C32 106.85(15) . . ?	C10 C11 H11 119.6 . . ?
C14 H14 0.9500 . ?	O9 S2 C32 107.05(15) . . ?	C13 C12 C11 120.1(3) . . ?
C15 N3 1.470(4) . ?	C24 S2 C32 107.62(14) . . ?	C13 C12 H12 120.0 . . ?
C16 C17 1.485(5) . ?	C3 O1 H1 109.5 . . ?	C11 C12 H12 120.0 . . ?
C16 H16A 0.9900 . ?	C4 O2 H2 109.5 . . ?	C14 C13 C12 120.2(3) . . ?
C16 H16B 0.9900 . ?	C6 O3 H3 109.5 . . ?	C14 C13 H13 119.9 . . ?
C17 C18 1.382(5) . ?	C7 O4 H4 109.5 . . ?	C12 C13 H13 119.9 . . ?
C17 C22 1.384(5) . ?	C5 C1 N1 121.9(3) . . ?	C13 C14 C15 119.5(3) . . ?
C18 C19 1.402(6) . ?	C5 C1 C2 118.4(2) . . ?	C13 C14 H14 120.2 . . ?
C18 H18 0.9500 . ?	N1 C1 C2 119.1(2) . . ?	C15 C14 H14 120.2 . . ?
C19 C20 1.380(9) . ?	C5 C1 H1A 92.6 . . ?	C14 C15 C10 122.0(3) . . ?
C19 H19 0.9500 . ?	N1 C1 H1A 92.6 . . ?	C14 C15 N3 115.1(3) . . ?
C20 C21 1.360(9) . ?	C2 C1 H1A 92.6 . . ?	C10 C15 N3 122.8(3) . . ?
C20 H20 0.9500 . ?	C1 C2 C4 113.8(3) . . ?	C17 C16 C9 113.9(3) . . ?
C21 C22 1.339(7) . ?	C1 C2 C3 111.9(2) . . ?	C17 C16 H16A 108.8 . . ?
C21 H21 0.9500 . ?	C4 C2 C3 110.0(3) . . ?	C9 C16 H16A 108.8 . . ?
C22 H22 0.9500 . ?	C1 C2 H2A 106.9 . . ?	C17 C16 H16B 108.8 . . ?
C23 C24 1.477(4) . ?	C4 C2 H2A 106.9 . . ?	C9 C16 H16B 108.8 . . ?
C23 N1 1.553(4) . ?	C3 C2 H2A 106.9 . . ?	H16A C16 H16B 107.7 . . ?
C23 H23A 0.9900 . ?	O1 C3 C2 110.3(3) . . ?	C18 C17 C22 119.9(4) . . ?
C23 H23B 0.9900 . ?	O1 C3 H3A 109.6 . . ?	C18 C17 C16 120.9(3) . . ?
C24 C25 1.481(4) . ?	C2 C3 H3A 109.6 . . ?	C22 C17 C16 119.2(4) . . ?
C24 H24 1.0000 . ?	O1 C3 H3B 109.6 . . ?	C17 C18 C19 118.7(5) . . ?
C25 C26 1.516(4) . ?	C2 C3 H3B 109.6 . . ?	C17 C18 H18 120.7 . . ?
C25 H25A 0.9900 . ?	H3A C3 H3B 108.1 . . ?	C19 C18 H18 120.7 . . ?
C25 H25B 0.9900 . ?	O2 C4 C2 110.2(3) . . ?	C20 C19 C18 118.8(5) . . ?
C26 C27 1.374(4) . ?	O2 C4 H4A 109.6 . . ?	C20 C19 H19 120.6 . . ?
C26 C31 1.393(5) . ?	C2 C4 H4A 109.6 . . ?	C18 C19 H19 120.6 . . ?
C27 C28 1.386(5) . ?	O2 C4 H4B 109.6 . . ?	C21 C20 C19 121.6(5) . . ?
C27 H27 0.9500 . ?	C2 C4 H4B 109.6 . . ?	C21 C20 H20 119.2 . . ?
C28 C29 1.387(5) . ?	H4A C4 H4B 108.1 . . ?	C19 C20 H20 119.2 . . ?
C28 H28 0.9500 . ?	C1 C5 C6 112.5(2) . . ?	C22 C21 C20 119.6(6) . . ?
C29 C30 1.367(5) . ?	C1 C5 C7 115.2(3) . . ?	C22 C21 H21 120.2 . . ?
C29 H29 0.9500 . ?	C6 C5 C7 108.4(3) . . ?	C20 C21 H21 120.2 . . ?
C30 C31 1.389(5) . ?	C1 C5 H5 106.7 . . ?	C21 C22 C17 121.4(5) . . ?
C30 H30 0.9500 . ?	C6 C5 H5 106.7 . . ?	C21 C22 H22 119.3 . . ?
C31 H31 0.9500 . ?	C7 C5 H5 106.7 . . ?	C17 C22 H22 119.3 . . ?
C32 C37 1.378(4) . ?	O3 C6 C5 111.2(3) . . ?	C24 C23 N1 112.7(2) . . ?
C32 C33 1.389(4) . ?	O3 C6 H6A 109.4 . . ?	C24 C23 H23A 109.1 . . ?
C33 C34 1.380(5) . ?	C5 C6 H6A 109.4 . . ?	N1 C23 H23A 109.1 . . ?
C33 N2 1.457(4) . ?	O3 C6 H6B 109.4 . . ?	C24 C23 H23B 109.1 . . ?
C34 C35 1.373(5) . ?	C5 C6 H6B 109.4 . . ?	N1 C23 H23B 109.1 . . ?
C34 H34 0.9500 . ?	H6A C6 H6B 108.0 . . ?	H23A C23 H23B 107.8 . . ?
C35 C36 1.368(5) . ?	O4 C7 C5 113.4(2) . . ?	C23 C24 C25 118.5(2) . . ?
C35 H35 0.9500 . ?	O4 C7 H7A 108.9 . . ?	C23 C24 S2 121.8(2) . . ?
C36 C37 1.381(5) . ?	C5 C7 H7A 108.9 . . ?	C25 C24 S2 118.1(2) . . ?
C36 H36 0.9500 . ?	O4 C7 H7B 108.9 . . ?	C23 C24 H24 94.3 . . ?
C37 H37 0.9500 . ?	C5 C7 H7B 108.9 . . ?	C25 C24 H24 94.3 . . ?
loop_	H7A C7 H7B 107.7 . . ?	S2 C24 H24 94.3 . . ?
_geom_angle_atom_site_label_1	C9 C8 N1 115.3(2) . . ?	C24 C25 C26 114.8(3) . . ?
_geom_angle_atom_site_label_2	C9 C8 H8A 108.4 . . ?	C24 C25 H25A 108.6 . . ?
_geom_angle_atom_site_label_3	N1 C8 H8A 108.4 . . ?	C26 C25 H25A 108.6 . . ?
_geom_angle	C9 C8 H8B 108.4 . . ?	C24 C25 H25B 108.6 . . ?
_geom_angle_site_symmetry_1	N1 C8 H8B 108.4 . . ?	C26 C25 H25B 108.6 . . ?
_geom_angle_site_symmetry_3	H8A C8 H8B 107.5 . . ?	H25A C25 H25B 107.5 . . ?
_geom_angle_publ_flag	C8 C9 C16 116.3(3) . . ?	C27 C26 C31 119.2(3) . . ?
O5 S1 O6 120.88(14) . . ?	C8 C9 S1 117.1(2) . . ?	C27 C26 C25 119.8(3) . . ?
O5 S1 C9 107.60(14) . . ?	C16 C9 S1 116.5(2) . . ?	C31 C26 C25 121.0(3) . . ?
	C8 C9 H9 100.7 . . ?	C26 C27 C28 120.7(3) . . ?

C26 C27 H27 119.6...?
 C28 C27 H27 119.6...?
 C27 C28 C29 119.8(3)...?
 C27 C28 H28 120.1...?
 C29 C28 H28 120.1...?
 C30 C29 C28 119.8(3)...?
 C30 C29 H29 120.1...?
 C28 C29 H29 120.1...?
 C29 C30 C31 120.6(3)...?
 C29 C30 H30 119.7...?
 C31 C30 H30 119.7...?
 C30 C31 C26 119.8(3)...?
 C30 C31 H31 120.1...?
 C26 C31 H31 120.1...?
 C37 C32 C33 117.6(3)...?
 C37 C32 S2 118.3(2)...?
 C33 C32 S2 123.9(3)...?
 C34 C33 C32 121.7(3)...?
 C34 C33 N2 115.1(3)...?
 C32 C33 N2 123.1(3)...?
 C35 C34 C33 119.5(3)...?
 C35 C34 H34 120.2...?
 C33 C34 H34 120.2...?
 C36 C35 C34 119.5(3)...?
 C36 C35 H35 120.3...?
 C34 C35 H35 120.3...?
 C35 C36 C37 120.9(3)...?
 C35 C36 H36 119.5...?
 C37 C36 H36 119.5...?
 C32 C37 C36 120.7(3)...?
 C32 C37 H37 119.7...?
 C36 C37 H37 119.7...?
 C1 N1 C8 110.8(2)...?
 C1 N1 C23 113.5(3)...?
 C8 N1 C23 108.4(2)...?
 O11 N2 O12 123.6(3)...?
 O11 N2 C33 118.8(3)...?
 O12 N2 C33 117.5(3)...?
 O7 N3 O8 124.5(3)...?
 O7 N3 C15 118.5(3)...?
 O8 N3 C15 116.9(3)...?

 loop_
 _geom_torsion_atom_site_label_1
 _geom_torsion_atom_site_label_2
 _geom_torsion_atom_site_label_3
 _geom_torsion_atom_site_label_4
 _geom_torsion
 _geom_torsion_site_symmetry_1
 _geom_torsion_site_symmetry_2
 _geom_torsion_site_symmetry_3
 _geom_torsion_site_symmetry_4
 _geom_torsion_publ_flag
 C5 C1 C2 C4 -114.6(3)...?
 N1 C1 C2 C4 56.4(3)...?
 C5 C1 C2 C3 119.9(3)...?
 N1 C1 C2 C3 -69.0(3)...?
 C1 C2 C3 O1 -163.7(2)...?
 C4 C2 C3 O1 68.8(3)...?
 C1 C2 C4 O2 60.4(3)...?
 C3 C2 C4 O2 -173.2(2)...?
 N1 C1 C5 C6 121.5(3)...?
 C2 C1 C5 C6 -67.7(3)...?
 N1 C1 C5 C7 -113.5(3)...?
 C2 C1 C5 C7 57.3(4)...?
 C1 C5 C6 O3 -165.8(2)...?

 C7 C5 C6 O3 65.6(3)...?
 C1 C5 C7 O4 60.3(4)...?
 C6 C5 C7 O4 -172.6(3)...?
 N1 C8 C9 C16 125.3(3)...?
 N1 C8 C9 S1 -90.4(3)...?
 O5 S1 C9 C8 171.7(2)...?
 O6 S1 C9 C8 41.1(2)...?
 C10 S1 C9 C8 -73.3(2)...?
 O5 S1 C9 C16 -44.1(2)...?
 O6 S1 C9 C16 -174.7(2)...?
 C10 S1 C9 C16 71.0(2)...?
 O5 S1 C10 C15 22.6(4)...?
 O6 S1 C10 C15 153.7(3)...?
 C9 S1 C10 C15 -92.8(3)...?
 O5 S1 C10 C11 -160.6(3)...?
 O6 S1 C10 C11 -29.5(3)...?
 C9 S1 C10 C11 84.1(3)...?
 C15 C10 C11 C12 2.3(5)...?
 S1 C10 C11 C12 -174.8(3)...?
 C10 C11 C12 C13 0.7(6)...?
 C11 C12 C13 C14 -2.6(7)...?
 C12 C13 C14 C15 1.4(7)...?
 C13 C14 C15 C10 1.8(6)...?
 C13 C14 C15 N3 -176.7(4)...?
 C11 C10 C15 C14 -3.6(5)...?
 S1 C10 C15 C14 173.3(3)...?
 C11 C10 C15 N3 174.8(3)...?
 S1 C10 C15 N3 -8.3(5)...?
 C8 C9 C16 C17 -92.2(3)...?
 S1 C9 C16 C17 123.3(3)...?
 C9 C16 C17 C18 -71.3(4)...?
 C9 C16 C17 C22 111.1(4)...?
 C22 C17 C18 C19 0.2(5)...?
 C16 C17 C18 C19 -177.3(3)...?
 C17 C18 C19 C20 1.0(6)...?
 C18 C19 C20 C21 -2.1(8)...?
 C19 C20 C21 C22 1.9(8)...?
 C20 C21 C22 C17 -0.7(7)...?
 C18 C17 C22 C21 -0.4(6)...?
 C16 C17 C22 C21 177.2(4)...?
 N1 C23 C24 C25 -64.1(3)...?
 N1 C23 C24 S2 131.0(2)...?
 O10 S2 C24 C23 -154.2(2)...?
 O9 S2 C24 C23 -23.8(3)...?
 C32 S2 C24 C23 91.4(2)...?
 O10 S2 C24 C25 40.9(3)...?
 O9 S2 C24 C25 171.3(2)...?
 C32 S2 C24 C25 -73.5(2)...?
 C23 C24 C25 C26 -92.1(3)...?
 S2 C24 C25 C26 73.3(3)...?
 C24 C25 C26 C27 -108.1(3)...?
 C24 C25 C26 C31 72.3(4)...?
 C31 C26 C27 C28 -1.1(5)...?
 C25 C26 C27 C28 179.4(3)...?
 C26 C27 C28 C29 -0.7(6)...?
 C27 C28 C29 C30 1.4(6)...?
 C28 C29 C30 C31 -0.2(6)...?
 C29 C30 C31 C26 -1.6(6)...?
 C27 C26 C31 C30 2.2(5)...?
 C25 C26 C31 C30 -178.2(3)...?
 O10 S2 C32 C37 -149.6(3)...?
 O9 S2 C32 C37 80.5(3)...?
 C24 S2 C32 C37 -35.3(3)...?
 O10 S2 C32 C33 24.7(3)...?
 O9 S2 C32 C33 -105.3(3)...?
 C24 S2 C32 C33 139.0(3)...?

APPENDIX 9
CRYSTAL STRUCTURE DATA FOR **19**



```

data_cmca (Dimethyl diazomalonate)

_audit_creation_method      SHELXL-97
_chemical_name_systematic;
?
;
_chemical_name_common      ?
_chemical_melting_point    ?
_chemical_formula_moiety   'C5 H6 N2 O4'
_chemical_formula_sum       'C5 H6 N2 O4'
_chemical_formula_weight    158.12

loop_
_atom_type_symbol
_atom_type_description
_atom_type_scat_dispersion_real
_atom_type_scat_dispersion_imag
_atom_type_scat_source
'C' 'C' 0.0033 0.0016
'International Tables Vol C Tables 4.2.6.8 and 6.1.1.4'
'H' 'H' 0.0000 0.0000
'International Tables Vol C Tables 4.2.6.8 and 6.1.1.4'
'N' 'N' 0.0061 0.0033
'International Tables Vol C Tables 4.2.6.8 and 6.1.1.4'
'O' 'O' 0.0106 0.0060
'International Tables Vol C Tables 4.2.6.8 and 6.1.1.4'

_symmetry_cell_setting     'Orthorhombic'
_symmetry_space_group_name_H-M 'C m c a'

loop_
_symmetry_equiv_pos_as_xyz
'x, y, z'
'-x, -y+1/2, z+1/2'
'-x, y+1/2, -z+1/2'
'x, -y, -z'
'x+1/2, y+1/2, z'
'-x+1/2, -y+1, z+1/2'
'-x+1/2, y+1, -z+1/2'
'x+1/2, -y+1/2, -z'
'-x, -y, -z'
'x, y-1/2, -z-1/2'
'x, -y-1/2, z-1/2'
'-x, y, z'
'-x+1/2, -y+1/2, -z'
'x+1/2, y, -z-1/2'
'x+1/2, -y, z-1/2'
'-x+1/2, y+1/2, z'

_cell_length_a            6.3203(7)
_cell_length_b            20.753(2)
_cell_length_c            11.0951(12)
_cell_angle_alpha          90.00
_cell_angle_beta           90.00
_cell_angle_gamma          90.00
_cell_volume              1455.3(3)
_cell_formula_units_Z      8
_cell_measurement_temperature 183(2)
_cell_measurement_reflns_used 988
_cell_measurement_theta_min 1.96
_cell_measurement_theta_max 28.270

_exptl_crystal_description 'fragment'
_exptl_crystal_colour      'yellow'

_exptl_crystal_size_max     .1
_exptl_crystal_size_mid     .1
_exptl_crystal_size_min     .08
_exptl_crystal_density_meas ?
_exptl_crystal_density_diffn 1.443
_exptl_crystal_density_method 'not measured'
_exptl_crystal_F_000        656
_exptl_absorpt_coefficient_mu 0.127
_exptl_absorpt_correction_type 'none'
_exptl_absorpt_correction_T_min ?
_exptl_absorpt_correction_T_max ?
_exptl_absorpt_process_details ?

_exptl_special_details
;
?
;

_diffrn_ambient_temperature 183(2)
_diffrn_radiation_wavelength 0.71073
_diffrn_radiation_type      MoK $\alpha$ 
_diffrn_radiation_source    'fine-focus sealed tube'
_diffrn_radiation_monochromator graphite
_diffrn_measurement_device_type ?
_diffrn_measurement_method   ?
_diffrn_detector_area_resol_mean ?
_diffrn_standards_number    ?
_diffrn_standards_interval_count ?
_diffrn_standards_interval_time ?
_diffrn_standards_decay_% ?
_diffrn_reflns_number        7096
_diffrn_reflns_av_R_equivalents 0.0303
_diffrn_reflns_av_sigmaI/netI 0.0184
_diffrn_reflns_limit_h_min   -8
_diffrn_reflns_limit_h_max   8
_diffrn_reflns_limit_k_min   -27
_diffrn_reflns_limit_k_max   27
_diffrn_reflns_limit_l_min   -14
_diffrn_reflns_limit_l_max   14
_diffrn_reflns_theta_min     1.96
_diffrn_reflns_theta_max     28.27
_reflns_number_total         988
_reflns_number_gt             961
_reflns_threshold_expression >2sigma(I)

_computing_data_collection ?
_computing_cell_refinement ?
_computing_data_reduction ?
_computing_structure_solution 'SHELXS-97 (Sheldrick, 1990)'
_computing_structure_refinement 'SHELXL-97 (Sheldrick, 1997)'
_computing_molecular_graphics ?
_computing_publication_material ?

_refine_special_details
;
Refinement of F2 against ALL reflections. The weighted R-factor wR and goodness of fit S are based on F2, conventional R-factors R are based on F, with F set to zero for negative F2. The threshold expression of F2 > 2sigma(F2) is used only for calculating R-factors(gt) etc. and is not relevant to the choice of reflections for refinement. R-factors based on F2 are statistically about twice as large as those based on F, and R-

```

factors based on ALL data will be even larger.

;

_refine_ls_structure_factor_coef Fsqd
_refine_ls_matrix_type full
_refine_ls_weighting_scheme calc
_refine_ls_weighting_details
'calc w=1/[s^2^(Fo^2^)+(0.0719P)^2^+0.5057P]
P=(Fo^2^+2Fc^2^)/3'
_atom_sites_solution_primary direct
_atom_sites_solution_secondary difmap
_atom_sites_solution_hydrogens geom
_refine_ls_hydrogen_treatment constr
_refine_ls_extinction_method none
_refine_ls_extinction_coeff ?
_refine_ls_number_reflins 988
_refine_ls_number_parameters 69
_refine_ls_number_restraints 0
_refine_ls_R_factor_all 0.0486
_refine_ls_R_factor_gt 0.0475
_refine_ls_wR_factor_ref 0.1283
_refine_ls_wR_factor_gt 0.1272
_refine_ls_goodness_of_fit_ref 1.165
_refine_ls_restrained_S_all 1.165
_refine_ls_shift/su_max 0.000
_refine_ls_shift/su_mean 0.000

loop_
_atom_site_label
_atom_site_type_symbol
_atom_site_fract_x
_atom_site_fract_y
_atom_site_fract_z
_atom_site_U_iso_or_equiv
_atom_site_adp_type
_atom_site_occupancy
_atom_site_symmetry_multiplicity
_atom_site_calc_flag
_atom_site_refinement_flags
_atom_site_disorder_assembly
_atom_site_disorder_group
O2 O 0.5000 0.22276(7) 0.20199(11) 0.0450(4) Uani 1 2 d S ..
O1 O 0.5000 0.08943(6) 0.10896(11) 0.0404(3) Uani 1 2 d S ..
N1 N 0.5000 0.10326(7) 0.42323(12) 0.0355(4) Uani 1 2 d S ..
N2 N 0.5000 0.08539(8) 0.51769(14) 0.0526(5) Uani 1 2 d S ..
C3 C 0.5000 0.19531(8) 0.29726(14) 0.0339(4) Uani 1 2 d S ..

loop_
_geom_bond_atom_site_label_1 C4 H4B 0.9800 . ?
_geom_bond_atom_site_label_2 C4 H4C 0.9800 . ?
_geom_bond_distance
_geom_bond_site_symmetry_2
_geom_bond_publ_flag
O2 C3 1.201(2) . ?
O1 C2 1.202(2) . ?
N1 N2 1.112(2) . ?
N1 C1 1.3251(19) . ?
C3 O4 1.3327(18) . ?
C3 C1 1.460(2) . ?
C2 O3 1.342(2) . ?
C2 C1 1.456(2) . ?
O3 C4 1.444(2) . ?
O4 C5 1.440(2) . ?
C5 H5A 0.9800 . ?
C5 H5B 0.9800 . ?
C5 H5C 0.9800 . ?
C4 H4A 0.9800 . ?

C2 C 0.5000 0.07761(8) 0.21502(14) 0.0314(4) Uani 1 2 d S ..
O3 O 0.5000 0.01774(5) 0.26081(11) 0.0398(3) Uani 1 2 d S ..
O4 O 0.5000 0.22346(6) 0.40523(11) 0.0428(4) Uani 1 2 d S ..
C1 C 0.5000 0.12536(8) 0.31119(12) 0.0316(4) Uani 1 2 d S ..
C5 C 0.5000 0.29286(9) 0.40451(19) 0.0590(6) Uani 1 2 d S ..
H5A H 0.4896 0.3088 0.4874 0.088 Uiso 0.50 1 calc PR ..
H5B H 0.3789 0.3085 0.3577 0.088 Uiso 0.50 1 calc PR ..
H5C H 0.6315 0.3085 0.3679 0.088 Uiso 0.50 1 calc PR ..
C4 C 0.5000 -0.03366(9) 0.17315(18) 0.0483(5) Uani 1 2 d S ..
H4A H 0.4748 -0.0748 0.2139 0.073 Uiso 0.50 1 calc PR ..
H4B H 0.6373 -0.0350 0.1322 0.073 Uiso 0.50 1 calc PR ..
H4C H 0.3879 -0.0260 0.1138 0.073 Uiso 0.50 1 calc PR ..

where loop_
_atom_site_aniso_label
_atom_site_aniso_U_11
_atom_site_aniso_U_22
_atom_site_aniso_U_33
_atom_site_aniso_U_23
_atom_site_aniso_U_13
_atom_site_aniso_U_12
O2 0.0687(9) 0.0419(7) 0.0243(6) 0.0020(4) 0.000 0.000
O1 0.0551(8) 0.0442(7) 0.0219(6) -0.0019(4) 0.000 0.000
N1 0.0436(8) 0.0388(7) 0.0240(7) 0.0001(5) 0.000 0.000
N2 0.0764(12) 0.0558(10) 0.0256(8) 0.0090(7) 0.000 0.000
C3 0.0415(8) 0.0388(9) 0.0213(7) -0.0015(5) 0.000 0.000
C2 0.0307(7) 0.0389(8) 0.0245(7) -0.0014(6) 0.000 0.000
O3 0.0550(7) 0.0350(6) 0.0293(6) -0.0033(5) 0.000 0.000
O4 0.0694(9) 0.0376(7) 0.0215(6) -0.0032(4) 0.000 0.000
C1 0.0372(8) 0.0389(9) 0.0189(7) 0.0016(5) 0.000 0.000
C5 0.1042(19) 0.0359(10) 0.0369(10) -0.0078(7) 0.000 0.000
C4 0.0675(12) 0.0375(9) 0.0399(9) -0.0112(7) 0.000 0.000

_geom_special_details ;
All esds (except the esd in the dihedral angle between two l.s. planes) are estimated using the full covariance matrix. The cell esds are taken into account individually in the estimation of esds in distances, angles and torsion angles; correlations between esds in cell parameters are only used when they are defined by crystal symmetry. An approximate (isotropic) treatment of cell esds is used for estimating esds involving l.s. planes. ;

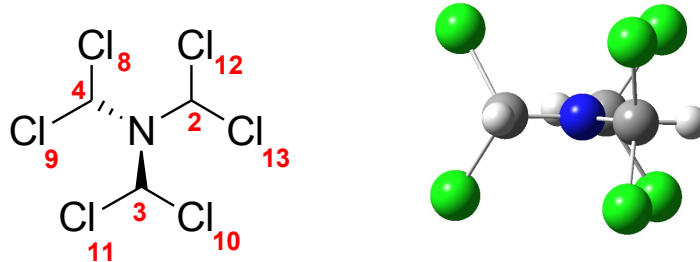
N1 C1 C2 116.86(15) . ?
N1 C1 C3 116.33(14) . ?
C2 C1 C3 126.81(14) . ?
O4 C5 H5A 109.5 . ?
O4 C5 H5B 109.5 . ?
H5A C5 H5B 109.5 . ?
O4 C5 H5C 109.5 . ?
H5A C5 H5C 109.5 . ?
H5B C5 H5C 109.5 . ?
O3 C4 H4A 109.5 . ?
O3 C4 H4B 109.5 . ?
H4A C4 H4B 109.5 . ?
O3 C4 H4C 109.5 . ?
H4A C4 H4C 109.5 . ?
H4B C4 H4C 109.5 . ?
_diffrn_measured_fraction_theta_max 0.999
_diffrn_reflins_theta_full 28.27
_diffrn_measured_fraction_theta_full 0.999

```
_refine_diff_density_max  0.216  
_refine_diff_density_min -0.269  
_refine_diff_density_rms  0.062
```

Appendix 10

Computational Details of **11, 20, 84, 85, 86, 87, 153, 106** and **107**.

1. Tris(dichloromethyl)amine, 107.



DFT/6-311 G (d, p) NBO 3.1 Second Order Perturbation Theory Analysis of Fock Matrix in NBO Basis & Occupancy.

$E_{DFT} = -2932.23878130$ a. u.

Donor NBO (i)	Acceptor NBO (j)	E(2)	E(j)-E(i)	F(i,j)	Occupancy
LP (1) N 1	BD*(1) C 2 - C 12	13.19	0.36	0.065	LP (1) N 1 1.72281
LP (1) N 1	BD*(1) C 2 - C 13	13.19	0.36	0.065	BD*(1) C 2 - Cl 13 0.09296
LP (1) N 1	BD*(1) C 3 - C 10	13.19	0.36	0.065	BD*(1) C 3 - Cl 10 0.09296
LP (1) N 1	BD*(1) C 3 - C 11	13.19	0.36	0.065	BD*(1) C 3 - Cl 11 0.09296
LP (1) N 1	BD*(1) C 4 - C 8	13.19	0.36	0.065	BD*(1) C 4 - Cl 8 0.09296
LP (1) N 1	BD*(1) C 4 - C 9	13.19	0.36	0.065	BD*(1) C 4 - Cl 9 0.09296

Bond lengths and bond angles of optimized structure

N1-C2 = 1.418 Å C3-N1-C4 = 120.000°
 N1-C3 = 1.418 Å C4-N1-C2 = 120.000°
 N1-C4 = 1.418 Å C2-N1-C3 = 120.000°
 Av. N-C = 1.418 Å sum C-N-C = 360.000° h = 0.000 Å

HF/6-311 G (d, p) NBO 5.9 Second Order Perturbation Theory Analysis of Fock Matrix in NBO Basis & Occupancy.

$E_{HF} = -2926.83208105$ a.u.

Donor NBO (i)	Acceptor NBO (j)	E(2)	E(j)-E(i)	F(i,j)	Occupancy
LP (1) N 1	BD*(1) C 2 - C 12	16.34	0.73	0.101	LP (1) N 1 1.80563
LP (1) N 1	BD*(1) C 2 - C 13	16.34	0.73	0.101	BD*(1) C 2 - Cl 13 0.06509
LP (1) N 1	BD*(1) C 3 - C 10	16.34	0.73	0.101	BD*(1) C 3 - Cl 10 0.06509
LP (1) N 1	BD*(1) C 3 - C 11	16.34	0.73	0.101	BD*(1) C 3 - Cl 11 0.06509
LP (1) N 1	BD*(1) C 4 - C 8	16.34	0.73	0.101	BD*(1) C 4 - Cl 8 0.06509
LP (1) N 1	BD*(1) C 4 - C 9	16.34	0.73	0.101	BD*(1) C 4 - Cl 9 0.06509

Bond lengths and bond angles of optimized structure.

N1-C2 = 1.415 Å C3-N1-C4 = 120.000°
 N1-C3 = 1.415 Å C4-N1-C2 = 120.000°
 N1-C4 = 1.415 Å C2-N1-C3 = 120.000°
 Av. N-C = 1.415 Å sum C-N-C = 360.000° h = 0.000 Å
Expt. Data: Av. N-C = 1.418 Å sum C-N-C = 360.000° h = 0.000 Å

HF/6-311 G (d, p) NBO 5.9 Energetic analysis

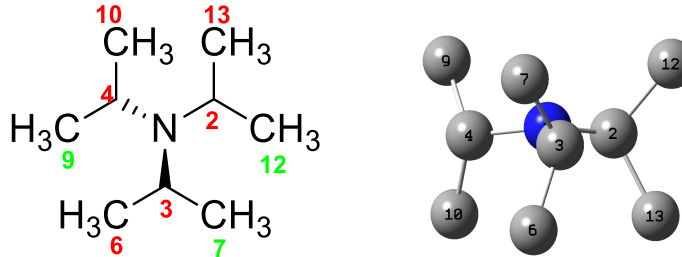
Deletion of interacting BD* orbitals gave;

- I. $E_{del} = 152.684$ kcal/mol after 2 iterations $\sum E (2) = 98.04$ kcal/mol.
- II. Lone pair occupancy on N 1 increased from 1.80563 to 1.98662.

Deletion of Fock matrix elements (N 1 and interacting BD* orbitals) gave;

- I. $E_{del} = 67.329$ kcal/mol after 2 iterations 31.32% lower than the $\sum E (2) = 98.04$ kcal/mol.
- II. Lone pair occupancy on N 1 increased from 1.80563 to 1.98641.

2. Triisopropylamine, 11.



DFT/6-311 G (d, p) NBO 3.1 Second Order Perturbation Theory Analysis of Fock Matrix in NBO Basis & Occupancy.

$E_{\text{DFT}} = -410.46510819$ a.u.

Donor NBO (i)	Acceptor NBO (j)	E(2)	E(j)-E(i)	F(i,j)	Occupancy
		kcal/mol	a.u.	a.u.	
LP (-1) N 1	BD*(-1) C 2 - C 12	4.94	0.60	0.050	LP (-1) N 1 1.86234
LP (-1) N 1	BD*(-1) C 2 - C 13	8.37	0.59	0.064	BD*(-1) C 2 - C 12 0.02489
LP (-1) N 1	BD*(-1) C 3 - C 6	8.37	0.59	0.064	BD*(-1) C 2 - C 13 0.03217
LP (-1) N 1	BD*(-1) C 3 - C 7	4.94	0.60	0.050	BD*(-1) C 3 - C 6 0.03217
LP (-1) N 1	BD*(-1) C 4 - C 9	4.94	0.60	0.050	BD*(-1) C 3 - C 7 0.02489
LP (-1) N 1	BD*(-1) C 4 - C 10	8.37	0.59	0.064	BD*(-1) C 4 - C 9 0.02489
					BD*(-1) C 4 - C 10 0.03217

Bond lengths and bond angles of optimized structure

N1-C2 = 1.467 Å C3-N1-C4 = 118.527°
 N1-C3 = 1.467 Å C4-N1-C2 = 118.528°
 N1-C4 = 1.467 Å C2-N1-C3 = 118.528°
 Av. N-C = 1.467 Å sum C-N-C = 355.583° h = 0.179 Å

HF/6-311 G (d, p) NBO 5.9 Second Order Perturbation Theory Analysis of Fock Matrix in NBO Basis & Occupancy.

$E_{\text{HF}} = -407.570454360$ a.u.

Donor NBO (i)	Acceptor NBO (j)	E(2)	E(j)-E(i)	F(i,j)	Occupancy
		kcal/mol	a.u.	a.u.	
LP (-1) N 1	BD*(-1) C 2 - C 12	7.16	0.99	0.077	LP (-1) N 1 1.89509
LP (-1) N 1	BD*(-1) C 2 - C 13	10.92	1.00	0.095	BD*(-1) C 2 - C 12 0.02058
LP (-1) N 1	BD*(-1) C 3 - C 6	10.92	1.00	0.095	BD*(-1) C 2 - C 13 0.02531
LP (-1) N 1	BD*(-1) C 3 - C 7	7.16	0.99	0.077	BD*(-1) C 3 - C 6 0.02531
LP (-1) N 1	BD*(-1) C 4 - C 9	7.16	0.99	0.077	BD*(-1) C 3 - C 7 0.02058
LP (-1) N 1	BD*(-1) C 4 - C 10	10.92	1.00	0.095	BD*(-1) C 4 - C 9 0.02058
					BD*(-1) C 4 - C 10 0.02531

Bond lengths and bond angles of optimized structure

N1-C2 = 1.457 Å C3-N1-C4 = 118.892°
 N1-C3 = 1.457 Å C4-N1-C2 = 118.892°
 N1-C4 = 1.457 Å C2-N1-C3 = 118.892°
 Av. N-C = 1.457 Å sum C-N-C = 356.676° h = 0.154 Å

Expt. Data: Av. N-C = 1.469 Å sum C-N-C = 349.2° h = 0.282 Å

HF/6-311 G (d, p) NBO 5.9 Energetic analysis

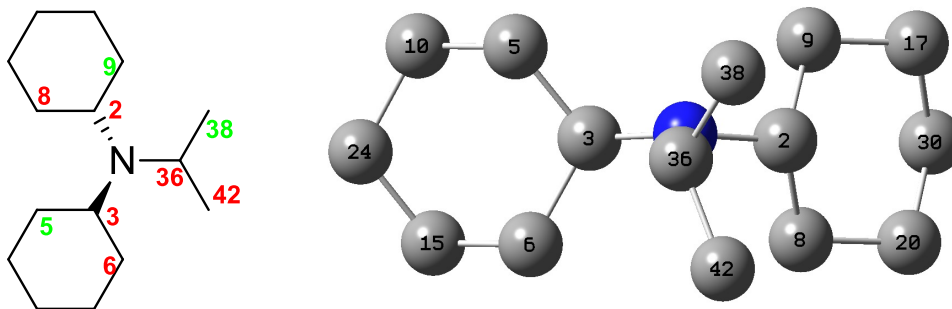
Deletion of interacting BD* orbitals gave;

- I. $E_{\text{del}} = 76.004$ kcal/mol after 2 iterations $\sum E (2) = 54.24$ kcal/mol.
- II. Lone pair occupancy on N 1 increased from 1.89509 to 1.98054.

Deletion of Fock matrix elements (N 1 and interacting BD* orbitals) gave;

- I. $E_{\text{del}} = 42.306$ kcal/mol after 2 iterations 22.00% lower than the $\sum E (2) = 54.24$ kcal/mol.
- II. Lone pair occupancy on N 1 increased from 1.89509 to 1.98034.

3. Dicyclohexylisopropylamine, 106.



DFT/6-311 G (d, p) NBO 3.1 Second Order Perturbation Theory Analysis of Fock Matrix in NBO Basis & Occupancy.

$E_{DFT} = -643.99259497$ a. u.

Donor NBO (i)	Acceptor NBO (j)	E(2)	E(j)-E(i)	F(i,j)	Occupancy
LP (1) N 1	BD*(1) C 2 - C 8	8.18	0.59	0.064	LP (1) N 1 1.86090
LP (1) N 1	BD*(1) C 2 - C 9	5.22	0.60	0.051	BD*(1) C 2 - C 9 0.03776
LP (1) N 1	BD*(1) C 3 - C 5	5.27	0.60	0.051	BD*(1) C 3 - C 5 0.03193
LP (1) N 1	BD*(1) C 3 - C 6	8.14	0.59	0.064	BD*(1) C 3 - C 6 0.03221
LP (1) N 1	BD*(1) C 36 - C 38	5.36	0.59	0.052	BD*(1) C 36 - C 38 0.03793
LP (1) N 1	BD*(1) C 36 - C 42	8.10	0.59	0.063	BD*(1) C 36 - C 42 0.02599

Bond lengths and bond angles of optimized structure

N1-C2 = 1.455 Å C3-N1-C36 = 119.004°

N1-C3 = 1.455 Å C36-N1-C2 = 118.702°

N1-C36 = 1.457 Å C2-N1-C3 = 119.190°

Av. N-C = 1.456 Å sum C-N-C = 356.896° h = 0.150 Å

HF/6-311 G (d, p) NBO 5.9 Second Order Perturbation Theory Analysis of Fock Matrix in NBO Basis & Occupancy.

$E_{HF} = -639.506005163$

Donor NBO (i)	Acceptor NBO (j)	E(2)	E(j)-E(i)	F(i,j)	Occupancy
LP (1) N 1	BD*(1) C 2 - C 8	10.58	0.99	0.093	LP (1) N 1 1.89470
LP (1) N 1	BD*(1) C 2 - C 9	7.32	1.00	0.078	BD*(1) C 2 - C 9 0.02979
LP (1) N 1	BD*(1) C 3 - C 5	7.33	1.00	0.078	BD*(1) C 3 - C 5 0.02596
LP (1) N 1	BD*(1) C 3 - C 6	10.61	0.99	0.093	BD*(1) C 3 - C 6 0.02609
LP (1) N 1	BD*(1) C 36 - C 38	7.45	1.00	0.078	BD*(1) C 36 - C 38 0.03000
LP (1) N 1	BD*(1) C 36 - C 42	10.61	0.99	0.094	BD*(1) C 36 - C 42 0.02103

Bond lengths and bond angles of optimized structure

N1-C2 = 1.463 Å C3-N1-C36 = 119.238°

N1-C3 = 1.464 Å C36-N1-C2 = 118.881°

N1-C36 = 1.466 Å C2-N1-C3 = 119.286°

Av. N-C = 1.464 Å sum C-N-C = 357.405° h = 0.136 Å

Expt. Data: No crystal data

HF/6-311 G (d, p) NBO 5.9 Energetic analysis

Deletion of interacting BD* orbitals gave;

I. $E_{del} = 92.233$ kcal/mol after 2 iterations $\sum E (2) = 54.10$ kcal/mol.

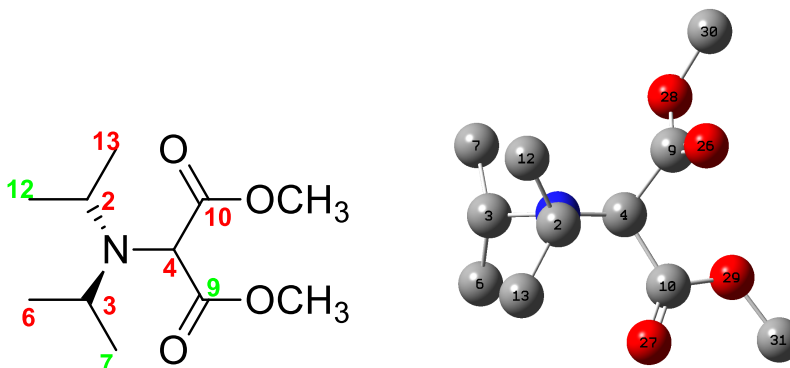
II. Lone pair occupancy on N 1 increased from 1.89470 to 1.97816.

Deletion of Fock matrix elements (N 1 and interacting BD* orbitals) gave;

I. $E_{del} = 41.598$ kcal/mol after 2 iterations 22.82% lower than the $\sum E (2) = 53.9$ kcal/mol.

II. Lone pair occupancy on N 1 increased from 1.89470 to 1.97801.

4. Dimethyl 2-(diisopropylamino)propanedioate, 84.



DFT/6-311 G (d, p) NBO 3.1 Second Order Perturbation Theory Analysis of Fock Matrix in NBO Basis & Occupancy.

$E_{\text{DFT}} = -787.68501282 \text{ a.u.}$

Donor NBO (i)	Acceptor NBO (j)	$E(2)$ kcal/mol	$E(j)-E(i)$ a.u.	$F(i,j)$ a.u.	Occupancy
LP (-1) N 1	BD*(-1) C 2 - C 12	5.83	0.61	0.055	LP (-1) N 1 BD*(-1) C 2 - C 12 0.02561
LP (-1) N 1	BD*(-1) C 2 - C 13	6.10	0.61	0.056	BD*(-1) C 2 - C 13 0.02593
LP (-1) N 1	BD*(-1) C 3 - C 6	7.13	0.60	0.060	BD*(-1) C 3 - C 6 0.02795
LP (-1) N 1	BD*(-1) C 3 - C 7	5.61	0.60	0.054	BD*(-1) C 3 - C 7 0.02512
LP (-1) N 1	BD*(-1) C 4 - C 9	6.98	0.57	0.057	BD*(-1) C 4 - C 9 0.08346
LP (-1) N 1	BD*(-1) C 4 - C 10	10.38	0.56	0.069	BD*(-1) C 4 - C 10 0.09732

Bond lengths and bond angles of optimized structure

N1-C2 = 1.474 Å C3-N1-C4 = 118.819°
 N1-C3 = 1.467 Å C4-N1-C2 = 119.960°
 N1-C4 = 1.436 Å C2-N1-C3 = 120.278°
 Av. N-C = 1.459 Å sum C-N-C = 359.057° h = 0.082 Å

HF/6-311 G (d, p) NBO 5.9 Second Order Perturbation Theory Analysis of Fock Matrix in NBO Basis & Occupancy.

$E_{\text{HF}} = -782.878928091 \text{ a.u.}$

Donor NBO (i)	Acceptor NBO (j)	$E(2)$ kcal/mol	$E(j)-E(i)$ a.u.	$F(i,j)$ a.u.	Occupancy
LP (-1) N 1	BD*(-1) C 2 - C 12	7.87	1.01	0.081	LP (-1) N 1 BD*(-1) C 2 - C 12 0.02108
LP (-1) N 1	BD*(-1) C 2 - C 13	7.98	1.01	0.082	BD*(-1) C 2 - C 13 0.02041
LP (-1) N 1	BD*(-1) C 3 - C 6	9.65	1.00	0.090	BD*(-1) C 3 - C 6 0.02272
LP (-1) N 1	BD*(-1) C 3 - C 7	7.24	1.00	0.078	BD*(-1) C 3 - C 7 0.01993
LP (-1) N 1	BD*(-1) C 4 - C 9	8.68	0.97	0.083	BD*(-1) C 4 - C 9 0.06714
LP (-1) N 1	BD*(-1) C 4 - C 10	14.70	0.97	0.108	BD*(-1) C 4 - C 10 0.07692

Bond lengths and bond angles of optimized structure

N1-C2 = 1.467 Å C3-N1-C4 = 118.681°
 N1-C3 = 1.460 Å C4-N1-C2 = 119.637°
 N1-C4 = 1.430 Å C2-N1-C3 = 120.254°
 Av. N-C = 1.452 Å sum C-N-C = 358.572° h = 0.101 Å

Expt. Data: No crystal data.

HF/6-311 G (d, p) NBO 5.9 Energetic analysis

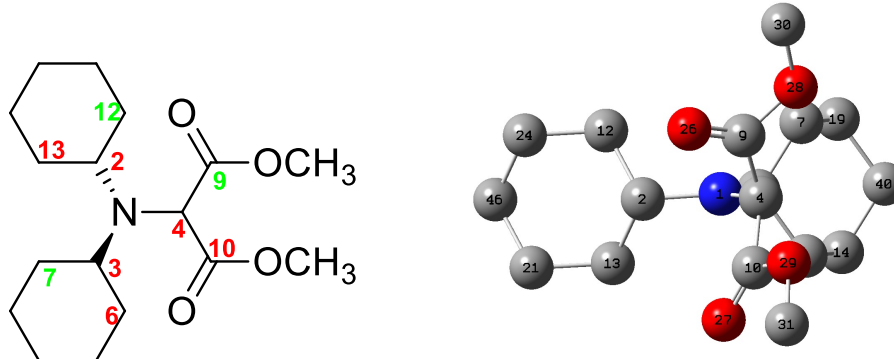
Deletion of interacting BD* orbitals gave;

- I. $E_{\text{del}} = 130.975 \text{ kcal/mol}$ after 2 iterations $\sum E(2) = 56.12 \text{ kcal/mol}$.
- II. Lone pair occupancy on N 1 increased from 1.88698 to 1.97547.

Deletion of Fock matrix elements (N 1 and interacting BD* orbitals) gave;

- I. $E_{\text{del}} = 42.480 \text{ kcal/mol}$ after 2 iterations 24.31% lower than the $\sum E(2) = 56.12 \text{ kcal/mol}$.
- II. Lone pair occupancy on N 1 increased from 1.88698 to 1.97513.

5. Dimethyl 2-dicyclohexylaminopropan-1,3-dioate, 86.



DFT/6-311 G (d, p) NBO 3.1 Second Order Perturbation Theory Analysis of Fock Matrix in NBO Basis & Occupancy.

$E_{\text{DFT}} = -1021.21279434$ a. u.

Donor NBO (i)	Acceptor NBO (j)	E(2)	E(j)-E(i)	F(i,j)	Occupancy
		kcal/mol	a.u.	a.u.	
LP (-1) N 1	BD*(-1) C 2 - C 12	6.24	0.61	0.057	LP (-1) N 1 1.83983
LP (-1) N 1	BD*(-1) C 2 - C 13	5.78	0.61	0.055	BD*(-1) C 2 - C 12 0.03269
LP (-1) N 1	BD*(-1) C 3 - C 6	6.67	0.60	0.058	BD*(-1) C 2 - C 13 0.03184
LP (-1) N 1	BD*(-1) C 3 - C 7	6.16	0.60	0.056	BD*(-1) C 3 - C 6 0.03368
LP (-1) N 1	BD*(-1) C 4 - C 9	7.67	0.56	0.060	BD*(-1) C 3 - C 7 0.03283
LP (-1) N 1	BD*(-1) C 4 - C 10	9.86	0.56	0.067	BD*(-1) C 4 - C 9 0.08477
					BD*(-1) C 4 - C 10 0.09719

Bond lengths and bond angles of optimized structure

N1-C2 = 1.471 Å C3-N1-C4 = 119.288°

N1-C3 = 1.465 Å C4-N1-C2 = 119.722°

N1-C4 = 1.435 Å C2-N1-C3 = 120.794°

Av. N-C = 1.457 Å sum C-N-C = 359.804° h = 0.037 Å

HF/6-311 G (d, p) NBO 5.9 Second Order Perturbation Theory Analysis of Fock Matrix in NBO Basis & Occupancy.

$E_{\text{HF}} = -1014.81476099$ a.u.

Donor NBO (i)	Acceptor NBO (j)	E(2)	E(j)-E(i)	F(i,j)	Occupancy
		kcal/mol	a.u.	a.u.	
LP (-1) N 1	BD*(-1) C 2 - C 12	7.89	1.01	0.082	LP (-1) N 1 1.88651
LP (-1) N 1	BD*(-1) C 2 - C 13	7.79	1.02	0.081	BD*(-1) C 2 - C 12 0.02628
LP (-1) N 1	BD*(-1) C 3 - C 6	9.46	1.01	0.089	BD*(-1) C 2 - C 13 0.02541
LP (-1) N 1	BD*(-1) C 3 - C 7	7.30	1.01	0.078	BD*(-1) C 3 - C 6 0.02772
LP (-1) N 1	BD*(-1) C 4 - C 9	8.95	0.96	0.084	BD*(-1) C 3 - C 7 0.02531
LP (-1) N 1	BD*(-1) C 4 - C 10	14.59	0.97	0.107	BD*(-1) C 4 - C 9 0.06147
					BD*(-1) C 4 - C 10 0.07693

Bond lengths and bond angles of optimized structure

N1-C2 = 1.465 Å C3-N1-C4 = 118.944°

N1-C3 = 1.458 Å C4-N1-C2 = 119.405°

N1-C4 = 1.430 Å C2-N1-C3 = 120.570°

Av. N-C = 1.451 Å sum C-N-C = 358.919° h = 0.087 Å

Expt. Data: Av. N-C = 1.460 Å sum C-N-C = 353.745° h = 0.157 Å

HF/6-311 G (d, p) NBO 5.9 Energetic analysis

Deletion of interacting BD* orbitals gave;

I. $E_{\text{del}} = 147.151$ kcal/mol after 2 iterations $\sum E (2) = 55.98$ kcal/mol.

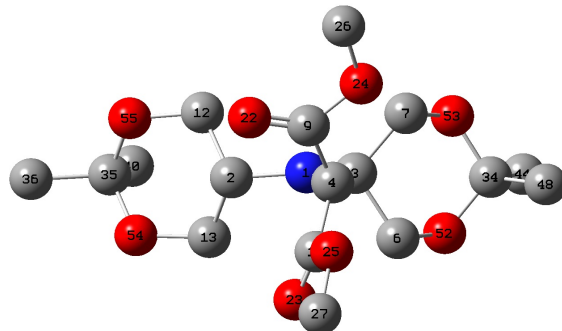
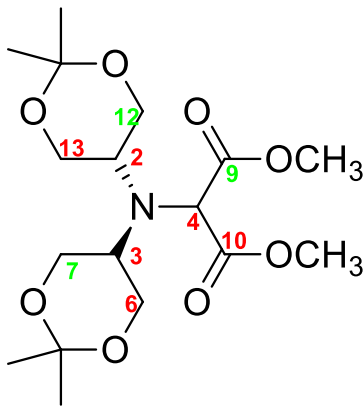
II. Lone pair occupancy on N 1 increased from 1.88651 to 1.9751.

Deletion of Fock matrix elements (N 1 and interacting BD* orbitals) gave;

I. $E_{\text{del}} = 41.865$ kcal/mol after 2 iterations 25.21% lower than the $\sum E (2) = 55.98$ kcal/mol.

II. Lone pair occupancy on N 1 increased from 1.88651 to 1.97322.

6. Dimethyl 2-(N,N-bis(4,4-dimethyl-3,5-dioxanyl)amino) malonate, 20.



DFT/6-311 G (d, p) NBO 3.1 Second Order Perturbation Theory Analysis of Fock Matrix in NBO Basis & Occupancy.

$E_{\text{DFT}} = -1322.14265074 \text{ a.u.}$

Donor NBO (i)	Acceptor NBO (j)	E(2)	$E(j)-E(i)$	F(i,j)	Occupancy
LP (1) N 1	BD*(1) C 2 - C 12	5.80	0.62	0.055	BD*(1) C 2 - C 12 0.03910
LP (1) N 1	BD*(1) C 2 - C 13	6.42	0.62	0.058	BD*(1) C 2 - C 13 0.04015
LP (1) N 1	BD*(1) C 3 - C 6	7.76	0.60	0.063	BD*(1) C 3 - C 6 0.04321
LP (1) N 1	BD*(1) C 3 - C 7	5.68	0.60	0.054	BD*(1) C 3 - C 7 0.03989
LP (1) N 1	BD*(1) C 4 - C 9	6.37	0.58	0.055	BD*(1) C 4 - C 9 0.08350
LP (1) N 1	BD*(1) C 4 - C 10	9.69	0.57	0.067	BD*(1) C 4 - C 10 0.09647

Bond lengths and bond angles of optimized structure

N1-C2 = 1.468 Å C3-N1-C4 = 119.200°

N1-C3 = 1.461 Å C4-N1-C2 = 118.971°

N1-C4 = 1.443 Å C2-N1-C3 = 120.315°

Av. N-C = 1.457 Å sum C-N-C = 358.486° h = 0.104 Å

HF/6-311 G (d, p) NBO 5.9 Second Order Perturbation Theory Analysis of Fock Matrix in NBO Basis & Occupancy.

$E_{\text{HF}} = -1314.30586538 \text{ a.u.}$

Donor NBO (i)	Acceptor NBO (j)	E(2)	$E(j)-E(i)$	F(i,j)	Occupancy
LP (1) N 1	BD*(1) C 2 - C 12	7.84	1.02	0.082	BD*(1) C 2 - C 12 0.03121
LP (1) N 1	BD*(1) C 2 - C 13	8.36	1.02	0.084	BD*(1) C 2 - C 13 0.03108
LP (1) N 1	BD*(1) C 3 - C 6	10.15	1.01	0.092	BD*(1) C 3 - C 6 0.03377
LP (1) N 1	BD*(1) C 3 - C 7	7.16	1.01	0.080	BD*(1) C 3 - C 7 0.03112
LP (1) N 1	BD*(1) C 4 - C 9	8.09	0.98	0.080	BD*(1) C 4 - C 9 0.06765
LP (1) N 1	BD*(1) C 4 - C 10	13.86	0.98	0.105	BD*(1) C 4 - C 10 0.07644

Bond lengths and bond angles of optimized structure

N1-C2 = 1.460 Å C3-N1-C4 = 119.207°

N1-C3 = 1.453 Å C4-N1-C2 = 118.992°

N1-C4 = 1.436 Å C2-N1-C3 = 120.264°

Av. N-C = 1.450 Å sum C-N-C = 358.463 ° h = 0.104 Å

Expt. Data: Av. N-C = 1.451 Å sum C-N-C = 358.320° h = 0.101 Å

HF/6-311 G (d, p) NBO 5.9 Energetic analysis

Deletion of interacting BD* orbitals gave;

I. $E_{\text{del}} = 148.517 \text{ kcal/mol}$ after 2 iterations $\sum E (2) = 54.85 \text{ kcal/mol}$.

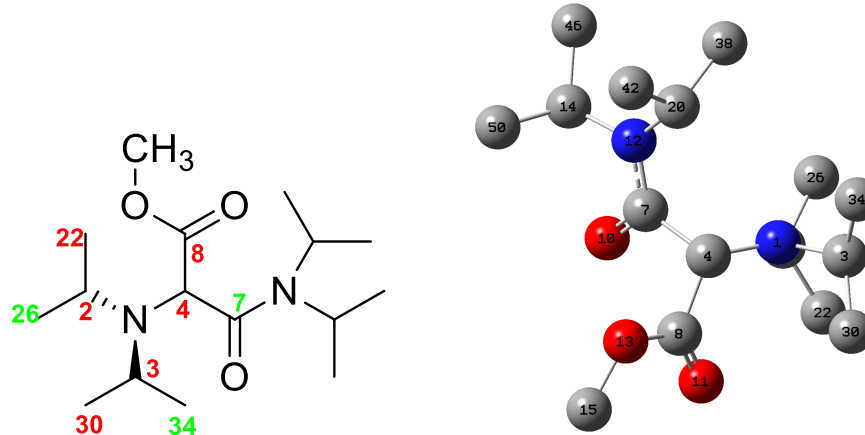
II. Lone pair occupancy on N 1 increased from 1.88500 to 1.96977.

Deletion of Fock matrix elements (N 1 and interacting BD* orbitals) gave;

I. $E_{\text{del}} = 40.869 \text{ kcal/mol}$ after 2 iterations 25.49% lower than the $\sum E (2) = 54.85 \text{ kcal/mol}$.

II. Lone pair occupancy on N 1 increased from 1.88500 to 1.96938.

7. 2-Diisopropylamino-N,N-diisopropylmalonamic acid methyl ester, 85.



DFT/6-311 G (d, p) NBO 3.1 Second Order Perturbation Theory Analysis of Fock Matrix in NBO Basis & Occupancy.

$E_{\text{DFT}} = -964.41906337$ a.u.

Donor NBO (i)	Acceptor NBO (j)	E(2)	E(j)-E(i)	F(i,j)	Occupancy
		kcal/mol	a.u.	a.u.	
LP (-1) N 1	BD*(-1) C 2 - C 22	6.28	0.62	0.057	BD*(-1) C 2 - C 22 0.02523
LP (-1) N 1	BD*(-1) C 26	4.69	0.62	0.049	BD*(-1) C 26 0.02414
LP (-1) N 1	BD*(-1) C 3 - C 30	7.73	0.61	0.063	BD*(-1) C 3 - C 30 0.02884
LP (-1) N 1	BD*(-1) C 34	4.50	0.61	0.048	BD*(-1) C 34 0.02353
LP (-1) N 1	BD*(-1) C 7	3.40	0.57	0.040	BD*(-1) C 7 0.07701
LP (-1) N 1	BD*(-1) C 8	12.29	0.58	0.076	BD*(-1) C 8 0.09810

Bond lengths and bond angles of optimized structure

N1-C2 = 1.484 Å C3-N1-C4 = 118.038°
 N1-C3 = 1.475 Å C4-N1-C2 = 118.660°
 N1-C4 = 1.446 Å C2-N1-C3 = 117.871°
 Av. N-C = 1.468 Å sum C-N-C = 354.569° h = 0.199 Å

HF/6-311 G (d, p) NBO 5.9 Second Order Perturbation Theory Analysis of Fock Matrix in NBO Basis & Occupancy.

$E_{\text{HF}} = -958.238032719$ a.u.

Donor NBO (i)	Acceptor NBO (j)	E(2)	E(j)-E(i)	F(i,j)	Occupancy
		kcal/mol	a.u.	a.u.	
LP (-1) N 1	BD*(-1) C 2 - C 22	8.04	1.03	0.083	BD*(-1) C 2 - C 22 0.02004
LP (-1) N 1	BD*(-1) C 26	6.49	1.02	0.074	BD*(-1) C 26 0.01945
LP (-1) N 1	BD*(-1) C 30	10.14	1.01	0.092	BD*(-1) C 30 0.02299
LP (-1) N 1	BD*(-1) C 34	6.04	1.01	0.071	BD*(-1) C 34 0.01890
LP (-1) N 1	BD*(-1) C 7	4.87	0.97	0.062	BD*(-1) C 7 0.06150
LP (-1) N 1	BD*(-1) C 8	16.15	0.99	0.114	BD*(-1) C 8 0.07781

Bond lengths and bond angles of optimized structure

N1-C2 = 1.476 Å C3-N1-C4 = 118.014°
 N1-C3 = 1.467 Å C4-N1-C2 = 118.535°
 N1-C4 = 1.439 Å C2-N1-C3 = 117.893°
 Av. N-C = 1.461 Å sum C-N-C = 354.442° h = 0.200 Å
Expt. Data: Av. N-C = 1.460 Å sum C-N-C = 353.745° h = 0.213 Å

HF/6-311 G (d, p) NBO 5.9 Energetic analysis

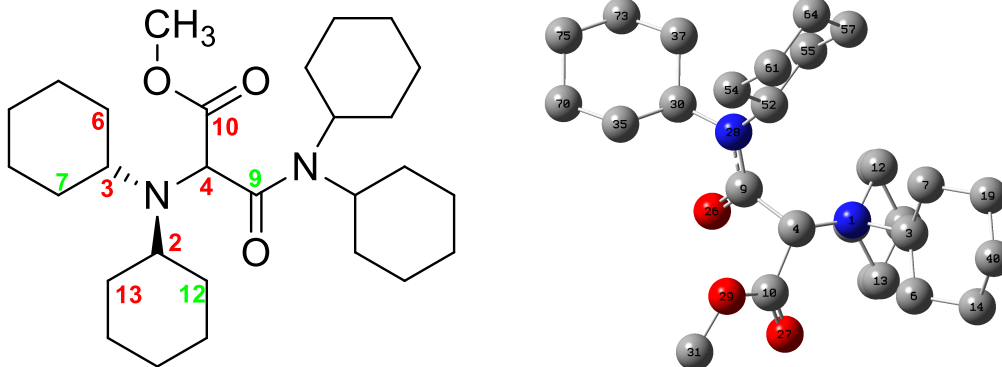
Deletion of interacting BD* orbitals gave;

- I. $E_{\text{del}} = 125.587$ kcal/mol after 2 iterations $\sum E (2) = 51.73$ kcal/mol.
- II. Lone pair occupancy on N 1 increased from 1.89499 to 1.97742.

Deletion of Fock matrix elements (N 1 and interacting BD* orbitals) gave;

- I. $E_{\text{del}} = 39.749$ kcal/mol after 2 iterations 23.16% lower than the $\sum E (2) = 51.73$ kcal/mol.
- II. Lone pair occupancy on N 1 increased from 1.89499 to 1.97716.

8. N,N-Dicyclohexyl-2-dicyclohexylaminomalonamic acid methyl ester, 87.



DFT/6-311 G (d, p) NBO 3.1 Second Order Perturbation Theory Analysis of Fock Matrix in NBO Basis & Occupancy.

$E_{\text{DFT}} = -1431.47255176$ a.u.

Donor NBO (i)	Acceptor NBO (j)	$E(2)$	$E(j)-E(i)$	$F(i,j)$	Occupancy
		kcal/mol	a.u.	a.u.	
LP (1) N 1	BD*(1) C 2 - C 12	4.72	0.62	0.050	LP (1) N 1 1.85682
LP (1) N 1	BD*(1) C 2 - C 13	6.22	0.62	0.057	BD*(1) C 2 - C 12 0.03057
LP (1) N 1	BD*(1) C 3 - C 6	7.58	0.61	0.062	BD*(1) C 2 - C 13 0.03155
LP (1) N 1	BD*(1) C 3 - C 7	4.58	0.61	0.049	BD*(1) C 3 - C 6 0.03512
LP (1) N 1	BD*(1) C 4 - C 9	3.40	0.57	0.040	BD*(1) C 3 - C 7 0.03076
LP (1) N 1	BD*(1) C 4 - C 10	12.36	0.57	0.076	BD*(1) C 4 - C 9 0.07553
					BD*(1) C 4 - C 10 0.09896

Bond lengths and bond angles of optimized structure

N1-C2 = 1.481 Å C3-N1-C4 = 117.939°

N1-C3 = 1.474 Å C4-N1-C2 = 118.957°

N1-C4 = 1.446 Å C2-N1-C3 = 118.060°

Av. N-C = 1.467 Å sum C-N-C = 354.956° h = 0.192 Å

HF/6-311 G (d, p) NBO 5.9 Second Order Perturbation Theory Analysis of Fock Matrix in NBO Basis & Occupancy.

$E_{\text{HF}} = -1422.10707788$ a.u.

Donor NBO (i)	Acceptor NBO (j)	$E(2)$	$E(j)-E(i)$	$F(i,j)$	Occupancy
		kcal/mol	a.u.	a.u.	
LP (1) N 1	BD*(1) C 2 - C 12	6.46	1.03	0.074	LP (1) N 1 1.89409
LP (1) N 1	BD*(1) C 2 - C 13	7.93	1.03	0.082	BD*(1) C 2 - C 12 0.02459
LP (1) N 1	BD*(1) C 3 - C 6	9.89	1.02	0.091	BD*(1) C 2 - C 13 0.02519
LP (1) N 1	BD*(1) C 3 - C 7	6.11	1.03	0.072	BD*(1) C 3 - C 6 0.02808
LP (1) N 1	BD*(1) C 4 - C 9	4.86	0.97	0.037	BD*(1) C 3 - C 7 0.02454
LP (1) N 1	BD*(1) C 4 - C 10	16.33	0.98	0.062	BD*(1) C 4 - C 9 0.06066
					BD*(1) C 4 - C 10 0.07835

Bond lengths and bond angles of optimized structure

N1-C2 = 1.474 Å C3-N1-C4 = 118.169°

N1-C3 = 1.466 Å C4-N1-C2 = 118.826°

N1-C4 = 1.440 Å C2-N1-C3 = 118.046°

Av. N-C = 1.460 Å sum C-N-C = 355.041° h = 0.190 Å

Expt. Data: Av. N-C = 1.461 Å sum C-N-C = 353.50° h = 0.217 Å

HF/6-311 G (d, p) NBO 5.9 Energetic analysis

Deletion of interacting BD* orbitals gave;

I. $E_{\text{del}} = 141.668$ kcal/mol after 2 iterations $\sum E (2) = 51.58$ kcal/mol.

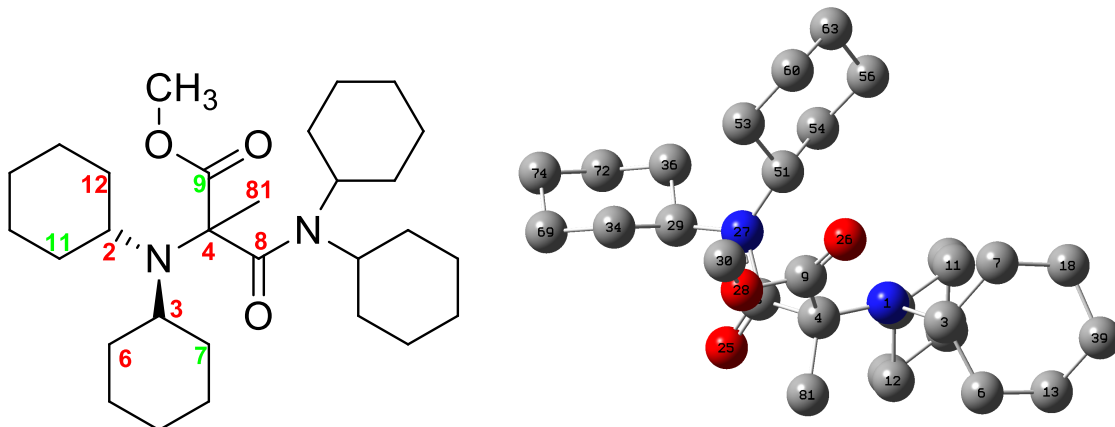
II. Lone pair occupancy on N 1 increased from 1.89409 to 1.97554.

Deletion of Fock matrix elements (N 1 and interacting BD* orbitals) gave;

I. $E_{\text{del}} = 39.126$ kcal/mol after 2 iterations 24.15% lower than the $\sum E (2) = 51.58$ kcal/mol.

II. Lone pair occupancy on N 1 increased from 1.89409 to 1.97529.

9. N,N-Dicyclohexyl-2-dicyclohexylamino-2-methylmalonamic acid methyl ester, 105.



DFT/6-311 G (d, p) NBO 3.1 Second Order Perturbation Theory Analysis of Fock Matrix in NBO Basis & Occupancy.

$E_{\text{DFT}} = -1470.77171999 \text{ a.u.}$

Donor NBO (i)	Acceptor NBO (j)	E(2)	E(j)-E(i)	F(i,j)	Occupancy
		kcal/mol	a.u.	a.u.	
LP (1) N 1	BD*(1) C 2 - C 11	1.89	0.63	0.032	LP (1) N 1 1.86895
LP (1) N 1	BD*(1) C 2 - C 12	9.61	0.61	0.070	BD*(1) C 2 - C 11 0.02598
LP (1) N 1	BD*(1) C 3 - C 6	7.44	0.61	0.062	BD*(1) C 2 - C 12 0.04088
LP (1) N 1	BD*(1) C 3 - C 7	4.31	0.62	0.047	BD*(1) C 3 - C 6 0.03652
LP (1) N 1	BD*(1) C 4 - C 9	3.98	0.57	0.043	BD*(1) C 3 - C 7 0.03039
LP (1) N 1	BD*(1) C 4 - C 81	8.74	0.58	0.065	BD*(1) C 4 - C 9 0.08768
					BD*(1) C 4 - C 81 0.03404

Bond lengths and bond angles of optimized structure

N1-C2 = 1.485 Å C3-N1-C4 = 113.296°
 N1-C3 = 1.499 Å C4-N1-C2 = 115.372°
 N1-C4 = 1.483 Å C2-N1-C3 = 122.921°
Av. N-C = 1.489 Å sum C-N-C = 351.589° $\hbar = 0.251 \text{ \AA}$

HF/6-311 G (d, p) NBO 5.9 Second Order Perturbation Theory Analysis of Fock Matrix in NBO Basis & Occupancy.

$E_{\text{HF}} = -1461.1081327 \text{ a.u.}$

Donor NBO (i)	Acceptor NBO (j)	E(2)	E(j)-E(i)	F(i,j)	Occupancy
		kcal/mol	a.u.	a.u.	
LP (1) N 1	BD*(1) C 2 - C 11	2.64	1.04	0.048	LP (1) N 1 1.90252
LP (1) N 1	BD*(1) C 2 - C 12	12.54	1.02	0.103	BD*(1) C 2 - C 11 0.02082
LP (1) N 1	BD*(1) C 3 - C 6	9.58	1.02	0.090	BD*(1) C 2 - C 12 0.03225
LP (1) N 1	BD*(1) C 3 - C 7	5.87	1.02	0.070	BD*(1) C 3 - C 6 0.02880
LP (1) N 1	BD*(1) C 4 - C 9	5.91	0.97	0.068	BD*(1) C 3 - C 7 0.02413
LP (1) N 1	BD*(1) C 4 - C 81	11.82	0.98	0.098	BD*(1) C 4 - C 9 0.07106
					BD*(1) C 4 - C 81 0.02637

Bond lengths and bond angles of optimized structure

N1-C2 = 1.478 Å C3-N1-C4 = 113.320°
 N1-C3 = 1.490 Å C4-N1-C2 = 115.765°
 N1-C4 = 1.473 Å C2-N1-C3 = 123.129°
Av. N-C = 1.480 Å sum C-N-C = 352.214° $\hbar = 0.240 \text{ \AA}$
Expt. Data: Av. N-C = 1.474 Å sum C-N-C = 350.78° $\hbar = 0.261 \text{ \AA}$

HF/6-311 G (d, p) NBO 5.9 Energetic analysis

Deletion of interacting BD* orbitals gave;

- I. $E_{\text{del}} = 122.093 \text{ kcal/mol}$ after 2 iterations $\sum E (2) = 48.36 \text{ kcal/mol}$.
- II. Lone pair occupancy on N 1 increased from 1.90252 to 1.97895.

Deletion of Fock matrix elements (N 1 and interacting BD* orbitals) gave;

- I. $E_{\text{del}} = 39.126 \text{ kcal/mol}$ after 2 iterations 25.30% lower than the $\sum E (2) = 48.36 \text{ kcal/mol}$.
- II. Lone pair occupancy on N 1 increased from 1.90252 to 1.97860.